19813

APPLICATIONS OF COAL PETROGRAPHY AND MICROSTRUCTURE TO GAS EMISSIONS, OUTBURST-PRONENESS INDICATIONS AND ALLEVIATION IN UNDERGROUND COAL MINES

JOINT COAL BOARD
HEALTH AND SAFETY TRUST

FINAL REPORT

March 1995

P.J. CROSDALE AND B.B. BEAMISH

COALSEAM GAS RESEARCH INSTITUTE

JAMES COOK UNIVERSITY OF NORTH QUEENSLAND

TABLE OF CONTENTS

SUMMARY

Coals from South Bulli Colliery (Southern Coalfield, NSW) and Central Colliery (Bowen Basin, Queensland) were investigated for methane sorption properties in relation to coal type. Bright and dull coal types were hand picked from a variety of sample types including in-seam drill cuttings and cores and strip samples. Coals were analysed as 'lump' (-5.60+2.00mm) and 'crushed' (-0.212mm) samples in both equilibrium moist and dry states. Lump samples were used to evaluate *in situ* methane desorption parameters. Crushed coals were used to evaluate methane adsorption isotherms and Langmuir volumes (the maximum amount of gas that can be adsorbed). Equilibrium moist samples best simulate *in situ* conditions but analysis of dry coals was also required to ensure a comparable data basis between samples.

Methane sorption testing was performed using high pressure microbalances. The technique allows small samples of about 1g to be used and is suitable for the hand picked coal types investigated. Maximum sample weight of 25g is possible at pressures up to 15MPa.

Adsorption isotherms were performed at 23°C at pressure steps of 0.5, 1, 2, 3, 5, 7 and 9MPa. Coals were shown to adsorb more gas when dry than when moist. Central Colliery coals generally have a larger capacity to adsorb methane than those from South Bulli, which is related to the higher coal rank at Central. Bright coal at Central has a greater methane storage capacity than its equivalent dull coal from the same site; at South Bulli, no strong trends were noted in relation to coal type. Estimation of the adsorption isotherm from proximate analysis found Central Colliery samples were better modelled than the South Bulli coals.

Lump samples (-5.60+2.00mm) were used to evaluate gas desorption to atmosphere from the estimated *in situ* gas pressure (2MPa for Central; 3MPa for South Bulli). Samples were resorbed with methane at 5MPa, followed by a pressure reduction to 2 or 3MPa and then release of the gas at atmospheric pressure. Sorption rates were

estimated using the effective diffusivity parameter (D_e) which uses the rate of gas release over the first 10 minutes.

Relationships of coal type to D_e are different for South Bulli and Central. South Bulli desorption rates are slower than at Central. At South Bulli, there appears to be little correlation of desorption rate and coal type (as measured by the vitrinite content). In contrast, Central coals have a trend of increasing D_e with decreasing vitrinite content i.e. the dull coals desorb more rapidly. More rapid desorption in dull coals at Central is related to differences in maceral properties, in particular to the higher percentage of open cell lumina associated with inertinites at Central.

Detailed analysis of pore distribution by mercury porosimetry showed D_e of the lump samples is strongly related to the pore structure of the coal. Bright coals have smaller mean pore diameters and lower D_e than equivalent dull coals.

Crushed samples were also desorbed to atmosphere from the estimated *in situ* gas pressure for comparison with the lump samples. Results showed crushed coal desorption rates are an order of magnitude greater than the lump samples. This phenomenon explains the rapid desorption rates associated with sheared coal at Central.

Adsorption isotherm results were used to evaluate the degree of gas saturation in the lump samples. Dry samples had higher degrees of gas saturation than moist samples. Central Colliery lump samples consistently achieved greater degrees of gas saturation than those from South Bulli, which is presumed to be related to a larger fracture network spacing at South Bulli and to differences in pore structure.

Microstructural analysis by SEM investigated how gas flow is affected by the nature of fractures and macropores and their degree and type of mineral infill. Detailed examination of the sheared coal allowed its rapid sorption behaviour to be explained in terms of grain size and large, open intergranular porosity. Other microstructural

analyses were inconclusive largely because of difficulties in quantifying the data, especially in relation to its effect on gas flow.

Microbalance desorption rates on lump samples were found to correspond to desorption rates in methane drainage holes at Central. It is inferred the microbalance could be used to predict methane drainage performance months in advance.

Highlights, Breakthroughs and Difficulties

Major achievements of this investigation are :

- recognition that significant differences occur in methane sorption properties between coals of the Sydney and Bowen Basins. Experiences gained in methane drainage in NSW and Queensland may not be directly interchangeable.

- at South Bulli, (NSW) coal type does not appear to play a major role in gas desorption rates and it is likely that targeting specific seam horizons will not greatly enhance methane drainage.

- at Central (Qld), dull coal types sorb methane more rapidly than bright coal types. Targeting dull horizons will increase gas make rates but may result in uneven seam drainage. This is of particular concern where bright coal types have been implicated in outbursting.

- tectonically disturbed (sheared) coals have greatly enhanced gas make rates because the coal has been crushed to small particle sizes and large (up to 5μm) open, interconnected spaces between the grains provide easy pathways for gas escape.

- laboratory studies using high pressure microbalances may provide reliable predictions of long term in-seam drainage performance.

Due to the novelty of the microbalance technique, a number of difficulties were experienced in determining the best experimental conditions for evaluation of gas sorption properties. These are not detailed in this final report but may be found in quarterly progress reports. It was anticipated that sample residence time in the balance of around two days would be sufficient to complete testing. However, a minimum time of 7 to 10 days was found necessary which significantly reduced sample throughput. Analysis of equilibrium moist samples was complicated by moisture loss during testing: no satisfactory solution was found to this problem.

Progress Against Milestones

Four main objectives were identified :

1. To investigate the different gas flow characteristics of coal types from South Bulli and German Creek.
2. To determine the influence of coal microstructure on gas emissions and outburst-proneness.
3. To identify target drilling horizons in seam to assist optimum gas drainage
4. To identify proximity to seam dislocations and disturbances.

The first three objectives have been directly addressed in this report. Insufficient data was gathered to allow objective 4. to be evaluated.

Details of Intellectual Property with Commercial Value

Intellectual property with potential commercial value relates to gas sorption testing services using high pressure microbalances. New techniques developed include methane adsorption isotherm analysis and helium density determination. Estimation of long term methane drainage from microbalance studies has potential commercial value, however, additional research is required to prove this technology.

Intellectual property rights relating to coal microstructure analysis belonged to James Cook University prior to commencement of this study.

RECOMMENDATIONS FOR FURTHER WORK

1. Laboratory studies have been shown to be valuable estimators of longer term in-seam drainage. One hour of laboratory desorption may estimate 6 months of drainage but calibration requires further work. Problems exist in correlating these studies to other factors affecting drainage rates, especially the relation to water make. Further work is required on how water make influences methane drainage rates.

2. Maceral controls on gas release rate and storage are indicated. However, the sample suite investigated has not been sufficiently broad in scope for complete understanding of the significance of maceral composition. Additional sorption and petrographic analyses are required from a variety of coal ranks in both the Sydney and Bowen Basins.

3. Significant differences have been found in methane sorption characteristics between coals of the Sydney and Bowen Basins. To understand these differences, further work is required in the areas of pore characterisation, including evaluation of the relative significance of different pore systems (macro-, meso- and micro-pores).

4. Microstructural analysis by SEM shows considerable promise for evaluation of gas transport pathways. However, the technique requires further refinement with more quantitative information required on fracture spacing, pore sizes and degrees of infill. Image analysis packages could be used to provide this information.

5. The role of carbon dioxide and mixed gases needs to be addressed. Initially, fundamental work is required on CO_2 sorption before the mixed gas question can be evaluated.

ACKNOWLEDGMENTS

Staff at South Bulli and Central Collieries and Shell Australia are thanked for assistance in sample collection and advice on many aspects of the project. Bruce Robertson is thanked for fruitful discussions relating to the LW306 drainage project at Central Colliery. The Geology Department at the University of Auckland, New Zealand, is acknowledged for substantial in-kind support, especially for use of coal petrologic microscope facilities, including reflectance analysis, and coal proximate analysis using thermogravimetric techniques.

1. INTRODUCTION

The two major gases associated with coal seams are methane and carbon dioxide. Methane is generated as a result of the coalification process (Juntgen and Karweil, 1966). Carbon dioxide is often introduced to the seam as a result of the presence of igneous intrusions (Stutzer, 1936; Smith and Gould, 1980), which may or may not be in contact with the seam. Both gases pose a hazard when encountered in sufficient quantities in the seam. Methane may explode in the concentration range of 5-15 percent in air, provided an ignition source is present. Carbon dioxide is not a life supporting gas, and at concentrations above 1-2 percent in air it begins to have major detrimental physiological effects.

Under certain mining and geological conditions, violent ejections of coal (up to thousands of tonnes) and large releases of gas (up to hundreds of thousands of cubic metres) can occur simultaneously. These events are referred to as instantaneous outbursts (Hargraves, 1958). Carbon dioxide outbursts tend to be more violent, although there is always the added risk of a subsequent explosion accompanying a methane outburst. Fatalities continue to occur from outbursts and the phenomenon is not totally understood with respect to the gas/coal system.

1.1 Previous Gas in Coals Research

1.1.1 General

Fundamental investigations concerning the gases found in coal seams can be related back to the earliest coal mining (von Meyer, 1872, 1873; Thomas 1876; Fischer *et al.*, 1932). The primary concern at that time was to assess gas content and composition for ventilation purposes, in order to reduce the hazard of either methane emissions and subsequent explosions (Curl, 1978) or outbursting of coal and gas (Hargraves, 1958; Jackson, 1984). This work is still continuing as higher production operations must combat larger quantities of gas into workings (Hargraves, 1993), and the complexity of

the gas/coal system is recognised (Levine, 1992).

1.1.2 Australian Experience

In Australia there has been considerable research related to gas in coals. Several symposia have presented research findings of the Australian and related experience with respect to this topic:

1. Symposium on the Occurrence, Prediction and Control of Outburst in Coal Mines, Brisbane, 1980.
2. The Co-ordinating Committee on Outburst Related Research Mini-Seminar series -
   - No.1 - Regional outburst-proneness of coal seams, Leichhardt, 1981.
   - No.2 - Prediction techniques currently in use and being researched in Australian coal mines (R.J. Williams editor), Bowen, 1982.
   - No.3 - Alleviation of coal and gas outburst in coal mines (R.D. Lama editor), Sydney, 1983.
   - No.4 - Outburst control in Australian coal mines, (A.J. Hargraves editor), Sydney, 1984.
3. Symposium on Seam Gas Drainage with Particular Reference to the Working Seam (A.J. Hargraves editor), Wollongong, 1982.
4. Symposium on Gas in Australian Coals (J. Bamberry and A. Depers editors), Sydney, 1991.
5. Symposium on Coalbed Methane Research and Development in Australia (B.B. Beamish and P.D. Gamson editors), Townsville, 1992.

A symposium cum workshop on the management and control of outbursts in underground coal mines is proposed for March 1995 to be held in Wollongong, Australia. The holding of this event acknowledges the threat that the outburst problem poses to the future of underground mining in Australia. A history of outbursting in Australian coal mines is presented in Table 1.1. Both the major coal producing basins,

Bowen and Sydney have suffered from this phenomenon at depth. Coal mine explosions also pose a hazard to underground operations in Australia, with the most recent occurring at Moura in 1994.

Most previous research and development on gas from coal seams prior to 1990 has been performed by the Australian Coal Industry Research Laboratories (ACIRL), the Commonwealth Scientific and Industrial Research Organisation (CSIRO), the University of New South Wales (NSW) and the University of Wollongong in association with coal mining companies. Since then there has been a wider research effort boosted by interest in the coalseam methane prospects of the Bowen and Sydney Basins. The major work to date has covered :

1. investigation of gas adsorption/desorption and comparison of methane and carbon dioxide (e.g. Beamish and O'Donnell, 1992; Faiz *et al.*, 1992; Lama, 1986; Bartosiewicz and Hargraves, 1985; Bartosiewicz *et al.*, 1983 in Rixon, 1983).
2. investigations of permeability of Australian coals (e.g. Paterson et al., 1992; Koenig *et al.*, 1992a,b; Davidson, 1992; Battino, 1991; Xue and Thomas, 1991; Bartosiewicz and Hargraves, 1985; Lingard *et al.*, 1984).
3. computer modelling of fluid flow (by University of NSW and ACIRL, e.g. Stevenson *et al.*, 1991; Ivanovic *et al.*, 1985).
4. well completion, stimulation and production testing (e.g. Koenig *et al.*, 1992a,b; Jeffrey *et al.*, 1992; Lewis *et al.*, 1992; Morales and Davidson, 1992; Paterson and Wold, 1992; Jeffrey, 1990).
5. investigations of gas outburst phenomena, in-seam drainage and mine gas flows (e.g. Caffery *et al.*, 1992; Thomson and Hungerford, 1992; Lunarzewski, 1992; Williams *et al.*, 1992; Williams, 1991a,b; Battino, 1986; Beamish *et al.*, 1985; TDM, 1984; Rixon, 1983; Marshall, 1981).

Gas assessment work in Australia has been performed by measuring gas contents of coal in the Sydney and Bowen Basins as input to underground mine planning of

ventilation. Regional outburst-prone areas have also been identified by applying desorbable gas content limits of 9 m^3/t for methane and 5 m^3/t for carbon dioxide, although these have been reviewed following the past two outburst occurrences (Table 1.1). Truong and Williams (1989) looked at gas content and composition of Australian coals, and highlighted the variations that occur. They concluded the processes controlling the eventual in-situ gas content of coal are highly complex and cannot be explained by simple geologic factors.

Table 1.1 Summary of Australian outburst occurrences (modified from Hargraves, 1983)

Date	Colliery	Seam	Depth (m)	Number	Maximum size (t)	Gas
Sydney Basin						
1895 +	Metropolitan	Bulli	400-450	15	200	Firedamp
1925	Metropolitan	Bulli	400	1	140	Blackdamp
1949	Metropolitan	Bulli	425	1	5	Blackdamp
1954	Metropolitan	Bulli	425	1	90	CO_2
1961 +	Metropolitan	Bulli	425	Many	300	CO_2 or mixed
1911	North Bulli	Bulli	370	1	1	Firedamp
1961	Coal Cliff	Bulli	450	2	2	Mixed
1967	Corrimal	Bulli	400	3	50	Mixed
1969	Appin	Bulli	520	3	60	CH_4
1972	Bulli	Bulli	380	1	100	Mixed
1977 +	West Cliff	Bulli	480	200 +	400	CH_4 and CO_2
1980	Kemira	Bulli	220	2	100	Mixed
1981 +	Tahmoor	Bulli	410	30 +	50	Mixed
1981	Tower	Bulli	480	4	40	CH_4
to 1991	South Bulli	Bulli	370	14	<30	CH_4
1991	South Bulli	Bulli	370	1	120	CO_2
Bowen Basin						
1954	Collinsville State	Bowen	220	1	500	CO_2
1960	Collinsville State	Bowen	215-225	9	360	CO_2
1961	Collinsville State	Bowen	230-235	3	60	CO_2
1972	No.3 Mine	Bowen	230	2	1	CO_2
1978	No.2 Mine	Bowen	260-265	4	25	CO_2
1980 +	No.2 Mine	Bowen	250	3	35	CO_2
1975 +	Leichhardt	Gemini	370	Many	500	CH_4
1980 +	Moura	C Upper	130	2 +	20	CH_4

A gas content measurement standard has been drawn up by the Australian Standards Association after consultation with coal industry, university and research institution representatives (Australian Standard AS 3980-1991 Guide to the determination of desorbable gas content of coal seams - Direct Method). It defines the desorbable gas content (Q_D) as the sum of lost gas content (Q_1) and measurable gas content (Q_2). The total desorbable gas content (Q_{TD}) is the sum of lost gas content, measurable gas content and residual gas content (Q_3).

$$Q_{TD} = Q_1 + Q_2 + Q_3$$

1.2 Effect of Coal Type and Physical Properties on Sorption Behaviour

The effects of coal type are poorly understood in terms of gas emission and outbursting (Jackson, 1984) and have generally been overshadowed by the inferred relationships with coal rank. Hargraves (1980) noted the physical nature of coals is more poorly understood than its chemical nature. Some early workers referred to coal type as a basis of outburst-proneness (Hargraves, 1958), but there appears to be little substantiation of this in Australian experience, with only one published example known to the authors (Hunt and Botz, 1986). An association of inertinite-rich coal characteristics with outbursting in Australian coal mines was advocated by Botz and Hart (1983) but the evidence appears to be more symptomatic of fault prediction than the outburst tendency of the coal itself.

Hargraves (1962) commented that some variation has been noticed in emission of the various coal types within one seam at one location, but to date this has not been studied in great detail. Tests on -14+25 mesh samples, with CO_2 as the seamgas indicated a higher desorption rate for duro-clarain samples as opposed to vitrain samples. This variation is also displayed by direct gas content measurements on seam sub-samples.

Detailed studies on the effects of coal type in relation to gas outburst phenomena were performed by Platt (1959), Platt *et al.* (1965), Pooley *et al.* (1966) and Pooley (1968) on British coals. These authors examined bright fractions of coal of different rank and found a change in surface structure with rank. The roughness variation between high and low rank bright coal varied by a factor of ten to one, the low rank coal being far rougher than the high rank coal. Bright coals have smooth, homogeneous fracture surfaces, whereas dull coals have extremely rough and irregular surfaces.

The pore nature of coal is well documented for US coals (Gan *et al.*, 1972; Walker *et al.*, 1988), but little published data exists on Australian coals. To fully understand sorption mechanisms requires a better understanding of pore sizes and distributions in the coals of interest. With this knowledge it is possible to predict the sorption behaviour of the coal, and apply it to field observations.

Lama and Mitchell (1981) found that for the Gemini seam, Leichhardt Colliery, Blackwater, the porosity of bright coals was less than that of dull coals, while bright coal internal surface area was greater. The bright coals therefore had a greater capacity to store gas, but lower permeability. They concluded the higher internal surface area, lower porosity, and finer pore size distribution of bright coals helps explain the higher frequency of outbursts in areas where coal seams contain a higher percentage of bright bands. Similar tests on the Castor seam at Cook Colliery (Lama, 1980) yielded higher porosity values than the Gemini seam at Leichhardt. No outbursts have been recorded at Cook Colliery.

Most previous laboratory gas sorption work has focused on bulk sample testing, which confuses the issue of coal rank and coal type effects. Recent investigations of smaller sample sizes (Beamish and O'Donnell, 1992; Levine et al., 1993; Crosdale and Beamish, 1993) using high pressure microbalances are providing clearer distinctions between the two coal parameters. Bartosiewicz *et al.* (1983, in Rixon (1983)) assessed sorption of gas on bright, dull and mixed coal types from Cordeaux and Appin Collieries, NSW. They concluded that bright coal generally adsorbed more gas in these samples in the lower pressure range of 0 - 1 MPag.

1.3 Gas Sorption Studies

Gas sorption in this report is used as a general term to refer to the reversible processes of gas adsorption (gas attaching onto the internal surfaces of coal pores) and gas desorption (gas releasing off the internal surfaces of coal pores). The more common definition of sorption is the combined processes of gas adsorption and gas absorption.

The parameters influencing gas sorption by coals play an important role in the extraction of coal with associated gas emissions and outbursting phenomena, and recovery of the gas by drainage methods. Without a better understanding of these parameters it is difficult ,if not impossible, to appreciate the complexities that arise during both these operations. Data have been compiled from laboratory measurements of gas sorption using coals from Central Colliery, Bowen Basin, Queensland, and South Bulli Colliery, Sydney Basin, New South Wales (Figure 1.1) to assess the fundamental parameters of gas sorption behaviour.

Laboratory methane sorption studies of coal are an integral part of assessing the coal/gas system. Two main parameters established during these tests are the sorption capacity and the diffusivity behaviour of the coal. The primary aim of the work was to establish the fundamental links between coal characteristics and these parameters, as well as to provide a better understanding of the sorption kinetics and their influence on gas emission behaviour. One of the main difficulties encountered in performing this task has been attributed to the use of bulk samples (Beamish and O'Donnell, 1992), where identifying relationships is strongly reliant on representative sampling and a great deal of statistical inference. To remove this problem a new technique for sorption testing has been developed at the Coalseam Gas Research Institute, James Cook University using high pressure microbalances.

In summary this report attempts to show the basis for the link between coal sorption behaviour, its pore nature and the likely resulting experiences of gas emission and outbursting.

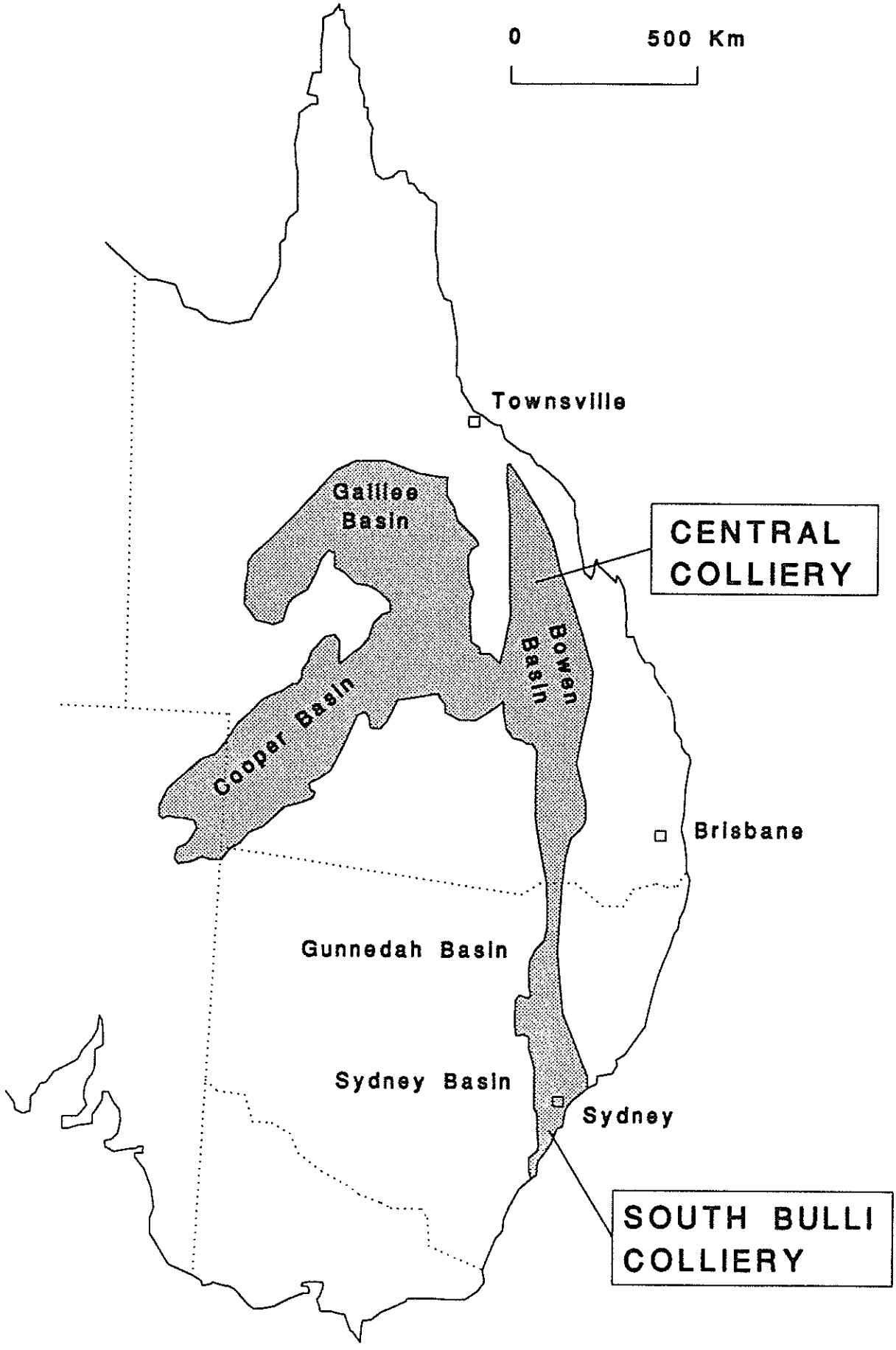

Figure 1.1 Location of collieries investigated in New South Wales and Queensland

2. METHODS

2.0 Project Description and Work Programme Outline

Three main objectives were identified :

- to investigate the different gas flow characteristics of coal types from South Bulli and German Creek
- to determine the influence of coal microstructure on gas emissions and outburst-proneness
- to identify target drilling horizons in seam to assist optimum gas drainage

To achieve these objectives, the following work programme was proposed :

- description of seam profiles in exposed workings with collection of strip samples for testing
- analyse samples, including cuttings from in-seam boreholes by :
  - dividing into bright and dull coal fractions to isolate coal type influences
  - gas sorption testing using high pressure microbalances, including sorption isotherms and desorption rate
  - SEM analysis for microstructural information
  - proximate analysis of samples
  - petrographic analysis to characterise coal type
  - coal density, porosity and surface area measurements
  - gas content estimation from proximate analysis data for comparison with field and laboratory measurement
- comparison with mine emission data

2.1 Samples

Samples were selected from South Bulli Colliery (NSW) and Central Colliery (German Creek, Queensland). Three types of sample collection procedures were undertaken :

- lithotype logging followed by collection of selected sample intervals
- core from in-seam drilling
- cuttings from in-seam drilling

A full list of samples investigated is given in Table 2.1. Sample locations within the mines and details of lithotype profiles for Central Colliery are shown in Figures 2.1 and 2.2 and for South Bulli Colliery in Figures 2.3 and 2.4

Lithotype logging was performed in accordance with Australian Standards (Anon., 1986b). Samples and logs from Central Colliery (Figure 2.2) were provided by mine staff. Seam profiles were divided into plies (A, B, C etc.) and strip samples from each ply collected. Bright and dull coals were hand picked from selected plies. Profiles at South Bulli Colliery (Figure 2.4) were divided into macroscopically similar units on site and selected units sampled for analysis.

In-seam drilling samples were supplied from both mines. Chip samples were provided from Central Colliery and core samples from South Bulli. Bright and dull coal types were hand picked from the chip samples following sieving to remove coal too fine to pick. Core samples were not picked separately for coal types.

Sample Preparation

Sample preparation was governed by sorption analysis requirements. Two main factors considered were particle size and moisture state.

Particle size has significant effect on sorption rate. Increasing particle size reduces sorption rates until a critical size is reached, at which fracture networks within grains are the governing factor (Bielicki, 1972; Nandi and Walker, 1975; Barker-Read and Radchenko, 1989). It is therefore essential that a consistent particle size is used for intersample comparisons. Selection of the upper limit for particle size was affected by two competing influences. Firstly, the desire that grains be as large as practical so as to give the best indication of *in situ* desorption parameters. Secondly, that a reasonable time frame be maintained. The main constraint on maximum grain size was the in-seam

Table 2.1 Sample numbers (JCB numbers) and locations of coals tested. Pairs of bright and dull coal types have been analysed from each site.

Sample Number	Litho type	Colliery	Sample Type	Location
JCB4	B D	Central	in-seam drill cuttings	306, hole 14, 71m
JCB7	B D	Central	in-seam drill cuttings	306, hole 14, 143m
JCB9	B D	Central	in-seam drill cuttings	306, hole 14, 195m
JCB12	B D	Central	in-seam drill cuttings	306, hole 14, 279m
JCB15	B D	Central	strip sample	GBS 122a, 305MG, 9c/t ply B
JCB19	B D	Central	strip sample	GBS 122a,305MG, 9c/t ply D
JCB21	B D	Central	strip sample	GBS 122a, 305MG, 9c/t ply E
JCB25 JCB27	D B	South Bulli	strip sample	T11, 12c/t, 70m I/B LH rib
JCB29 JCB32	B D	South Bulli	strip sample	T11, 6c/t, 52m I/B LH rib
JCB35 JCB37	B D	South Bulli	strip sample	T Main, Z Hdg, 40m I/B 32c/t, RH rib
JCB40 JCB42	B D	South Bulli	strip sample	W main, B Hdg, 35m I/B 36 c/t RH rib
JCB65 JCB66	D B	South Bulli	strip sample	Cataract North, Z Hdg, 55m O/B 7c/t
JCB74	BD	South Bulli	in-seam drill core	
JCB76	BD	South Bulli	in-seam drill core	Cataract North, A7 Hdg, Borehole CN17
JCB82	B D	Central	strip sample	GBS 123a, 305MG 15 c/t, ply C
JCB92	B D	Central	strip sample	GBS 124a, 305 MG, 19c/t, ply D
JCB95	Sheared	Central	strip sample	305MG, 9c/t, mid seam shear

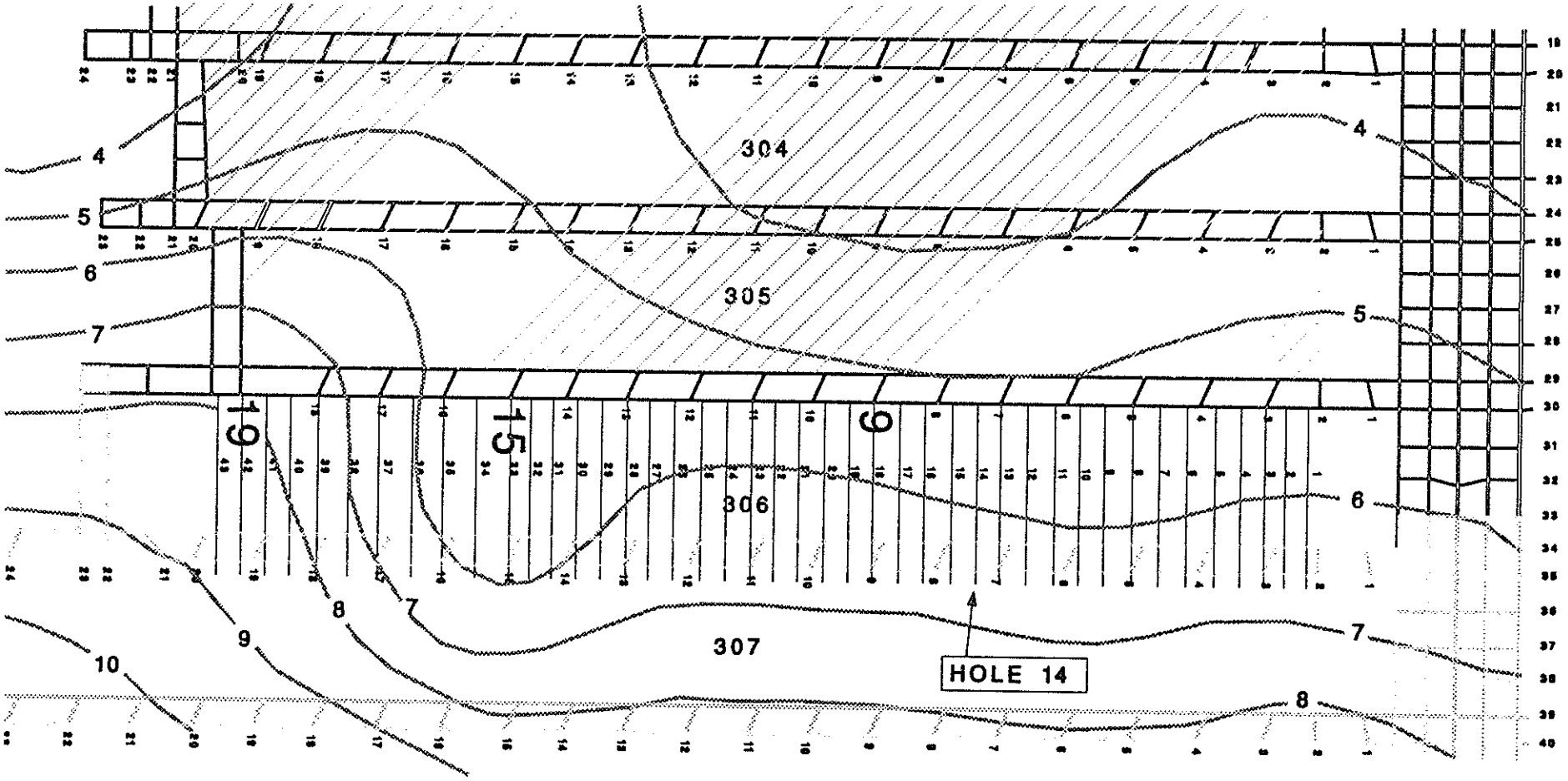

Figure 2.1 Plan of Central Colliery, German Creek. Samples from 306 panel gas drainage hole 14 and cut-throughs 9,15 and 19. Contours indicate gas content in m^3/t.

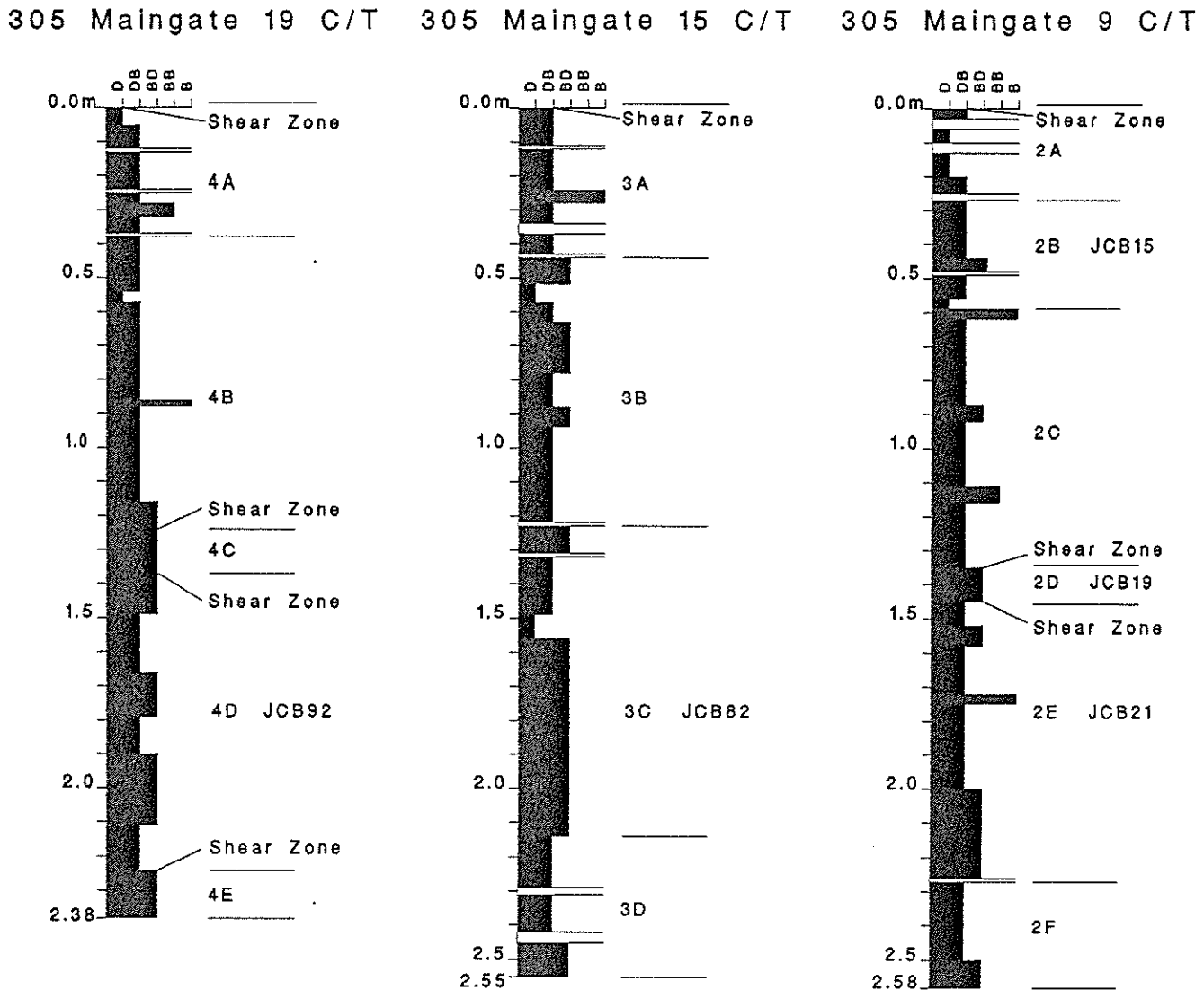

Figure 2.2 Lithotype profiles and sample details for Central Colliery

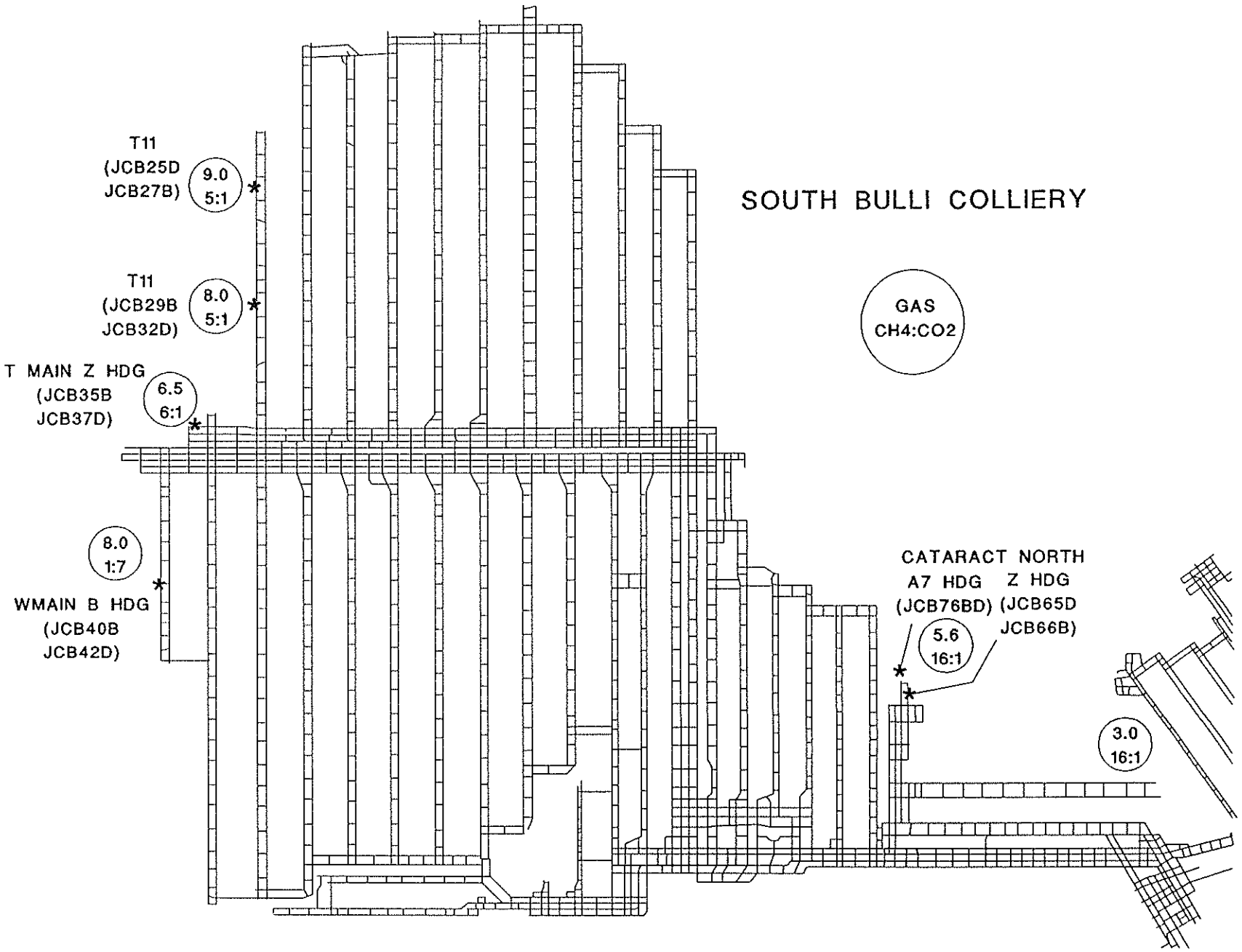

Figure 2.3 Plan of South Bulli Colliery showing details of sample locations, gas contents (m3/t) and CH4:CO2 ratio.

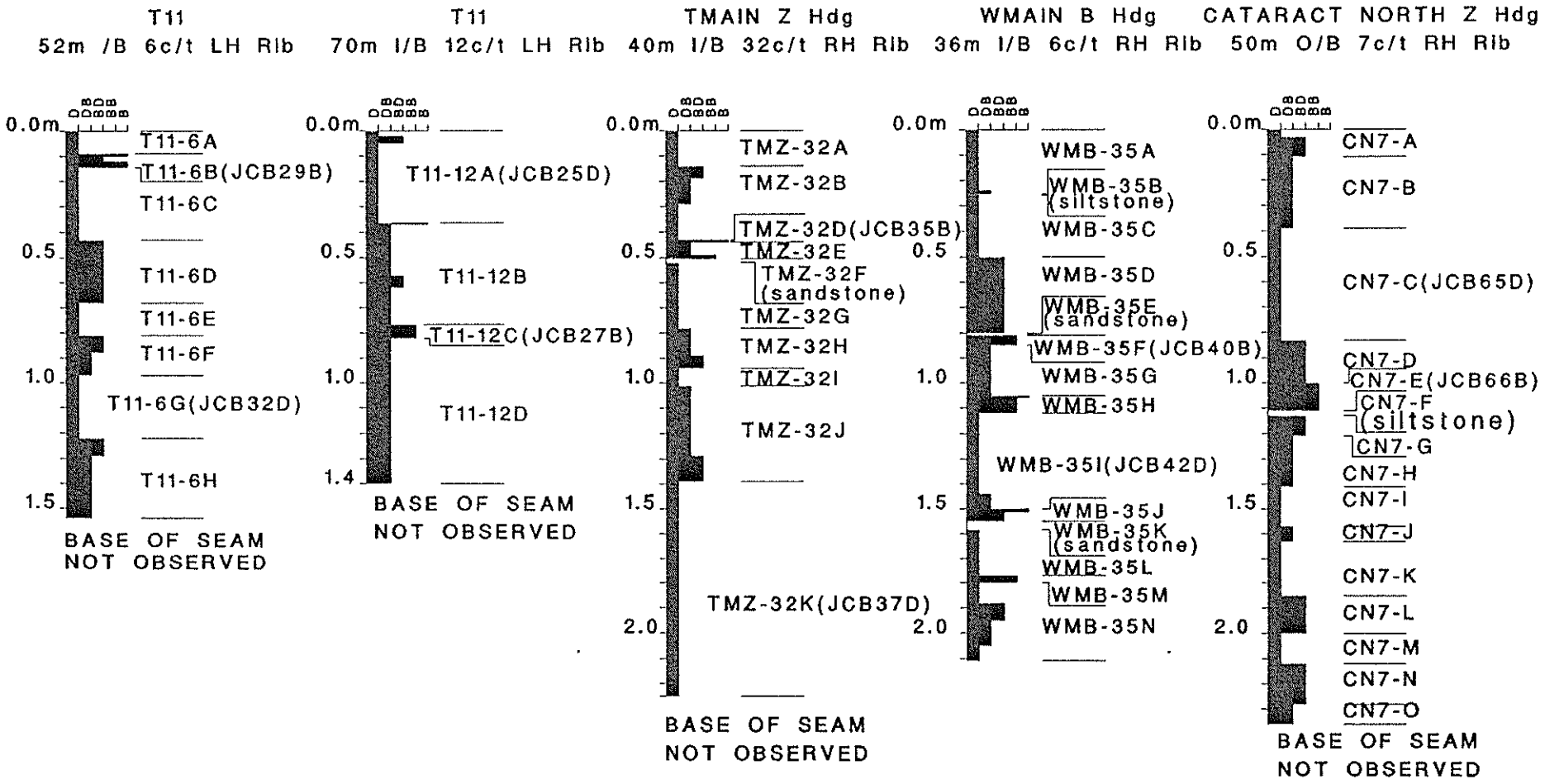

Figure 2.4 Lithotype profiles and sample details for South Bulli Colliery

drilling chip samples. Few grains were greater than 5.60mm in diameter and this set the upper limit. A lower limit of 2.00mm was selected so that there was neither a large size variation nor a significant amount of rapidly desorbing fine coal. An additional constraint was the sample containers within the microbalance sorption apparatus which limit maximum diameters to 15mm. Grains for sorption rate analysis were therefore selected in the range -5.60mm +2.00mm.

A disadvantage of grains of this size is that the sorption analysis takes about two weeks to complete and it is uncertain that the coals were fully sorbed with gas at the commencement of the analysis. Gas is sorbed back onto the coal prior to desorption analysis. More rapidly sorbing coals may therefore have higher initial gas contents and an incorrect impression will be gained of the relative sorption capacity of the different coals. Sorption isotherm analysis was also conducted on -0.212mm samples to measure true sorbable gas contents.

Moisture state of the coal is crucial in terms of both sorption rate and sorption capacity (Joubert *et al.*, 1973, 1974). Moist coals have both lower sorption rates and lower sorption capacities than dry coals. As a primary objective of the study was estimation of *in situ* parameters, coal in a moist state was desirable. All samples were therefore brought to an equilibrium moist state as described by Australian Standards (Anon., 1989a). However, data interpretation is complicated by moisture loss during sorption analysis. To ensure validity of intersample comparisons, samples were also analysed on a dry basis.

2.2 Gas Sorption Isotherms

Two main methods are available for adsorption/desorption testing of coal samples :

1. volumetric, where a fixed volume of gas is introduced to the sample chamber and gas sorption monitored by changes in pressure (e.g. Ruppel *et al.*, 1972).
2. gravimetric, where gas pressure is fixed and gas sorption evaluated by weight changes (e.g. Daines, 1968; Lama and Bartosiewicz, 1982).

In determining the most appropriate method, factors to be considered are the purpose of testing, sample size fraction and quantity to be used. Most gas sorption capacity testing uses bulk quantities (80 - 150 g) of fine coal (<250 μm), which normally provides broad relationships between parameters.

The gravimetric technique was selected as previous experience at CGRI (Beamish and Gamson, 1993) showed this is the most appropriate method for evaluation of gas sorption in relation to coal type, a major objective of the work programme. Testing at CGRI was being performed using an existing Sartorius M25D-P high pressure microbalance (referred to as microbalance 1) and a second microbalance of the same type (referred to as microbalance 2) was purchased to facilitate throughput of samples. The microbalances are fully self-contained units capable of highly accurate measurement of weight change in samples associated with adsorption/desorption under a wide range of pressure and temperature conditions and are amenable to automated measurement. Microbalance 2 was ordered in December, 1992 immediately upon commencement of the project and arrived in March, 1993. Installation was delayed until June, 1993 immediately following which a fault developed that was repaired in July, 1993. Effective use of the second instrument was therefore delayed by six months.

The sorption equipment is schematically presented in Figure 2.5. On-site construction required manufacture of a housing frame for the microbalance to isolate the unit from vibration, installation of high pressure gas lines, valves, pressure gauges and transducers. Additional electronic components were required to connect the balance to a computer for automatic data logging. Steps involved in commissioning the microbalances have been described elsewhere (Crosdale, 1993).

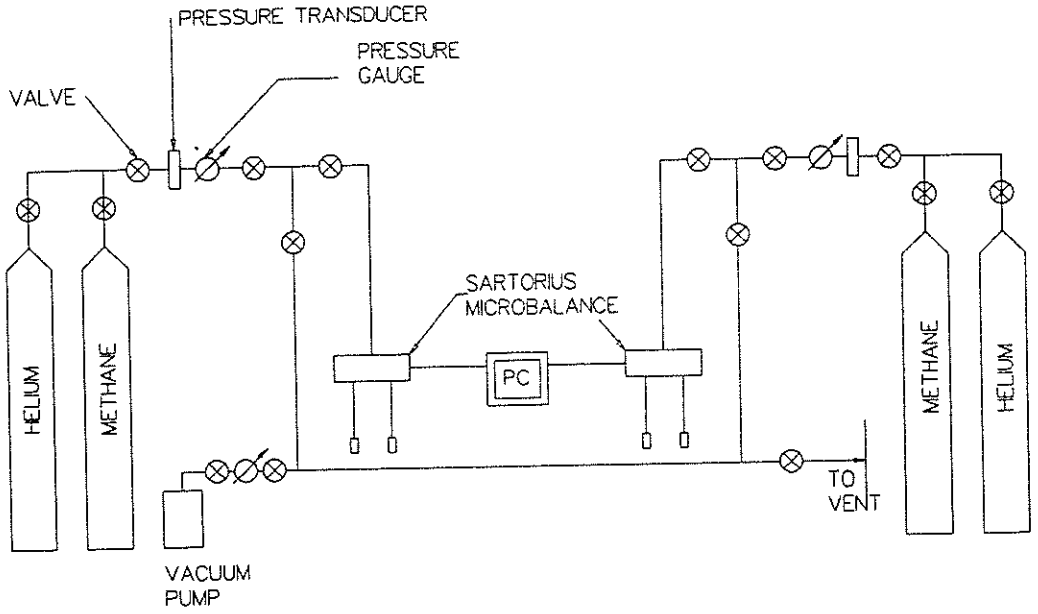

Figure 2.5 Schematic of microbalance setup

2.2.1 Micrograviметric Determination of Methane Sorption Isotherms

With the gravimetric method using a beam balance, weight changes represent the combined influence of change in sample mass during sorption and gas buoyancy at the specified pressure. Calculation of sorbed gas weight requires subtraction of the buoyant force. The value of the buoyancy correction depends upon volume and temperature differences between the sample and other balance components (counter weight, sample pans, weighing arms, connection wires etc) (Gregg and Sing, 1967) and should include a correction for the compressibility of the adsorbate. A correction for the volume change of the sample due to sorbed gas may also be applied (Levine *et al.*, 1993).

The balance is initially tared under vacuum so all weight changes represent the combined effect of buoyancy and gas sorption.

Parameters required for gas content calculation are :

- initial sample weight (determined in the microbalance)
- sample weight during adsorption/desorption
- correction for buoyancy involving :
    - volume of the sample (derived from its helium density)
    - volume of the microbalance (derived experimentally)
    - density of the gas in the microbalance at a given pressure (derived theoretically)

Buoyancy Correction

The buoyant force applied equals the weight of fluid displaced, which equals the volume of fluid multiplied by its density.

Gas density is estimated by :

$$\rho_g = \frac{Mp}{zRT}$$

where ρ_g = gas density (g/cc)
z = compressibility factor of the adsorbate
M = molecular weight of the adsorbate
(CH_4 = 16.043; CO_2 = 44.010; He = 4.0026)
T = temperature of the sample (= 296.6K)
p = pressure (atm)
R = universal gas constant (= 82.0562 cm^3 atm K^{-1} mol^{-1})

The volume of the gas is estimated by the volume of the microbalance (including pans, counterweights etc) and the volume of the sample (including the volume of sorbed gas).

Total volume = $V_{mb} + V_{cwt} - V_c = V_{mb} + V_{cwt} - (V_{dc} + V_w + V_s)$

where V_c = Volume of coal sample (cc)
V_{cwt} = Volume of counter weight (cc)
V_{dc} = Volume of dry coal (cc)
V_{mb} = Volume of microbalance (cc)
V_w = Volume of water (cc)
V_s = Volume of sorbate (cc)

The final weight of the sample is then equal to the weight determined in the microbalance less the buoyancy

$$W_f = W_m - B_t$$

The final weight of the sample is the sum of its initial dry weight, weight of water and weight of sorbate

$$W_{dc} + W_w + W_s = W_m - \rho_g(V_{mb} + V_{cwt} - V_{dc} - V_w - V_s)$$

$$W_s = W_m - W_{dc} - W_w - \rho_g(V_{mb} + V_{cwt} - W_{dc}/\rho_{dc} - W_w/\rho_w - W_s/\rho_s)$$

$$W_s(1-\rho_g/\rho_s) = W_m - W_{dc} - W_w - \rho_g(V_{mb} + V_{cwt} - W_{dc}/\rho_{dc} - W_w/\rho_w)$$

if the microbalance has been tared, then $W_m = W_{dc} + W_w + W_{mb}$

$$W_s = W_{dc} + W_w + W_{mb} - W_{dc} - W_w - \rho_g(V_{mb} + V_{cwt} - V_{dc} - V_w - V_s)$$

$$W_s = W_{mb} - \rho_g(V_{mb} + V_{cwt} - V_{dc} - V_w - V_s)$$

$$W_s = W_{mb} - \rho_g(V_{mb} + V_{cwt} - W_{dc}/\rho_{dc} - W_w/\rho_w - W_s/\rho_s)$$

$$W_s(1 - \rho_g/\rho_s) = W_{mb} - \rho_g(V_{mb} + V_{cwt} - W_{dc}/\rho_{dc} - W_w/\rho_w)$$

where B_t = total buoyancy
W_{dc} = dry coal weight (g)
W_f = final weight (g)
W_m = measured weight without taring the microbalance (g)
W_{mb} = weight displayed by microbalance after taring (g)
W_s = sorbate weight (g)
W_w = water (moisture) weight (g)
ρ_{dc} = dry coal density (g/cc)
ρ_g = gas density (g/cc)
ρ_w = water density (g/cc)
ρ_s = sorbate density (g/cc)

Volumes of the coal and counter weight are determined from their dry weight and dry helium density. Volume of the water is determined from the percent moisture of the sample. Volume of the microbalance is experimentally determined (Crosdale, 1993). Volume of the sorbate is estimated for methane using a density for adsorbed methane on coal of 618.9g/l (van der Sommen *et al.*, 1955).

A complication arises with moist coal of moisture loss during the analysis. Attempts to maintain a constant humidity atmosphere (e.g. Levine *et al.*, 1993) proved unsuccessful due to an inability to maintain equal humidity levels on each side of the balance. Humidification of the gas prior to entry into the balance is necessary, however, the manufacturer (Sartorius) advises that high humidity conditions may cause damage to the balance. Moisture loss is handled by assuming a constant rate of loss during the experiment. Validity of this assumption cannot be proven but no method is presently available for determining moisture loss rates during adsorption and desorption phases. The following equation applies :

$$W_s(1 - \rho_g/\rho_s) = W_{mb} + W_{wloss} - \rho_g(V_{mb} + V_{cwt} - W_{dc}/\rho_{dc} - W_w/\rho_w + W_{wloss}/\rho_w)$$

where W_{wloss} = weight of water lost

Weight of water lost is determined by calculating the rate of water loss, assuming it to be constant and linear, and multiplying by the time at each measurement.

Calculation of the Gas Compressibility Factor (z)

The gas compressibility factor (z) has been calculated using the Hall-Yarborough equations (Dake, 1978; Figure 2.6) :

$$z = \frac{0.06125\, p_{pr}\, t\, e^{-1.2(1-t)}}{y}$$

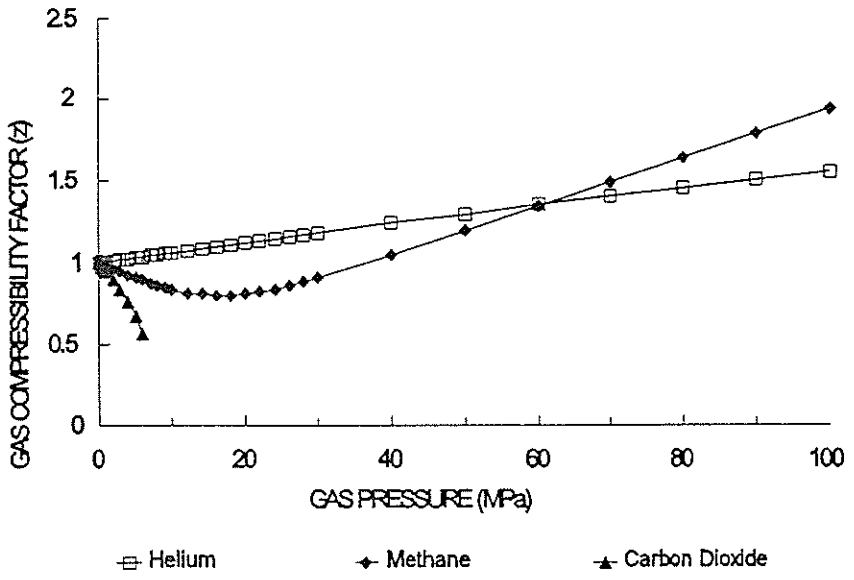

Figure 2.6 Gas compressibility factor (z) at 296.5°K determined from the Hall-Yarborough equations

where p_{pr} = pseudo reduced pressure
= pressure/critical pressure
t = reciprocal of the pseudo reduced temperature
= critical temperature/temperature
y = reduced density

The value for y is obtained by solving :

$$(-0.06125\,p_{pr}\,t\,e^{-1.2(1-t)^2}) + \frac{y+y^2+y^3-y^4}{(1-y)^3} - (14.76t-9.76t^2+4.58t^3)y^2$$

$$+ (90.7t-242.2t^2+42.4t^3)y^{(2.18+2.82t)} = 0$$

An iterative technique is used to numerically solve for y. An initial estimation of y (y_k) can be better approximated (y_{k+1}) by a first order Taylor series expansion :

$$y_{k+1} = y_k - f_k / \frac{df_k}{dy}$$

where

$$\frac{df}{dy} = \frac{1+4y+4y^2-4y^3+y^4}{(1-y)^4} - (29.52t-19.52t^2+9.16t^3)y$$

$$+ (2.18+2.82t)(90.7t-242.2t^2+42.4t^3)y^{(1.18+2.82t)}$$

Compressibility Factor (z) for Methane

Calculated values for z at 290K and 300K compare favourably with published values (Anon, 1976). A least squares linear regression was used to estimate the z value at 296.5K for the region 0.1 to 7.0 MPa :

$$z = -0.01799\ MPa + 0.9986 \qquad r^2 = 0.9991$$

For the range 0 to 10MPa compressibility may be estimated by :

$$z = e^{(-0.01838\ MPa\ -\ 0.001888)} \qquad r^2 = 0.9985$$

Pressures greater than 10MPa are not used at CGRI so the above equations are adequate. However, neither equation estimates compressibility at greater pressures.

Compressibility Factor (z) for Carbon Dioxide

Attempts were made at evaluation of carbon dioxide sorption parameters (Appendix 7) which required the compressibility of CO_2 to be known. A fit to the 296.5K values for the region 0.1 to 5.0 MPa gives :

$$z = \sqrt[3]{-0.13659MPa + 0.992193} \qquad r^2 = 0.9997$$

Note that CO_2 liquefies at P > 5MPa at 293.15K (20°C) and P > 7MPa at 303.15K (30°C).

Compressibility Factor (z) for Helium

Helium is used in determination of the density of the sample and its compressibility can be estimated by a least squares linear regression :

$$z = 0.006234 \text{ MPa} - 0.99983 \qquad r^2 = 0.99999$$

Microbalance volume determination

Volumes of the microbalances must be determined for each set of initial conditions. The microbalances were initially supplied with quartz weighing pans, which were found to be unsatisfactory due to static charge build-up. Stainless steel weighing pans were manufactured in-house to overcome this problem. Both PVC and stainless steel have been used as counter weights.

Volume of the microbalance including the weighing pans is derived from a plot of gas density versus weight at different gas pressures. The empty weighing pans are pressurised and the volume is specific to the set of pans. Negative volume refers to the weighing pan side having a larger volume than the tare pan side.

The volume of microbalance 1 was initially determined in methane using the more sensitive balance range II and the supplied quartz weighing pans (Table 2.2). After manufacture of the stainless steel weighing pans, the volume was redetermined using helium (Table 2.2). A PVC counterweight was added to the system to increase the small volume and obtain more accurate results.

The volume of microbalance 2 was determined using only the in-house manufactured stainless steel weighing pans (Table 2.2). Initially a PVC counterweight was used in the balance but, following testing using CO_2, PVC was found to be unsatisfactory and it was replaced with stainless steel. The volume of the balance was re-evaluated with the new counterweight (Table 2.2)

Table 2.2 Volume determination of microbalances 1 and 2 under a variety of initial configurations

MICROBALANCE 1						MICROBALANCE 2					
Quartz weighing Pans			Stainless Steel Weighing Pans			Stainless Steel Weighing Pans			Stainless steel weighing pans with stainless steel counterweight		
Weight (mg)	CH_4 Pressure (Mpa)	CH_4 Density (mg/ml)	Weight (mg)	Helium Pressure (MPa)	Helium Density (mg/ml)	Weight (mg)	Helium Pressure (MPa)	Helium Density (mg/ml)	Weight (mg)	CO_2 Pressure (MPa)	CO_2 Density (mg/ml)
-1.752	8.57	65.42	-5.29	9.43	14.47	398.92	8.00	12.38	0.919	5.05	134.35
-1.682	8.24	62.52	-5.07	9.02	13.87	398.99	7.00	10.90	0.670	4.21	100.61
-1.441	7.14	53.09	-4.54	8.03	12.42	399.07	6.07	9.50	0.380	2.96	63.17
-1.222	6.11	44.58	-3.96	6.97	10.85	399.14	5.10	8.03	0.222	1.94	38.46
-1.023	5.16	37.00	-3.41	5.94	9.30	399.23	4.03	6.39	0.081	1.01	19.01
-0.824	4.15	29.20	-2.87	4.97	7.83	399.31	3.06	4.88			
-0.619	3.11	21.47	-2.32	3.99	6.32	399.40	2.10	3.37			
-0.428	2.12	14.37	-1.77	3.01	4.80	399.44	1.50	2.41			
-0.328	1.57	10.54	-1.21	1.99	3.19	399.48	0.99	1.60			
-0.235	1.09	7.25	-0.64	1.00	1.61	399.52	0.46	0.75			
-0.134	0.55	3.62	-0.35	0.47	0.76						
LINEAR REGRESSION [weight = a.(gas density) + b]											
X Coefficient (a)		-0.02633			-0.36097			-0.05276			0.00699
Constant (b)		-0.04561			-0.05341			399.565			-0.03532
R Squared		0.99971			0.99995			0.99945			0.99593
weight PVC (g)					0.49418						
volume PVC (cc)					0.35526						
vol bal +pvc (cc)					-0.36097						
Balance volume (cc)		**-0.02633**			**-0.00571**			**-0.0528**			**0.0070**

Conversion of Digital Output from Pressure Transducers and Microbalances

Output signals from the two microbalances and pressure transducers are automatically recorded using the National Instruments Measure for Lotus 1-2-3 data acquisition package. Output voltages must be converted into their corresponding real values.

Pressures are monitored using WikaTronic pressure transducers (Typ 891.13.520) with ranges of 0-160 bar (microbalance 1) and 0-250 bar (microbalance 2). Theoretical conversion of the signal from the transducer to a pressure is described in the manual "Measure for Lotus 1-2-3, Data Acquisition Module Reference", p5-3. Formulae were confirmed by monitoring transducer outputs against gauge pressures :

pressure = ([output] - 2047)*10/4096*160/5/10(microbalance 1)

pressure = ([output] - 2042)*10/4096*250/5/10 - 0.1013(microbalance 2)

A linear correlation was used to convert electrical output signal from the microbalance to a weight recorded by the data logger :

weight = 0.009703 [output] - 29.8795 (microbalance 1)

weight = 0.009721 [output] - 29.9088 (microbalance 2)

2.2.2 Procedure for Adsorption Isotherm Determination

Approximately one gram of coal is crushed to -0.212mm and placed under equilibrium moist conditions for at least 24hours. Equilibrium moist conditions incorporate application of a partial vacuum, which is considered adequate for degassing the sample. The moist coal is placed in the balance, weighed and evacuated with a high pressure vacuum pump for one minute. A short period of evacuation is used to maintain moisture levels in the sample. After evacuation, methane is introduced at a number of pressure steps (0.5, 1, 2, 3, 5, 7 and 9 MPa) and held at each pressure for at least 2 hours. Sorption rate information is gathered during degassing for comparison with the larger grains of the same sample. Degassing takes place by reduction of pressure to

5MPa, maintaining this for 2 hours, reducing to 3MPa (South Bulli samples) or 2 MPa (Central samples) and maintaining this for 2 hours before degassing to atmosphere. This procedure simulates that for sorption rate determination of the larger grains.

Moist samples are then dried at 105°C for 12 hours. The sample is reweighed and evacuated for one hour prior to helium density determination, following which the sample is again evacuated for one hour before methane is again introduced. The same sequence of methane pressures is followed as for the moist sample but after degassing to atmosphere, vacuum is applied for one hour.

An example is given of a methane adsorption isotherm using microbalance 1 with quartz pans and a PVC counterweight (Table 2.3; Figure 2.7). Adsorption isotherm data from JCB7, bright, crushed coal has been used. Corrected microbalance readings relate to corrections applied for buoyancy, including gas density and sample and sorbate volumes.

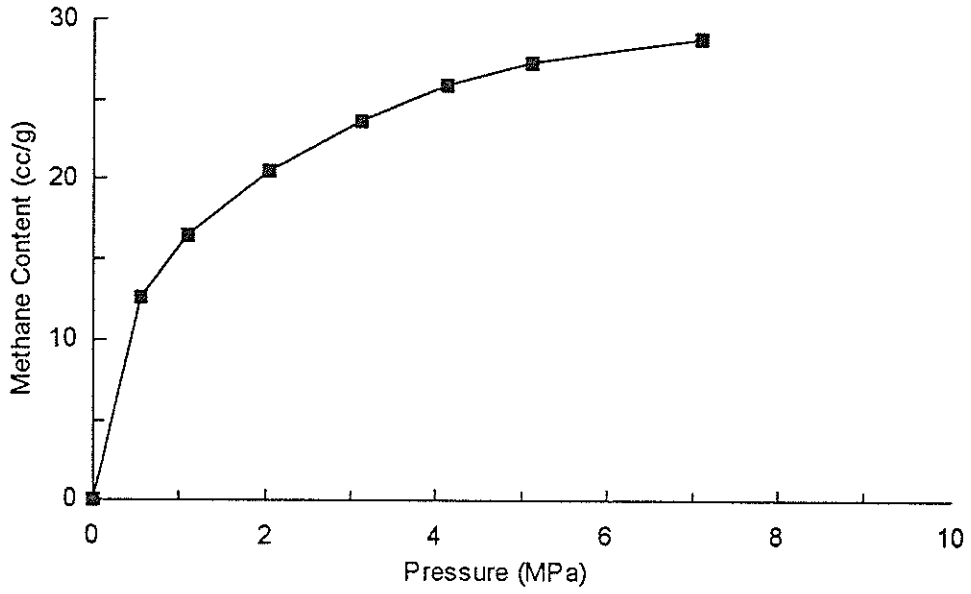

Figure 2.7 Methane adsorption isotherm indicating the adsorbable gas content of a coal at each pressure step at a fixed temperature.

Table 2.3 Example of parameters used and calculated gas contents for a methane adsorption isotherm

weight	coal moist (g)	1.0012
	coal dry (g)	0.9892
	PVC counterweight (g)	0.9925
	CH_4 (molecular weight)	16.043
moisture	coal (%)	1.20
density	dry coal in helium (g/cc)	1.325
	sorbate (g/cc)	0.6189
	PVC counterweight (g/cc)	1.3895
	gas (g/cc)	Mp/zRT
volume	microbalance (cc)	-0.02633
	PVC counterweight (cc)	0.71429
	dry coal (cc)	0.66613
	moisture (cc)	0.012
z factor	methane (0-10MPa)	e^(-0.01838 MPa - 0.001888)
specific volume CH_4	at 21degC, 101.3 kPa	1.479 cu m/kg
	at 15.54degC, 101.3 kPa	1.452 cc/mg

Calculated gas contents

Pressure (MPa)	Microbalance Reading (mg)	Corrected Reading (mg)	Methane Content (mg/g)	Methane Content (cc/g)
0.55	8.53	8.54	8.53	12.6
1.08	11.13	11.18	11.18	16.5
2.03	13.73	13.90	13.89	20.5
3.11	15.69	16.04	16.02	23.7
4.10	17.02	17.55	17.53	25.9
5.10	17.75	18.48	18.46	27.3
7.08	18.38	19.52	19.50	28.8

2.2.3 Procedure for Sorption Rate Determination

Approximately one gram of coal of size fraction -5.60 +2.00mm is placed under equilibrium moist conditions for at least 7 days. Equilibrium moist conditions incorporate application of a partial vacuum, which is considered adequate for degassing the sample. The moist coal is placed in the balance, weighed and evacuated with a high pressure vacuum pump for one minute. A short period of evacuation is used to maintain moisture levels in the sample. After evacuation, methane is introduced at 5MPa and

held until no appreciable change in weight is observed (less than 0.02mg/hr) or at least 3 days have passed. Pressure is then reduced to the estimated *in situ* gas pressure (2MPa for Central Colliery; 3MPa for South Bulli Colliery) and held until no appreciable change in weight is observed (less than 0.02mg/hr) or at least one day. Samples are then degassed to atmosphere until no appreciable change in weight is observed (less than 0.02mg/hr) or at least 3 days have passed. All data is recorded as a function of time at one minute intervals. Examples of adsorption and desorption for moist and dry coals are given in Figures 2.8 and 2.9. Sorption curves for moist samples are corrected for moisture loss as previously described.

Moist samples are then dried at 105°C for 12 hours. The dry sample is reweighed and evacuated for one hour before methane is again introduced with the same sequence of methane pressures as for the moist sample. Following degassing to atmosphere, a vacuum may be applied. Gas content calculations are the same as for adsorption isotherms but rate information is also collected to permit calculation of desorption rates.

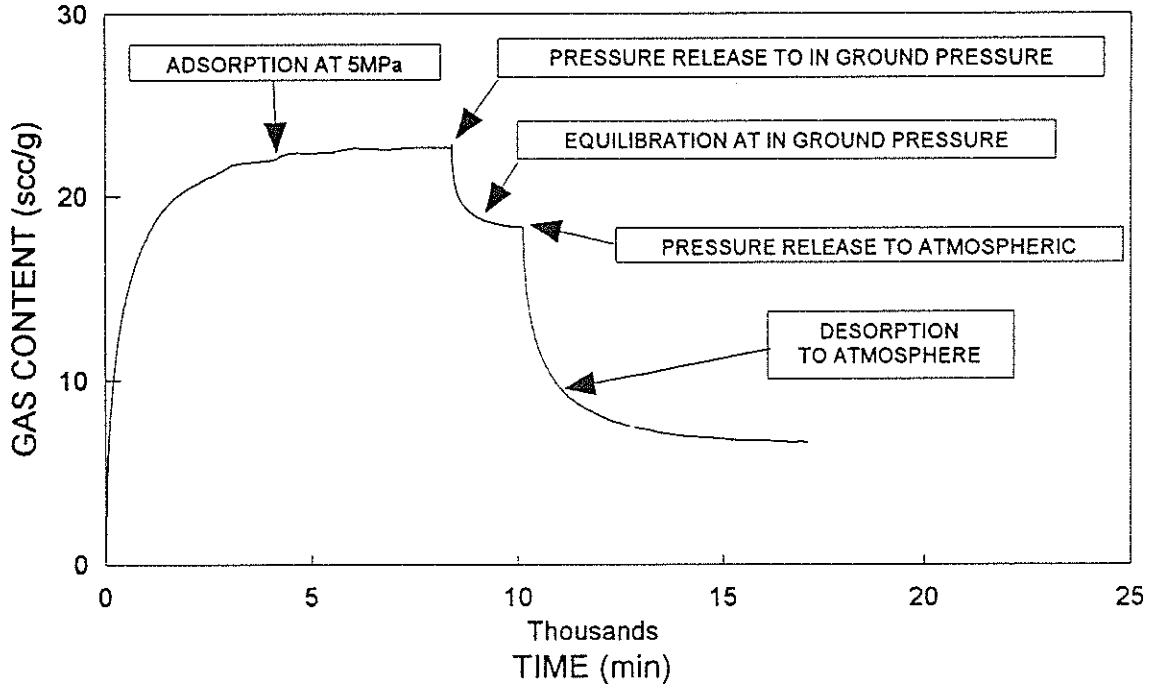

Figure 2.8 Adsorption and desorption curves for dry lump (-5.60 +2.00mm) samples.

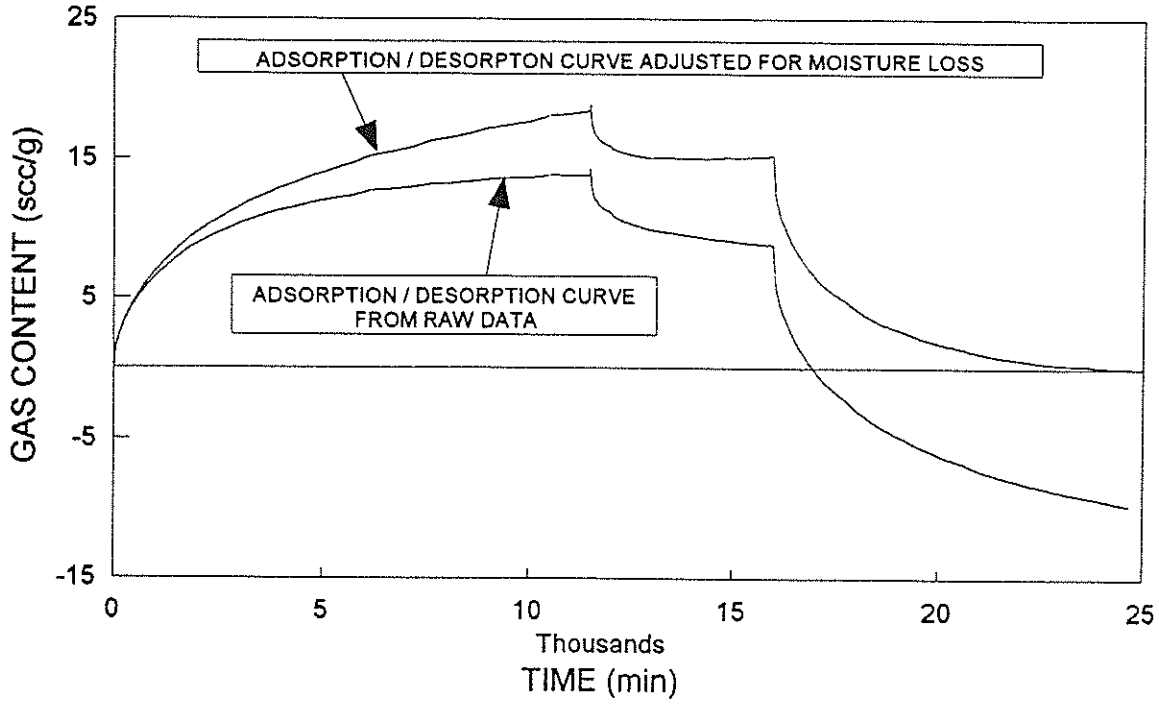

Figure 2.9 Adsorption and desorption curves for moist lump (-5.60 +2.00mm) samples. A correction factor is applied to account for moisture loss during testing.

2.2.4 Calculation of Diffusion Coefficients

Diffusion coefficients of gases through solid coal are very small, between 10^{-11} cm^2/sec (Sevenster, 1959) and 10^{-5} cm^2/sec (Thimons and Kissell, 1973; Smith and Williams, 1984b). The coefficients may be calculated from sorption kinetic studies, such as from the microbalance, or directly determined experimentally using gas chromatographic techniques.

Calculation from kinetic data relies on the rate of sorption being proportional to the square root of time and assumes a uniform pore distribution. Neither assumption is usually true and only the initial part of the sorption curve is used to estimate effective diffusivity (Smith and Williams, 1984a). For describing methane desorption over long time periods (days to months), these diffusivities have proven unsuitable (Smith and Williams, 1984a). However, in the absence of direct experimental determination,

effective diffusivities have been calculated from desorption kinetics determined in the microbalance :

$$\frac{V}{V_\infty} = 1 - \frac{6}{\pi^2} \sum_{n=1}^{\infty} \frac{1}{n^2} e^{(-D_e n^2 \pi^2 t)}$$

where D_e = effective diffusivity
V = volume of desorbed gas
V_∞ = total desorbable gas
t = time

For short time, this simplifies to

$$\frac{V}{V_\infty} = \frac{6}{\sqrt{\pi}} \sqrt{D_e t}$$

Desorption over the first 600 seconds is used to calculate effective diffusivity (Smith and Williams, 1984a, b).

Total desorbable gas content is taken as the amount of gas desorbed during the experiment. This is in contrast to Beamish and Gamson (1993) who use the amount of gas adsorbed prior to release to atmosphere. For dry coal, it is shown experimentally (Chapter 3) that excess gas is retained by the coal under normal conditions which requires either vacuum or heating to displace it.

Effective diffusivity determined for moist coal samples depends on moisture rate loss assumptions. Moisture loss during the course of testing results in final sample weights significantly less than initial weight. Rate of moisture loss has been assumed constant during the course of testing and the final gas content of the coal assumed to be zero.

2.3 DETERMINATION OF HELIUM DENSITY

Density of the coal sample is critical in calculation of the gas content. To correct for buoyancy in the microbalance the volume of the coal must be known, which is calculated from knowledge of its density and weight. Several methods for density

determination are available, most of which involve displacement of a fluid such as methylated spirits, water or helium (Mahajan and Walker Jr, 1978; Anon., 1983). Helium was chosen as the most suitable fluid because :

1. sample density could be determined in the microbalance on the sample used for methane sorption and

2. helium is regarded as giving the most accurate evaluation of true density because its small molecular size permits the greatest penetration into the coal micropores.

2.3.1 Procedure

Helium densities of samples were routinely determined during the course of methane adsorption isotherm analysis. Following adsorption isotherm determination on the moist sample, samples were dried at 105°C, allowed to cool for one hour in the microbalance, evacuated for a further hour and then helium density determined prior to testing for the methane adsorption isotherm of the dry coal.

Following evacuation, helium is introduced up to a pressure of 7 to 9MPa and the system allowed to equilibrate for 30 minutes. The weight of the sample is recorded and the gas pressure released in 1MPa steps to atmospheric. Fifteen minutes is allowed at each pressure step. The volume of the sample + microbalance is determined from a plot of gas density versus weight. The previously determined volume of the microbalance (Table 2.2) is subtracted. Gas density is derived from the Hall - Yarborugh equations (Section 2.2.1; Dake, 1978).

In addition, densities were determined on some lump samples (-5.60+2.00mm) and on some samples in the moist state. It was anticipated that the moist sample density would give a better indication of the total volume of the moist coal. However, results were variable and sometimes unrealistic. The procedure was discontinued in favour of assuming the density of moisture in the coal is 1g/cc and calculating its volume based on the moisture content.

Results obtained using this technique have been confirmed by comparison with other laboratory measurements. A sample from a previous research project (sample 7 bright, Beamish and Gamson, 1993) had a measured helium density by pcynometry of 1.321 g/cc compared with a microbalance determination of 1.315 g/cc. Similarly, a kaolinite sample tested at 2.658 g/cc compares with a known density range of 2.61 - 2.68 g/cc (Deer *et al.*, 1966) .

2.3.2 Example Calculations

Example calculations are given for density determinations of PVC (Table 2.4) and coal (Table 2.5; Fig 2.10) in helium. PVC has been used as a counterweight in the tare side of the balance and, like coal samples, its volume must be assessed to determine buoyancy corrections.

Table 2.4 Determination of the density of PVC using helium

	Weight (mg)	Pressure (MPa)	Gas Density (mg/ml)
	3.60	7.38	11.46
	3.39	6.94	10.81
	3.22	6.55	10.22
	2.99	6.05	9.47
	2.53	5.07	7.98
	2.07	4.07	6.45
	1.55	3.00	4.78
	1.08	2.00	3.21
	0.84	1.49	2.40
	0.61	1.00	1.61
	0.34	0.46	0.75
LINEAR REGRESSION [weight = a.(gas density) + b]			
X Coefficient(s)			0.3039
Constant			0.1100
R Squared			0.99997
weight pvc (g)			0.49553
vol of pvc + balance (cc)			0.3039
vol of balance (cc)			-0.0528
density pvc (g/cc)			**1.390**

Table 2.5 Determination of the density of coal using helium

	Weight (mg)	Pressure (MPa)	Gas Density (mg/ml)
	-4.14	8.81	13.57
	-3.76	7.98	12.35
	-3.30	6.99	10.88
	-2.84	5.99	9.38
	-2.39	5.02	7.91
	-1.90	3.98	6.31
	-1.44	3.00	4.78
	-0.96	2.01	3.22
	-0.48	1.00	1.61
	0.00	0.10	0.16
LINEAR REGRESSION [weight = a.(gas density) + b]			
X Coefficient (a)			-0.3071
Constant (b)			0.0344
R Squared			0.99995
weight of coal (g)			0.4661
volume of coal + balance (cc)			-0.3071
volume of balance (cc)			-0.00571
density of coal			**1.546**

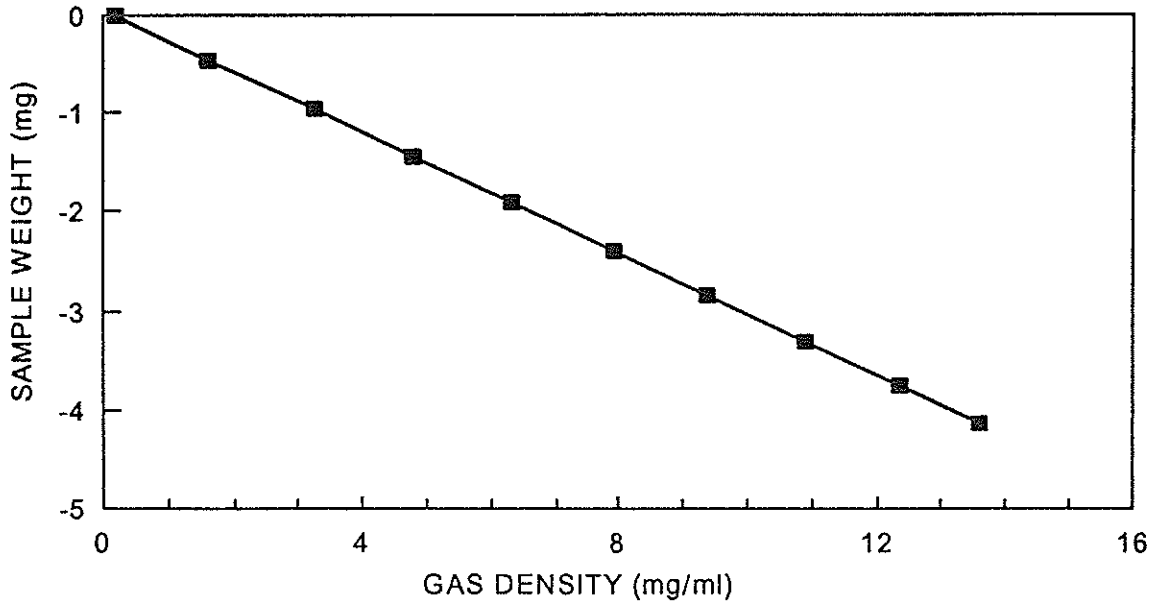

Figure 2.10 Linear relationship between gas density at different pressures and the weight of coal at that pressure (Table 2.5). The slope of the line equals the volume of the coal sample, which allows its density to be determined.

2.4 Proximate Analysis

A thermogravimetric technique for proximate analysis was developed as a collaborative project at the University of Auckland, New Zealand (Beamish, 1994; Appendix 3). This method is the most appropriate because the small sample size (15mg) allowed coals sorption tested in the microbalance to be analysed directly. Proximate analysis using standard procedures (e.g. Anon., 1989b) requires greater than 6g of sample, which, in many cases, was not available. Thermogravimetric analysis enabled much better control on the material being tested without the complications of representative subsampling. Sample amounts less than 20 mg produced results within acceptable repeatability and reproducibility limits (Anon., 1989b).

Approximately 15 mg of sample is heated under nitrogen to 110°C at 50°C per minute and held at this temperature for 5 minutes. Weight loss recorded is the moisture content of the coal, which correlated well with that measured by standard moisture tests. Simulating standard ash and volatile matter determinations required some ingenuity because ash is normally measured by combusting the coal at temperatures up to 815°C, where as volatile matter must be analysed in non-combusting conditions at 900°C. This difficulty was overcome by heating the coal from 110°C up to 900°C at 50°C per minute under nitrogen, holding for a fixed time, then switching the gas flow to air. The weight loss before the switch to air correlates well with volatile matter determined by standard procedures, while the weight of residue after the combustion stage correlates well with the ash content as determined by standard methods. The technique was found to be suitable for both Australian and New Zealand coals.

2.5 Petrographic Analysis

Coals were crushed to -1mm, embedded in epoxy resin and polished in accordance with standard procedures (Anon., 1986a). Maceral and reflectance analyses were conducted in accordance with standard methods (ICCP, 1963; Anon., 1986a). In addition, it was attempted to classify large pores within the coal, especially cell lumina in inertinites, as

mineralised or unmineralised. These large pores play an important role in transportation of gas through the coal when the laminar flow phase is reached. Reflectance analyses were conducted at the University of Auckland, New Zealand, using a Leitz Orthoplan microscope and MPV2 photomultiplier system.

Maceral analysis samples were sub-samples when sufficient coal was available or half the -5.60+2.00mm sample used in the microbalance when coal quantities were small (JCB4, JCB7, JCB9, JCB12, JCB21).

Table 2.6 Coal maceral nomenclature

Maceral Group	Maceral	Pore Fabric
Vitrinite	Telocollinite	unmineralised fractures
		mineralised fractures
	Desmocollinite	
Liptinite	Sporinite	
	Resinite	
	Cutinite	
	Alginite	
Inertinite	Semifusinite	unmineralised cell lumen
		mineralised cell lumen
	Fusinite	unmineralised cell lumen
		mineralised cell lumen
	Micrinite	
	Macrinite	
	Inertodetrinite	
Mineral Matter	Clay	
	Quartz	
	Carbonate	
	Pyrite	

2.6 Pore Distribution and Surface Area

Analysis of pore distribution and surface area have been conducted by the CSIRO Division of Coal and Energy Technology at Lucas Heights. Tests included determination

of the surface area using CO_2 and N_2, total porosity by difference in mercury and helium density and pore distribution by mercury porosimetry.

2.7 Microstructural Analysis

Microstructural analysis by scanning electron microscopy (SEM) of bright and dull coal types from the Bowen Basin has identified significant differences which influence gas flow through coal (Beamish and Gamson, 1993; Gamson *et al.*, 1993). SEM provides an ideal method of examining coal in relation to microstructural properties by allowing observation of :

1. coal microstructure in 3-dimension and, therefore, provides information on the shape, size and cross-sectional area of the microstructures and their bearings to the face and butt cleat and bedding.
2. fracture density, orientation and continuity.
3. connectivity of cleats, microfractures and cavities.
4. individual bright and dull coal bands over several centimetres.
5. connectivity between dull and bright coal bands.
6. greater textural detail of the macerals.

The term microstructure refers to structures not visible in hand specimen, which distinguishes them from macrofractures or cleats. Observed microstructures are considered to represent original features and are not due to sampling or stress release since : 1) most are infilled with secondary minerals, 2) fractures are rarely observed between the coal and the mineralisation infilling the pore space, and 3) the observed microstructures have not been found in all samples studied.

Coal Microstructures

Coal microstructures fall into two broad categories of micron-sized fractures (microfractures) and micron-sized cavities (microcavities) (Beamish and Gamson, 1993;

Gamson *et al.*, 1993). Microstructures vary in width from 0.01μm to 20 μm which, according to pore classifications, belong to meso- and macro-pores. Gas-storing micropores are significantly smaller (<0.0012μm) and cannot be imaged using SEM. In relation to coal type, the microfractures are generally associated with the bright coals and tend to form a continuous structural fabric through the coal layers. In contrast, the dull coals predominantly contain microcavities that are part of the phyteral and matrix porosity.

Bright Coal

Two fracture sizes are recognised in bright coals : the larger macrofractures or cleats, and smaller microfractures between the cleats.

Three different types of cleat (face, butt and a third cleat direction) may be present (Table 2.7). Both the face an butt cleats commonly occur as planar, orthogonal sets oriented perpendicular to the bedding and are not continuous through the coal seam but are largely restricted to bright coal bands. A third curviplanar cleat direction is commonly present which cuts across both the face and butt cleats.

Five different types of microfracture are recognised in between the cleats of the bright coals: vertical microcleats, horizontal microcleats, blocky fractures, conchoidal fractures and striae (Table 2.7). Microfractures are commonly mineralised.

Analogous to cleats, microcleats are associated only with bright coal bands and terminate at their boundaries. Vertical microcleats parallel the face and butt cleat directions while horizontal microcleats parallel bedding. The cleat-defined blocks of bright coal commonly exhibit an irregular, blocky fracture pattern, with fractures often conchoidal, showing no regular relationship to bedding or the cleat direction and irregularly spaced.

At maximum magnification of 80,000x bright coals exhibit a striated fracture pattern

made up of closely packed parallel laminations or sheet-like layers termed striae. Their small size, continuity and their constant spacing suggest they represent planes of weakness corresponding to layers of secondary cell wall thickening and basic layer-plane structures recognised in vitrinite.

Dull Coal

Dull coal predominantly contains a phyteral and matrix porosity of microcavities.

Phyteral porosity represents the void space associated with the original plant fragments. Microstructures associated with these organic components are abundant in the dull coal bands and form microcavities, as opposed to microfractures. A common component of the phyteral porosity is numerous sheet-like structures arranged in a series of stacked layers parallel to bedding which represent remnants of wood fibres. In cross-section the sheets are smooth, apparently homogeneous and are separated by long, cylinder-like microcavities (cell lumina).

Although the original cavities were rectangular in cross-section and form sieve-like structures, many have since been broken and compressed. This has resulted in various morphological structures, namely: needle (fragmented cell walls resulting in network of pointed, needle-shaped splinters), compressed (cell walls that have been crushed together almost to lines of compression, but are not broken), bogen (cell walls that have been broken and pushed into one another), bogen-compressed (bogen structure that has been compressed) and highly-compressed. Mineral infillings are common.

Table 2.7 Characterisation of microstructures observed in coal using SEM

Microstructures	Width of pathway	Length of pathway	Spacing	Orientation	Association
Fracture Porosity					
Macrofractures					
- cleats (face, butt, others)	0.1-2mm	100μm - core	0.3 - 2mm	90° to bedding	restricted to bright
Microstructures					
- vertical microcleats	5-20μm	50-500μm	30-100μm	90° to bedding	restricted to bright
- horizontal microcleats	0.5-2μm	50-300μm	5-10μm	parallel to bedding	restricted to bright
- blocky fractures	1-15μm	50-200μm	<100μm	irregular	restricted to bright
- conchoidal fractures	0.05-0.1μm	1-100μm	0.05-0.1μm	irregular	restricted to bright
- striae	0.1μm	5-100μm	0.1-0.3μm	60-90° to bedding	restricted to bright
Phyteral Porosity					
- cavities associated with organic components	2-4μm	10μm-core	1-20μm	parallel to bedding	restricted to dull
Matrix Porosity					
- between maceral fragments	0.05-50μm	0.05-50μm	0.05-50μm	irregular	restricted to dull
- between minute particles	0.01-0.05μm	0.01-0.05μm	0.01-0.05μm	irregular	restricted to dull
- between clays	0.1-2μm	1-20μm	irregular	parallel to bedding	restricted to dull

Matrix porosity represents cavities associated with pore space separating particles and occurs in three forms:

1. in between a coarse (10-50μm) granular matrix of maceral fragments, such as vitrinite and fusinite.
2. within a chaotic mass of minute (1-5μm), angular to rounded particles.
3. as microcavities in between clay particles.

In relation to coal type, clays in bright coals occur predominantly as fracture infill. In contrast, clays in dull coals occur as bands/lenses, as disseminated fine particles , as cavity infill, and/or interbedded between maceral fragments. Cavities between the clay particles and granular aggregates vary from 0.1-2μm wide and up to 20μm long.

Microstructure and the Effect on Sorption Behaviour

The differences in gas sorption behaviour and the effect of a macropore and micropore component shown between the dull and bright coal samples can be explained in terms of microstructure and extent of mineralisation. Both bright and dull coals can be categorised into fast (Class A) and slow (Class B) desorbing types.

Faster sorbing bright coals contain a well defined cleat grid network, where cleats are moderately tightly infilled with clay and connecting pore space exists between the clay particles. In addition, they contain open, unmineralised blocky fractures, microcleats, conchoidal fractures and striae. The rapid sorption behaviour is related to a high proportion of macropores. Slow sorbing bright coals exhibit fewer macropores and microfractures and have more tightly infilled cleats and microfractures.

In dull coals, rapid sorption is related to a higher proportion of open, unmineralised macropores, and probably relates to laminar flow through them. In contrast, slow sorption behaviour is related to fewer macropores and a higher proportion of micropores due to mineralisation.

Samples for Microstructural Analysis

To understand the relationship between coal type, microstructure and gas flow behaviour, selected samples characterised by sorption analyses in the microbalances and surface area / porosity were examined by SEM to determine their microstructure. Samples were representative of those used for sorption testing and 4 pieces of bright and dull coal approximately 5mm in diameter were examined for each sample number. Bright coals pieces were generally bounded by the face and butt cleats and the influence of these cleats on gas flow is more difficult to establish. All samples were carbon coated prior to SEM evaluation of microstructures outlined by Table 2.7.

3. RESULTS

3.1 Proximate analysis

Proximate analysis results of air-dried coals are presented in Table 3.1. Bright coals from Central Colliery are low volatile bituminous in rank and are higher in rank than the medium volatile bituminous South Bulli samples. Bright coals are distinguished from dull coals by their lower ash and higher volatile matter contents. Dull coals from Central Colliery typically have higher ash contents than dull coals from South Bulli.

3.2 Methane Adsorption Isotherms

Methane adsorption isotherms on crushed (-0.212mm), equilibrium moist and dry samples are used to determine the amount of gas the coal is capable of storing at a particular pressure as well as the maximum storage capacity of the sample (the Langmuir Volume or V_L). The isotherm value at the estimated *in situ* gas pressure (2MPa for Central; 3MPa for South Bulli) has been used to evaluate the degree of gas saturation in the lump samples prior to desorption to atmosphere.

Results are summarised as Langmuir volumes for the raw coals as well as recalculated to an ash free basis (Table 3.2). Adsorption isotherms on a dry basis are illustrated in Section 4.1.5 where they are compared to those predicted by the model of Kim (1977). The degree of saturation of the lump samples (Table 3.3) is generally equal to or better than 80% compared to the adsorption isotherm sample, indicating the procedure used to resorb methane onto the sample has achieved close to saturation in most cases.

Lump samples with greater than 100% gas saturation are related to moist coals. Short analysis time for adsorption isotherms (several hours) means the moisture state of the coal is little altered. Longer residence times for the lump samples (several days) allows them to partially dry out and adsorb more gas than expected, resulting in apparent oversaturation.

Table 3.1 Proximate Analysis Results for Central and South Bulli Collieries (%, air-dried basis)

Sample	Moisture (%)	Volatile Matter (%)	Fixed Carbon (%)	Ash (%)
Central Colliery				
JCB4B	1.6	17.5	74.5	6.4
JCB4D*	7.9	17.1	59.8	15.2
	5.0	17.9	61.0	16.1
	3.5	18.1	62.1	16.3
JCB7B	1.8	17.8	75.3	5.1
JCB7D	1.8	14.5	63.6	20.1
JCB9B	0.8	18.0	78.9	2.3
JCB9D	1.7	15.6	60.3	22.4
JCB12B	1.5	17.2	77.5	3.8
JCB12D	1.3	14.6	64.0	20.1
JCB21B	1.2	17.5	77.9	3.4
JCB21D	1.3	15.8	69.3	13.6
JCB82B	1.0	18.2	79.1	1.7
JCB82D	1.0	15.3	70.2	13.5
JCB92B	1.0	17.7	79.3	2.0
JCB92D	1.2	14.7	64.2	19.9
JCB95	2.0	14.8	56.7	26.5

Sample	Moisture (%)	Volatile Matter (%)	Fixed Carbon (%)	Ash (%)
South Bulli Colliery				
JCB27B	1.0	25.8	72.3	0.9
JCB25D	1.9	16.4	63.2	18.5
JCB29B	1.2	27.5	69.6	1.7
JCB32D	1.2	20.7	66.1	12.0
JCB35B	1.2	25.6	71.7	1.5
JCB37D	0.8	18.3	72.6	8.3
JCB40B	0.8	25.9	69.4	3.9
JCB42D	2.0	18.1	70.9	9.0
JCB66B	0.9	25.7	72.2	1.2
JCB65D	1.4	18.2	71.6	8.8
JCB74BD	1.1	22.1	63.7	13.1
JCB76BD	0.8	22.7	68.7	7.8

*This sample was not completely air-dried when received, as shown by repeated testing over a week.

Note: Samples JCB76BD, JCB40B, JCB66B and JCB27B were all high swell coals and were analysed using alumina powder dilution. Samples JCB35B and JCB29B were also high swell coals and were analysed using smaller subsamples. JCB32D only had 11.90 mg of sample supplied.

Table 3.2 Langmuir volumes (V_L) of moist and dry coals as analysed and recalculated to an ash free basis.

Sample	Lithotype	V_L (raw coal) (cc/g)		V_L (ash free) (cc/g)	
		Moist	Dry	Moist	Dry
Central Colliery					
JCB4B	B	31.6	33.0	33.9	35.5
JCB4D	D		31.7		38.5
JCB7B	B	33.3	35.1	35.3	37.2
JCB7D	D	24.5	27.6	31.4	35.5
JCB9B	B	30.5	37.5	31.3	38.5
JCB9D	D	33.2	28.6	44.1	37.9
JCB12B	B	23.3	29.1	24.3	30.4
JCB12D	D	25.5	28.1	32.7	36.1
JCB21B	B	33.0	32.7	34.3	33.9
JCB21D	D	24.6	27.1	28.9	31.8
JCB82B	B	25.2	30.1	25.7	30.6
JCB82D	D	22.7	25.6	26.6	30.1
JCB92B	B	26.7	32.1	27.3	32.9
JCB92D	D	20.9	23.5	26.8	30.1
JCB95	Sheared	23.8	22.6	33.6	31.9
South Bulli Colliery					
JCB27B	B	25.7	25.3	26.0	25.5
JCB25D	D	28.6	30.4	35.9	38.1
JCB29B	B		27.3		27.8
JCB32D	D	20.5	24.5	23.6	28.2
JCB35B	B	23.7	27.5	24.1	27.9
JCB37D	D	30.2	28.3	33.2	31.2
JCB40B	B	20.0	24.6	20.9	25.7
JCB42D	D		25.3		28.1
JCB66B	B	30.2	33.9	30.6	34.3
JCB65D	D	24.4	27.8	27.0	30.7
JCB74BD	BD	21.8	23.9	25.5	27.9

Table 3.3 Degree of gas saturation of lump samples prior to desorption analysis in relation to the methane adsorption isotherm.

Sample	Lithotype	Moisture Content (%)	crushed (-0.212mm)		lump (-5.60+2.00mm)		% gas saturation of lumps
			Pressure (MPa)	Gas Content (cc/g)	Pressure (MPa)	Gas Content (cc/g)	
Central Colliery							
JCB4B	B	3.32	2.08	13.0	1.88	10.9	84
JCB4B	B	0	2.11	17.6	1.97	18.6	105
JCB4D	D	moist			2.01	9.4	
JCB4D	D	0	2.09	15.8	1.97	14.4	91
JCB7B	B	2.52	1.98	13.4	1.84	13.7	102
JCB7B	B	0	2.08	17.1	1.83	18.2	107
JCB7D	D	4.56	2.03	10.6	2.02	11.1	105
JCB7D	D	0	2.10	16.6	2.02	15.0	90
JCB9B	B	1.28	2.07	15.5	2.02	13.3	86
JCB9B	B	0	2.12	20.8	2.13	18.8	90
JCB9D	D	3.12	2.05	11.9	2.14	12.2	102
JCB9D	D	0	2.05	13.3	2.21	15.9	119
JCB12B	B	1.88	2.07	13.0	1.95	15.5	119
JCB12B	B	0	2.02	18.4	1.99	18.7	102
JCB12D	D	2.46	2.02	9.6	1.92	12.1	126
JCB12D	D	0	2.13	16.1	2.11	15.4	95
JCB21B	B	3.36	2.03	17.2	1.98	9.5	55
JCB21B	B	0	2.05	17.3	2.05	17.4	100
JCB21D	D	3.37	2.03	10.8	2.07	6.2	57
JCB21D	D	0	2.00	14.9	2.10	15.1	101
JCB82B	B	1.84	2.00	12.0	2.07	6.7	56
JCB82B	B	0	2.05	17.0	2.07	17.8	105
JCB82D	D	2.11	2.09	11.3	2.17	8.4	74
JCB82D	D	0	2.24	15.6	2.23	14.5	93
JCB92B	B	1.94	2.03	13.2	2.09	6.4	48
JCB92B	B	0	2.20	18.3	2.01	14.7	80
JCB92D	D	2.54	2.19	10.3	2.12	9.9	96
JCB92D	D	0	2.10	12.8	2.06	14.9	116
JCB95	Sheared	6.54	1.99	11.4	1.98	13.8	121
JCB95	Sheared	0	2.10	13.2	2.06	13.9	106
South Bulli Colliery							
JCB25D	D	1.70	3.13	13.2	3.01	8.0	60
JCB25D	D	0	3.05	15.5	3.08	13.6	87
JCB27B	B	1.55	3.04	11.5	3.05	6.3	55
JCB27B	B	0	3.07	15.6	3.07	15.4	99
JCB29B	B	2.95	3.14	7.7			
JCB29B	B	0	3.10	15.8	2.99	7.6	48
JCB32D	D	2.02	3.05	11.2	3.15	7.4	66
JCB32D	D	0	3.04	15.6	3.05	13.4	86
JCB35B	B	1.42	3.16	10.5			
JCB35B	B	0	3.00	13.8			
JCB37D	D	5.23	3.05	15.0			
JCB37D	D	0	3.08	17.1			
JCB40B	B	1.91	3.03	11.2	2.97	9.6	85
JCB40B	B	0	3.12	15.0	2.87	15.5	103
JCB42D	D	moist					
JCB42D	D	0	3.07	15.5	2.91	14.8	96
JCB65D	D	2	3.13	15.3	3.06	10.4	68
JCB65D	D	0	3.07	17.9	2.96	16.0	89
JCB66B	B	1.73	3.11	16.4	2.96	8.4	51
JCB66B	B	0	3.08	19.8	3.00	14.3	72
JCB74	BD	1.68	3.05	12.8	2.95	11.3	88
JCB74	BD	0	2.99	14.7	3.08	11.9	81

3.3 Desorption Rates

Desorption rate studies have been performed on lump (-5.60+2.00mm) samples. Results are reported for raw coals in equilibrium moist and dry states. Samples have been resorbed with methane at 5MPa gas pressure prior to desorption to the estimated *in situ* pressure (2MPa for Central; 3MPa for South Bulli) and finally release to atmosphere. In some instances, vacuum has been applied to the dry coals after completion of desorption to atmosphere.

Graphical results for Central (Figs 3.1 to 3.16) and South Bulli Collieries (Figs 3.17 to 3.28) show the combined analyses for dull and bright coal pairs in both equilibrium moist and dry states for each sample site.

Central Colliery

Adsorption to 5MPa

Bright, dry coals have the greatest methane content at 5MPa followed by dull, dry samples, with the exception of JCB92(bright) (Figs 3.1, 3.3, 3.5, 3.7, 3.9, 3.11, 3.13 and 3.15). Most dry samples had effectively completed gas adsorption at 5MPa with the exceptions of JCB4 dull and JCB92 bright.

For sample JCB92 dull, dry coal has the highest gas content at 5MPa but at 2MPa bright and dull dry samples are similar. Bright coal was still adsorbing gas at 5MPa, even after 100 hours (4 days), which accounts for its lower gas content than the dull coal for which adsorption was effectively complete at 5MPa.

Moist sample gas contents are more difficult to evaluate due to moisture loss. Although gas pressures were maintained until sample weight changes were small, after application of the moisture loss algorithm it appears that gas adsorption was still occurring at the end of the 5MPa stage. Comparison with the adsorption isotherm data

shows most moist samples were between 50 to 80% adsorbed at 5MPa and confirms further significant adsorption could have taken place. This suggests the applied moisture loss algorithm is appropriate. It can be seen that at any given time the amount of gas adsorbed by the moist coal is significantly less than adsorbed by the dry coal indicating a much slower adsorption rate for moist samples. Similar to the dry samples, moist bright coals have adsorbed more gas than their equivalent dull coal.

Desorption from 5MPa to 2MPa

Reduction in gas pressure to 2MPa is designed to bring the samples to an *in situ* state. Bright, dry coals have the highest gas contents followed by the dull, dry samples. Dry samples are generally greater than 80% saturated with gas at the end of the 2MPa stage (Table 3.3).

Moist coals show varying degrees of gas saturation with several around the 50% level (Table 3.3). The shape of the isotherm, after moisture loss correction, often indicates continuing adsorption at the end of the 2MPa stage which is consistent with undersaturation of some samples. Bright, moist coals have higher gas contents than their equivalent dull coal.

Despite some coals being undersaturated at the 5MPa pressure, all samples show gas desorption when pressure is reduced to 2MPa. Some of these coals then appear to be saturated at 2MPa while others maintain significant degrees of undersaturation because of very slow diffusion rates to adsorption sites.

Desorption from 2MPa to atmosphere

Gas release to atmospheric pressure is designed to simulate gas release when the coal surface is suddenly exposed to the atmosphere. For comparison, all samples have been normalised to a desorbed gas ratio, which is the ratio of the gas content at a particular time to the final gas content of the sample (Figs 3.2, 3.4, 3.6, 3.8, 3.10, 3.12, 3.14 and

3.16). Desorbed gas ratio is plotted against the square root of time (in seconds). The first 600 seconds of this plot is used to estimate the effective diffusivity (D_e; Table 3.4) of the sample.

All dry samples retain significant gas quantities after completion of desorption to atmosphere. This gas is equivalent to the residual gas determined by finely crushing samples following canister desorption testing. Moist samples have zero final gas contents because of the moisture loss correction algorithm, however, moist samples would be expected to have residual gas contents similar to the dry coals.

Comparison of gas release rates is made from desorbed gas ratio plots (Fig 3.2, 2.4, 3.6, 3.8, 3.10, 3.12, 3.14 and 3.16). Plots should be asymptotic towards a gas ratio of one. Non-asymptotic samples (e.g. JCB4, Figs 3.1 and 3.2) indicate desorption was incomplete at atmosphere. A number of trends are observed :

1. most moist coals desorb at rates slower than their dry coal equivalent. Exceptions are JCB4 samples (Fig 3.2) and dull coal of JCB21 (Fig 3.10) .

2. dull samples usually desorb more rapidly than their bright coal equivalent for the same moisture state.

3. some coals exhibit no apparent differences in desorption rates in relation to coal type or moisture state e.g. JCB4 (Fig 3.2); JCB9 moist samples (Fig 3.6).

4. the sheared coal shows very rapid desorption, especially in the dry state.

Desorption during application of vacuum

Vacuum was applied to some dry samples (JCB82B, JCB82D, JCB95) following completion of desorption testing to atmosphere. The procedure was not applied to moist coals where moisture loss problems would be exacerbated. Evacuation times were

three to five hours and resulted in gas reductions from 8.8 to 6.9cc/g (JCB82 bright); 7.1 to 5.0cc/g (JCB82 dull); and 3.9 to 0cc/g (JCB95). These results indicate that much of the residual gas may be removed and is consistent with vacuum procedures currently employed in methane drainage operations.

South Bulli Colliery

South Bulli Colliery samples are illustrated by Figures 3.17 to 3.28. General comments on analytical procedures for Central Colliery (above) also apply to South Bulli.

Adsorption to 5MPa

In contrast to Central Colliery, South Bulli coals show no strong trend of coal type and maximum gas content at 5MPa (Figs 3.17, 3.19, 3.21 and 3.23).

Moisture state is again an important influence with dry coals adsorbing the most methane. Most dry samples had effectively completed gas adsorption at 5MPa while for moist coals adsorption appears incomplete after application of the moisture loss algorithm. Comparison with the adsorption isotherm data shows most moist samples were between 50 to 80% adsorbed at 5MPa. At any given time the amount of gas adsorbed by the moist coal is significantly less than adsorbed by the dry coal indicating a much slower adsorption rate for moist samples. Similar to the dry samples, moist coals exhibit no strong trend in amount of gas adsorbed in relation to coal type .

Desorption from 5MPa to 3MPa

Reduction in gas pressure to 3MPa is designed to bring the samples to an *in situ* state. Despite some coals being undersaturated at the 5MPa pressure, all samples show gas desorption when pressure is reduced to 3MPa.

No strong trends are apparent relating coal type to quantity of adsorbed methane in

either moist or dry states.

Moisture state is again an important factor with dry samples adsorbing the most gas. Although high degrees of gas saturation (80 to 90%) have been achieved for the dry samples, the level appears to be consistently lower than achieved for Central Colliery (Table 3.3).

Moist coals have lower degrees of gas saturation with most around the 50% level, which is also consistently lower than achieved for Central Colliery (Table 3.3). The shape of the isotherm, after moisture loss correction, often indicates continuing adsorption at the end of the 3MPa stage, consistent with methane undersaturation.

Desorption from 3MPa to atmosphere

Gas release to atmospheric pressure is designed to simulate gas release when the coal surface is suddenly exposed to the atmosphere. For comparison, all samples have been normalised to a desorbed gas ratio and plotted against the square root of time (Figs 3.18, 3.20, 3.22, 3.24, 3.26 and 3.28). The first 600 seconds of this plot is used to estimate the effective diffusivity (D_e; Table 3.4).

All dry samples retain significant gas quantities after completion of desorption to atmosphere, which is equivalent to the residual gas content. Moist samples have zero final gas contents because of the moisture loss correction algorithm. However, it is unlikely this is the case and moist samples would be expected to have residual gas contents similar to the dry coals.

Observed trends are similar to those of Central Colliery :

1. most moist coals desorb at rates slower than their dry coal equivalent.
2. dull samples usually desorb more rapidly than their bright coal equivalent for the same moisture state.

3. some coals exhibit no apparent differences in desorption rates in relation to moisture state e.g. JCB76 (Fig 3.28).

Desorption during application of vacuum

Vacuum was applied to JCB32D (dull, dry) following completion of desorption testing to atmosphere. Gas content was reduced from 6.3 to 4.2cc/g during evacuation for 5 hours.

Table 3.4 Effective diffusivities determined from rate information over the first 600 seconds of desorption to atmosphere.

Sample	Lithotype	Effective Diffusivity (De) (sec^{-1})			
		Moist		Dry	
		Crushed	Lump	Crushed	Lump
Central Colliery					
JCB4B	B	3.8E-05	6.3E-06	2.7E-05	3.1E-06
JCB4D	D		8.6E-06	3.4E-05	6.6E-06
JCB7B	B		3.7E-06		3.2E-06
JCB7D	D	3.1E-05	7.2E-06	2.4E-05	5.5E-06
JCB9B	B	2.2E-05	1.5E-06	7.3E-05	1.2E-06
JCB9D	D	2.6E-05	2.5E-06	1.8E-05	4.5E-06
JCB12B	B	3.6E-05	1.2E-06	5.4E-05	2.3E-06
JCB12D	D	6.2E-05	3.3E-06	6.2E-05	3.8E-06
JCB21B	B	1.7E-05	2.2E-06	2.7E-05	1.7E-06
JCB21D	D	3.9E-05	7.5E-06	7.4E-05	3.8E-06
JCB82B	B	3.7E-05	2.9E-06	4.2E-05	1.2E-06
JCB82D	D	4.6E-05	4.8E-06	5.7E-05	2.0E-06
JCB92B	B	4.1E-05	2.0E-06	3.9E-05	1.3E-06
JCB92D	D	1.7E-05	3.1E-06	4.0E-05	3.4E-06
JCB95	Sheared	6.7E-05	9.3E-06	7.3E-05	6.5E-05
South Bulli Colliery					
JCB27B	B	3.2E-05	3.0E-06	2.1E-05	1.1E-06
JCB25D	D	4.7E-05	2.5E-06	5.4E-05	2.5E-06
JCB29B	B	1.3E-05		2.3E-05	7.8E-07
JCB32D	D	2.4E-05	4.6E-06	3.1E-05	2.9E-06
JCB35B	B	2.3E-05		3.7E-05	
JCB37D	D	3.6E-05		6.8E-05	
JCB40B	B	2.1E-05	6.4E-07	1.4E-05	6.4E-07
JCB42D	D	2.4E-05	1.8E-06	2.4E-05	2.0E-06
JCB66B	B	3.7E-05	1.3E-06	3.6E-05	1.1E-06
JCB65D	D	6.2E-05	2.7E-06	4.7E-05	2.9E-06
JCB74BD	BD	4.6E-05	4.4E-06	3.9E-05	2.7E-06
JCB76BD	BD		2.6E-06		2.3E-06

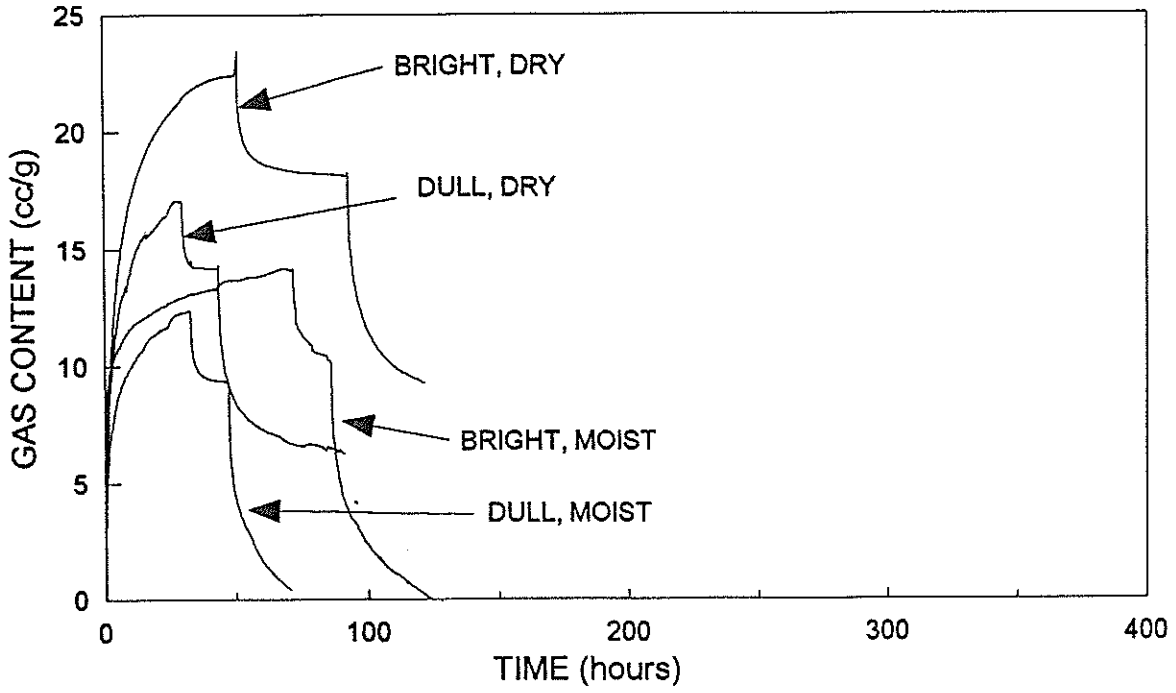

Figure 3.1 Central Colliery JCB4 lump samples (-5.60+2.00mm) showing methane sorption in equilibrium moist and dry raw coal. Initial adsorption at 5MPa is followed by pressure reduction to 2MPa and subsequent desorption to atmosphere. Moist samples are corrected for moisture loss during analysis.

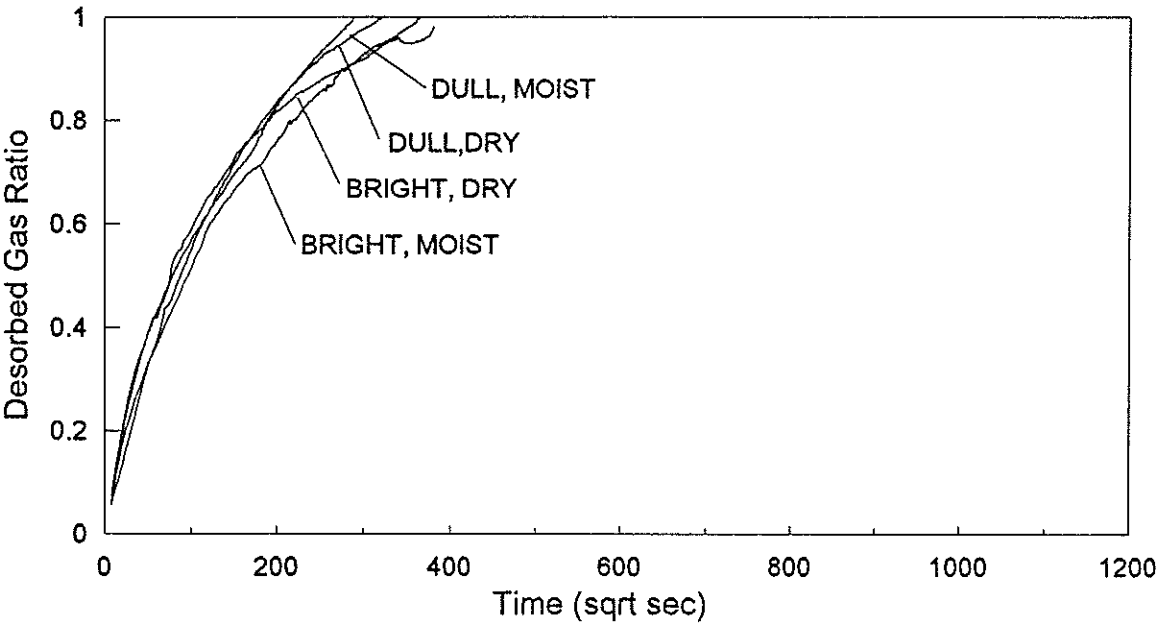

Figure 3.2 Central Colliery JCB4 lump samples (-5.60+2.00mm) showing methane desorption rate at atmospheric pressure after release from 2MPa.

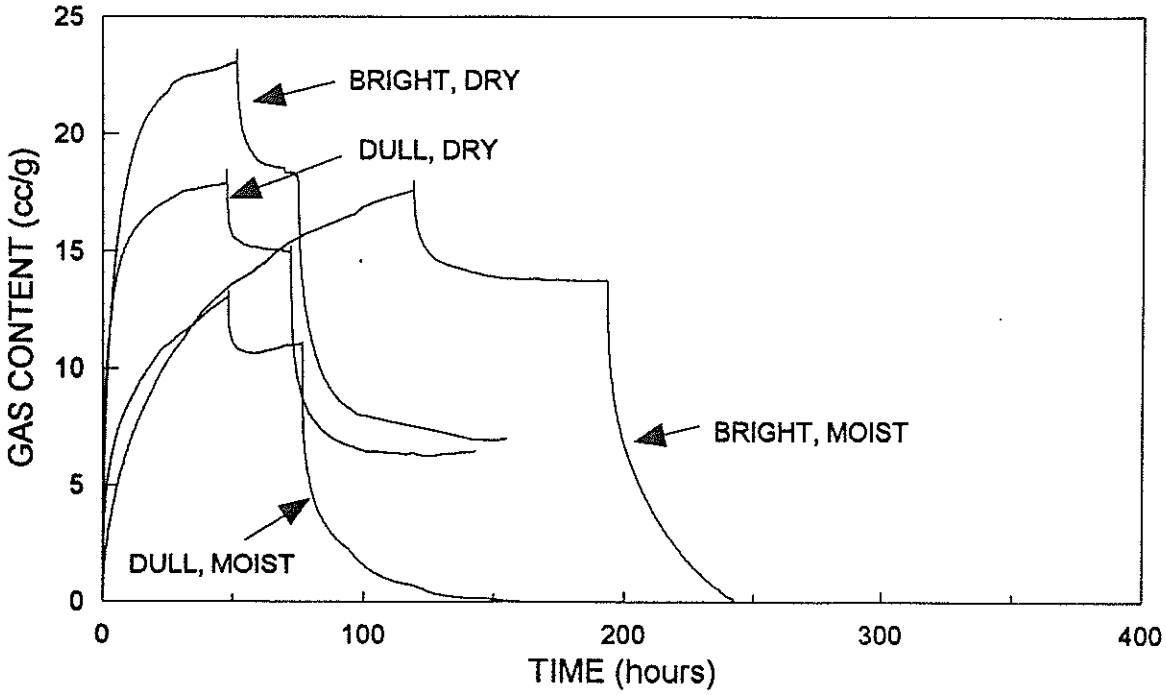

Figure 3.3 Central Colliery JCB7 lump samples (-5.60+2.00mm) showing methane sorption in equilibrium moist and dry raw coal. Initial adsorption at 5MPa is followed by pressure reduction to 2MPa and subsequent desorption to atmosphere. Moist samples are corrected for moisture loss during analysis.

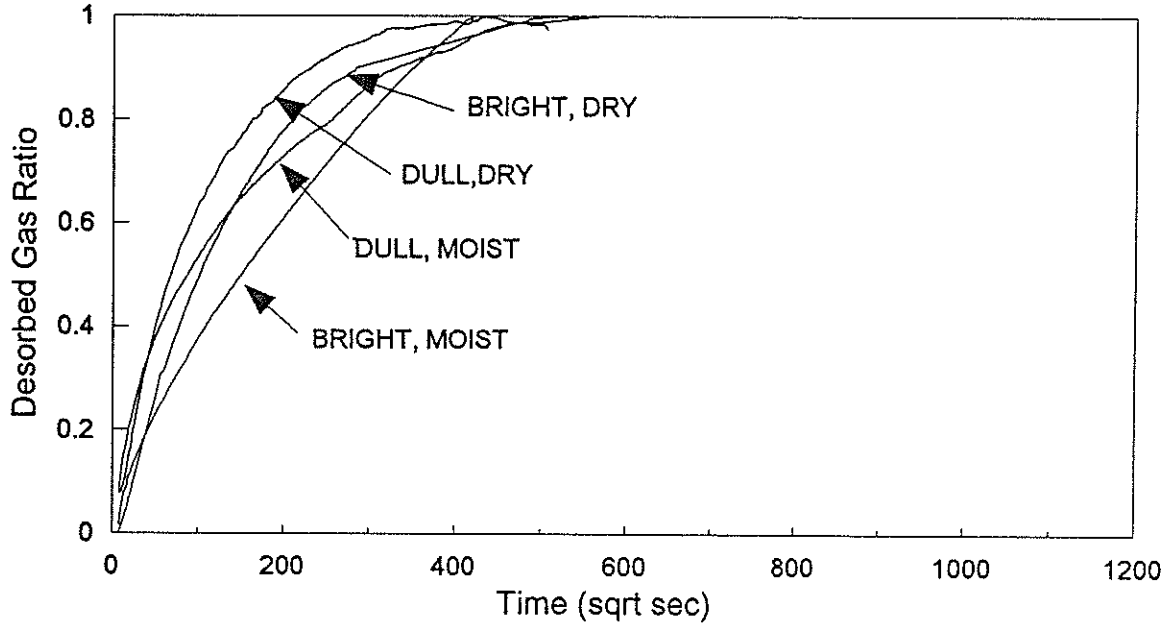

Figure 3.4 Central Colliery JCB7 lump samples (-5.60+2.00mm) showing methane desorption rate at atmospheric pressure after release from 2MPa.

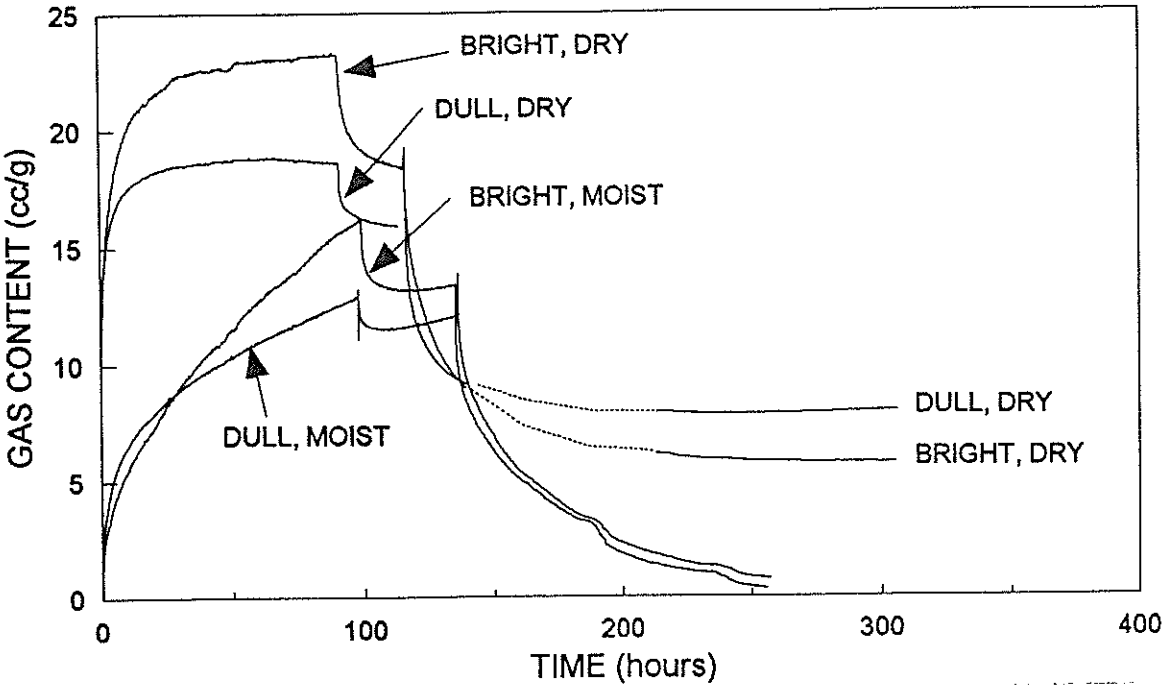

Figure 3.5 Central Colliery JCB9 lump samples (-5.60+2.00mm) showing methane sorption in equilibrium moist and dry raw coal. Initial adsorption at 5MPa is followed by pressure reduction to 2MPa and subsequent desorption to atmosphere. Moist samples are corrected for moisture loss during analysis.

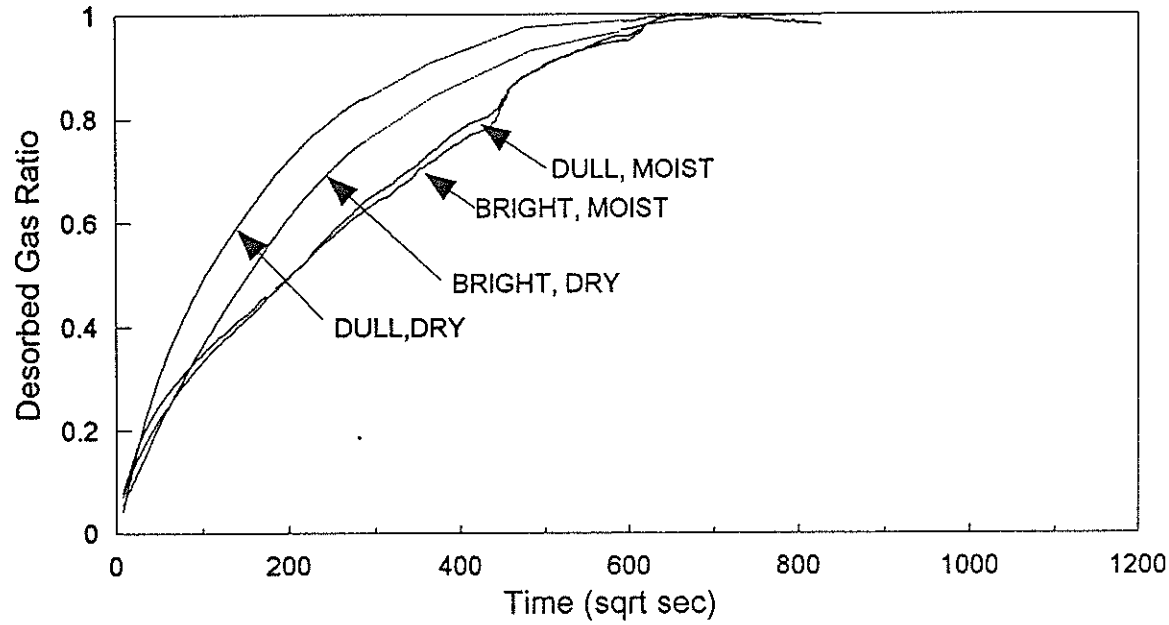

Figure 3.6 Central Colliery JCB9 lump samples (-5.60+2.00mm) showing methane desorption rate at atmospheric pressure after release from 2MPa.

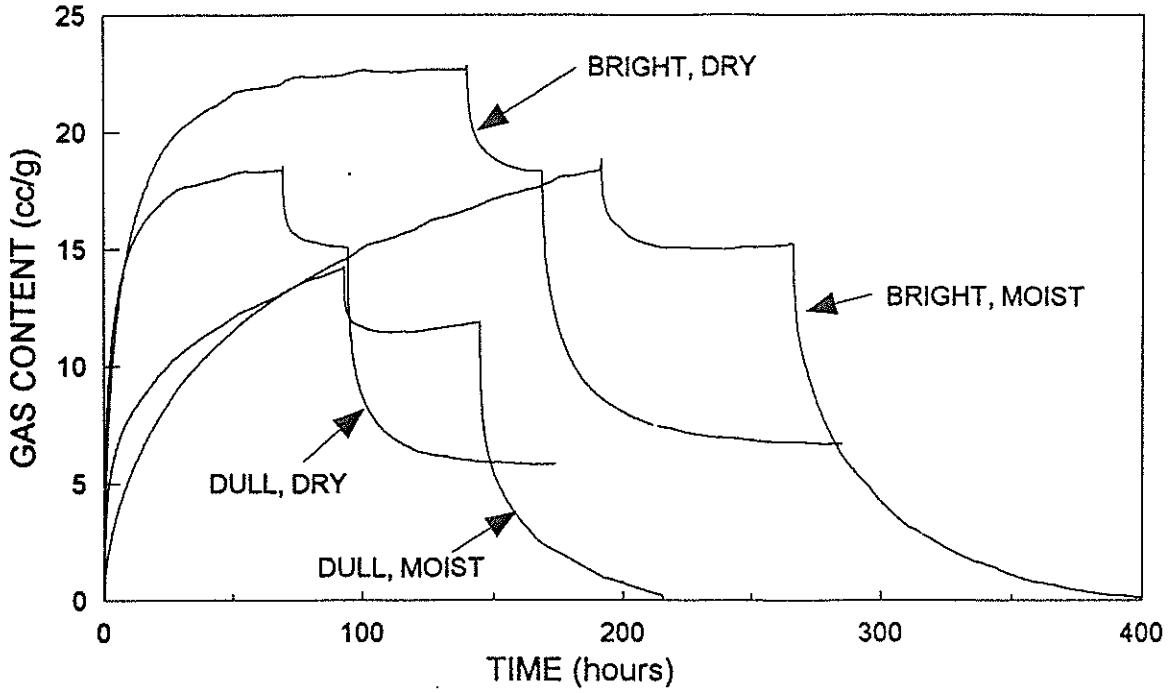

Figure 3.7 Central Colliery JCB12 lump samples (-5.60+2.00mm) showing methane sorption in equilibrium moist and dry raw coal. Initial adsorption at 5MPa is followed by pressure reduction to 2MPa and subsequent desorption to atmosphere. Moist samples are corrected for moisture loss during analysis.

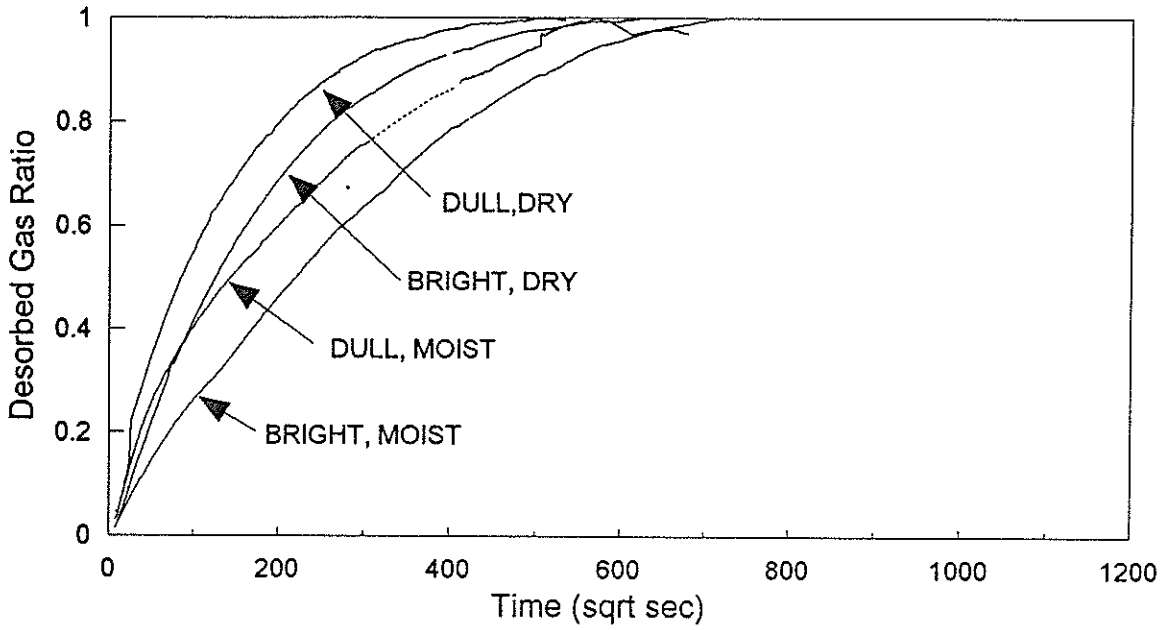

Figure 3.8 Central Colliery JCB12 lump samples (-5.60+2.00mm) showing methane desorption rate at atmospheric pressure after release from 2MPa.

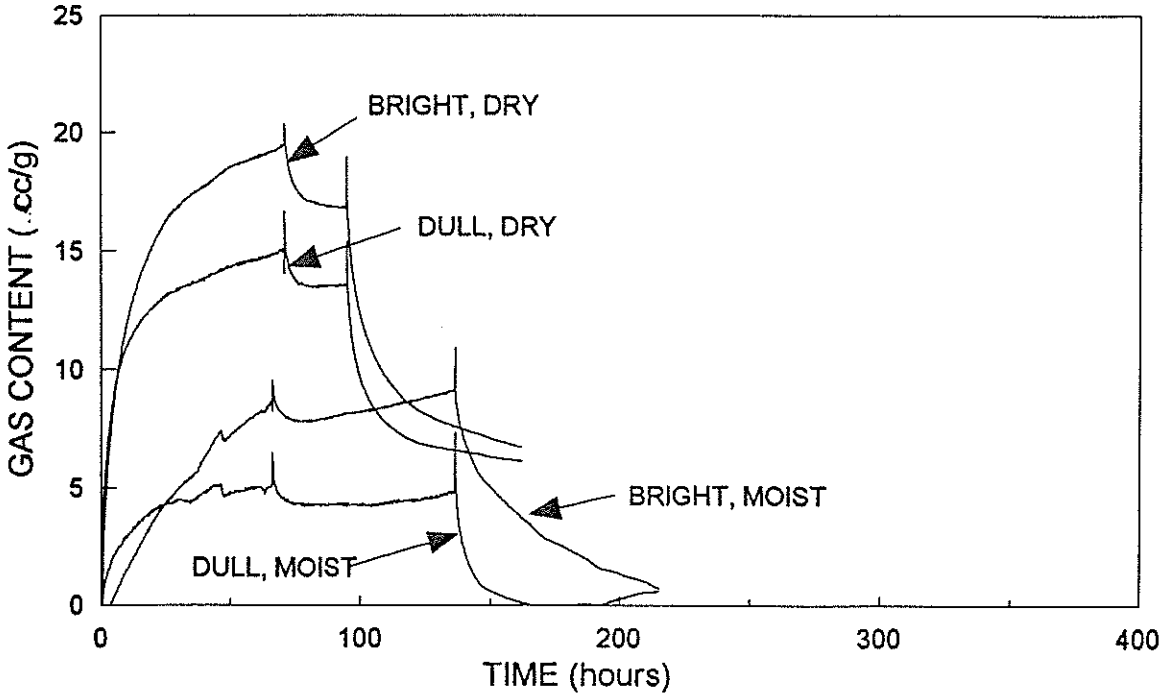

Figure 3.9 Central Colliery JCB21 lump samples (-5.60+2.00mm) showing methane sorption in equilibrium moist and dry raw coal. Initial adsorption at 5MPa is followed by pressure reduction to 2MPa and subsequent desorption to atmosphere. Moist samples are corrected for moisture loss during analysis. Vacuum has been applied to the dry sample after desorption to atmosphere.

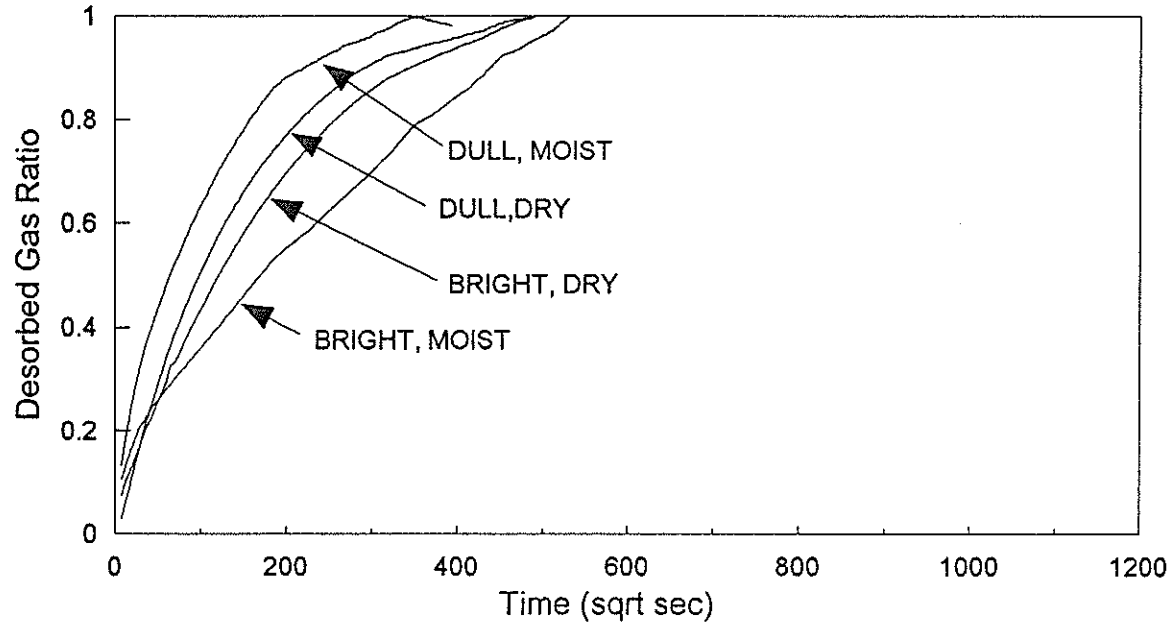

Figure 3.10 Central Colliery JCB21 lump samples (-5.60+2.00mm) showing methane desorption rate at atmospheric pressure after release from 2MPa.

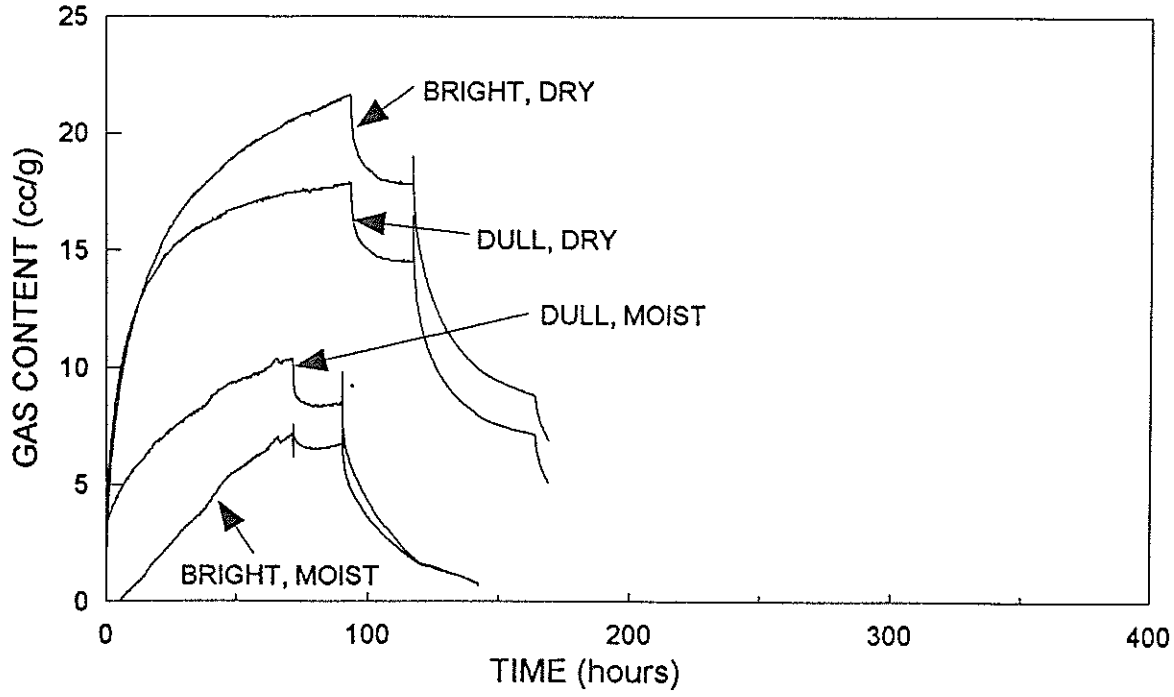

Figure 3.11 Central Colliery JCB82 lump samples (-5.60+2.00mm) showing methane sorption in equilibrium moist and dry raw coal. Initial adsorption at 5MPa is followed by pressure reduction to 2MPa and subsequent desorption to atmosphere. Moist samples are corrected for moisture loss during analysis.

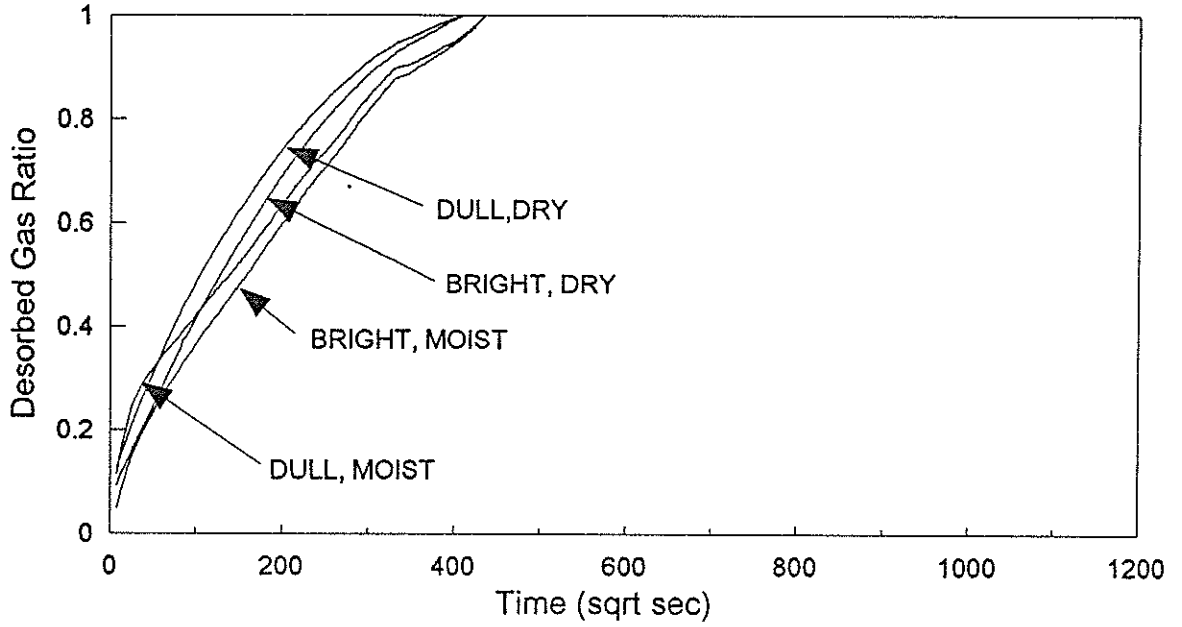

Figure 3.12 Central Colliery JCB82 lump samples (-5.60+2.00mm) showing methane desorption rate at atmospheric pressure after release from 2MPa.

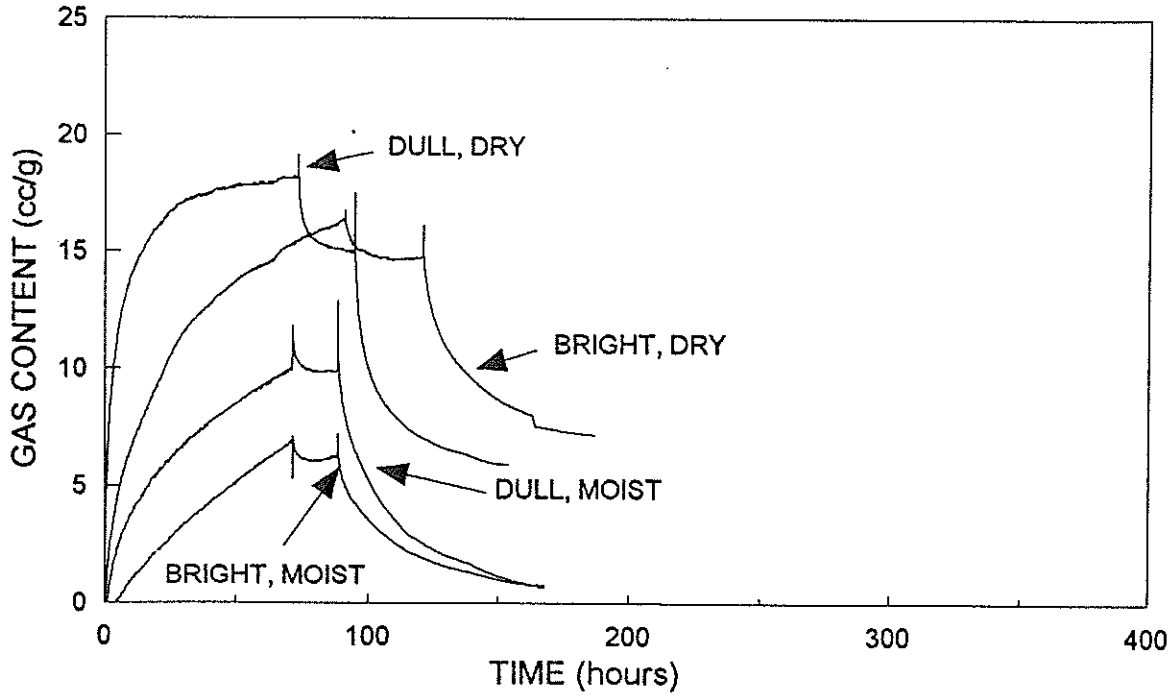

Figure 3.13 Central Colliery JCB92 lump samples (-5.60+2.00mm) showing methane sorption in equilibrium moist and dry raw coal. Initial adsorption at 5MPa is followed by pressure reduction to 2MPa and subsequent desorption to atmosphere. Moist samples are corrected for moisture loss during analysis. Vacuum has been applied to dry samples after desorption to atmosphere.

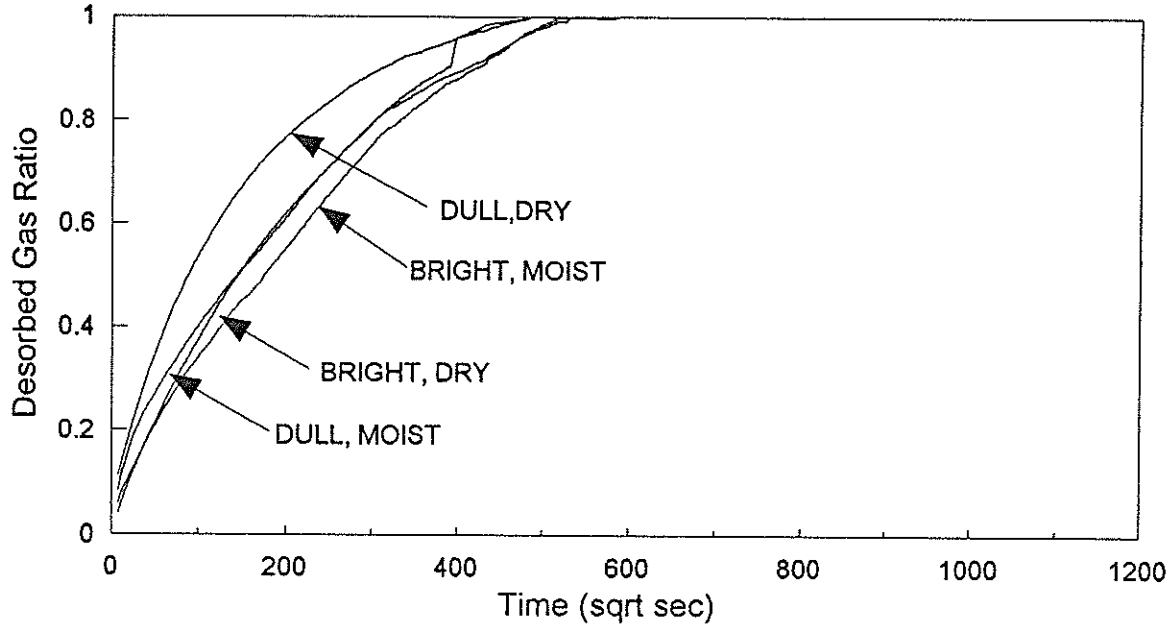

Figure 3.14 Central Colliery JCB92 lump samples (-5.60+2.00mm) showing methane desorption rate at atmospheric pressure after release from 2MPa.

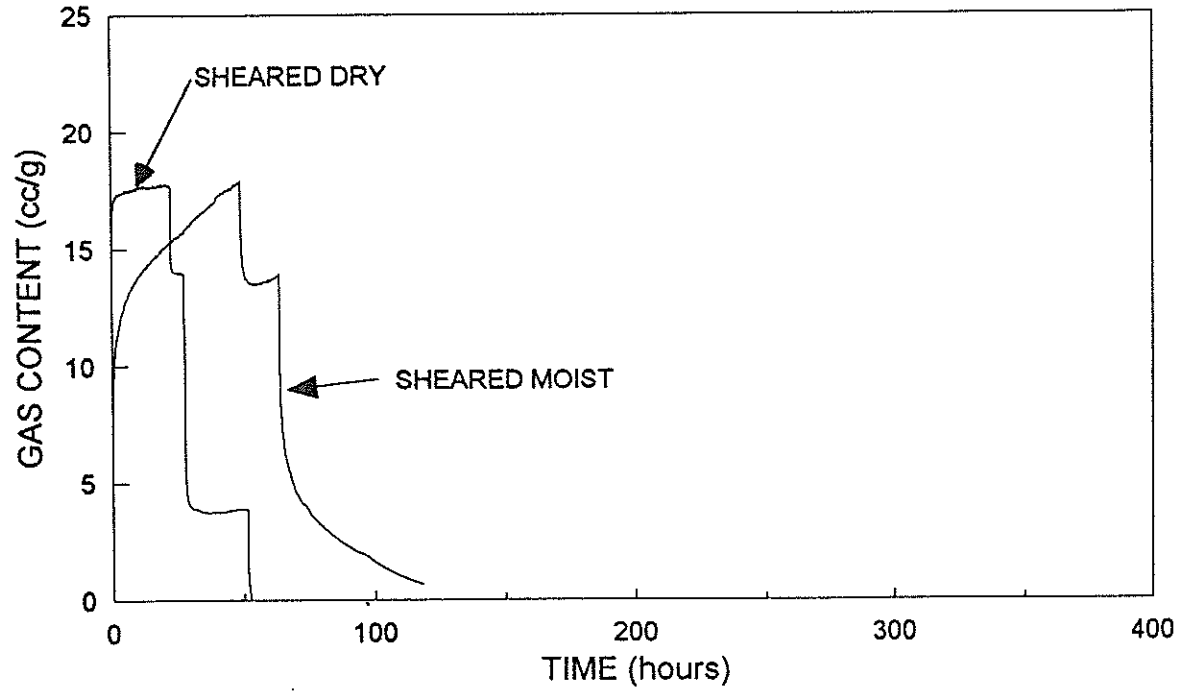

Figure 3.15 Central Colliery JCB95 lump samples (-5.60+2.00mm) showing methane sorption in equilibrium moist and dry raw coal. Initial adsorption at 5MPa is followed by pressure reduction to 2MPa and subsequent desorption to atmosphere. Moist samples are corrected for moisture loss during analysis.

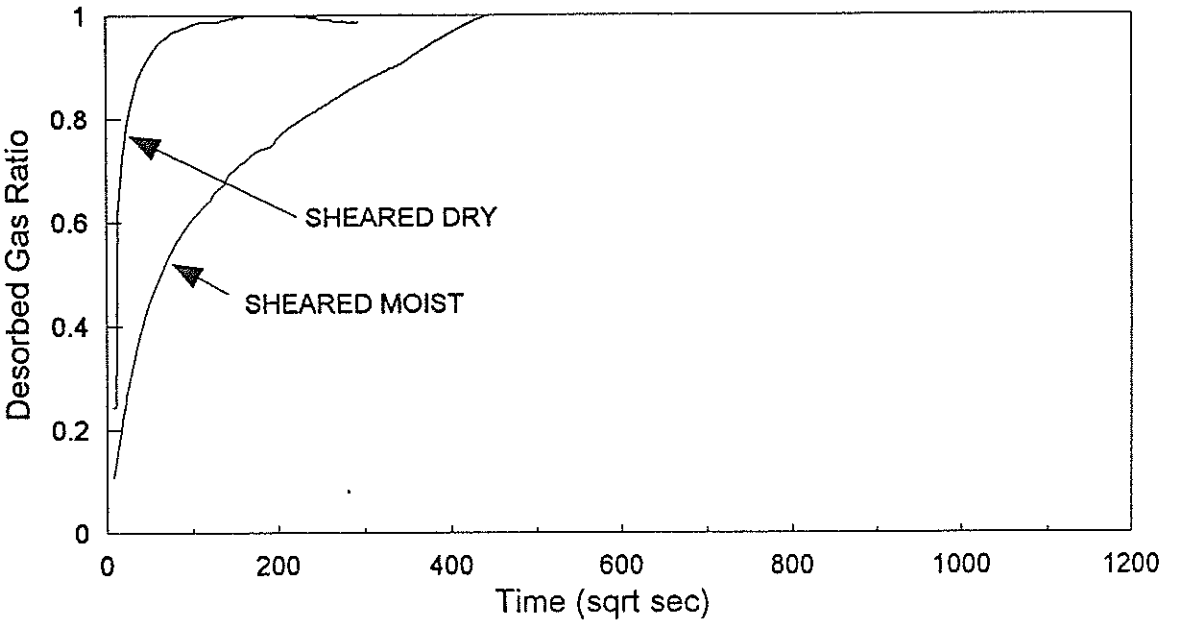

Figure 3.16 Central Colliery JCB95 lump samples (-5.60+2.00mm) showing methane desorption rate at atmospheric pressure after release from 2MPa.

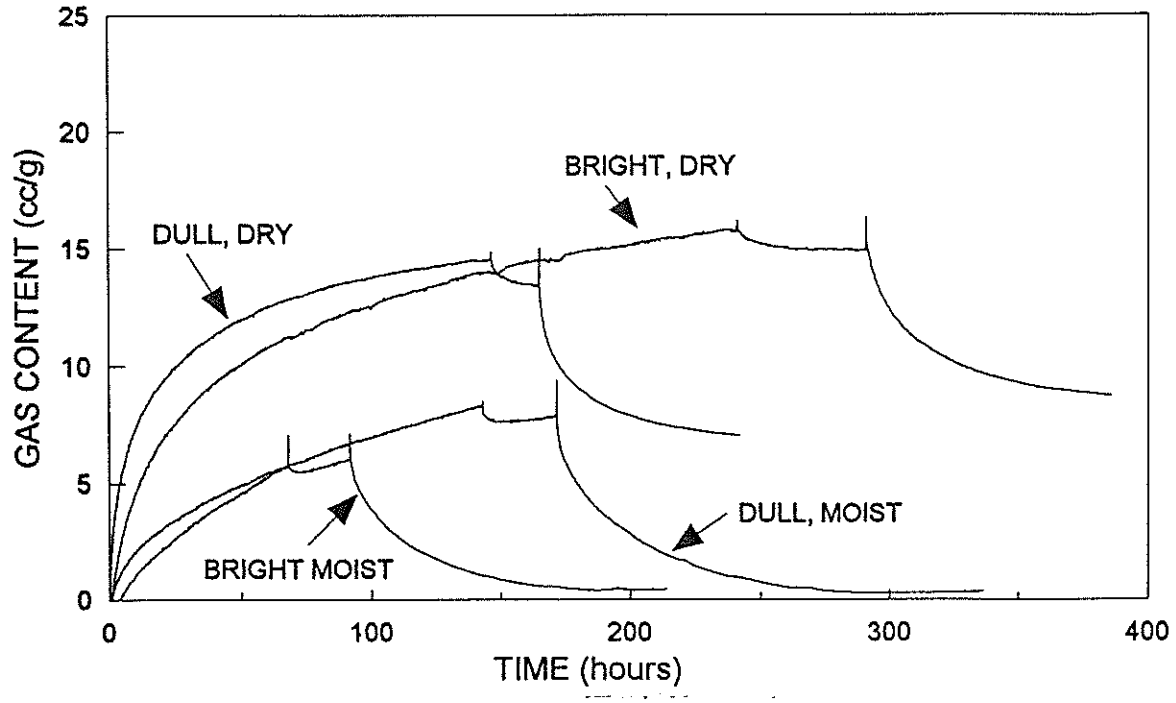

Figure 3.17 South Bulli Colliery JCB25D and JCB27B lump samples (-5.60+2.00mm) showing methane sorption in equilibrium moist and dry raw coal. Initial adsorption at 5MPa is followed by pressure reduction to 3MPa and subsequent desorption to atmosphere. Moist samples are corrected for moisture loss during analysis.

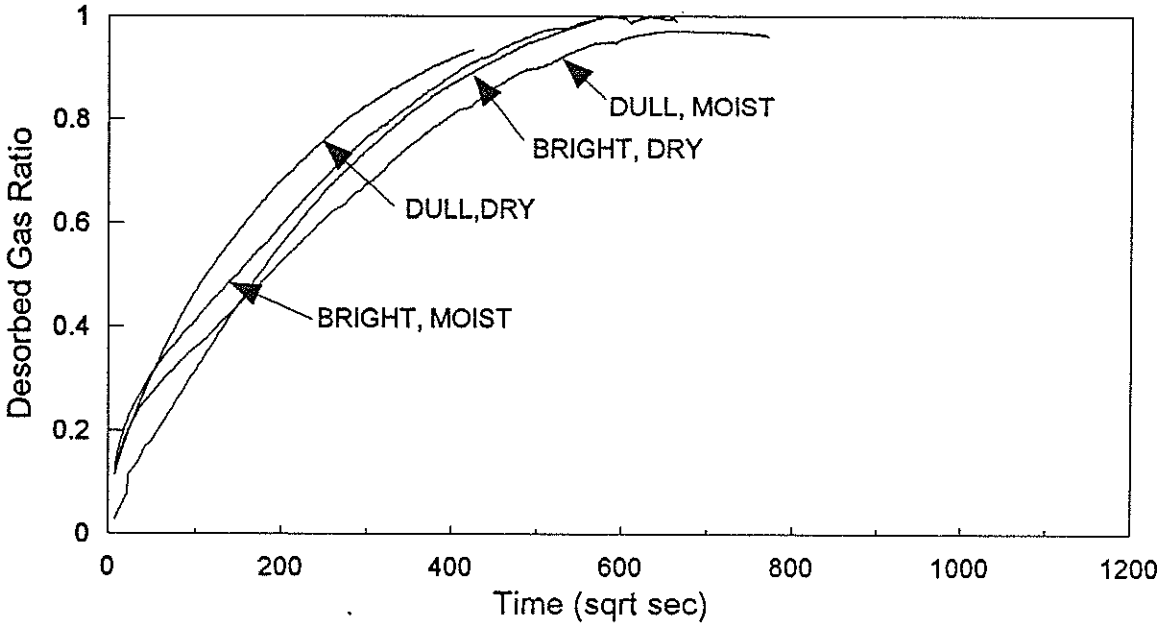

Figure 3.18 South Bulli Colliery JCB25D and JCB27B lump samples (-5.60+2.00mm) showing methane desorption rate at atmospheric pressure after release from 3MPa.

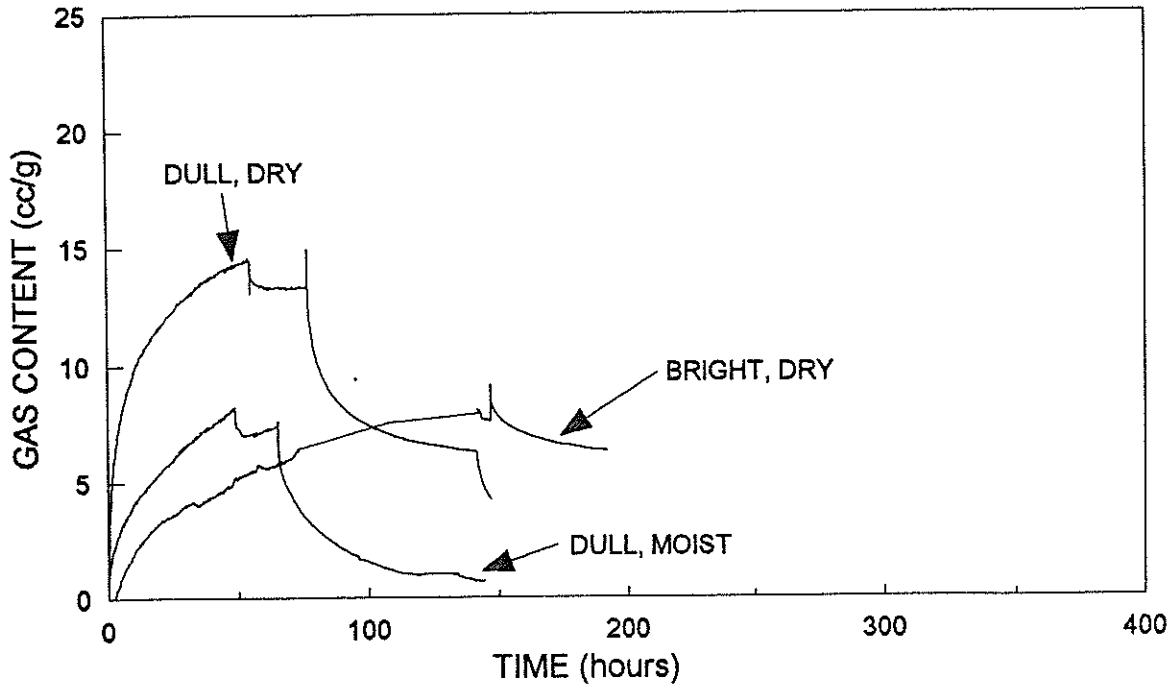

Figure 3.19 South Bulli Colliery JCB29B and JCB32D lump samples (-5.60+2.00mm) showing methane sorption in equilibrium moist and dry raw coal. Initial adsorption at 5MPa is followed by pressure reduction to 3MPa and subsequent desorption to atmosphere. Moist samples are corrected for moisture loss during analysis. Vacuum has been applied to dry samples after desorption to atmosphere.

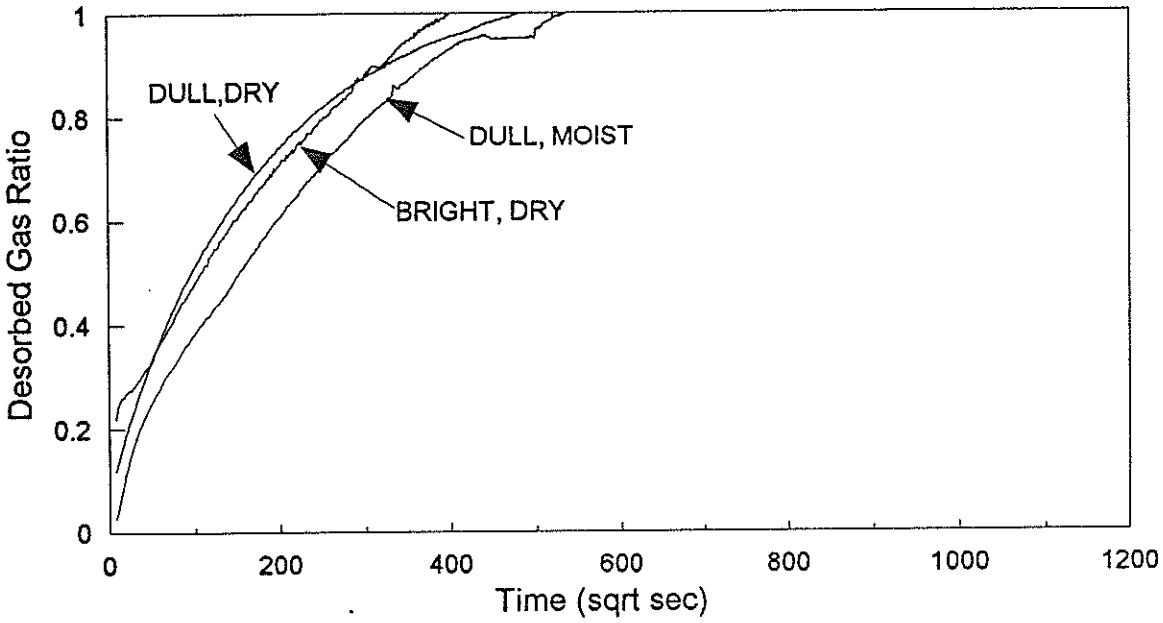

Figure 3.20 South Bulli Colliery JCB29B and JCB32D lump samples (-5.60+2.00mm) showing methane desorption rate at atmospheric pressure after release from 3MPa.

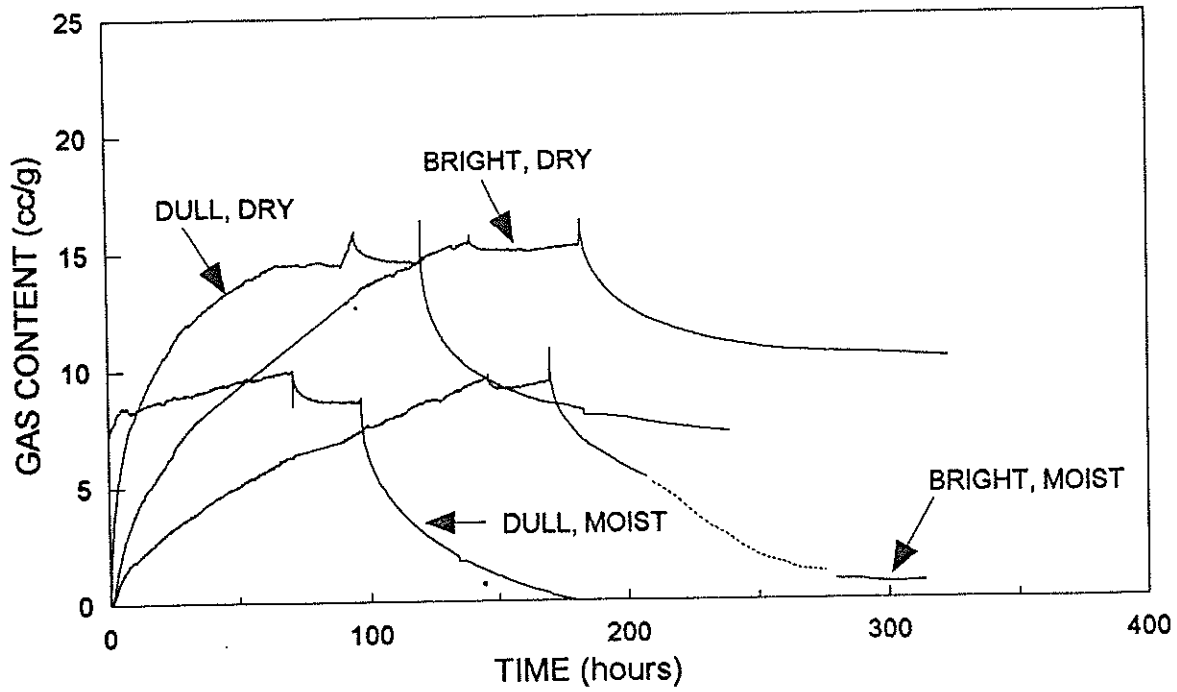

Figure 3.21 South Bulli Colliery JCB40B and JCB42D lump samples (-5.60+2.00mm) showing methane sorption in equilibrium moist and dry raw coal. Initial adsorption at 5MPa is followed by pressure reduction to 3MPa and subsequent desorption to atmosphere. Moist samples are corrected for moisture loss during analysis.

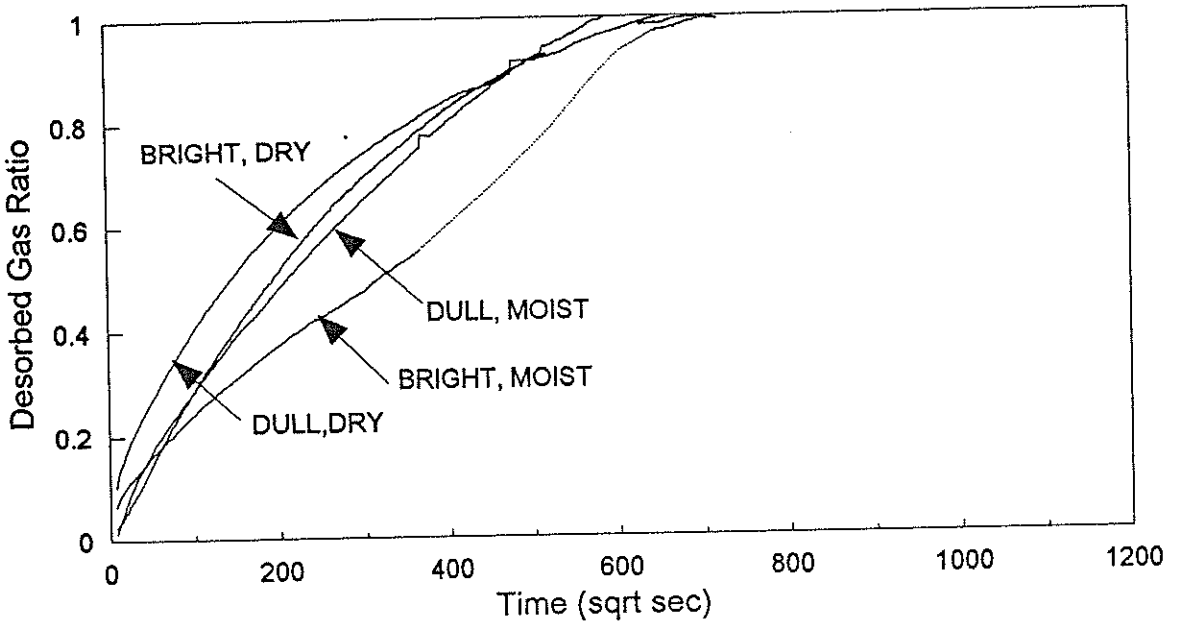

Figure 3.22 South Bulli Colliery JCB40B and JCB42D lump samples (-5.60+2.00mm) showing methane desorption rate at atmospheric pressure after release from 3MPa.

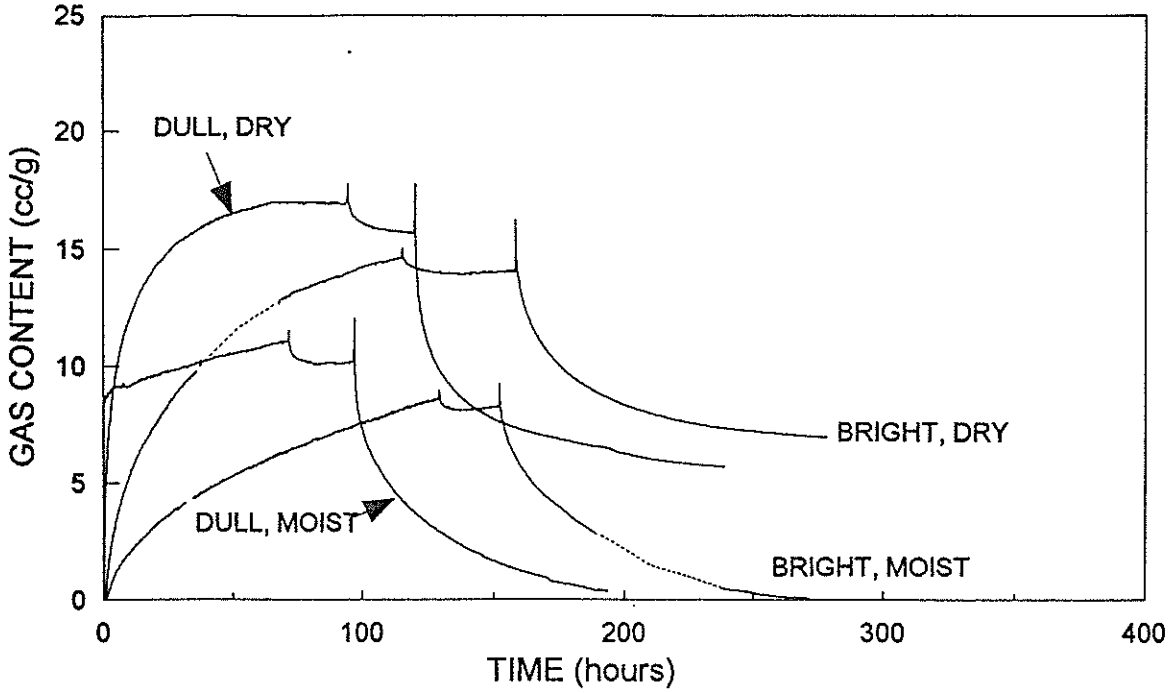

Figure 3.23 South Bulli Colliery JCB65D and JCB66B lump samples (-5.60+2.00mm) showing methane sorption in equilibrium moist and dry raw coal. Initial adsorption at 5MPa is followed by pressure reduction to 3MPa and subsequent desorption to atmosphere. Moist samples are corrected for moisture loss during analysis.

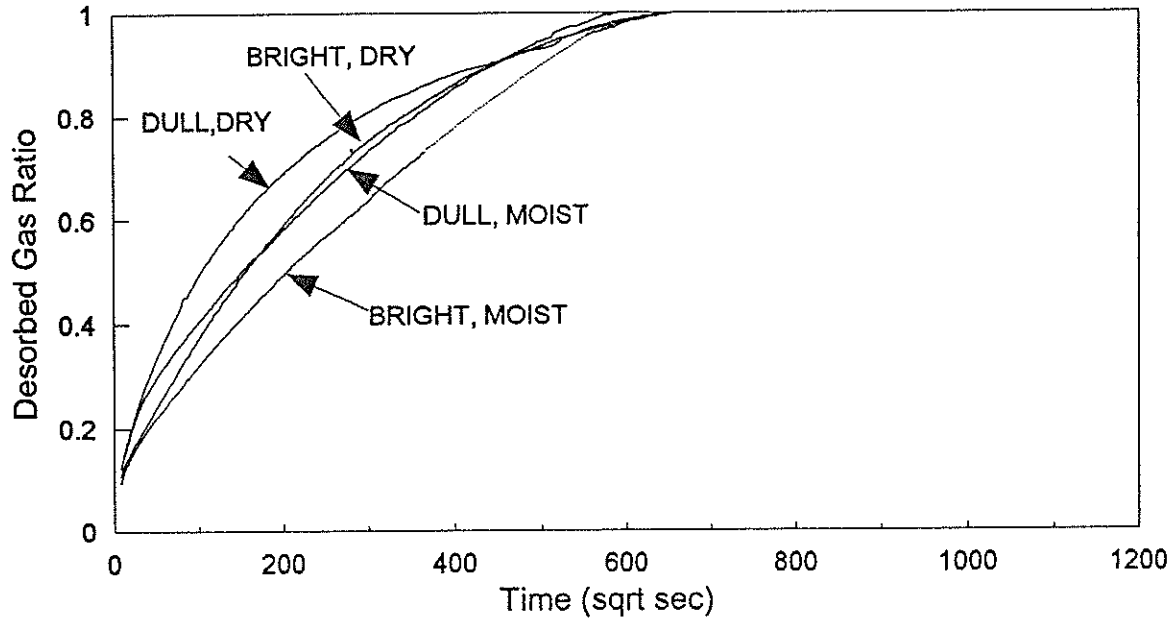

Figure 3.24 South Bulli Colliery JCB65D and JCB66B lump samples (-5.60+2.00mm) showing methane desorption rate at atmospheric pressure after release from 3MPa.

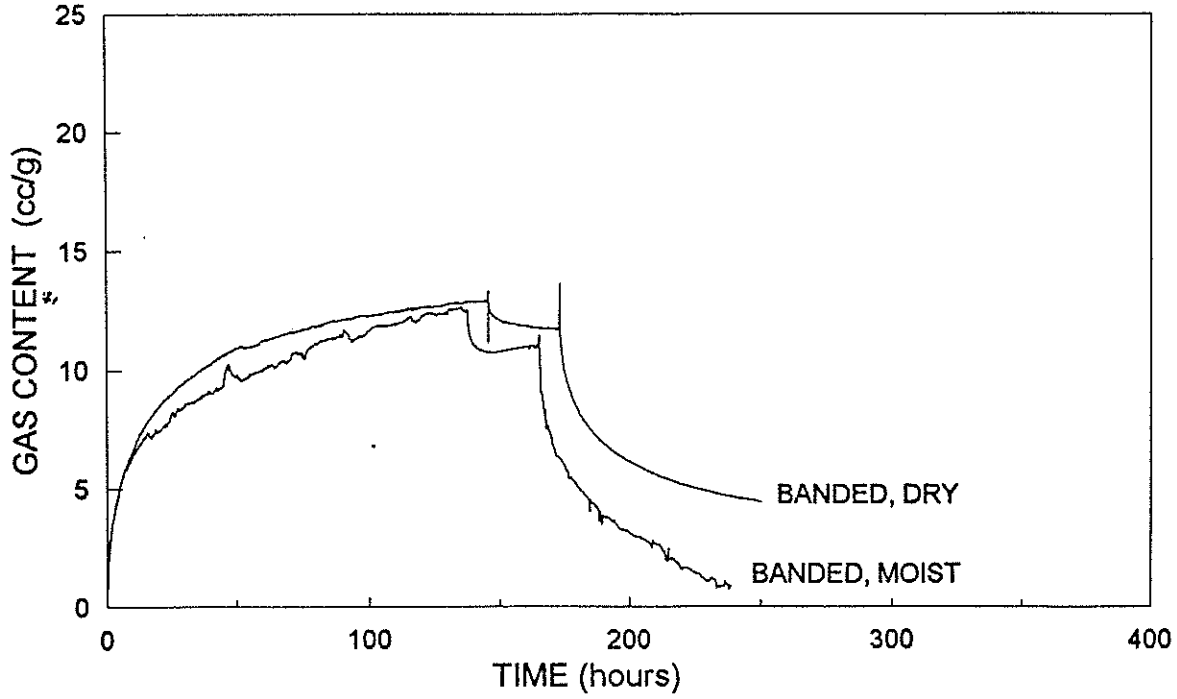

Figure 3.25 South Bulli Colliery JCB74BD lump samples (-5.60+2.00mm) showing methane sorption in equilibrium moist and dry raw coal. Initial adsorption at 5MPa is followed by pressure reduction to 3MPa and subsequent desorption to atmosphere. Moist samples are corrected for moisture loss during analysis.

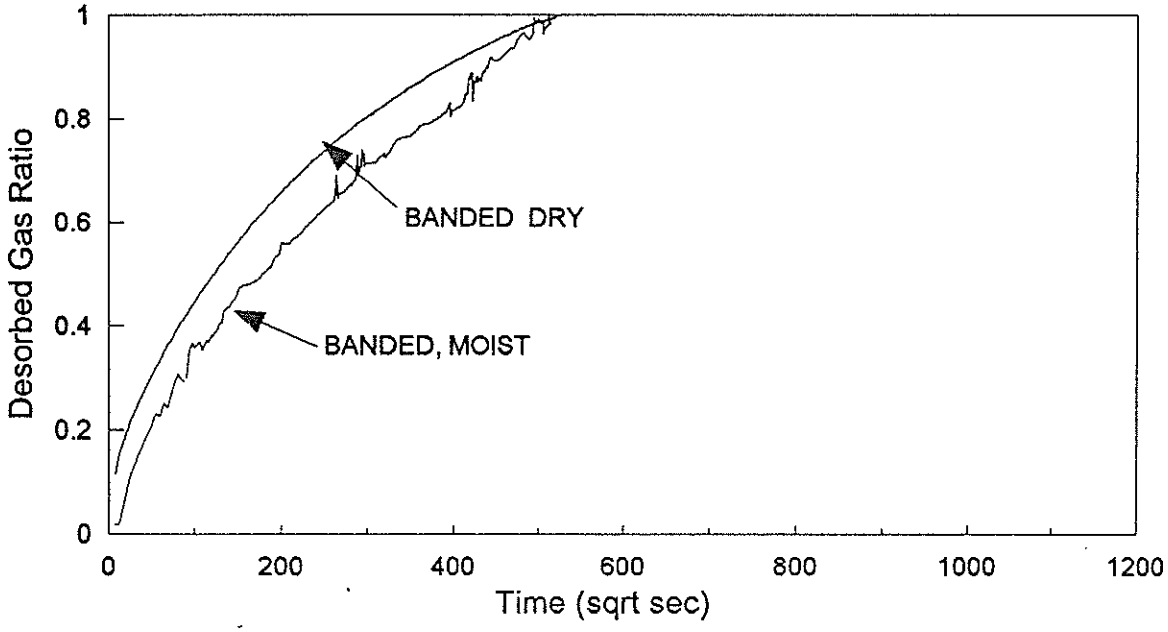

Figure 3.26 South Bulli Colliery JCB74BD lump samples (-5.60+2.00mm) showing methane desorption rate at atmospheric pressure after release from 3MPa.

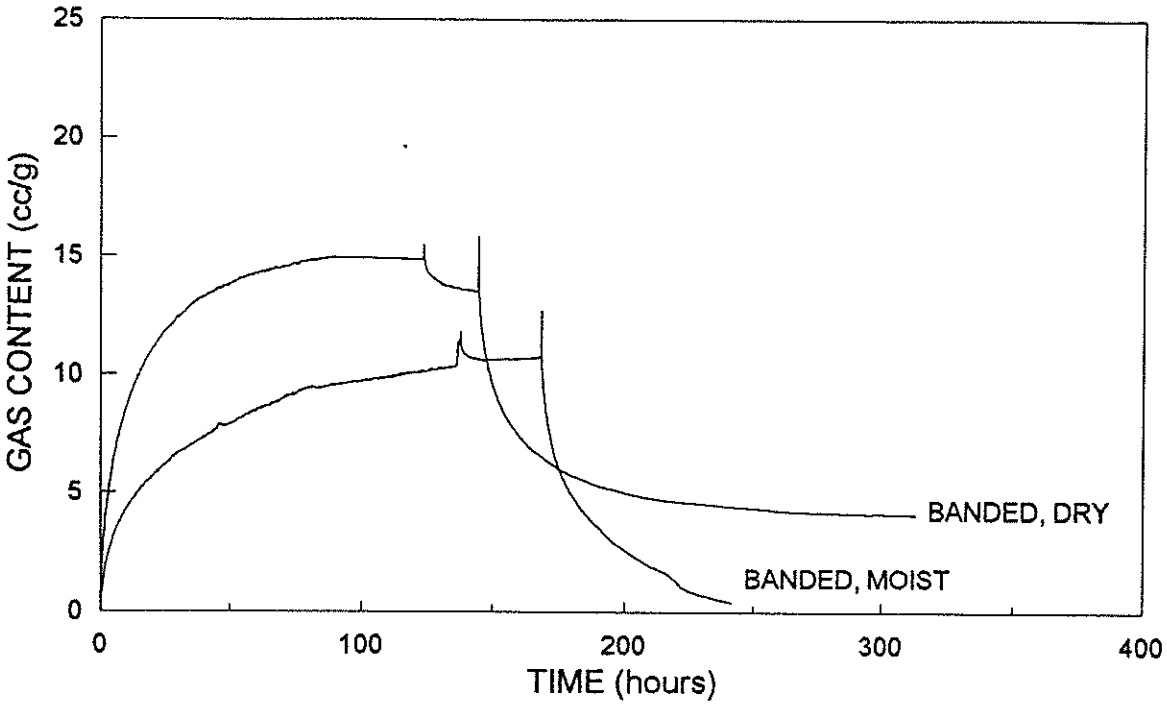

Figure 3.27 South Bulli Colliery JCB76BD lump samples (-5.60+2.00mm) showing methane sorption in equilibrium moist and dry raw coal. Initial adsorption at 5MPa is followed by pressure reduction to 3MPa and subsequent desorption to atmosphere. Moist samples are corrected for moisture loss during analysis.

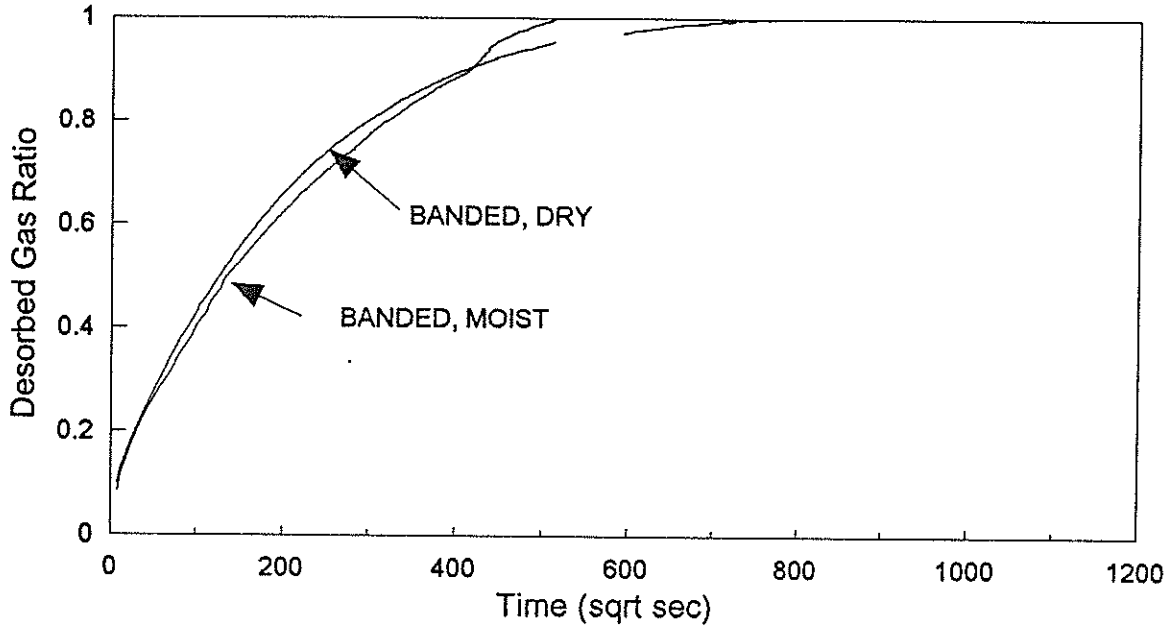

Figure 3.28 South Bulli Colliery JCB76BD lump samples (-5.60+2.00mm) showing methane desorption rate at atmospheric pressure after release from 3MPa.

3.4 Petrographic Analysis

Petrographic analyses are summarised in Table 3.5. Coal rank is such that most liptinites can no longer be recognised and only total liptinite is reported, the majority of which is resinite associated with telocollinite. Mineral types of clays, quartz, carbonates and pyrite were observed but only undifferentiated mineral matter (MM - undiff) is given. While cell lumina in inertinites are readily identified, recognition of mineralisation within them is difficult using reflected light microscopy, especially as most mineralisation appeared to be clays or quartz. However, mineralised (MM - lumina) and unmineralised (open lumina) are reported as these have an influence on the gas flow properties of the coal. Although a variety of macropore types were counted (Section 2) only results of cell lumina are reported. Unmineralised fracture systems could not be ascribed as being primary and may have resulted from sample preparation; these have been excluded from the analysis.

Whole coal samples from Central Colliery are representative splits of the bulk sample and can be used to evaluate the relative concentration of macerals in the hand picked bright and dull coal types. Relative to the whole coal, bright samples are enriched in vitrinites and depleted in inertinites and mineral matter. Conversely, the dull samples are enriched in inertinites but also show relative depletion of mineral matter as mineral bands are excluded during hand picking.

Bright coals from both Central and South Bulli Collieries are dominated by telocollinite (over 80%). More variable composition is observed at Central Colliery where a greater amount of mineral matter in the form of clays is found, often infilling cell lumina in telocollinite.

Dull coals are more variable in composition but show a significant depletion of vitrinite, especially telocollinite. Compared to South Bulli, Central Colliery samples contain more vitrinite with associated detrital mineral matter and less inertinite (Plates 3.1 - 3.6). However, the Central Colliery inertinites contain a greater proportion of preserved cell

lumina, most of which appear unmineralised.

Coal from the mid-seam shear zone at Central Colliery (JCB95 - sheared coal) is characterised by fine brecciation (Plates 3.7 and 3.8). Vitrinite has been classified as desmocollinite although the brecciation makes this difficult to substantiate and much may be crushed telocollinite. Mineral matter occurs both intimately associated with this brecciation and also forms discrete lenses around which the fractures anastomose. The intense fracturing is responsible for the very weak mechanical strength of the coal and provides numerous pathways for gas release. There is no optical evidence of secondary mineralisation infilling the fractures to restrict gas flow or provide additional mechanical strength.

Mean maximum reflectance values (Romax) are for telocollinite only and are therefore indicative of rank. In general, only bright coal types were measured as bright and dull coals from the same seam in the same locality will have the same degree of thermal maturation. Central Colliery has an average Romax of 1.72%, indicating a low volatile bituminous coal. South Bulli samples average 1.23%, which is typical of medium volatile bituminous coals. Reflectances are consistent with coal rank based on volatile matter determinations.

Table 3.5 Coal maceral composition (vol. %) and telocollinite reflectance

Sample	Lithotype[1]	Telocollinite	Desmocollinite	Total Vitrinite	Total Liptinite	Semifusinite	Fusinite	Inertodetrinite	Micrinite	Macrinite	Total Inertinite	MM (undiff)[2]	MM (lumina)[3]	Total MM	Open Lumina[4]	Total	Romax (%)
Central Colliery																	
JCB 4	whole coal	36.4	8.9	45.3	0.7	23.6	1.2	3.2	0.0	0.0	28.0	20.1	1.9	22.0	3.3	99.3	1.69
JCB4B	B	80.4	4.7	85.1	0.0	7.4	0.0	0.9	0.0	0.0	8.3	4.8	0.0	4.8	1.3	99.5	
JCB4D	D	13.1	22.6	35.7	0.0	40.0	0.1	8.0	0.0	0.0	48.1	11.1	1.1	12.2	3.5	99.5	
JCB 7	whole coal	39.0	9.5	48.5	0.0	10.4	1.0	2.1	0.0	0.0	13.5	36.0	0.5	36.5	0.6	99.1	1.75
JCB7B	B	92.7	3.4	96.1	0.0	0.5	0.5	0.1	0.0	0.0	1.1	2.5	0.0	2.5	0.0	99.7	
JCB7D	D	20.5	26.7	47.2	0.0	28.2	1.2	6.1	0.0	0.0	35.5	11.7	1.0	12.7	3.9	99.3	
JCB 9	whole coal	38.1	15.8	53.9	0.0	28.1	3.8	3.1	0.0	0.0	35.0	7.0	1.7	8.7	1.8	99.4	1.71
JCB9B	B	88.5	3.7	92.2	0.0	3.7	0.0	1.1	0.0	0.0	4.8	2.4	0.0	2.4	0.1	99.5	
JCB9D	D	9.2	21.7	30.9	0.0	45.4	1.4	2.9	0.0	0.0	49.7	7.5	4.5	12.0	6.9	99.5	
JCB 12	whole coal	32.5	18.7	51.2	0.0	16.9	3.2	2.5	0.3	0.3	23.2	21.1	0.9	22.0	2.6	99.0	1.73
JCB12B	B	83.3	9.0	92.3	0.0	3.0	0.3	1.1	0.0	0.0	4.4	2.6	0.1	2.7	0.1	99.5	
JCB12D	D	18.6	29.1	47.7	0.0	24.6	1.2	7.0	0.0	0.0	32.8	14.3	1.0	15.3	3.7	99.5	
JCB21B	B	96.6	1.1	97.7	0.0	0.7	0.1	0.1	0.0	0.0	0.9	1.0	0.0	1.0	0.0	99.6	
JCB21D	D	26.6	34.3	60.9	0.0	19.1	0.3	3.1	0.0	0.0	22.5	12.0	0.3	12.3	3.8	99.5	
JCB82B	B	95.5	2.0	97.5	0.0	1.8	0.1	0.0	0.0	0.0	1.9	0.3	0.0	0.3	0.0	99.7	
JCB82D	D	25.0	21.2	46.2	0.0	32.8	1.4	7.2	0.0	0.0	41.4	8.2	0.6	8.8	3.6	100.0	
JCB92B	B	89.2	5.7	94.9	0.0	1.4	0.5	0.5	0.0	0.0	2.4	2.2	0.1	2.3	0.0	99.6	
JCB92D	D	18.7	23.6	42.3	0.1	35.7	0.5	6.5	0.0	0.1	42.8	7.5	2.2	9.7	4.5	99.4	
JCB95	sheared	9.5	46.5	56.0	0.0	7.6	0.5	4.6	0.0	0.3	13.0	30.1	0.0	30.1	0.1	99.2	
South Bulli																	
JCB27B	B	94.9	0.7	95.6	3.5	0.1	0.0	0.3	0.0	0.0	0.4	0.1	0.0	0.1	0.0	99.6	1.28
JCB25D	D	0.5	1.3	1.8	0.1	75.1	1.3	9.7	0.0	0.0	86.1	2.3	6.6	8.9	2.4	99.3	
JCB29B	B	93.1	2.0	95.1	0.0	1.6	0.0	0.7	0.0	0.0	2.3	2.3	0.0	2.3	0.0	99.7	1.23
JCB32D	D	12.8	8.2	21.0	0.0	56.0	0.3	10.9	0.0	0.0	67.2	7.1	0.5	7.6	3.7	99.5	
JCB35B	B	83.0	8.1	91.1	0.0	4.4	0.0	3.7	0.0	0.0	8.1	0.6	0.0	0.6	0.0	99.8	1.25
JCB37D	D	0.0	10.2	10.2	0.0	53.7	0.0	26.5	0.0	0.0	80.2	3.3	0.1	3.4	5.8	99.6	
JCB40B	B	92.0	4.6	96.6	0.0	0.9	0.0	0.3	0.0	0.0	1.2	1.9	0.0	1.9	0.0	99.7	1.24
JCB42D	D	6.5	10.3	16.8	0.0	61.6	0.7	15.3	0.0	0.0	77.6	0.8	1.1	1.9	2.9	99.2	
JCB66B	B	98.4	0.7	99.1	0.0	0.1	0.0	0.3	0.0	0.0	0.4	0.1	0.0	0.1	0.0	99.6	1.30
JCB65D	D	0.8	2.6	3.4	0.1	73.3	2.8	14.5	0.0	0.0	90.6	0.3	2.1	2.4	3.1	99.6	1.24
JCB74BD	BD	9.4	25.0	34.4	0.0	47.3	0.0	8.0	0.0	0.0	55.3	3.5	0.1	3.6	6.3	99.6	1.16
JCB75BD	BD	21.0	35.1	56.1	0.2	29.1	3.2	4.3	0.0	0.1	36.7	1.8	1.4	3.2	3.2	99.4	1.16
JCB76BD	BD	61.1	20.2	81.3	0.0	10.8	0.6	1.6	0.0	0.0	13.0	4.4	0.4	4.8	1.0	100.1	1.24

1. B = bright; D = dull; BD = banded in inertinite
2. undifferentiated mineral matter
3. mineral matter within cell lumina in inertinite
4. unmineralised cell lumina

3.5 Pore Characterisation and Surface Area

Selected samples have been characterised by CO_2 and N_2 surface areas as well as for pore distribution by mercury porosimetry (Table 3.6). Density values are given for both raw coal and recalculated to a daf basis (van Krevelen, 1961) :

$$d_{daf} = \frac{(100 - A)\, d_t\, d_a}{(100\, d_a - d_t\, A)}$$

where A = weight percent ash
d_{daf} = density of the dry, ash free coal
d_a = average density of the ash constituents (= 3g/cc; van Krevelen, 1961; Beamish et al., under review)
d_t = true density of the ash containing coal

Calculated values of total pore volume represent pores less than 20μm in diameter and are estimated by the difference of the density of the coal determined in helium and mercury :

$$\text{Total pore volume} = 1/\rho_{Hg} - 1/\rho_{He}$$

Percent total porosity of the dry, ash free coal is determined from the calculated total pore volume times the mercury density (daf).

Determination of surface area by CO_2 adsorption is thought to give the best representation of the internal surface area of the coal as it has maximum penetration of the micropore network. Nitrogen has poorer penetration of the micropores and gives consistently much lower surface areas. The surface areas reflect the micro-pore surface area, which is the site of methane adsorption in the coal.

For the samples examined, bright coal surface areas are larger than their equivalent dull coal (Table 3.6). Central Colliery bright coals have larger surface areas than South Bulli Colliery brights but no regular difference is found for the dull coals. The larger surface areas for Central are consistent with increased microporosity associated with

higher rank.

Mercury intrusion gives information on pore size distribution. Mercury will fill pores down to about 20μm in diameter at atmospheric pressure. This allows the total volume of pores less than 20μm in diameter to be determined by difference with the helium density, which assumes helium fills all available porosity (Table 3.6). Under pressure, mercury will intrude pores down to 36Å in size, which represents the macro- and meso-porosity of the coal. Mercury intrusion results therefore reflect characteristics of the macro- and meso-pore systems (the pores in which free flow occurs during methane desorption).

Total intrusion volumes for the Central and South Bulli coal types show no regular pattern (Table 3.6). Total pore areas are consistently larger for bright coals than their equivalent dull coal but no systematic variation is observed between Central and South Bulli Collieries. Histograms of the mercury intrusion data indicate a bimodal distribution for pores larger than 36Å. Most pores occur around a mode at 7 to 9nm which is toward the lower limit of the intrusion data. For both South Bulli and Central Collieries, a small proportion have a mode centred on 5μm. For bright coals this represents 3 to 5% of the total porosity while for dull coals it is 8 to 11% of the total porosity

Table 3.6 Surface area and pore characterisation mercury porosimetry and helium density.

Sample	Surface Area		Helium density		Mercury density		Mercury Intrusion				Calculated	
	CO_2 (m^2/g)	N_2 (m^2/g)	dry (cc/g)	daf (cc/g)	dry (cc/g)	daf (cc/g)	Total Intrusion Volume (cc/g)	Total Pore Area (m^2/g)	Mean Pore Diameter (nm)	Porosity (%)	Total Pore Volume (cc/g, daf)	Porosity (%) (daf)
Central Colliery												
JCB21B	228	1.28	1.350	1.324	1.289	1.264	0.0422	20.411	8.3	5.44	0.036	4.56
JCB21D	186	1.42	1.477	1.366	1.454	1.343	0.0351	15.421	9.1	5.10	0.013	1.70
JCB82B	225	1.28	1.356	1.343	1.278	1.265	0.0408	19.685	8.3	5.22	0.046	5.79
JCB82D	185	1.42	1.524	1.414	1.434	1.325	0.0339	15.689	8.6	4.86	0.048	6.33
JCB92B	247	1.88	1.367	1.352	1.289	1.274	0.0391	19.104	8.2	5.04	0.045	5.78
JCB92D	206	2.52	1.514	1.346	1.441	1.274	0.0401	16.555	9.7	5.78	0.042	5.34
South Bulli Colliery												
JCB27B			1.430	1.423	1.268	1.261	0.0893				0.090	11.37
JCB25D			1.560	1.403	1.360	1.207	0.0943				0.116	14.02
JCB29B	210	1.29	1.319	1.306	1.261	1.248	0.0383	18.675	8.2	4.83	0.036	4.46
JCB32D	191	3.12	1.531	1.434	1.434	1.337	0.0373	16.598	9.0	5.35	0.051	6.76
JCB40B	215	1.39	1.381	1.351	1.287	1.257	0.0368	17.960	8.2	4.73	0.055	6.96
JCB42D	208	2.33	1.428	1.356	1.354	1.282	0.0372	17.188	8.7	5.04	0.042	5.44
JCB66B			1.320	1.311	1.280	1.271	0.0237				0.024	3.05
JCB65D			1.430	1.360	1.380	1.311	0.0253				0.028	3.65
JCB74BD	179	1.41	1.396	1.291	1.346	1.241	0.0375	16.908	8.9	5.04	0.031	3.84

3.6 Microstructural Studies by R.G. Riel

Detailed results, including photographs and figures, are given as Appendix 8.2. Analytical procedure and sample descriptions are given below.

3.6.1 Procedure

Specimens were examined optically at up to 40X magnification. Sample size was highly variable; where only a few small fragments were available, all were mounted for examination. Larger specimens were divided into representative pieces and mounted to facilitate analysis of significant cleat systems, textures, or other features of interest. Where only two or three small pieces were supplied for analysis, all were mounted; orientation was adjusted to optimise viewing of features such as cleat systems or texture variations likely to impact gas desorption kinetics.

Each specimen was mounted on an aluminium stub using a carbon paste adhesive. These were coated under vacuum with 200-300 angstroms evaporated carbon to enhance electrical conductivity. Examination was made on a JEOL JXA-840A Scanning Electron Microprobe at 25 kV accelerating voltage. Probe current and working distance were variable. Energy Dispersive Spectroscopy (EDS) was used to chemically characterise features of interest.

3.6.2 Results

Evaluation of probable sorption behaviour of each specimen is complicated by the small volume of some specimens, the possibility that some specimens may not be representative of bulk material, difficulty in determining microstructural orientation, and the lack of classification for bulk specimens. As some specimens had been crushed and possibly sized, certain microstructures may have been selectively preserved while others were damaged or removed. Summaries of data for Central and South Bulli Collieries are provided in Tables 3.7 and 3.8 respectively, and these compilations list

the pertinent photographs supporting interpretation. A description of each sample's most prominent microstructural features is provided below.

Central Colliery

Sample JCB21B. Five small fragments were available for analysis. Optically, no face/butt cleat system could be defined, however numerous closely spaced cleats bearing reddish infill were observed. Three pieces were mounted for SEM examination; study of these revealed a dominant system of open cleats 5-15 μm wide arbitrarily categorised as face cleats, and a curvilinear 3rd cleat system tightly infilled with clay. No butt cleats were observed. The open cleat system argues for respectable permeability, while clay nodules argue against.

Sample JCB21D. A single piece of coal was provided for analysis; it was mounted for examination on the SEM in transverse section. Loosely infilled microcleats were noted perpendicular to the bedding plane. The overwhelming bulk of this material was either highly compressed dull coal or matrix clay, neither of which support good sorption kinetics. Behaviour of this dull coal is almost certainly strongly class B.

Sample JCB82B. Four small pieces of bright coal were supplied, of which three were mounted for SEM analysis. No cleat systems were preserved, however the volume of matrix clay was high, consisting of both Si-Al clay and calcium phosphate. One might infer from the amount of clay present in the bright coal that sorption kinetics were not particularly fast.

Sample JCB82D. Four pieces of dull coal were available for analysis, of which 3 were examined on the SEM. The specimen consisted entirely of either highly compressed dull coal, heavily infilled, or matrix clay rich in carbonates, from which Class B sorption behaviour may be inferred.

Sample JCB92B. Of three pieces bright coal available, two were mounted for SEM

examination, one in plan view and the other in transverse orientation. Two distinct cleat types were observed, or a single cleat system sometimes open, sometimes infilled with amorphous calcium sulfate. Open conchoidal fractures were noted. This specimen might represent Class A material by reason of open cleats and a lack of clay infill, although this interpretation is far from certain.

Sample JCB92D. All three pieces of dull coal provided were examined on the SEM. A small amount (5%) of open sieve structure was observed, however the balance of this specimen was highly compressed and tightly infilled, suggesting Class B behaviour.

Sample JCB95(sheared). This specimen consisted of a single large fragment which was broken into 3 pieces for SEM analysis. Although no dominant cleat system was observed, the sample was bounded by smooth, slickensided shear planes which contained a series of steps and striations. They had a mottled appearance due to chemical inhomogeneity of the sample. Surfaces normal to the shear planes were extremely rough. In the vicinity of the bounding shears occurred sets of closely spaced, sub-parallel fractures with significant porosity, which accounted for the stepped appearance. Other shear planes and fracture systems cut the sample at an angle of approximately 30 - 45° to the bounding shears at 1 to 2mm spacings. Surface roughness was caused by a highly irregular fracture through mineral dominated matrix and along grain boundaries, although individual grains were often difficult to observe. Coal/mineral grains were less 20μm in diameter and had significant associated intergranular porosity, with individual pores up to 5μm in diameter. Mineral matrix had high chemical variablity from point to point. Sorption kinetics for this specimen might well be typical of Class A coal based on the high degree of intergranular porosity and its likely high degree of interconnectivity as well as the unmineralised fracture network.

South Bulli Colliery

Sample JCB25D. A single piece of coal was provided for analysis; it was broken into two sections for SEM analysis. The specimen contained a high fraction of matrix clay

(15%), and the remaining dull coal was either highly compressed or bogen compressed in structure, heavily infilled. Sorption behaviour for this material would most probably be typically Class B.

Sample JCB27B. Although only four small fragments were available for inspection, at least two discrete cleat systems were visible optically. These were too distorted to make a standard face cleat/butt cleat system, however one set of cleats was tightly infilled with Si-Al-K clay, while the other was open. Class A behaviour is possible for this coal, though far from demonstrated.

Sample JCB29B. Four pieces were available for analysis, however each was a relatively solid fragment whose sides may once have been cleats. Optical and SEM examination revealed a single cleat system tightly infilled with Si-Al clay. Too little information was available from this specimen to support a guess as to sorption behaviour.

Sample JCB32D. All four small fragments were mounted for SEM examination. A small amount (5%) of open sieve microstructure was observed, however the balance of this specimen was characterised as either highly compressed or bogen compressed, heavily infilled with Si-Al-K clay. As 10% by volume was Si-Al-K matrix clay, sorption behaviour of this sample is most likely Class B.

Sample JCB40B. This specimen was similar to JCB29(B) in that each of the 3 pieces supplied for analysis was a relatively solid fragment whose sides may once have been cleats. In addition to conchoidal fracture, SEM analysis identified one very narrow but open cleat system (which may have been an artefact of fracture during preparation) and two infilled cleat systems (or a single cleat system with two types of infill). Insufficient information was available to hazard a guess regarding sorption behaviour.

Sample JCB42D. Three of four small pieces were mounted for SEM analysis. Thick bands of matrix clay parallel to the bedding plane were noted, and the overwhelmingly

predominant microstructure was highly compressed dull coal tightly infilled with Si-Al-K clay. Sorption behaviour of such coal would be very much Class B.

Sample JCB65D. This specimen consisted of a single large piece which was mounted whole for SEM analysis. A loosely infilled 3rd cleat system was observed, but the microstructure was predominantly highly compressed, infilled with either Si-Al-Ca clay or Sr-Ba phosphates. Gas sorption would probably tend more to Class B than Class A.

Sample JCB66B. A single large fragment was supplied; this was broken into several smaller pieces of which two were mounted for SEM examination, one in transverse view, the other in plan view. A single macrocleat system was observed, fairly narrow, and tightly infilled. Vertical microcleats, also infilled, were observed in various orientations. Although very little information is available for this sample, nothing observed either optically or on the SEM would support an interpretation of rapid sorption or desorption kinetics.

Sample JCB74BD. A single large fragment was available for analysis. Optically, numerous cleats were visible at 40X or below, some infilled with red material, others with white. The specimen proved highly friable. Two sections were mounted for SEM analysis to provide both plan and transverse views of the microstructure. Two cleat systems were apparent; even though they were not oriented perpendicular to one another, one was large and infilled, while the other was smaller and open, suggesting a face cleat/but cleat relationship. A third cleat (possibly a face cleat extending from bright through dull coal) was also noted. Dull coal was highly compressed, and contained a very large fraction of matrix clay (both Si-Al clay and rutile). The highly friable texture of this specimen precluded an accurate classification, although banded would not be far from the truth. In any case, the high percentage of matrix clay in the dull coal (40%) strongly suggests Class B behaviour for this sample.

Table 3.7 Microstructural characteristics of samples from Central Colliery.

Samples		Microstructural Characteristics					Sorption	Photos (Appendix 8.2)	
Sample No.	Coal Type	Feature Type	Orientation	Proportion (%)	Width (μm)	Infilling (type/morphology/tightness/major elements)	Permeability	Figure	Photo No.
JCB21B	Bright		Side View					1	2156
			Plan View					1	2151
		Face Cleat	90° Bedding		5-15	Open	High	1	2154
		3rd Cleat	90° Bedding, Curvilinear		10-30	Clay/Grains&flakes/tight/Si,Al	Low	2	2153
		Inclusion	Random		1-10	Clay/Grains/tight/Si,Al plus Na,Cl	Low	2	2157
JCB21D	Dull		Side View					3	2152
		Vertical microcleat	⊥ Bedding		< 3	Clay/grains/loose/Si,Al	Low	3	2153
		Highly Compressed	0° Bedding	70	1-5	Clay/grains/tight/Si,Al, Trace S, K, Ti	Low	4	2156,7
		Matrix Clay	0° Bedding	30	1-10	Clay/grains/loose/Ca,S, Trace Si, Al, Mg, Na	Low	5	2154,5
JCB82B	Bright		Side View					6	8201,2
			Plan View					6	8205
		Matrix Clay	0° Bedding	10	1-15	CaP/grains/tight/Ca,P, + Clay/grains/tight/Si,Al	Low	7	8203,4
JCB82D	Dull		Side View					8	8251,2,6
		Highly Compressed	Random	85	1-5	Clay/grains/tight/Si,Al, trace K	Low	9	8253
		Matrix Clay	0° Bedding	15	1-10	Clay/grains/tight/Si,Al + carbonate/grains/tight/Fe,Ca,Mg	Low	9	8254
JCB92B	Bright		Side View					10	9201
		Face Cleat	90° Bedding		5-10	CaS/amorphous/tight	Low	10	9202
		Face Cleat	90° Bedding		5-10	Open	High	10	9205
		Conchoidal	Random		10-20	Open	Low	11	9203
JCB92D	Dull		Side View					12	9251
		Highly Compressed	Random	80	1-10	Clay/grains/loose/Si,Al	Low	12	9253
		Bogen Compressed	0° Bedding	5	1-5	Clay/grains/loose/Si,Al	Low	12	9254
		Sieve	0° Bedding	5	10-30	Open	High	12	9256
		Matrix Clay	0° Bedding	10	1-10	Clay/grains/tight/Si,Al	Low	13	9252,55
JCB95	sheared		Side View					14	9501,2
		Nodule	Random		<1-5	Crystals/loose/Sr,Ba,S,Al, trace Ca,Fe,Na	Mod	15	9503
		Dull Coal	Random			Clay/amorphous/loose/Si,Al,K, trace Ca,Fe,S	High	15-19	9504,6, 10-17

Table 3.8 Microstructural characteristics of samples from South Bulli Colliery.

Samples		Microstructural Characteristics					Sorption	Photos (Appendix 8.2)	
SampleNo.	Coal Type	Feature Type	Orientation	Proportion (%)	Width (µm)	Infilling (type/morphology/tightness/major elements)	Permeability	Figure	Photo No.
JCB25D	Dull		Side View					20	2501,2
		Highly Compressed	Random	80	< 3	Clay/grains/tight/Si,Al,K	Low	20	2504
		Bogen Compressed	0° Bedding	5	1-5	Clay/grains/tight/Si,Al,K,Ti	Low	21	2505,6
		Matrix Clay	Random	15	1-10	Clay/grains/tight/Si,Al,K,Ti, +BaP crystals	Low	22	2503
JCB27B	Bright		Plan View					23	2701,2,6
		3rd Cleat	90° bedding		10-20	Clay/amorphous/tight/Si,Al,K	Low	24	2703
		4th Cleat	90° bedding		10-20	Open	High	24	2704
JCB29B	Bright		Side View					25,26	2901,2,3
		3rd Cleat	Unknown		3-7	Clay/amorphous/tight/Si,Al	Low	27	2905,6
JCB32D	Dull		Overviews					28	3201,6
		Highly Compressed	Random	80	1-5	Clay/grains/tight/Si,Al,K	Low	29	3202,3
		Bogen Compressed	0° Bedding	5	5-20	Clay/grains/tight/Si,Al,K	Low	30	3204,5
		Sieve	0° Bedding	5	1-10	Clay/grains/open	High	31	3207
		Matrix Clay	0° Bedding	10	1-20	Clay/grains/tight/Si,Al,K	Low	31	3206
JCB40B	Bright		Overview					32	4001
		3rd Cleat	90° bedding		< 1	Clay/grains/open	Low	32	4006
		4th Cleat	90° bedding		1-5	Fe/amorphous/tight/Fe	Low	32	4002
		5th Cleat	90° bedding		2-5	Clay/grains/loose/Si,Al	High	33	4003,4
		Conchoidal	Random		1-2	Clay/grains/open	Mod-Low	33	4005
JCB42D	Dull		Side View					34	4201,2
		Highly Compressed	Random	95	1-5	Clay/grains/tight/Si,Al,K	Low	35	4204,5
		Matrix Clay	Random	5	1-100	Clay/grains/tight/Si,Al,K,Fe,Mn,Mg,Ti	Low	36	4203
JCB65D	Dull		Side View					37	6501
		3rd Cleat	90° bedding		5-15	Clay/grains/loose/Si,Al or Ba,Ti,S	Mod	37,38	6504,5
		Highly Compressed	Random	95	1-10	Clay/grains/Sr,Ba,P or Si,Al,Ca	Low	39	6502,6
		Bogen Compressed	Random	5	1-5	Clay/grains/tight/Si,Al,K	Low	40	6503
JCB66B	Bright		Side View					41	6601,2
		3rd Cleat	90° bedding		4-10	Clay/grain/tight/Si,Al,Fe	Low	42	6603,7
		Vertical microcleat	Various		2-5	Clay/blocky/tight/Si,Al	Low	43	6605,6
JCB74BD	Banded		Plan View					44	7401,2
			Side View					44	7405
		Face Cleat	+/- 45° BC		10-30	Clay/grains/tight/Si,Al	Low	45	7403
		Butt Cleat	+/- 45° FC		5-10	Clay/grains/open	High	45	7404
		3rd Cleat	0° bedding		10-50	Clay/amorphous/tight/Si,Al	Low	44	7402
		Highly Compressed	Random	60	1-10	Clay/grains/tight/Si,Al or Si	Low	46	7407
		Matrix Clay	0° bedding	40	1-10	Clay/amorphous/tight/Si,Al clay or rutile/Ti	Low	47	7406

4. DISCUSSION

4.1 Factors Affecting Gas Content

The maxiumum amount of gas a coal can adsorb is assessed by the adsorption isotherm, which, however, may not reflect the *in situ* quantity of gas in the coal. Gas quantities in place must be evaluated by desorption testing. The adsorption isotherm provides a useful basis for evaluating fundamental coal properties that affect gas contents. The main factors influencing methane content of coals are rank, moisture content, mineral matter content and petrographic composition (Ruppel *et al.*, 1972; Joubert *et al.*, 1973; Kim, 1977; Lamberson and Bustin, 1993).

4.1.1 Rank

Increasing coal rank is associated with an increase in methane sorptive capacity at any given pressure and temperature (Kim, 1977; Yalçin and Durucan, 1991; Moxon *et al.*, 1992). Low volatile bituminous coals from Central Colliery would be expected to have a greater methane sorptive capacity than medium volatile bituminous coals from South Bulli. The Langmuir volume, ash free of the dry coal has been used as a measure of sorptive capacity and compared with the volatile matter (daf) of the bright coal fractions as a rank parameter (Fig 4.1). In general, the Central coals have higher sorption capacities than those of South Bulli, which is consistent with the expected trend.

4.1.2 Moisture Content

An increase in moisture content by 1% typically reduces the sorptive capacity of coal by 15 to 25% depending on gas pressure and temperature (Jolly *et al.*, 1968). Sorptive capacity decreases with increasing moisture up to a critical level after which no further reduction takes place (Joubert *et al.*, 1973, 1974). To reduce the effects of variable moisture content, coals are often analysed either dry or air-dry. However, these states do not accurately reflect the *in situ* state of the coal, which is normally saturated with

moisture. Gas sorption properties have therefore been evaluated at both equilibrium moist and dry states.

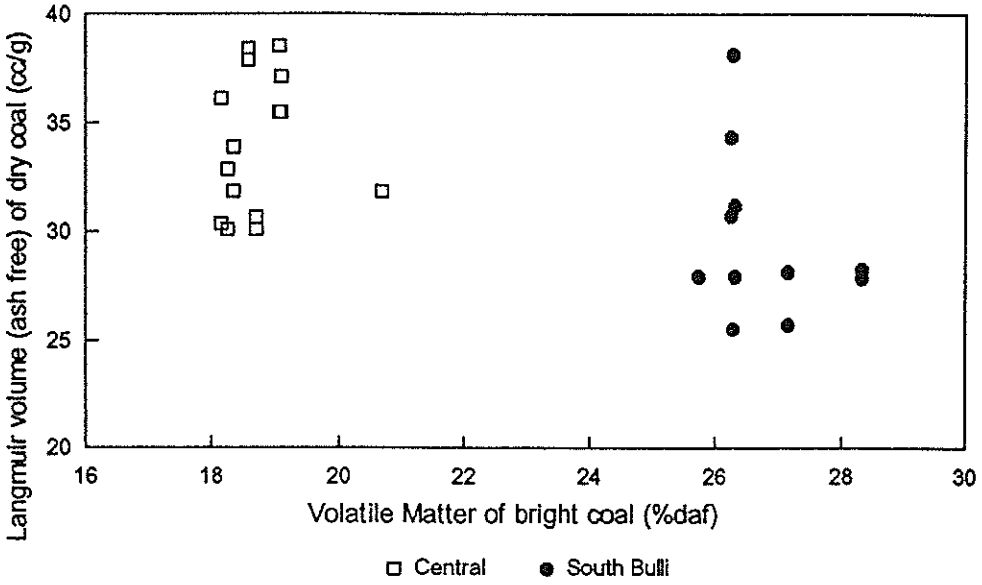

Figure 4.1 Methane sorptive capacity (expressed as Langmuir volume) in relation to coal rank (expressed as Volatile Matter (daf) of the bright coal component).

Effects of moisture on gas adsorption at Central and South Bulli Collieries has been assessed by the Langmuir volumes of the crushed samples (Fig 4.2). The majority of samples show the expected trend of dry coals adsorbing more gas than moist coals (samples falling above the line in Fig 4.2). The increase in adsorbed gas content is within the expected range of 15 to 25% for the moisture content of the coals at around 1%. However, some coals appear to sorb more gas on a moist basis (samples below the line of Fig 4.2). It is likely the correction algorithm for moisture loss during analysis was not valid for these samples.

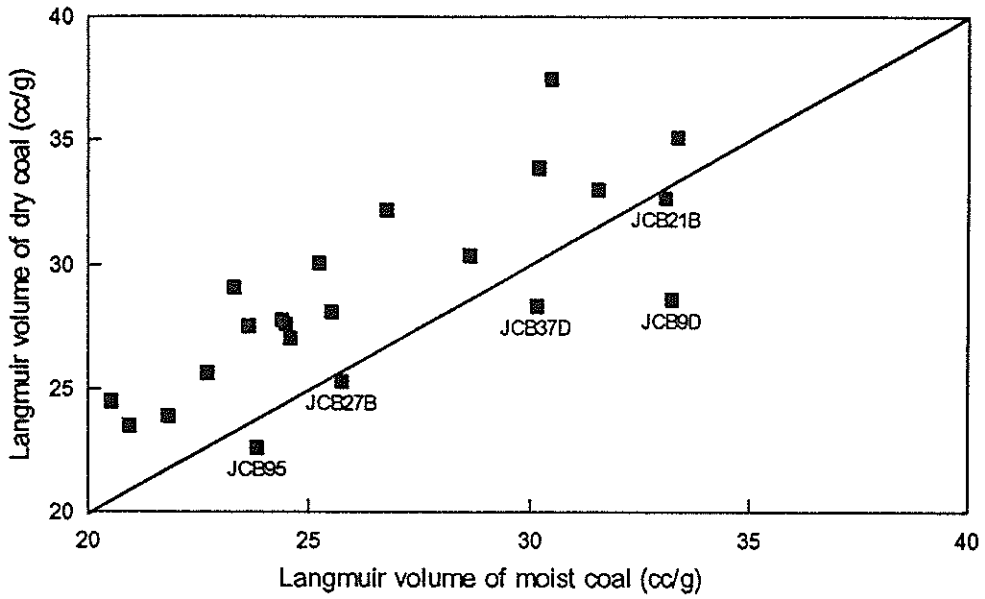

Figure 4.2 Relationship of maximum gas holding capacity as expressed by the Langmuir volume of coals from South Bulli and Central Collieries to moisture state. Line of equal Langmuir volumes shown for reference.

4.1.3 Mineral Matter Content

Mineral matter represents a non-gas-sorbing phase in the coal and acts as a dilutent. Gas contents are therefore often recalculated to an ash or mineral matter free basis for comparison. A strong relationship is usually observed between ash content (as an estimator of the mineral matter content) and methane sorptive capacity, with increasing ash accompanied by decreasing methane content (Barker-Read and Radchenko, 1989).

Decreasing methane content with increasing ash is observed in Central Colliery coals (Fig 4.3) where the line of best fit passes through 95% ash at zero methane content. At South Bulli no strong trend is observed. The most likely reason is the composition of the mineral matter. Carbonate minerals decompose during ashing which leads to underestimation of mineral matter using ash content.

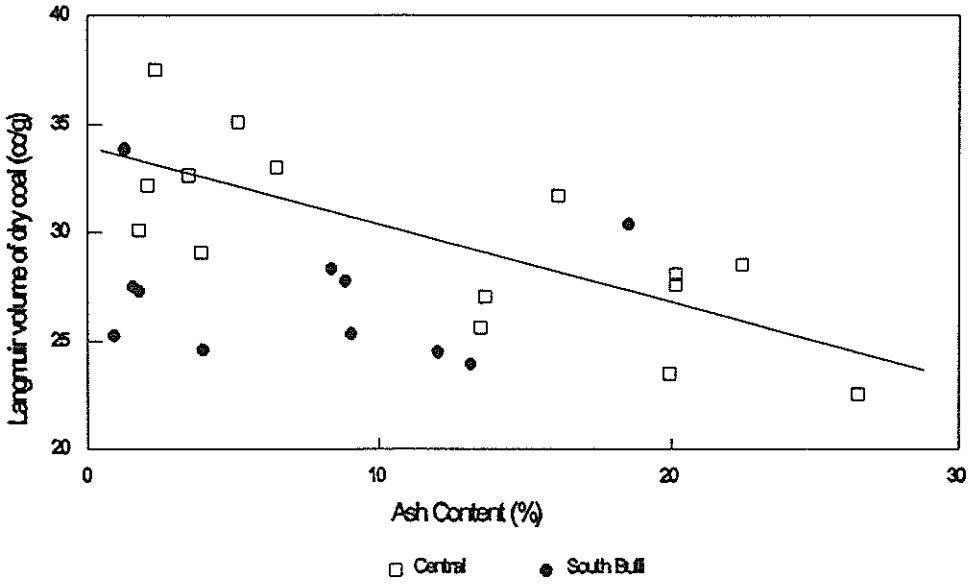

Figure 4.3 Relationship of maximum methane sorptive capacity expressed as Langmuir volume to ash content. Line of best fit shown for Central Colliery (V_L = -0.36 Ash + 33.8 ; r^2 = 0.56)

4.1.4 Maceral Composition

Maceral composition has been shown to have a strong effect on methane sorption capacity which may be more significant than rank-related effects (Lamberson and Bustin, 1993). In general, high vitrinite contents are associated with higher gas sorption capacity. This effect is attributed to the pore nature of the vitrinites, which are more microporous than inertinites.

Gas sorption capacity, expressed as the Langmuir volume, and maceral composition, as percent vitrinite, have been compared on an inorganic free basis to remove mineral matter dilution effects. At South Bulli and Central Collieries no strong association is observed of maceral composition to gas sorption capacity for either equilibrium moist or dry coals (Fig 4.4).

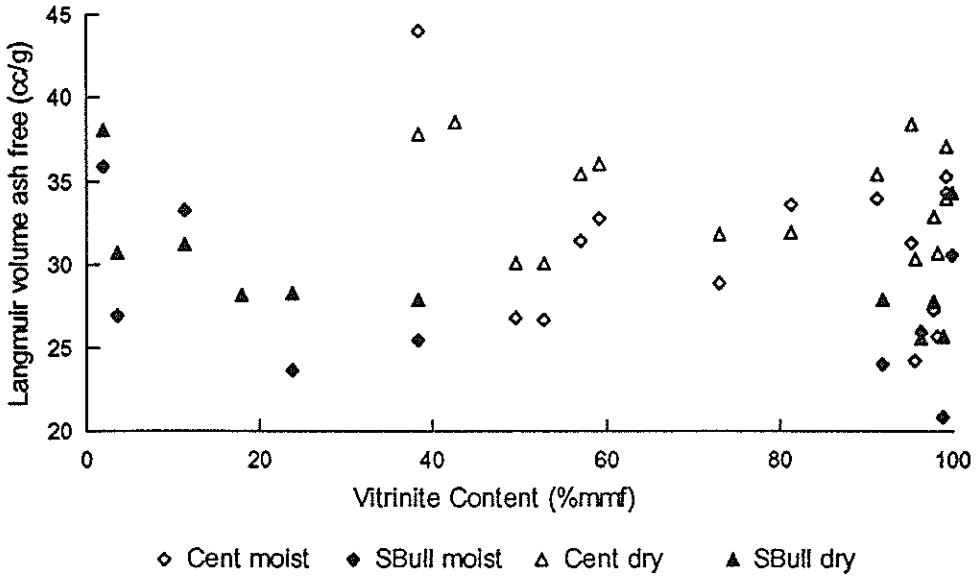

Figure 4.4 Relationship between coal compsition and methane sorption capacity

However, a more detailed evaluation of bright and dull coal pairs (Figs 4.5 and 4.6) reveals a number of trends :

1. Central Colliery samples indicate the bright coal fraction has a greater maximum sorption capacity than the equivalent dull coal on a dry-ash-free basis in most cases.

2. The same trend does not apply to the South Bulli coals. It was noted during proximate analysis South Bulli bright coals had unusually high swelling capabilities. This may be related to a supermicroporosity which inhibits access to sorption sites, thus reducing the maximum sorption capacity of the coal.

3. Langmuir volume on an ash containing basis reflects the in-seam state. Bright coals have a definite greater sorption capacity than their dull equivalents in the Central Colliery samples (see section 4.1.3; Fig 4.3). In this case the inert effect of the coal mineral matter (non-adsorbing) is the main contributor.

4. South Bulli coals do not display this trend.

Therefore, there are appreciable differences between the sorption capacity of the Central Colliery coals and the South Bulli Colliery coals which is not readily explainable by their chemical nature.

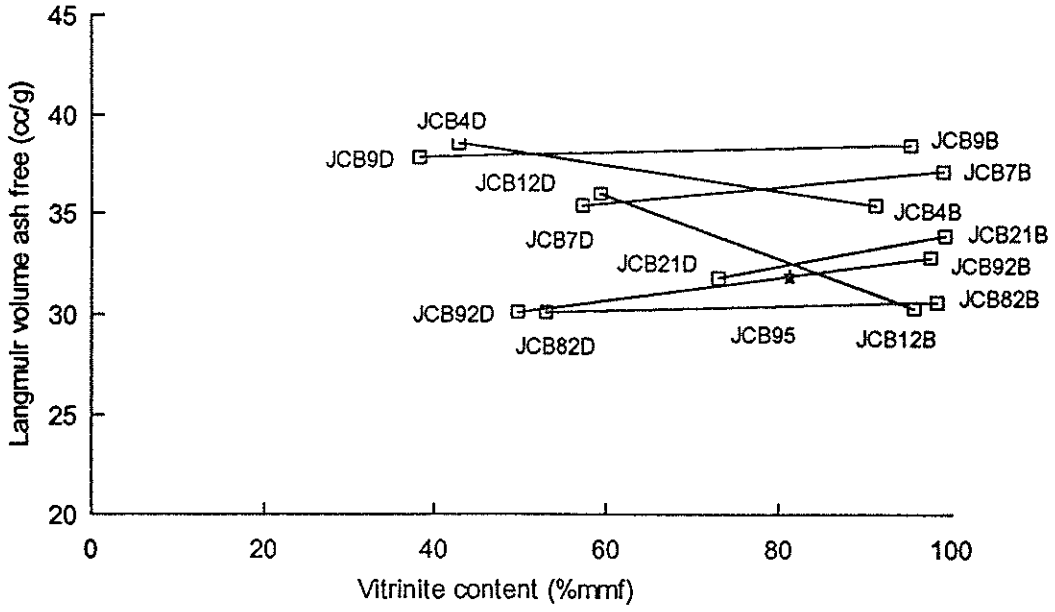

Figure 4.5 Central Colliery methane sorption capacity of dry dull and bright coal pairs along with sheared coal (JCB95 represented by a star).

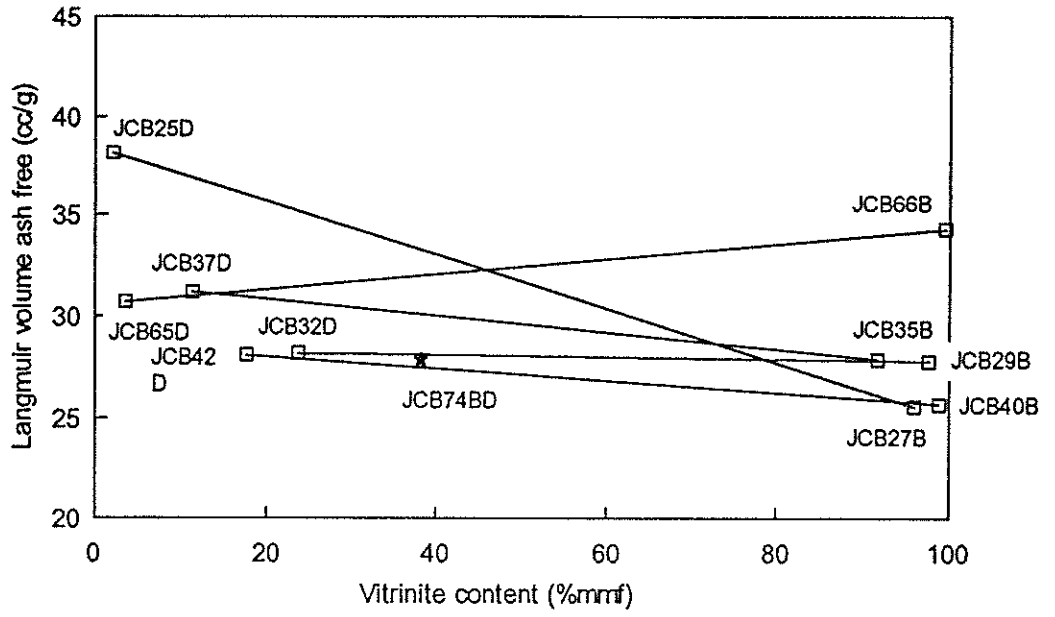

Figure 4.6 South Bulli Colliery methane sorption capacity of dry dull and bright coal pairs along with banded coal (JCB74 represented by a star).

4.1.5 Adsorption Equation Estimated from Analytical Data (Kim, 1977)

Adsorption testing of Australian coals has shown they may be closely modelled by the Langmuir isotherm (Lama, 1986). An empirical relationship between proximate analysis and adsorption isotherm has been devised for American sub-bituminous to anthracite rank coals (), which takes into account rank (by volatile matter) and moisture content. Reasonable agreement has been found between estimates of methane contents based on the adsorption equation with the direct method of gas determination (McCulloch and Diamond, 1976; Feng *et al.*, 1984). Applicability of the adsorption isotherm equation of Kim (1977) to coals from Central and South Bulli Collieries is assessed.

According to Kim (1977), the relationship between the volume of gas adsorbed by the coal, and pressure and temperature can be described by the equation:

$$V = \frac{V_w}{V_d}(KP^N - bT)$$

where,
- V = volume of gas adsorbed, in cc/g of moisture, ash-free coal (maf)
- P = pressure, in atmospheres
- T = temperature, in degrees Centigrade
- K = a constant, in cubic centimetres per gram per atmosphere
- N = a constant
- b = a constant, in cubic centimetres per gram per degree Centigrade
- Vw/Vd = ratio of volumes of gas adsorbed on wet and dry coal, moisture reduction factor.

Kim also established from the coals tested :

$$K = 0.79\ FC/VM + 5.6$$
$$N = 0.39 - 0.013K$$
$$b = 0.14\ cc/g/^{\circ}C$$
$$Vw/Vd = 1/(0.25\ MC + 1)$$

where,
- FC = fixed carbon content
- VM = volatile matter content
- MC = moisture content

The form of the above equation is similar to a Freundlich isotherm, which may explain its applicability to the wide range of coals tested by Kim. The constants K and N build

in a rank factor to the equation. Kim's values for K and N have been modified to better reflect the original data (Beamish, in prep) :

$$K = 5.15\ (FC/VM)^{0.46}$$
$$N = 0.84\ (K)^{-0.54}$$

Comparisons made of this equation for the dry coal adsorption isotherms (i.e. Vw/Vd = 1.00) (Figs 4.7 to 4.11) show :

1. The modified Kim equations show the closer fit to the experimental data in most cases.

2. The equation appears to apply more consistently to the Central Colliery samples than South Bulli Colliery samples.

3. Dull and bright separates do not form a consistent pattern with this equation.

4. The Central Colliery sheared sample (JCB95), which is not a dull or bright category, is modelled remarkably well using the equation, presumably because Kim's original data was for bulk coal.

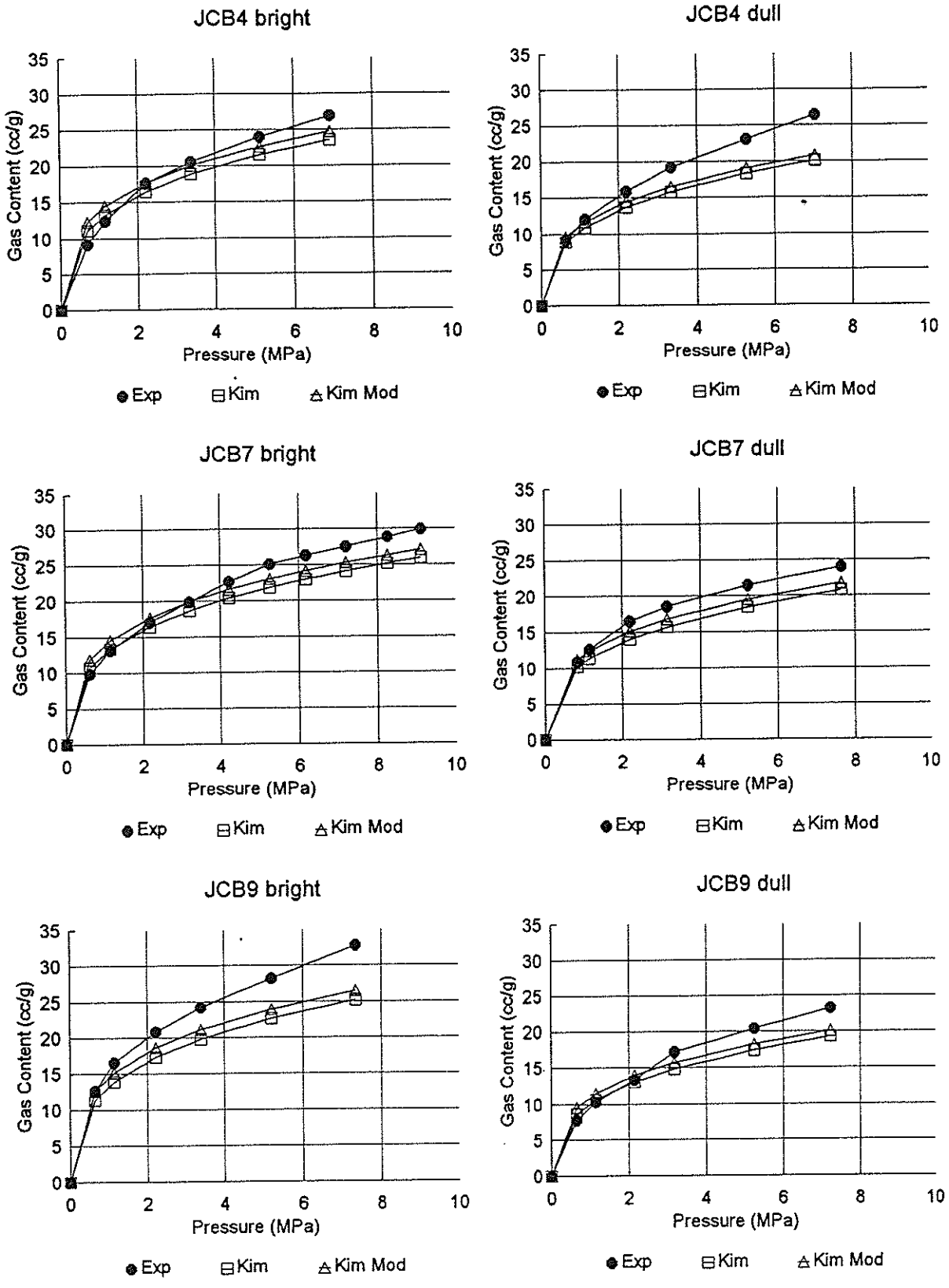

Figure 4.7 Methane adsorption isotherms for Central Colliery on dry coal experimentally determined (Exp) and modelled using the algorithm of Kim (1977) (Kim) and a modified alogorithm (Kim Mod).

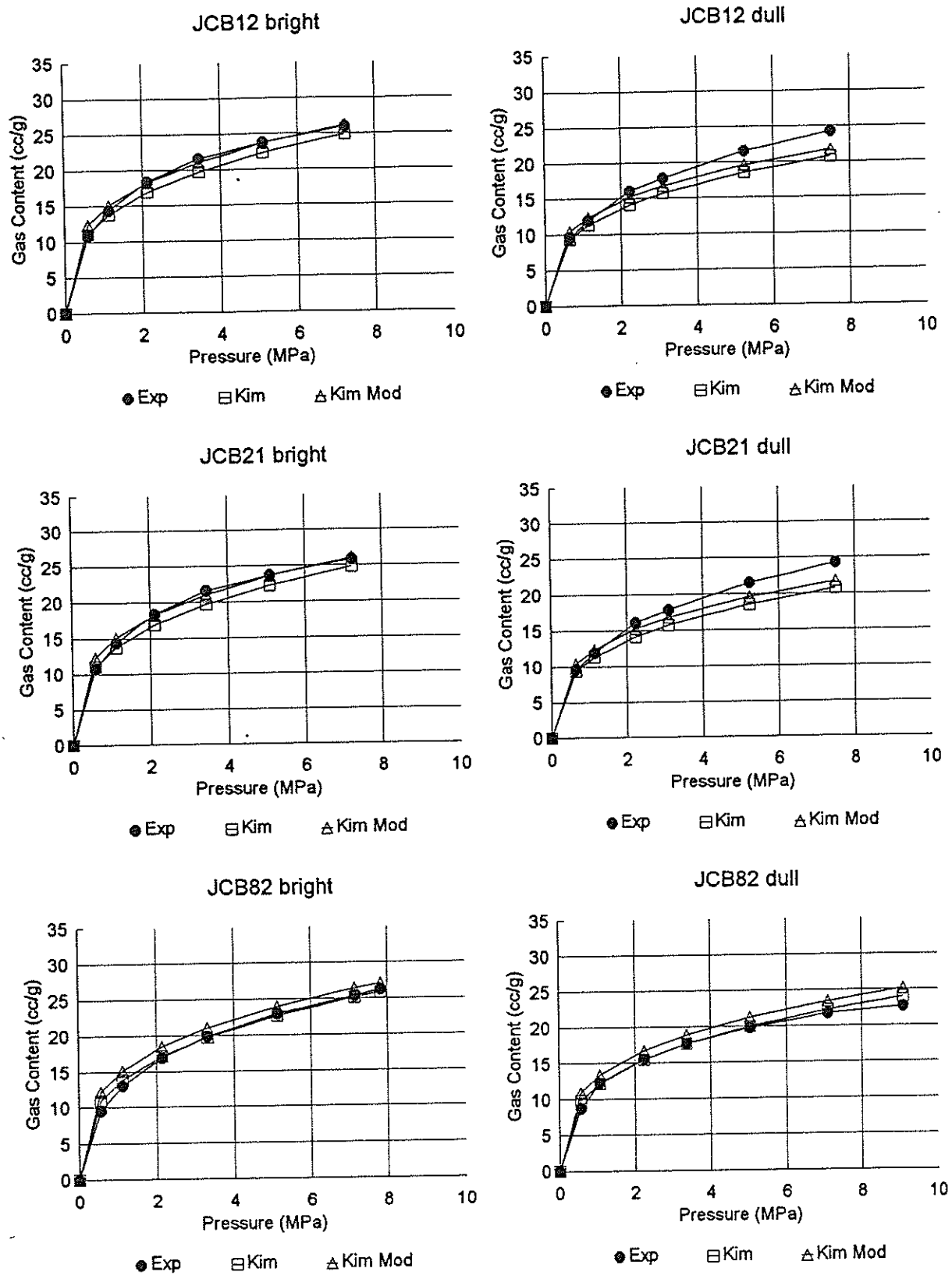

Figure 4.8 Methane adsorption isotherms for Central Colliery on dry coal experimentally determined (Exp) and modelled using the algorithm of Kim (1977) (Kim) and a modified alogorithm (Kim Mod).

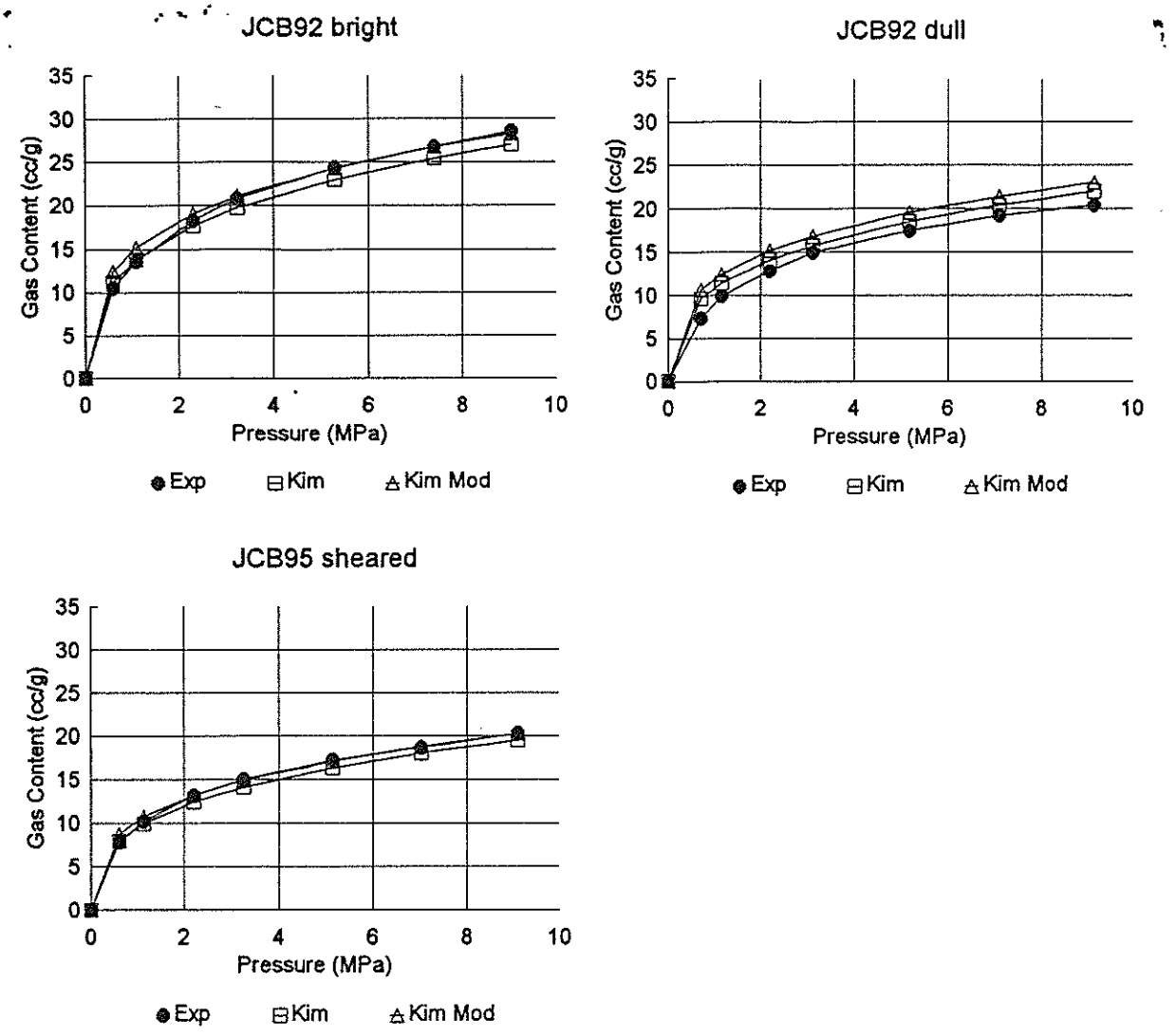

Figure 4.9 Methane adsorption isotherms for Central Colliery on dry coal experimentally determined (Exp) and modelled using the algorithm of Kim (1977) (Kim) and a modified alogorithm (Kim Mod).

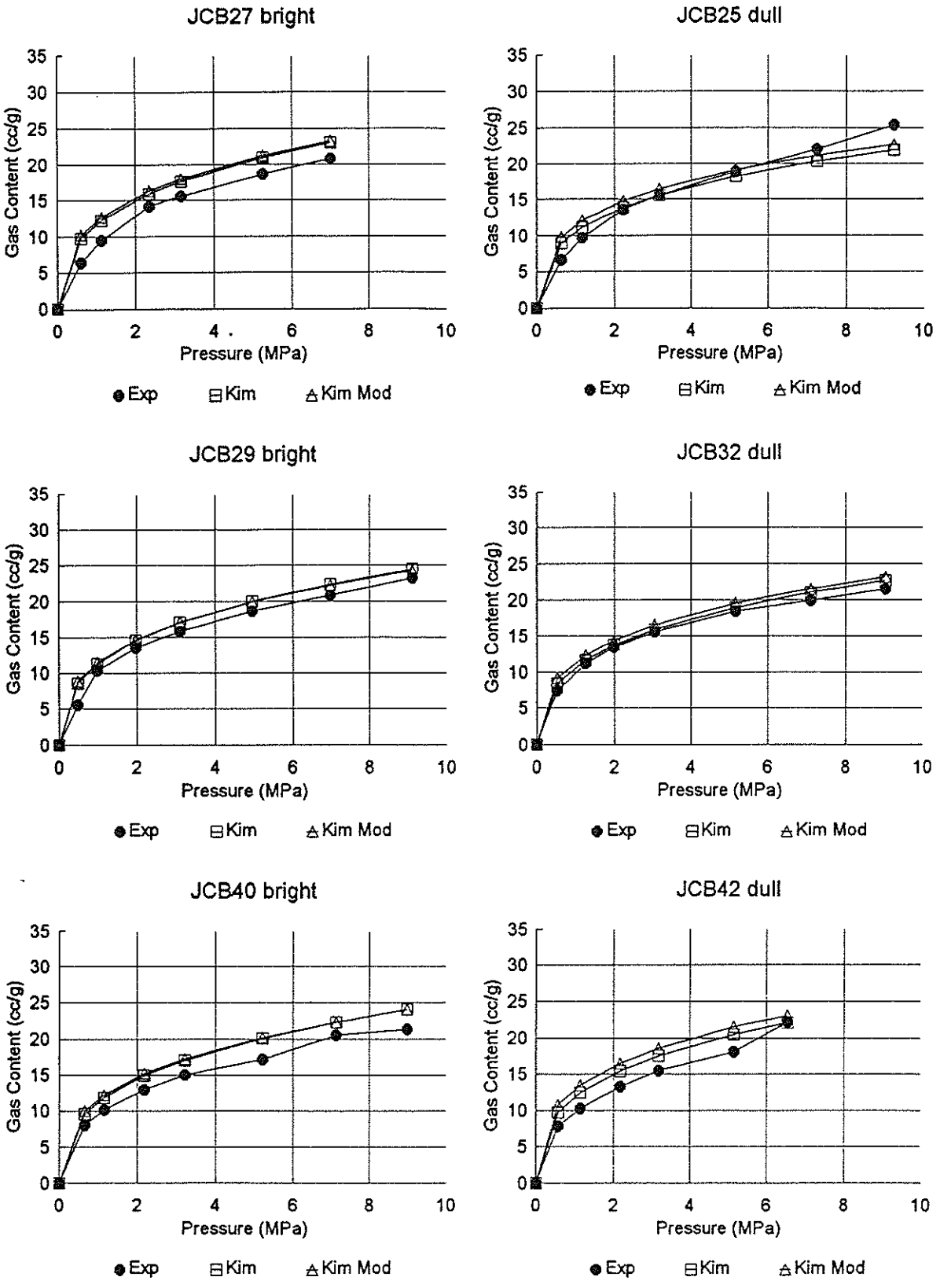

Figure 4.10 Methane adsorption isotherms for South Bulli Colliery on dry coal experimentally determined (Exp) and modelled using the algorithm of Kim (1977) (Kim) and a modified alogorithm (Kim Mod).

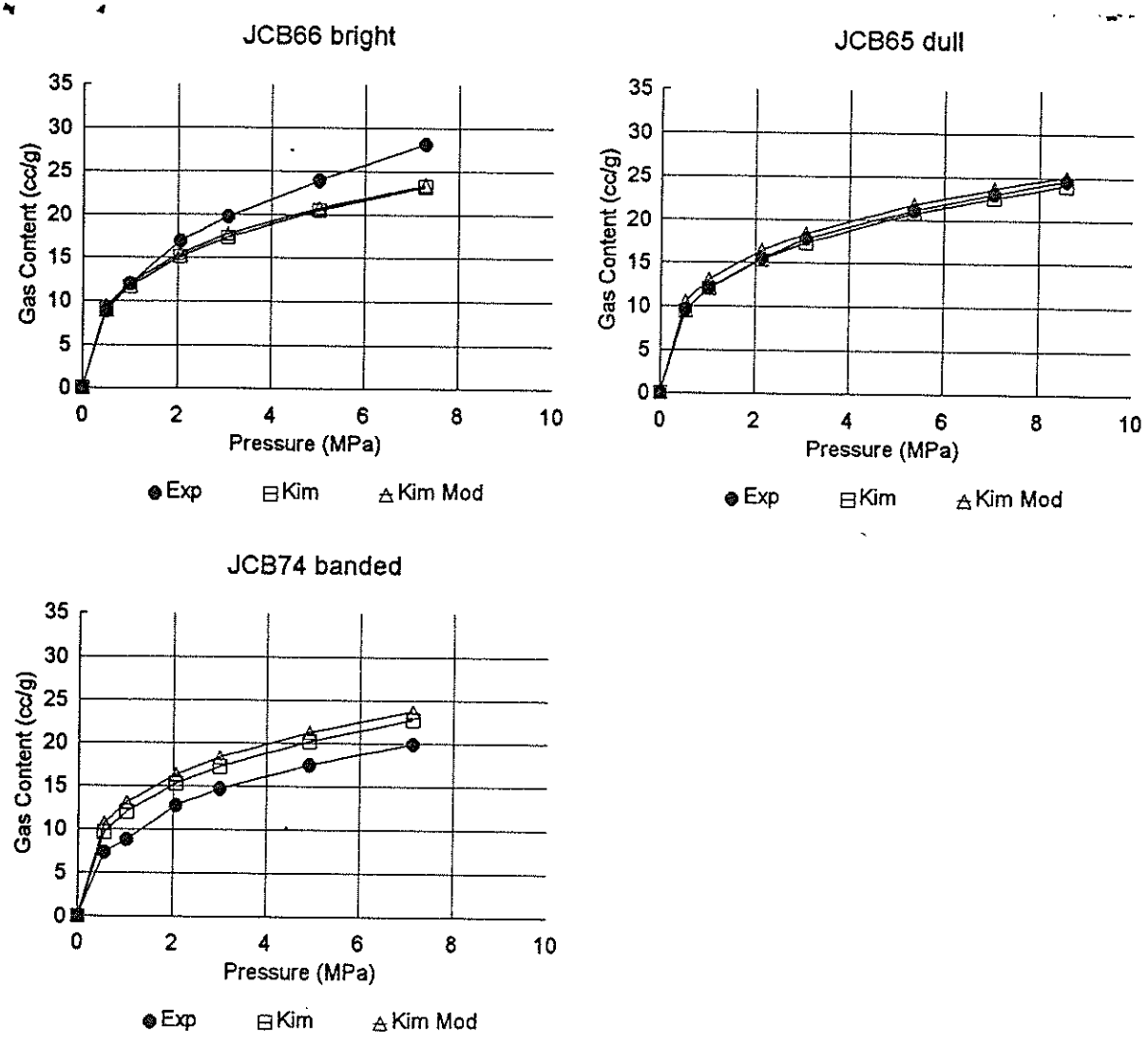

Figure 4.11 Methane adsorption isotherms for South Bulli Colliery on dry coal experimentally determined (Exp) and modelled using the algorithm of Kim (1977) (Kim) and a modified alogorithm (Kim Mod).

4.1.6 Helium Density Relationships

Helium densities of coals from Central and South Bulli Collieries have been plotted against ash content, along with additional data from an earlier ERDC study of Bowen Basin coals at the CGRI (Figure 4.12). The three data sets show separate trend lines in accordance with their respective ranks.

A clear distinction is found in density between vitrinite-rich and inertinite-rich samples which, as well as being a primary property related to maceral composition, is partly affected by ash content and rank. Maceral effects can contribute as much to density variation of a given coal as rank effects.

At greater than 4% ash, the coals are generally inertinite-rich. Differences are observed in the density trends with high volatile bituminous coals of the ERDC study generally having the highest densities; the South Bulli coals the lowest densities; and the Central Colliery samples intermediate density.

At less than 4% ash , the coals are generally vitrinite-rich. Central Colliery densities are the highest while the South Bulli and ERDC samples are similar. The lack of expected differentiation of density relating to coal rank for the bright coals is presumably related to the original mineral matter present in the coal. High carbonate contents, for example, result in low determined ash contents due to carbonate decomposition during proximate analysis.

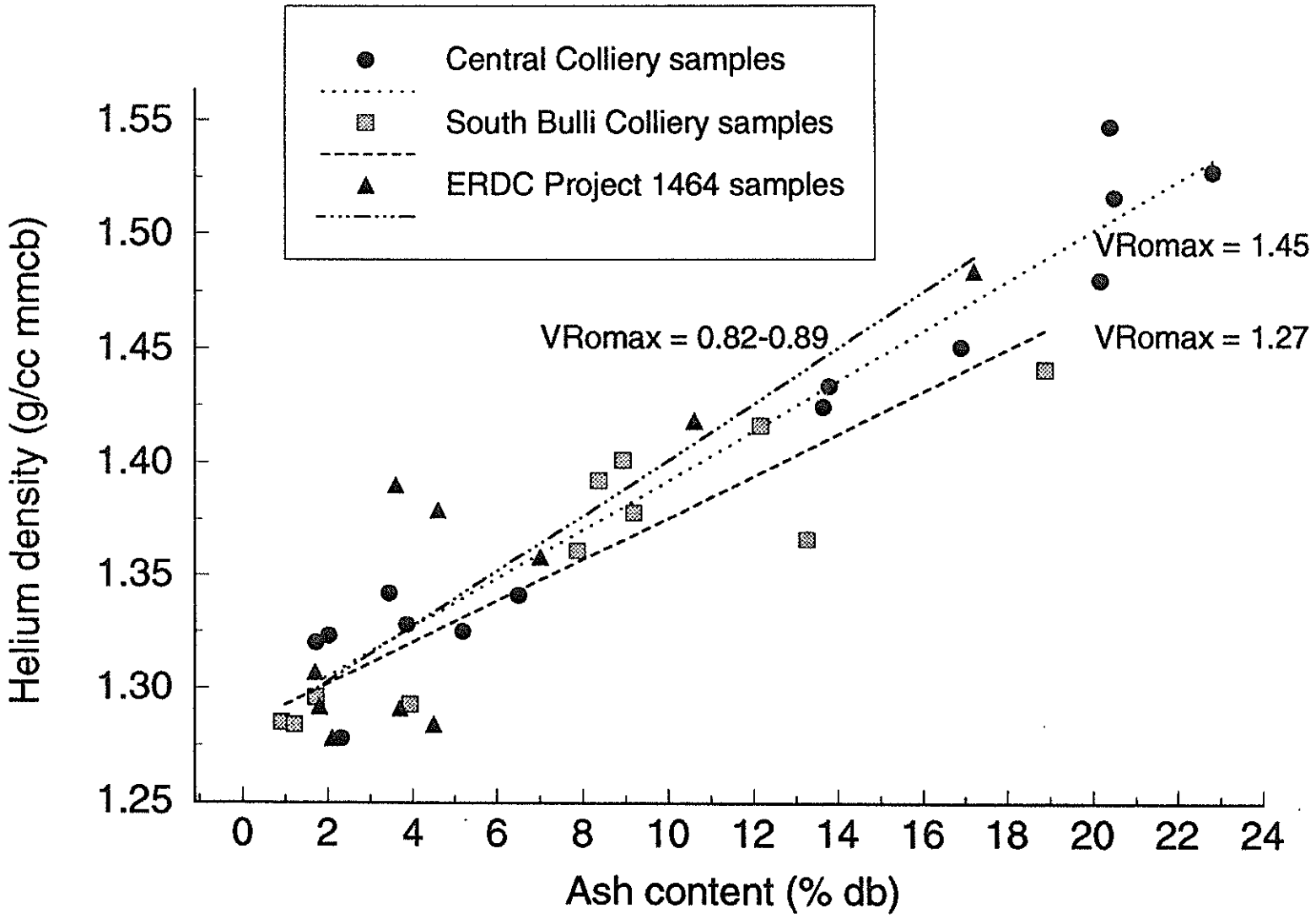

Figure 4.12 Helium density to ash relationships for Central Colliery, South Bulli Colliery and samples from ERDC Projec 1464

4.1.7 Relationship of Surface Area to Gas Content

Surface areas of coals are determined from the adsorption isotherm of gases, usually CO_2 and N_2.Nitrogen and CO_2 molecules are of similar size and would be expected to give similar surface areas, however, in microporous substances such as coal large differences are often found. The lower temperature of the N_2 analysis (72K) compared to the CO_2 analysis (273K) means nitrogen molecules do not have sufficient energy to penetrate all the micropores, resulting in a lower determined surface area. In relation to coal type, N_2 indicates dull coals have the greatest surface area (Table 3.6), which is opposite to the CO_2 trend. Again this is related to the micropore nature of the coal with bright coals having a greater proportion of micropores which cannot be fully penetrated by N_2.

Methane contents of coals determined from the adsorption isotherm would be expected to correlate closely with surface area measurements as both are evaluated from gas adsorption. The Langmuir volume of the coal is the monolayer capacity of methane and therefore a measure of the surface area. However, some differences are expected due to different experimental condtions (especially temperature which is 296K for methane) and different sizes of the CH_4 and CO_2 molecules. In general, coals with larger CO_2 surface areas can adsorb larger amounts of methane (Fig 4.13). Bright coals have both greater surface areas and larger Langmuir volumes than their dull coal equivalents. This effect is more marked in the Central Colliery samples and is related to the higher rank of the coals with its associated increase in microporosity.

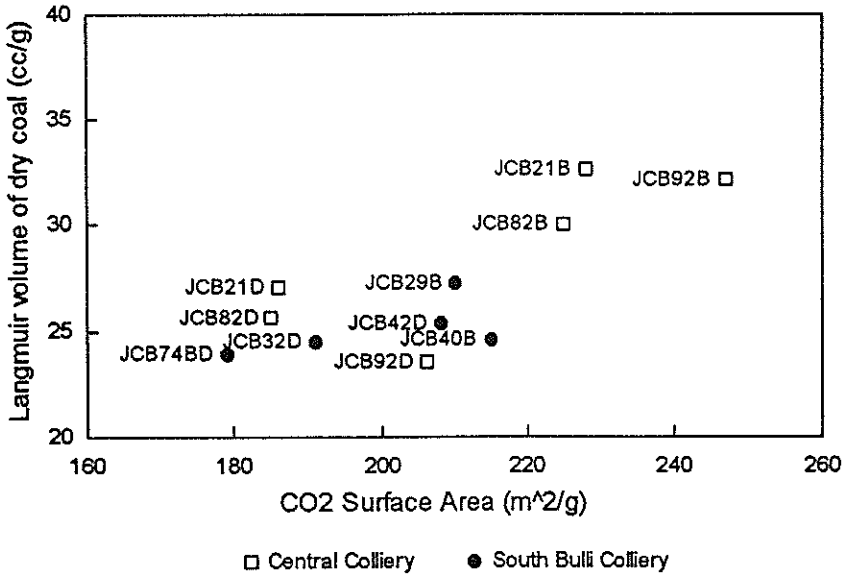

Figure 4.13 Relationship of coal surface area to its maximum methane capacity

4.2 Factors Affecting Desorption Rate (Methane Drainage)

Methane resides in coal primarily as an adsorbed layer on internal coal surfaces (Wyman, 1984; Gray, 1987). Adsorption occurs as a monomolecular layer capproximately 4Å thick (Wyman, 1984) which accounts for 90 to 98% of total methane; the remainder occurs in a gaseous state in macropores and fractures (Gray, 1987; Barker-Read and Radchenko, 1989).

Gas movement through coal occurs via a number of steps. Initially, the gas desorbs and diffuses out of the micropores, where strong gas - pore wall interactions can result in activated or molecular sieve diffusion. Subsequent movement through mesopores, macropores and cleats may occur by Knudsen diffusion or laminar flow depending on the relative mean free path of the diffusing gas to the pore size (Harpalani and Schraufnagel, 1990a,b).

Desorption rates are strongly influenced by degree of fracturing. Diffusion occurs in solid, unfractured coal in response to concentration gradients. Diffusion is very slow and

is governed by the size of the methane molecule in relation to the micropore system and how well the pores are interconnected. Open fractures allow rapid gas flow because they are much larger than the size of the methane molecule. Flow through fractures is assumed to be in accordance with D'Arcy's law and operates in response to a pressure gradient from the inside to the outside of the particle.

Methane emission rates are controlled by the slower of the processes of diffusion or laminar flow (Barker-Read and Radchenko, 1989).

4.2.1 Particle Size Effects

Particle size effects are well established for gas sorption on coal, with smaller particles sorbing more rapidly (Bielicki *et al.*, 1972; Nandi and Walker, 1975; Barker-Read and Radchenko, 1989). Gas sorption rates decrease as particle size increases up to a size determined by the fracture network spacing. For many coals this is around 1mm but may exceed 12mm (Bielicki *et al.*, 1972). For particles greater than the fracture network spacing size, sorption rate is independent of size distribution.

Effective diffusivities at South Bulli and Central are in the order of 10^{-5}/sec for crushed (-0.212mm) and 10^{-6}/sec for lump (-5.60+2.00mm) samples (Table 3.4), indicating more rapid sorption in the finer particles. These diffusivities in relation to particle size are similar to those reported for US coals (Bielicki *et al.*, 1972).

There appears to be no systematic difference in the crushed samples from the two mines or in relation to coal type.

For the lump samples, the diffusivities are generally lower at South Bulli compared with Central for both bright and dull coal types. The sheared coal (JCB95) has the greatest D_e of the lump samples and approaches that of the crushed coals.

In order to determine fracture network spacings, three or more particle sizes need to be

investigated. Although only two sizes investigated in this study, some inferences may be made on the fissure network spacing based on the degree of gas saturation of the lump samples. Central Colliery lump samples probably exceeded the fissure network spacing because many had high degrees of gas saturation (90 to 100%). In contrast, South Bulli lump samples had much lower degrees of gas saturation, suggesting a fissure network spacing exceeding the size of the particles and much greater than that of Central Colliery.

Previous studies relating gas sorption characteristics to coal type (e.g. Lamberson and Bustin, 1993) have reported on the relative sorptive capacity but have been unable to distinguish the importance of maceral content on gas flow. This study shows the distinction between coal types is less important at small particle sizes.

Larger grains retain large pores which are an essential part of the gas desorption mechanism. Gas flow in coal occurs by two processes : initially by diffusion until a large pore space is encountered following which free flow takes place. Crushing the samples results in progressive loss of these free flow pathways.

The sheared sample, although high in vitrinite content, displayed desorption characteristics more similar to the crushed samples. The rapid desorption is due to the fine particle size by brittle failure of the sample during tectonic shearing.

4.2.2 Maceral Composition

Methane content of coal is known to vary with coal type (Ettinger *et al.*, 1966; Lamberson and Bustin, 1993; Section 4.1.4) but the relationship of type to gas emission rate is less well understood. Studies in the Bowen Basin have indicated possible relationships of petrographic composition to outburst-proneness and gas emission rates (Hunt and Botz, 1986; Beamish and Crosdale, 1995). Inertinite-rich coals are implicated in high gas emission rates but contradictions occur at a maceral level where inertodetrinite has been associated with both rapid and slow emission. However, it has

also been suggested that coal type has little influence on gas emission rates (Faiz and Cook, 1991).

Comparison of maceral composition to effective diffusivity shows little relationship for the crushed samples (Fig 4.14). However, significant differences are observed for the lump samples (Fig 4.15). At South Bulli, effective diffusivities are very low for the high vitrinite bright coals and increase slightly in the low vitrinite dull coals but generally show little variation with vitrinite content. At Central Colliery, a marked increase in effective diffusivity is observed with decreasing vitrinite content.

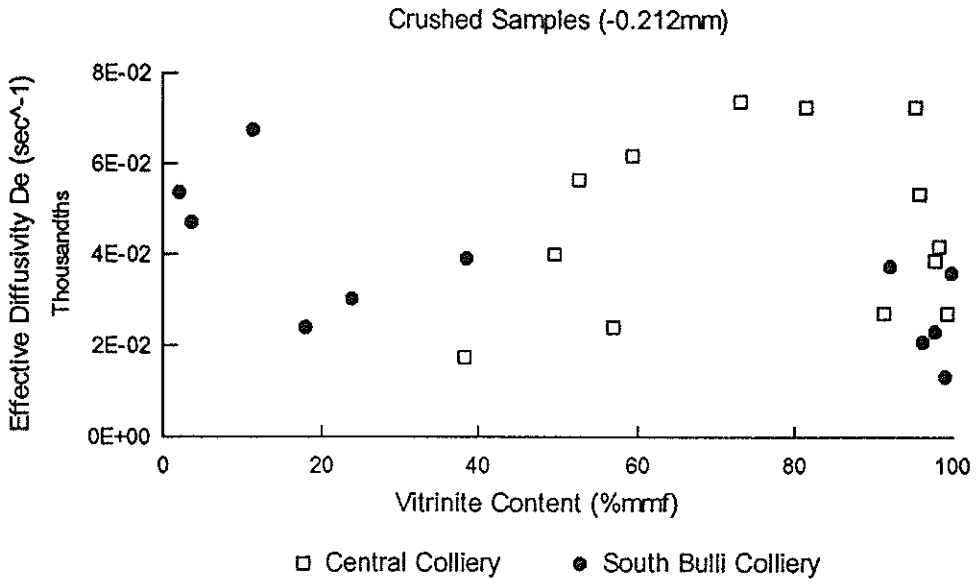

Figure 4.14 Relationship of effective diffusivity to vitrinite content for crushed (-0.212mm) coals

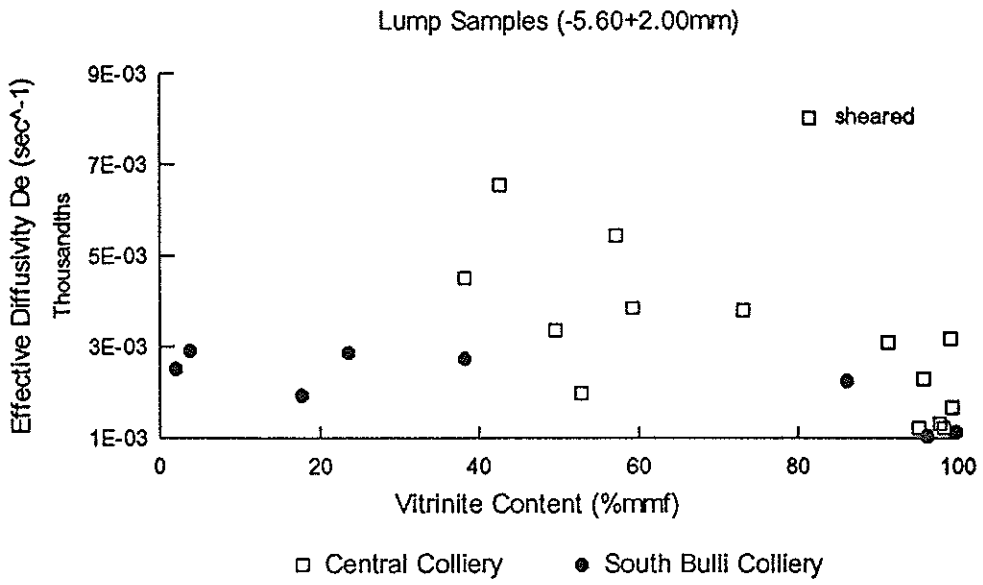

Figure 4.15 Relationship of effective diffusivity to vitrinite content for lump (-5.60+2.00mm) samples

Maceral analyses show the expected trend of bright coals having the greatest vitrinite contents (Table 3.5), especially telocollinite. Dull coals are more variable in composition and include significant amounts of inertinite and mineral matter. Central Colliery samples are distinguished by their generally lower total inertinite and inertodetrinite, higher mineral matter and greater proportion of cell lumina in inertinites expressed as a ratio to either total inertinite or semifusinite + fusinite.

Maceral composition effects on gas flow are best observed in the coarser grains.

Previous studies in the Southern Coalfield of the Sydney Basin (Faiz and Cook, 1991; Faiz *et al.*, 1992) concluded there is little correlation of gas sorption properties to maceral content. For the Southern Coalfield of NSW, our results also suggest increasing inertinite contents are not associated with marked changes in gas desorption rates.

Contrary findings have been found in coals of the Bowen Basin (Beamish and Gamson,

1993; Beamish *et al.*, 1993) where high inertinite contents are associated with rapid desorption. Results from Central Colliery support these conclusions.

A fundamental difference is therefore found between coals of the two basins. Inertinites in the Southern Coalfield typically contain fewer macropores as cell lumina and are more inertodetrinite-rich. South Bulli inertinites contain 5 to 13% cell lumina (Fig 4.16) while Central inertintes contain 8 to 20% cell lumina. Scanning Electron Microscope studies have suggested that, when unmineralised, cell lumina provide important flow pathways and assist rapid desorption of gas (Gamson *et al.*, 1993).

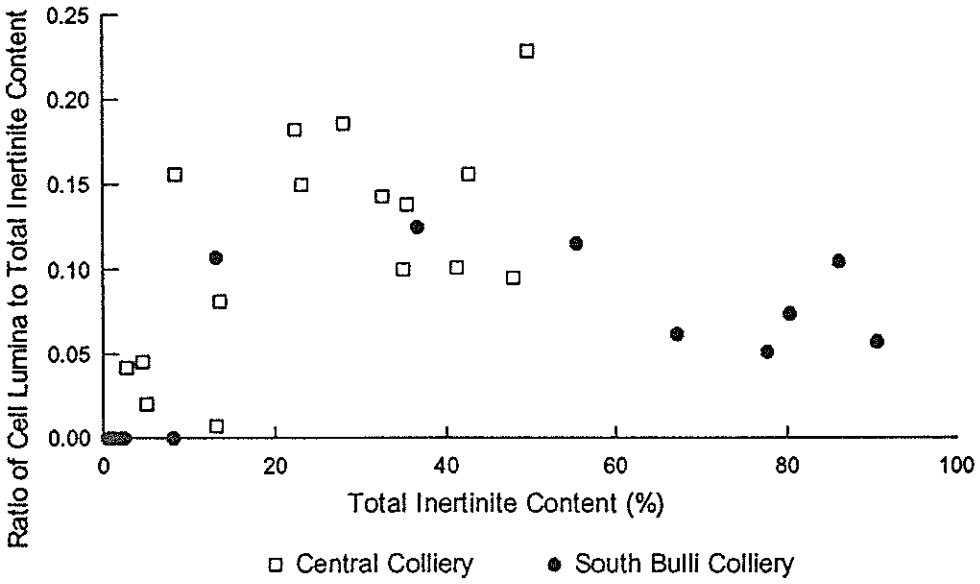

Figure 4.16 Amount of cell lumina in inertinites in relation ot the total inertinite content. Central Colliery inertinites have a greater proportion of associated cell lumina.

4.2.3 Pore Distribution

Mercury porosimetry characterises pores greater than 36Å in size, which are the transport pores for methane desorption. A strong correlation exists between the mean pore diameter (Table 3.6) and the effective methane diffusivity of the lump samples (Fig 4.17). Dull coals with the greatest mean pore diameters have the largest effective diffusivities. Central Colliery coals generally have greater mean pore diameters than

South Bulli samples for equivalent coal types.

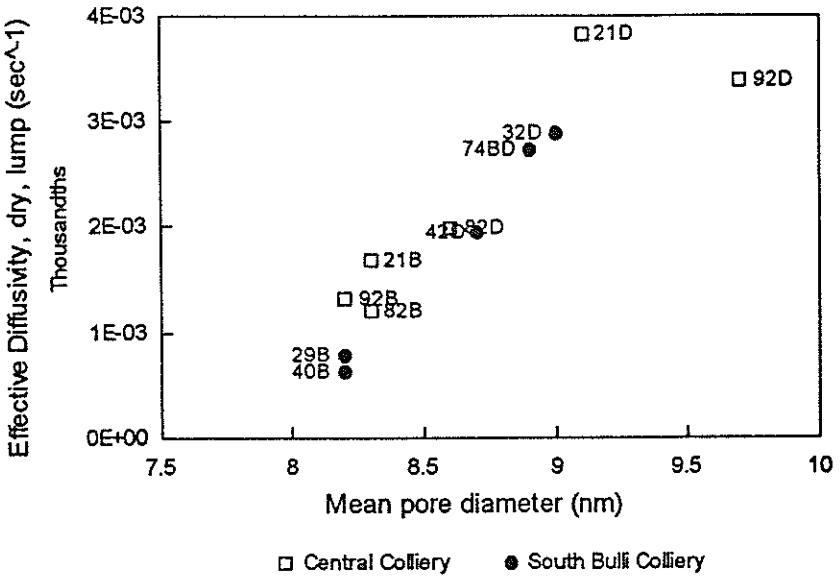

Figure 4.17 Relationship of mean pore diameter to effective diffusivity (D_e).

4.2.4 Influences of Coal Microstructure

Coal microstructures are inferred to have strong influences on gas sorption behaviour (Gamson and Beamish, 1992; Gamson *et al.*, 1993). Fractures and large pores provide transport pathways and SEM allows these to be assessed in terms of size, connectivitiy and degree of mineral infill. Results are generally descriptive and allow broad categorisation into rapid (Class A) and slow (Class B) desorbing coals.

As with previous studies, bright coal microstructures were formed by a variety of fracture types. Dull coals were dominated by highly compressed structures. Comparison with the maceral data suggests compressed material is likely to be desmocollinite dominated at Central and semifusinte dominated at South Bulli.

Sheared coal from Central was found to have an extensive network of open pores at grain boundaries as well as open fractures and unmineralised, open shear planes. Coal of this type had not been previously examined for microstructural analysis. The sample

could be considered analogous with the crushed coal which explains its extremely rapid desorption rate.

With the exception of the sheared coal, microstructural studies at South Bulli and Central have provided little detailed insight into factors controlling gas sorption at these sites. Assessment proved difficult by the use of hand-pick dull and bright coal types, which is different to the normal banded samples. No systematic differneces were found between the two mines in relation to fracture size or spacing; degree, tightness or type of mineral infill.

4.2.5 Central Colliery LW306 Drainage Project

Samples JCB4, JCB7, JCB9 and JCB12 were derived from cuttings from drill hole 14 of the Central Colliery Longwall 306 drainage project, whose objective was to reduce methane contents of 5 - 10 m^3/t down to 3m^3/t. Methane drainage was achieved in LW306 by the use of 54 in-seam holes of 265m minimum length (285m for hole 14), spaced 40 to 50m apart (B. Robertson, pers. comm. 1993). A number of drilling strategies were employed to assess drainage in relation to geological features, especially a mid-seam shear zone (see Fig 2.2). Holes were placed above, below and within the shear zone; hole 14 was drilled below the shear zone. Most holes required 3 to 6 shifts to complete, hole 14 requiring 5. Monitoring of total water make of the system and gas flow of individual holes was made on a regular basis. A vacumm pump was connected to the system on 4/5/93.

Results of monitoring for hole 14 are presented in Fig 4.18 for the period 11/11/92 to 12/6/93. The seam initially dewaters over the first few weeks with associated increase in gas flow. Peak gas flow develops as dewatering tails off, after which gas flow decreases exponentially. The increase in gas flow after 170 days is related to connection of the vacuum system. Exponential decrease in gas flow can be modelled (B. Robertson, pers. comm. 1993) :

$$f = a.\exp^{(bt)}$$

where f = flowrate in litres/minute/metre
a = initial flow rate constant
b = decay rate constant
t = time elapsed in days

For hole 14, a = 5.509; b = -0.014.

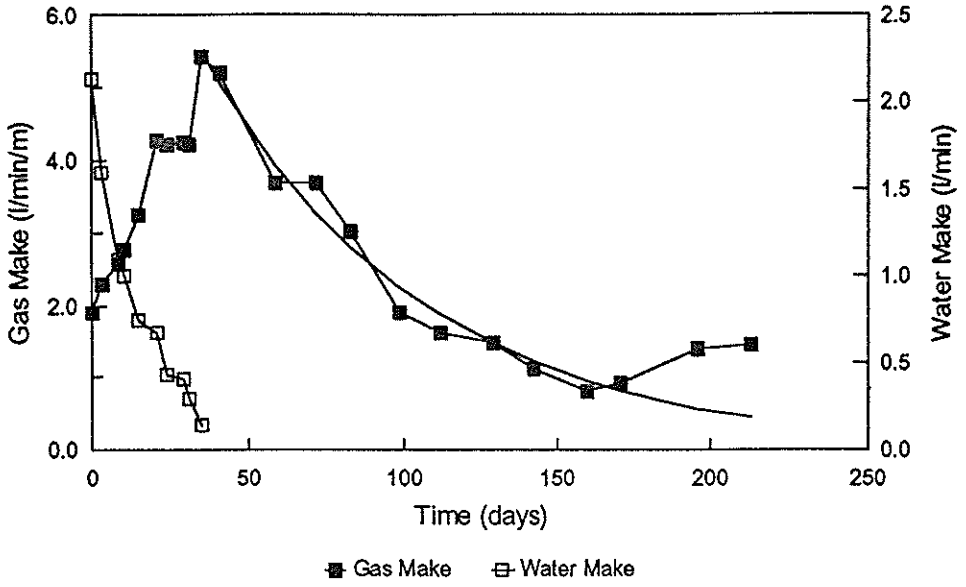

Figure 4.18 Results of gas drainage from hole 14, Central Colliery longwall 306 drainage project. Decay curve fitted for gas make following seam dewatering.

Hole 14 was drilled in a region where *in situ* gas contents range from 5.5 to 6.5m^3/t. Adsorption isotherm testing of the raw, moist coals indicate maximum sorption capacities of 23 to 33m^3/t (Table 3.2) and show the seam is undersaturated with respect to methane. Laboratory desorption testing of lump samples commenced at gas contents from 9 to 16m^3/t (Table 3.3) which is 2 to 3 times the *in situ* levels at this location, however, gas contents exceeding 10m^3/t are recorded in this panel.

The direct relationship of laboratory testing to degassing in the hole is complicated by :

- the dewatering process in the hole
- undersaturation of the seam with respect to methane
- the use of mean gas flow rates in relation to hole length
- the large gas reservoir available for the hole

- the longer time frame required to degas the hole

However, relative gas flow rates can be compared between hole 14 and laboratory tests. Flow rates within the hole are expressed as litres/minute/metre-of-hole-length. Metres of hole length are be converted into cm^2 to give gas make in relation to exposed surface area. Results are in the order of 10^{-3} to 10^{-4} l/min/cm^2.

External surface areas may be calculated for microbalance lump samples and thereby allow comparison to rates of gas make in the borehole (Fig 4.19). A number of models were tried assuming spherical particles with a density of 1.3 to 1.4g/cc and between 4 and 10 grains in the microbalance. These results also give rates in the order of 10^{-3} to 10^{-4} l/min/cm^2. Desorption rates of the same order of magnitude indicate the microbalance results are comparable to actual methane drainage processes operating in the mine.

An example is given using sample JCB12 (moist coal) (Fig 4.19). Microbalance desorption rates have been scaled to best fit Hole 14 rates. Laboratory testing shows a more or less regular decrease in gas make with time. Initial desorption does not model gas make in the hole as the in-seam rates are strongly controlled by the water make. Subsequent to seam dewatering, both data sets follow similar trends but at different time scales. From 0.2 to 1.0 hours, microbalance çgas make rates are similar to hole 14 for the period 35 to 213 days and indicates the microbalance simulates methane drainage hole over this period (Fig 4.19). Extrapolation of laboratory data indicates complete drainage of all desorbable gas would require more than 10 years, which is comparable to time frames indicated for coalbed methane production.

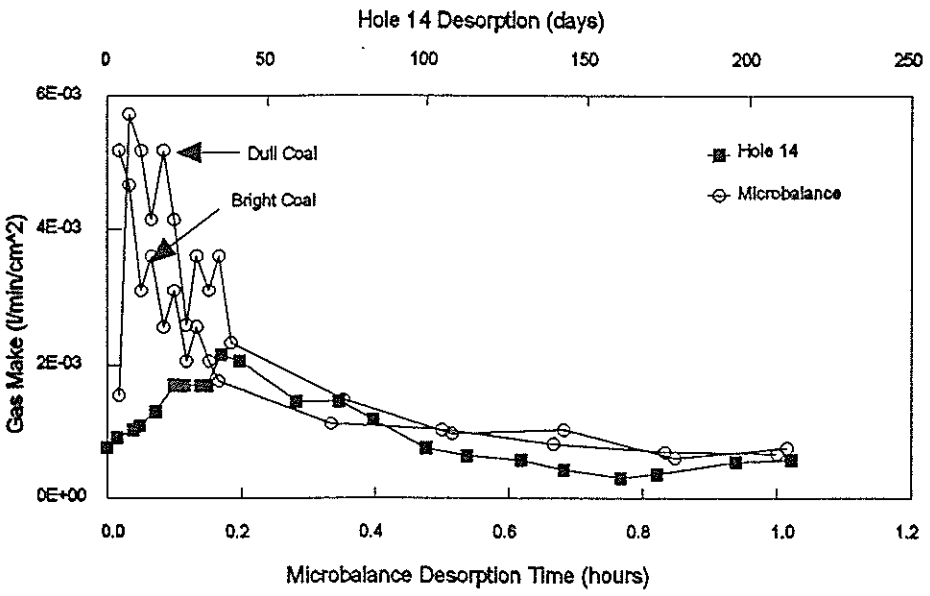

Figure 4.19 Comparison of gas make with time for LW306 drainage hole 14 and microbalance sample JCB12 (moist coal).

Increased gas make was observed after installation of the vacuum system in the LW306 drainage programme. A similar response was observed in the laboratory studies when vacuum was applied following apparent completion of desorption to atmosphere (Figs 3.9, 3.13 and 3.19) for both Central and South Bulli coals.

5. CONCLUSIONS

The main objectives of the work programme were determination of flow characteristics of different coal types from Central and South Bulli Collieries and to investigate parameters influencing methane flow, with particular reference to coal type. Fundamental differences have been found in methane sorption characteristics between the two mines and indicate results from the Sydney and Bowen Basins may not be directly interchangeable.

Gas Content

Factors significantly affecting gas contents are rank, moisture content, mineral matter content and coal type. Increased gas contents are associated with higher rank, lower moisture content and lower mineral matter content. Coal type relationships are more complex and vary between the two mines. At Central Colliery, bright coals are generally associated with higher gas capacities than their equivalent dull coals. At South Bulli Colliery, no firm trend has been established between coal type and gas content.

At both Central and South Bulli Colliery, comparison with the methane adsorption isotherm indicates the coal in ground is undersaturated. As mining becomes deeper, gas contents increase towards saturation levels.

Desorption Rates

Desorption rate is strongly influenced by particle size. Fine particles desorb gas more rapidly than coarse particles. This is of particular significance for tectonically disturbed coal (e.g. the sheared coal from Central) where very rapid *in situ* desorption can be attributed to the crushed state of the coal. Desorption rate progressively decreases with increasing particle size until a grain size is reached at which desorption rate no longer changes. This grain size defines the fracture network spacing. Although the range of samples required to define the fracture network spacing was not investigated, it is

inferred from a comarison of sorption in crushed and lump coals that Central Colliery samples probably exceeded the this spacing while South Bulli samples did not.

Coal Type Influences

Coals were classified into different types on a visual basis (bright and dull) followed by quantitative maceral analysis. Maceral analysis showed bright coals were essentially telocollinite (vitrinite A) in both mines but dull coals varied considerably. Central Colliery dull coals are dominated by desmocollinite (vitrinite B) with associated inertinite (mostly semifusinite) and mineral matter. South Bulli dull coals have greater amounts of inertinite (including greater amounts of inertodetrinite) and less vitrinite and mineral matter.

Coal type may affect both gas content (see above) and desorption rate. At South Bulli, no strong relationship was identified between desorption rate and coal type. However, at Central, a firm trend was found between decreasing vitrinite content and increasing desorption rate.

An important distinction appears between the inertinites in the two mines which has a bearing on gas sorption rates. Semifusinite and fusinite at Central Colliery have a larger proportion of open cell lumina which is associated with higher rates of gas desorption.

Microstructure Influences

Coal microstructure is an important influence on gas flow, as indicated by the extremely rapid gas sorption by the sheared coal from Central Colliery. However, with the exception of the sheared coal, microstructural influences on gas desorption rates proved difficult to quantify by SEM. The technique requires further development to assess the relative effect of different microstructures.

Use of microbalance samples for SEM assessment of rapid and slow desorbing

categories does not always appear appropriate as significant microstructural features may not be preserved in these samples. Previous success with this technique has been based on larger samples where infillings of macropore structures (including cleats) can be better evaluated.

Relevance to Methane Drainage

Very rapid desorption rates associated with sheared coal indicates it provides an efficient pathway for gas drainage. However, experience has shown its low mechanical strength causes severe drilling difficulties, including bogging of the drill string, and its enhanced permeability is difficult to capitalise on.

Microbalance analysis over the first half hour seems to give a good indication of gas release during long term (100 - 200 days) drainage by the use of in-seam holes. The technique may be useful as a long term predictor of methane drainage performance, although further evaluation is required.

At Central Colliery, it seems likely that targeting the duller horizons of the seam will enhance methane drainage rates but may leave higher than expected amounts of gas in the brighter horizons. Outburst proneness in the Bowen Basin has previously been related to higher vitrinite coals (%%1321(Williams & Rogis, 1980)%%).

At South Bulli Colliery, it does not appear that targeting horizons of either bright or dull coal will significantly enhance methane drainage.

6. REFERENCES

Chapter 1

Bartosiewicz, H. and Hargraves, A.J. (1985) Gas properties of Australian coal. *Bull. Proc. Australas. Inst. Min. Metall.*, 290(1):71-77.

Battino, S. (1986) Control of Methane emissions from strata into operating longwall units. NERDDC Report, NERDDP/Eg//665.

Battino, S. (1991) Determination of in situ permeability to gas for Australian coals. In W.J. Bamberry and A.M. Depers (eds), *Proc. Gas in Australian Coals*, Geological Society of Australia, Sydney, February:3-12.

Beamish, B.B. and O'Donnell, G. (1992) Microbalance applications to sorption testing of coal. In B.B. Beamish and P.D. Gamson (eds), *Proc. Symp. Coalbed Methane Research and Development in Australia*, Townsville, Qld., November, 4:31-41.

Beamish, B.B., Hungerford, F., McKavanagh, B. and Williams, R.J. (1985) Outburst Research, (Collinsville Coal Co., Qld. (Australia)). NERDDP-EG-495 Canberra, ACT, Australia. 760p.

Botz, R.W. and Hart, G.H. (1983). Mineralogical, petrographical and geochemical investigations of outbursting in Australian coal mines. *Proc. Australas. Inst. Min. Metall.*, 286:41-49.

Caffery, M., Smith, S., Beamish, B.B., Robertson, B., Phillips, R. and Crosdale, P. (1992) Applications of in-seam drilling and methane drainage at Central Colliery, Bowen Basin. In B.B. Beamish and P.D. Gamson (eds), *Proc. Symp. Coalbed Methane Res. Develop. in Australia*, Townsville, Qld., November, 3:69-77.

Crosdale, P.J. and Beamish, B.B. (1993) Maceral effects on methane sorption by coal. In J.W. Beeston (ed), *Proc. New Developments in Coal Geology Symp.*, Brisbane, November:95-98.

Curl, S.J. (1978) Methane production in coal mines: *London, International Energy Agency of Coal Research:* Report No. ICTIS/TR04.

Davidson, S. (1992) Some aspects of the transient testing of Bowen Basin coal seams. In B.B. Beamish and P.D. Gamson (eds), *Proc. Symp. Coalbed Methane Res. Develop. in Australia*, Townsville, Qld., November, 2:153-169.

Faiz, M.M., Aziz, N.I., Hutton, A.C. and Jones, B.C. (1992) Porosity and gas sorption capacity of some eastern Australian coals in relation to coal rank and composition. In B.B. Beamish and P.D. Gamson (eds), *Proc. Symp. Coalbed Methane Res. Develop. in Australia*, Townsville, Qld., November, 4:9-20.

Fischer, F., Peters, K. and Warnecke, A. (1932) Gases confined in coals. *Brennstoff-Chemie*, 13:209-216.

Gan, H., Nandi, S.P. and Walker, P.L. Jr. (1972) Nature of the porosity in American coals. *Fuel*, 51:272-277.

Hargraves, A.J., 1958. Instantaneous outbursts of coal and gas. *Proc. Australas. Inst. Min. Metall.*, 186:21-72.

Hargraves, A.J., 1962. Gas in face coal. *Proc. Australas. Inst. Min. Metall.*, 203:7-43.

Hargraves, A.J., 1980. A review of instantaneous outburst data. In *Proc. AusIMM Symp. on The Occurrence, Prediction and Control of Outbursts in Coal Mines*, Brisbane, Qld, September:1-18.

Hargraves, A.J. (1983) Instantaneous outbursts of coal and gas - a review. *Proc. Australas. Inst. Min. Metall.*, 285(3):1-37.

Hargraves, A.J. (1993) Update on instantaneous outburst of coal and gas. *Proc. Australas. Inst. Min. Metall.*, 298(2):3-17.

Hunt, J.W. and Botz, R.W. (1986) Outbursts in Australian coal mines: a petrographic factor. *Proc. Australas. Inst. Min. Metall.*, 291(1):59-63.

Ivanovic, D., Truong, D. and Williams, R.J. (1985) Methane Drainage. NERDDC Report NERDDP/EG/ 85/485.

Jackson, L.J. (1984) Outbursts in coal mines: *London, International Energy Agency of Coal Research:* Report No. ICTIS/TR25.

Jeffrey, R.G. (1990) Hydraulic fracturing and treating coalbed methane wells. In Paterson L. (ed), *Methane Drainage from Coal*, CSIRO, Division of Geomechanics:56-70.

Jeffrey, R.G., Enever, J.R., Moelle, D. and Davidson, S. (1992) Hydraulic fracturing experiments in vertical boreholes in the German Creek coal seam. In B.B. Beamish and P.D. Gamson (eds), *Proc. Symp. Coalbed Methane Res. Develop. in Australia*, Townsville, Qld., November, 3:1-21.

Juntgen, H. and Karweil, J. (1966) Formation and storage of gases in bituminous coal seams, Part 1 - Gas formation and Part 2 - Gas storage (English translation). *Erdöl und Kohle-Erdgas-Petrochemie*, 19:251-258, 339-344.

Koenig, R.A., Bocking, M.A., Forster, I., Enever, J.R. and Casey, D.A. (1992a) Experience with well testing and in-situ stress measurement in the Sydney Basin for evaluation of coalbed methane prospectivity. In B.B. Beamish and P.D. Gamson (eds), *Proc. Symp. Coalbed Methane Res. Develop. in Australia*, Townsville, Qld., November, 2:75-95.

Koenig, R., Dean, A. and Lupton, G. (1992b) Development and initial trials of a new multiphase well testing tool for coalbed methane evaluation. In B.B. Beamish and P.D. Gamson (eds), *Proc. Symp. Coalbed Methane Res. Develop. in Australia*, Townsville, Qld., November, 2:97-105.

Lama, R.D. (1980) Results of some index tests on coal at Cook Colliery, Queensland Coal Mining Company, Blackwater, Queensland. CSIRO Division of Applied Geomechanics, GCM Report No. 11, 19p, (February ,1980).

Lama, R.D. (1986) Improving the efficiency of gas drainage systems. NERDDP, Report No. 701, 88p, (October 1986).

Lama, R.M. and Mitchell, G.W. (1981) Investigations of geomechanical parameters in relation to outbursts of gas and coal at Leichhardt Colliery. CSIRO Division of Applied Geomechanics, GCM Report No. 9, 49p (July 1981).

Levine, J.R. (1992) Oversimplifications can lead to faulty coalbed gas reservoir analysis. *Oil & Gas J.*, November 23:63-69.

Levine, J.R., Johnson, P.W. and Beamish, B.B. (1993) High pressure microbalance sorption studies. *Proc. 1993 Internat. Coalbed Methane Symp.*, The University of Alabama/Tuscaloosa, Birmingham, Alabama, May 17-21:187-196.

Lewis, C., Allen, J. and Camp, B. (1992) An overview of the production and operations of the Hillview #1 and #2 coalbed methane wells near Moura Queensland. In B.B. Beamish and P.D. Gamson (eds), *Proc. Symp. Coalbed Methane Res. Develop. in Australia*, Townsville, Qld., November, 3:23-32.

Lingard, P.S., Doig, I.D. and Phillips, H.R. (1984) Laboratory studies of sorption characteristics and permeability of triaxially stressed coal samples. *Proc. Third Internat. Mine Ventilation Congr.*, Harrogate, England:143-150.

Lunarzewski, L. (1992) The role of predicted and measured gas emission in coal mine gas control. In B.B. Beamish and P.D. Gamson (eds), *Proc. Symp. Coalbed Methane Res. Develop. in Australia*, Townsville, Qld., November, 4:97-105.

Marshall, P. (1981) Gas drainage and outburst investigations. NERDDC end of grant Report No. 28.

Meyer, E. von (1872) Über die in einigen englischen Steinkohlen eingeschlossenen Gase. *Jour. f. praktishce Chemie*, 5:407pp.

Meyer, E. von (1873) Über die Beschaffenheit des in Inselbad bei Paderborn zur Inhalation gebrauchten Gases. *Jour. f. praktische Chemie*, 6:360pp.

Morales, H. and Davidson, S. (1992) Analysis of the hydraulic fracturing behaviour in the Bowen Basin (Australia). In B.B. Beamish and P.D. Gamson (eds), *Proc. Symp. Coalbed Methane Res. Develop. in Australia*, Townsville, Qld., November, 3:33-47.

Paterson, L. and Wold, M. (1992) Initial laboratory studies of the cavity completion process. In B.B. Beamish and P.D. Gamson (eds), *Proc. Symp. Coalbed Methane Res. Develop. in Australia*, Townsville, Qld., November, 4:87-96.

Paterson, L., Meaney, K. and Smyth, M. (1992) Measurements of relative permeability, absolute permeability and fracture geometry in coal. In B.B. Beamish and P.D. Gamson (eds), *Proc. Symp. Coalbed Methane Res. Develop. in Australia*, Townsville, Qld., November, 4:79-86.

Platt, J. (1959) The study of coal surfaces. *Colliery Guardian*, 197:369-371.

Platt, J., Pooley, F.D. and Henderson, W.J. (1965) Electron Microscopy Studies of Coal. *Colliery Guardian*, 210:534-536.

Pooley, F.D. (1968) The use of the electron microscope as a tool in mining research. *Mining Engineer*, 127(90):321-333.

Pooley, F.D., Platt, J. and Henderson, W.J. (1966) Surface micro-structure of some vitrains of British coals. *Nature*, 210:179-181.

Rixon, L.K. (1983). Geological Studies of instantaneous outbursts of coal and gas in Sydney and Bowen Basin coalfields. NERDDC Report NERDDP/EG/83/361.

Stutzer, (1936) Carbon dioxide eruptions from coal seams in Lower Silesia. *Economic Geology*, 31:441-452.

Smith, J.W. and Gould, K.W. (1980) An isotopic study of the role of carbon dioxide in outbursts in coal seams. *J. Geochem.*, 14:27-32.

Stevenson, M.D., Bagio, E., Somers, M.L. and Pinczewski, W.V. (1991) Adsorption / desorption of multi-component on coal at in-seam conditions. In *Proc. SPE Asia Pacific Conference*, Western Australia, 4-7 November 1991.

TDM (1984) Gas, Coal and stability investigations at Theiss Dampier Mitsui Coal Pty. Ltd., Moura, Qld. Final Report NERDDC Project No. 8111547.

Thomas, J.W. (1876) On the gases enclosed in cannel coals and jet. *J. Chem. Soc.*, 30 (2):144.

Thomson, S. and Hungerford, F. (1992) The "RIMDRIL" system - Application of horizontal drilling and RIM for the detection of outburst-prone structures. In B.B. Beamish and P.D. Gamson (eds), *Proc. Symp. Coalbed Methane Res. Develop. in Australia*, Townsville, Qld., November, 3:79-84.

Truong, D. and Williams, R.J. (1989) Gas content and composition of Australian coals. In *Proc. 23rd Newcastle Symp. Advances in the Study of the Sydney Basin.* University of Newcastle, NSW, Australia, March-April, 1989:247-254.
Walker, P.L. Jr., Verma, S.K., Rivera-Utrilla, J. and Davis, A. (1988) Densities, porosities and surface areas of coal macerals as measured by their interaction with gases, vapours and liquids. *Fuel*, 67:1615-1623.
Williams, R.J. (1991a) An update on long-hole drilling for mine gas emission control. In W.J. Bamberry and A.M. Depers (eds), *Proc. Gas in Australian Coals*, Geological Society of Australia, Sydney, February:131-140.
Williams, R.J. (1991b) Carbon dioxide and methane emission at Tahmoor Colliery. In W.J. Bamberry and A.M. Depers (eds), *Proc. Gas in Australian Coals*, Geological Society of Australia, Sydney, February:141-155.
Williams, R.J., Maddocks, P.I. and Gale, W.J. (1992) Longwall gas emission modelling: Practical application and research requirements. In B.B. Beamish and P.D. Gamson (eds), *Proc. Symp. Coalbed Methane Research and Development in Australia*, Townsville, Qld., November, 5:1-5.
Xue, S. and Thomas, I.J. (1991) The permeability of coal under various confining stresses. In W.J. Bamberry and A.M. Depers (eds), *Proc. Gas in Australian Coals*, Geological Society of Australia, Sydney, February:157-162.

Chapter 2

Anon. (1976) Gas Encyclopædia. Elsevier, Paris. 1150 pages. (L'air Liquide, Division Scientifique. English Translation by N. Marshall)
Anon. (1983) Australian Standard 1038.21-1983. Methods for the analysis and testing of coal and coke. Part 21 - Determination of the relative density and apparent relative density of hard coal. Standards Association of Australia, North Sydney. 10 pages.
Anon. (1986a) Australian Standard 2856-1986. Coal - Maceral Analysis. Standards Association of Australia, North Sydney. 24 pages.
Anon. (1986b) Australian Standard 2916-1986. Symbols for Grapical Representation of Coal Seams and Associated Strata. Standards Association of Australia, North Sydney. 12 pages.
Anon. (1989a) Australian Standard AS 1038.17-1989. Methods for the analysis and testing of coal and coke. Part 17: Determination of moisture holding capacity (equilibrium moisture) of higher rank coal. Australian Standards Association, North Sydney. 8 pages.
Anon. (1989b) Australian Standard 1038.3-1989. Methods for the analysis and testing of coal and coke. Part 3: Proximate analysis of higher rank coal. Standards Association of Australia, North Sydney. 16 pages.
Barker-Read, G.R. and Radchenko, S.A. (1989) Methane emission from coal and associated strata samples. *Internat. J. Mining Geol. Engin.*, 7:101-126.
Beamish, B.B. (1994) Proximate analysis of New Zealand and Australian coals by thermogravimetry. *N. Z. J. Geol. Geophysi.*, 37: 387-392.
Beamish, B.B. and Gamson, P.D. (1993) Volume 2 - Laboratory Studies : Sorption Behaviour and Microstructure of Bowen Basin Coals. In: Final Report EDRC Project 1464 - Prediction of Natural Gas Production from Coal Seams. (Ed: Oldroyd, G.C.) Energy Research Development Corporation, Canberra, 128.

Crosdale, P.J. (1993) Determination of Density and Methane Content of Coal Using a High Pressure Microbalance, Commissioning of Microbalance 2, Recommissioning of Microbalance 1. Department of Geology, James Cook University, Townsville. 18 pages. (Coalseam Gas Research Institute Technical Report CGRI TR93/5)

Daines, M.E. (1968) Apparatus for the determination of methane sorption on coal at high pressures by a weighing method. *Internat. J. Rock Mechanics and Mining Science,* 5:315-323.

Dake, L.P. (1978) Fundamentals of Reservoir Engineering. Elsevier, Amsterdam. 443 pages.

Deer, W.A., Howie, R.A. and Zussman, J. (1966) An introduction to the rock forming minerals. Longman, London. 528 pages.

Gamson, P.D., Beamish, B.B. and Johnson, D.P. (1993) Coal microstructure and micropermeability and their effects on natural gas recovery. *Fuel*, 72:87-99.

Gregg, S.J. and Sing, K.S.W. (1967) Adsorption, Surface Area and Porosity. Academic Press, London. 371 pages.

ICCP (1963) International Handbook of Coal Petrography. 2nd ed. Centre National de la Recherche Scientifique, Paris.

Joubert, J.I., Grein, C.T. and Bienstock, D. (1973) Sorption of methane in moist coal. *Fuel*, 52:181-185.

Joubert, J.I., Grein, C.T. and Bienstock, D. (1974) Effect of moisture on the methane capacity of American coals. *Fuel*, 53:186-191.

Lama, R.D. and Bartosiewicz, H. (1982) Determination of gas content of coal seams. In: Seam Gas Drainage with Particular Reference to the Working Seam. (Ed: Hargraves, A.J.) The Australasian Institute of Mining and Metallurgy, Illawarra Branch, Wollongong, 36-52. (Symposium Proceedings, University of Wollongong, 11-14 May, 1982)

Levine, J.R., Johnson, P.W. and Beamish, B.B. (1993) High pressure microgravimetry provides a viable alternative to volumetric method in gas sorption studies on coal. *Proc. 1993 Internat. Coalbed Methane Symp.*, The University of Alabama/Tuscaloosa, May 17-21, 1993, pp. 187-195.

Mahajan, O.P. and Walker Jr, P.L. (1978) Porosity of Coal and Coal Products. In: Analytical Methods for Coal and Coal Products. Vol. 1. (Ed: Karr Jr, C.) Academic Press, New York, 125-162.

Nandi, S.P. and Walker, P.L.J. (1975) Activated diffusion of methane from coals at elevated pressures. *Fuel*, 54:81-86.

Ruppel, T.C., Grein, C.T. and Bienstock, D. (1972) Adsorption of methane/ethane mixtures on dry coal at elevated pressure. *Fuel*, 51:297-303.

Sevenster, P.G. (1959) Diffusion of gases through coal. *Fuel*, 38:403-418.

Smith, D.M. and Williams, F.L. (1984a) Diffusion models for gas production models from coals - application to methane content determination. *Fuel*, 63:251-255.

Smith, D.M. and Williams, F.L. (1984b) Diffusion models for gas production from coal - Determiantion of diffusion parameters. *Fuel*, 63:256-261.

Thimons, E.D. and Kissell, F.N. (1973) Diffusion of methane through coal. *Fuel*, 52:274-280.

van der Sommen, J., Zweitering, P., Eillebrecht, B.J.M. and van Krevelen, D.W. (1955) Chemical structure and properties of coal XII - Sorption capacity for methane. *Fuel*, 34:444-448.

Chapter 3

Beamish, B.B., Crosdale, P.J., Pandolfo, T.G. and Killingley, J.S. (under review) Helium density of banded, hard coals from the Bowen Basin, Australia. *Fuel.*

van Krevelen, D.W. (1961) Coal. Elsevier, Amsterdam. 514 pages.

Chapter 4

Barker-Read, G.R. and Radchenko, S.A. (1989) Methane emission from coal and associated strata samples. *Internat. J. Mining and Geol. Engin.*, 7:101-126.

Beamish, B.B. (in prep) Sorption of gas by coal and associated phenomena in underground mining. Ph.D. Thesis, University of Auckland.

Beamish, B.B. and Crosdale, P.J. (1995) The influence of maceral content on the sorption of gases by coal and the association with outbursting. *Internat. Symp. Mangement and Control of High Gas Emissions and Outbursts in Underground Coal Mines.* (Ed: Lama, R.D.).

Beamish, B.B. and Gamson, P.D. (1993) Volume 2 - Laboratory Studies : Sorption Behaviour and Microstructure of Bowen Basin Coals. *Final Report EDRC Project 1464 - Prediction of Natural Gas Production from Coal Seams.* (Ed: Oldroyd, G.C.) Energy Research Development Corporation, Canberra, 128.

Beamish, B.B., Crosdale, P.J. and Gamson, P.D. (1993) Chracterising the methane sorption behaviour of banded coals in the Bowen Basin, Australia. *Proc. 1993 Internat. Coalbed Methane Symp.*, The University of Alabama/Tuscaloosa, May 17-21, 1993, pp. 145-150.

Bielicki, R.J., Perkins, J.H. and Kissell, F.N. (1972) Methane diffusion parameters for sized coal particles. US Bureau of Mines, Washington. 12 pages. (Bureau of Mines Report of Inveatigations RI 7697)

Ettinger, I., Eremin, I., Zimakov, B. and Yanovskaya, M. (1966) Natural factors influencing coal sorption properties I - Petrography and sorption properties of coals. *Fuel* , 45:267-275.

Faiz, M.M. and Cook, A.C. (1991) Influence of coal type, rank and depth on the gas retention capacity of coals in the Southern Coalfield, NSW. *Gas in Australian Coals.* (Symposium Proceedings 2) (Eds: Bamberry, W.J. and Depers, A.M.) Geological Society of Australia,, 19-29.

Faiz, M.M., Aziz, N.I., Hutton, A.C. and Jones, B.G. (1992) Porosity and gas sorption capacity of some eastern Australian coals in relation to coal rank and composition. *Symp. Coalbed Methane Res. Develop. in Australia*, 19-21 November 1992, Townsville 4, pp. 9-20.

Feng, K.K., Cheng, K.C. and Augsten, R. (1984) Preliminary evaluation of the methane production potential of coal seams at Greenhills Mine, Elkford, British Columbia. *CIM Bull.*, 77:56-61.

Gamson, P.D. and Beamish, B.B. (1992) Coal type, microstructure and gas flow behaviour of Bowen Basin coals. *Symp. Coalbed Methane Res. Develop. in Australia*, 19-21 November 1992, Townsville 4, pp. 43-66.

Gamson, P.D., Beamish, B.B. and Johnson, D.P. (1993) Coal microstructure and micropermeability and their effects on natural gas recovery. *Fuel*, 72:87-99.

Gray, I. (1987) Reservoir engineering in coal seams. Part 1 - The physical process of gas storage and movement in coal seams. SPE Paper #012514. In: SPE Reservoir Engineering.

Harpalani, S. and Schraufnagel, A. (1990a) Measurement of paramaters impacting methane recovery from coal seams. *Internat. J. Mining Geol. Engin.*, 8:369-384.

Harpalani, S. and Schraufnagel, R.A. (1990b) Shrinkage of coal matrix with release of gas and its impact on permeability of coal. *Fuel*, 69:551-556.

Hunt, J.W. and Botz, R.W. (1986) Technical note - outbursts in Australian coal mines: a petrographic factor. *Bull. Proc. Australas. Inst. Mining Metal.*, 291:59-63.

Jolly, D.C., Morris, L.H. and Hinsley, F.B. (1968) An investigation into the relationship between the methane sorption capacitry of coal and gas pressure. *The Mining Engineer*, 127:539-548.

Joubert, J.I., Grein, C.T. and Bienstock, D. (1973) Sorption of methane in moist coal. *Fuel*, 52:181-185.

Joubert, J.I., Grein, C.T. and Bienstock, D. (1974) Effect of moisture on the methane capacity of American coals. *Fuel*, 53:186-191.

Kim, A.G. (1977) Estimating the methane content of bituminous coals from adsorption data. US Department of the Interior, Washington. 22 pages. (Bureau of Mines Report of Investigations RI 8245)

Lama, R.D. (1986) Improving the efficiency of gas drainage systems. (End of Grant Report Number 701) National Energy Research, Development and Demonstration Program.

Lamberson, M.N. and Bustin, R.M. (1993) Coalbed methane characteristics of Gates Formation coals, northeastern British Columbia : effect of maceral composition. *Am. Assoc. Petrol. Geol. Bull.*, 77:2062-2076.

McCulloch, C.M. and Diamond, W.P. (1976) Inexpensive method helps predict methane content of coalbeds. *Coal Age*, 81:102-106.

Moxon, N.T., Mahoney, M.R. and Lunarzewski, L. (1992) Coal Properties Affecting Gas Desorption from Australian Coals. National Energy Research Development and Demonstration Program, Canberra. 114 pages. (Final Report - Project 1260)

Nandi, S.P. and Walker, P.L.J. (1975) Activated diffusion of methane from coals at elevated pressures. *Fuel,* 54:81-86.

Robertson, B. (1993) Central Colliery LW 306 Gas Drainage Project. Initial Assessment of Drainage Parameters. Unpublished Report, Shell Australia, Coal Division.

Ruppel, T.C., Grein, C.T. and Bienstock, D. (1972) Adsorption of methane/ethane mixtures on dry coal at elevated pressure. *Fuel,* 51:297-303.

Wyman, R.E. (1984) Gas resources in Elmworth coal seams. *Elmworth Case Study of a Deep Basin Gas Field.* (Ed: Masters, J.A.) AAPG, Tulsa, Oklahoma, 173-187. (Memoir 38).

Yalçin, E. and Durucan, S. (1991) Methane capacities of Zonguldak coals and the factors affecting methane adsorption. *Mining Sci. Technol.*, 13:215-222.

7. TECHNOLOGY TRANSFER ACTIVITIES

Four papers have been presented at conferences, including two to be presented at the International Symposium cum Workshop on Management and Control of High Gas Emission and Outburst in Underground Coal Mines to be held in Wollongong in March, 1995. These papers are reproduced in full as follows :

1. The influence of maceral content on the sorption of gases by coal and the association with outbursting. Beamish,B.B and Crosdale, P.J. (1995) International Symposium cum workshop on Management and Control of High Gas Emission and Outburst in Underground Coal Mines, Wollongong in March, 1995.

2. Methane Diffusivity at South Bulli (NSW) and Central (Qld) Collieries in relation to coal maceral compositionInternational. Crosdale, P.J. and Beamish, B.B. (1995) Symposium cum workshop on Management and Control of High Gas Emission and Outburst in Underground Coal Mines, Wollongong in March, 1995.

3. Methane sorption studies at South Bulli (NSW) and Central (Qld) Collieries using a high pressure microbalance. Crosdale, P.J. and Beamish, B.B. (1994) 28th Newcastle Symposium on Advances in the Study of the Sydney Basin, 15th to 17th April, 1994.

4. Maceral effects on methane sorption by coal. Crosdale, Peter and Beamish, Basil (1993) New Developments in Coal Geology : a Symposium, Brisbane, November, 1993.

Methane diffusivity at South Bulli (NSW) and Central (Qld) Collieries in relation to coal maceral composition

Peter J. Crosdale
Coalseam Gas Research Institute, James Cook University, Townsville, Australia

B. Basil Beamish
Department of Geology, The University of Auckland, Auckland, New Zealand

ABSTRACT : Dull and bright coal types from South Bulli (NSW) and Central (German Creek, Qld) Collieries have been investigated for methane sorption properties, including desorption rate, by microgravimetry in a high pressure balance. Crushed samples (-0.212mm) show little correlation of petrography to desorption rate as evaluated by the effective diffusivity (D_e). Lump samples (-5.60+2.00mm) show two different effects. At South Bulli there is little relationship between D_e and maceral content. However, at Central Colliery, increasing inertinite content is associated with more rapid desorption. Fundamental differences exist between inertinites at the two mines, with South Bulli having a greater percentage of fine-grained inertinite (inertodetrinite) and a smaller proportion of open cell lumina associated with semifusinite. It is inferred the relative reduction of very large pores in the dull coals from South Bulli inhibits free flow of gas through large particles.

1 INTRODUCTION

Methane content of coal is known to vary with coal type (Ettinger *et al.*, 1966; Lamberson and Bustin, 1993) but the relationship of type to gas desorption rate is less well understood. Studies in the Bowen Basin have indicated possible relationships of petrographic composition to outburst-proneness and gas emission rates (Hunt and Botz, 1986; Beamish and Crosdale, this volume). Inertinite-rich coals are implicated in high gas emission rates but contradictions occur at a maceral level where inertodetrinite has been associated with both rapid and slow emission. However, it has also been suggested that coal type has little influence on gas emission rates (Faiz and Cook, 1991).

To investigate the relationship of coal type to methane desorption, bright and dull coals from Central Colliery (Romax 1.72%) in the Bowen Basin and South Bulli Colliery (Romax 1.25%) in the Sydney Basin have been studied.

2 METHODS

Samples of bright and dull coal types from Central Colliery, German Creek, and South Bulli Colliery were hand picked from in-seam drill cuttings and core and stip samples after lithotype profiling. A particle size of -5.60+2.00mm was selected for sorption rate analysis as a compromise between completion of analysis within a reasonable time frame and evaluation of *in situ* parameters. Samples were also crushed to -0.212mm for evaluation of methane adsorption isotherms and desorption rate of the smaller particles. Analyses were conducted under both equilibrium moist and dry coal conditions but only results from the dry coals are reported.

Sartorious high pressure microbalances were used for gas sorption testing (Beamish and O'Donnell, 1992; Crosdale, 1993; Levine *et al.*, 1993.) Samples were considered to be fully desorbed before analysis as equilibrium moist conditions (under vacuum) were maintained for a minimum of one week and vacuum was applied after transferring into the balance. For sorption rate analysis on lump samples, methane was resorbed at 5MPa until gas uptake became small, following a reduction was made to the estimated *in situ* pressure (3MPa for South Bulli; 2MPa for Central). The *in situ* gas pressure was maintained until weight changes were small and then the gas released to atmosphere. Weight and pressure changes were recorded automatically every minute. The rate of gas release in the first 10 minutes of desorption to atmosphere

is used to estimate the effective diffusivity (D_e) (Smith and Williams, 1984a, b).

$$\frac{V}{V_\infty} = 1 - \frac{6}{\pi^2}\sum_{n=1}^{\infty}\frac{1}{n^2}e^{(-D_e n^2 \pi^2 t)}$$

where D_e = effective diffusivity (sec^{-1})
V = volume of desorbed gas (cc/g)
$V\infty$ = total desorbable gas volume (cc/g)
t = time (sec)

For short time this simplifies to :

$$\frac{V}{V_\infty} = \frac{6}{\sqrt{\pi}}\sqrt{D_e t}$$

A plot of the desorbed gas ratio for the first 600sec versus the square root of time is used for D_e estimation.

Methane adsorption isotherms were determined on moist and dry crushed (-0.212mm) samples at pressures up to 9MPa. Degassing from the highest pressure was performed in a similar manner to the lump samples and thereby allowed D_e to be determined.

Maceral composition of the samples was evaluated using standard point counting techniques on polished grain mounts. Additionally, open and infilled cell lumina in inertinites were counted.

3 RESULTS

Effective diffusivity is an order of magnitiude greater in the crushed than the lump samples (Table 1). There appears to be no systematic difference in the crushed samples from the two mines or in relation to coal type. For the lump samples, the diffusivities are generally lower at South Bulli compared with Central for both bright and dull coal types. The sheared coal (JCB95) has the greatest D_e of the lump samples and approaches that of the crushed coals.

Maceral analyses show the expected trend of bright coals having the greatest vitrinite contents (Table 1), especially telocollinite. Dull coals are more variable in composition and include significant amounts of inertinite and mineral matter. Central Colliery samples are distinguished by their generally lower total inertinite and inertodetrinite, higher mineral matter and greater proportion of cell lumina in inertinites expressed as a ratio to either total inertinite or semifusinite + fusinite.

Comparison of maceral composition to effective diffusivity shows little relationship for the crushed samples (Fig 1). However, significant differences are observed for the lump samples (Fig 2). At South Bulli, effective diffusivities are very low for the high vitrinite bright coals, increase slightly in the low vitrinite dull coals and show little variation with vitrinite content. At Central Colliery, a marked increase in effective diffusivity is observed with decreasing vitrinite content.

4. DISCUSSION

Effect of Particle Size

Particle size effects are well established for gas sorption on coal, with smaller particle sizes sorbing more rapidly (Nandi and Walker, 1975; Barker-Read and Radchenko, 1989). Most adsorption studies use finely ground coal (at least -0.212mm) to take advantage of this and allow rapid equilibration times. Previous studies relating gas sorption characteristics to coal type (e.g. Lamberson and Bustin, 1993) have reported on the relative sorptive capacity but have been unable to distinguish the importance of maceral content on gas flow. This study shows the distinction between coal types is less important at small particle sizes.

Larger grains retain large pores which are an essential part of the gas desorption mechanism. Gas flow in coal occurs by two processes : initially by diffusion until a large pore space is encountered following which free flow takes place. Crushing the samples results in progressive loss of these free flow pathways.

The sheared sample, although high in vitrinite content, displayed desorption characteristics more similar to the crushed samples. The rapid desorption is due to the fine particle size by brittle failure of the sample during tectonic shearing.

Effect of maceral composition

Maceral composition effects on gas flow are best observed in the coarser grains.

Previous studies in the Southern Coalfield of the Sydney Basin (Faiz and Cook, 1991; Faiz *et al.*, 1992) concluded there is little correlation of gas sorption properties to maceral content. For the Southern Coalfield of NSW, our results also suggest increasing inertinite contents are not associated with

marked changes in gas desorption rates.

Contrary findings have been found in coals of the Bowen Basin (Beamish and Gamson, 1993; Beamish *et al.*, 1993) where high inertinite contents are associated with rapid desorption. Results from Central Colliery support these conclusions.

A fundamental difference is therefore found between coals of the two basins. Inertinites in the Southern Coalfield typically contain fewer macropores as cell lumina and are more inertodetrinite-rich. Scanning Electron Microscope studies have suggested that, when unmineralised, cell lumina provide important flow pathways and assist rapid desorption of gas (Gamson *et al.*, 1993).

5 CONCLUSIONS

The effects of maceral composition on gas flow properties of coals cannot be established using fine particle sizes. Desorption rates in Central Colliery coals increase with increasing inertinite content and appears to be related with an increase in macroporosity as identified by preserved cell lumina. In contrast, South Bulli coals do not show a good relationship between desorption rate and petrographic composition. Inertinite types differ at South Bulli and appear to have a lower associated macroporosity.

ACKNOWLEDGMENTS

This work was sponsored by the New South Wales Joint Coal Board Health and Safety Trust.

REFERENCES

Barker-Read, G.R. and Radchenko, S.A. (1989) Methane emission from coal and associated strata samples. *Int. J. Min. Geol. Engng.* 7:101-126.

Beamish, B.B. and Gamson, P.D. (1993) Volume 2 - Laboratory Studies : Sorption Behaviour and Microstructure of Bowen Basin Coals. In: Final Report EDRC Project 1464 - Prediction of Natural Gas Production from Coal Seams. (Ed: Oldroyd, G.C.) Energy Research Development Corporation, Canberra, 128pp.

Beamish, B.B. and O'Donnell, G. (1992) Microbalance applications to sorption testing of coal. *Symp. Coalbed Methane Research and Development in Australia*, 19-21 November 1992, Townsville 4, pp. 31-41.

Beamish, B.B., Crosdale, P.J. and Gamson, P.D. (1993) Chracterising the methane sorption behaviour of banded coals in the Bowen Basin, Australia. *Proc. 1993 Int. Coalbed Methane Symp.*, The University of Alabama/Tuscaloosa, May 17-21, 1993, pp. 145-150.

Crosdale, P.J. (1993) High Pressure Microbalance Analysis. Department of Geology, James Cook University, Townsville. 20 pages. (Coalseam Gas Research Institute, Technical Report, CGRI TR93/4b)

Ettinger, I., Eremin, I., Zimakov, B. and Yanovskaya, M. (1966) Natural factors influencing coal sorption properties I - Petrography and sorption properties of coals. *Fuel* 45:267-275.

Faiz, M.M. and Cook, A.C. (1991) Influence of coal type, rank and depth on the gas retention capacity of coals in the Southern Coalfield, NSW. *In:* Gas in Australian Coals. (Symposium Proceedings 2) (Eds: Bamberry, W.J. and Depers, A.M.) Geological Society of Australia,, 19-29.

Faiz, M.M., Aziz, N.I., Hutton, A.C. and Jones, B.G. (1992) Porosity and gas sorption capacity of some eastern Australian coals in relation to coal rank and composition. *Symp. Coalbed Methane Research and Development in Australia*, 19-21 November 1992, Townsville 4, pp. 9-20.

Gamson, P.D., Beamish, B.B. and Johnson, D.P. (1993) Coal microstructure and micropermeability and their effects on natural gas recovery. *Fuel* 72:87-99.

Hunt, J.W. and Botz, R.W. (1986) Technical note - outbursts in Australian coal mines: a petrographic factor. *Bull. Proc. Australas. Inst. Mining Metall.* 291:59-63.

Lamberson, M.N. and Bustin, R.M. (1993) Coalbed methane characteristics of Gates Formation coals, northeastern British Columbia : effect of maceral composition. *Am. Assoc. Petrol. Geol. Bull.* 77:2062-2076.

Levine, J.R., Johnson, P.W. and Beamish, B.B. (1993) High pressure microgravimetry provides a viable alternative to volumetric method in gas sorption studies on coal. *Proc 1993 Int. Coalbed Methane Symp.*, The University of Alabama

/Tuscaloosa, May 17-21, 1993, pp. 187-195.

Nandi, S.P. and Walker, P.L.J. (1975) Activated diffusion of methane from coals at elevated pressures. *Fuel* 54:81-86.

Smith, D.M. and Williams, F.L. (1984a) Diffusion models for gas production from coal - Determination of diffusion parameters. *Fuel* 63:256-261.

Smith, D.M. and Williams, F.L. (1984b) Diffusion models for gas production models from coals - application to methane content determination. *Fuel* 63:251-255.

Table 1 Coal petrography and effective difusuvities of dry samples

Sample	Lithotype	Vit (%)	Lipt (%)	Semif + Fus (%)	Inertodet (%)	Total Inert (%)	MM (%)	Cell lumina (%)	De (sec^{-1}) crushed	De (sec^{-1}) lump
Central Colliery										
JCB4B	B	85.1	0.0	7.4	0.9	8.3	4.8	1.3	2.7E-5	3.1E-6
JCB4D	D	35.7	0.0	40.1	8.0	48.1	12.2	4.6		6.6E-6
JCB7B	B	96.1	0.0	1.0	0.1	1.1	2.5	0.0		3.2E-6
JCB7D	D	47.2	0.0	29.4	6.1	35.5	12.7	4.9	2.4E-5	5.5E-6
JCB9B	B	92.2	0.0	3.7	1.1	4.8	2.4	0.1	7.3E-5	1.2E-6
JCB9D	D	30.9	0.0	46.8	2.9	49.7	12.0	11.4	1.8E-5	4.5E-6
JCB12B	B	92.3	0.0	3.3	1.1	4.4	2.7	0.2	5.4E-5	2.3E-6
JCB12D	D	47.7	0.0	25.8	7.0	32.8	15.3	4.7	6.2E-5	3.8E-6
JCB21B	B	97.7	0.0	0.8	0.1	0.9	1.0	0.0	2.7E-5	1.7E-6
JCB21D	D	60.9	0.0	19.4	3.1	22.5	12.3	4.1	7.4E-5	3.8E-6
JCB82B	B	97.5	0.0	1.9	0.0	1.9	0.3	0.0	4.2E-5	1.2E-6
JCB82D	D	46.2	0.0	34.2	7.2	41.4	8.8	4.2	5.7E-5	2.0E-6
JCB92B	B	94.9	0.0	1.9	0.5	2.4	2.3	0.1	3.9E-5	1.3E-6
JCB92D	D	42.3	0.1	36.2	6.5	42.8	9.7	6.7	4.0E-5	3.4E-6
JCB95	sheared	56.0	0.0	8.1	4.6	13.0	30.1	0.1	7.3E-5	8.0E-6
South Bulli Colliery										
JCB27B	B	95.6	3.5	0.1	0.3	0.4	0.1	0.0	2.1E-5	1.1E-6
JCB 25D	D	1.8	0.1	76.4	9.7	86.1	8.9	9.0	5.4E-5	2.5E-6
JCB29B	B	95.1	0.0	1.6	0.7	2.3	2.3	0.0	2.3E-5	
JCB32D	D	21.0	0.0	56.3	10.9	67.2	7.6	4.2	3.1E-5	2.9E-6
JCB35B	B	91.1	0.0	4.4	3.7	8.1	0.6	0.0	3.7E-5	
JCB37D	D	10.2	0.0	53.7	26.5	80.2	3.4	5.9	6.8E-5	
JCB40B	B	96.6	0.0	0.9	0.3	1.2	1.9	0.0	1.4E-5	0.6E-6
JCB42D	D	16.8	0.0	62.3	15.3	77.6	1.9	4.0	2.4E-5	2.0E-6
JCB66B	B	99.1	0.0	0.1	0.3	0.4	0.1	0.0	3.6E-5	1.1E-6
JCB65D	D	3.4	0.1	76.1	14.5	90.6	2.4	5.2	4.7E-5	2.9E-6
JCB74BD	BD	34.4	0.0	47.3	8.0	55.3	3.6	6.4	3.9E-5	2.7E-6
JCB76BD	BD	81.3	0.0	11.4	1.6	13.0	4.8	1.4		2.2E-6

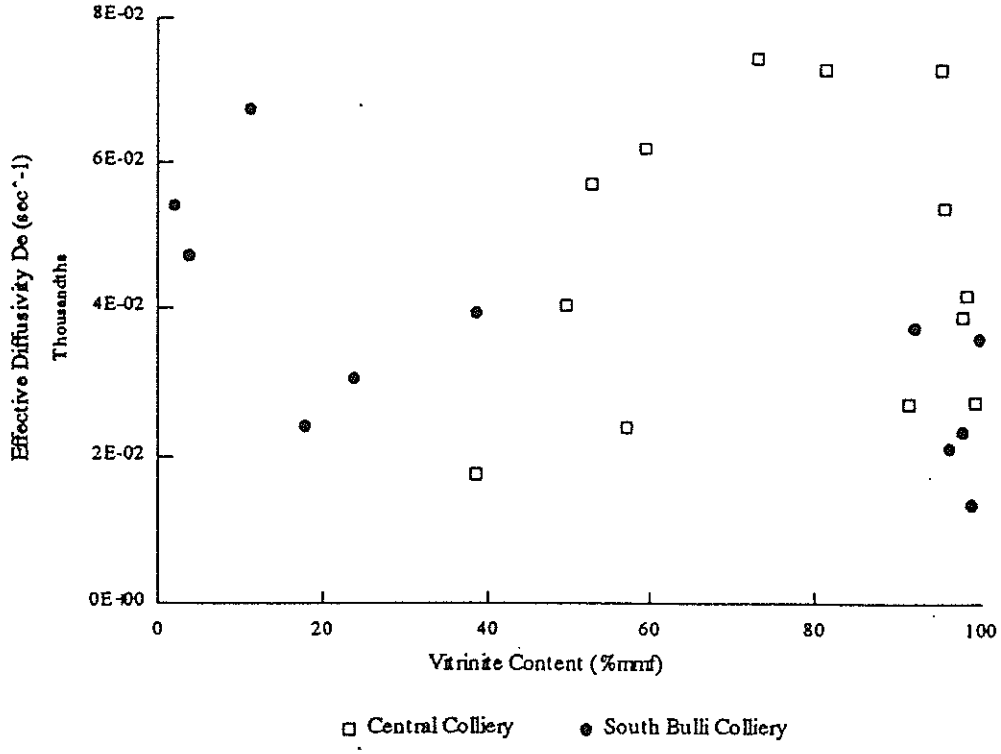

Figure 1 Relationship of vitrinite content to effective diffusivity for crushed samples (-0.212mm)

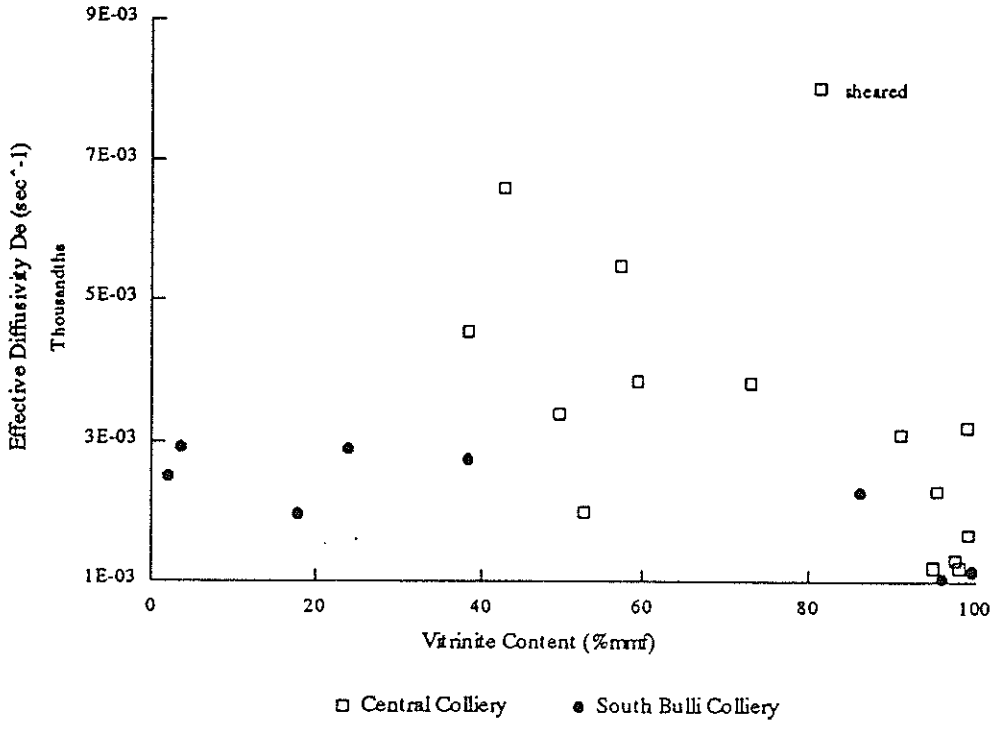

Figure 2 Relationship of vitrinite content to effective diffusivity for lump samples (-5.60+2.00mm)

MACERAL EFFECTS ON METHANE SORPTION BY COAL

Peter Crosdale & Basil Beamish, JCU

Methane sorption characteristics of Bowen Basin coals are shown to be strongly influenced by coal type. In isorank samples, vitrinite-rich coal has greater sorption capacity but slower sorption rate than inertinite-rich coal.

INTRODUCTION

A two year research programme at James Cook University has included the investigation of methane sorption behaviour of Bowen Basin coals as part of Energy Research Development Corporation (ERDC) project 1464 (Oldroyd, 1993).

Laboratory studies concentrated on characterising methane sorption and coal microstructure. Differences observed between bright and dull coal types were subsequently investigated by maceral analysis.

A variety of opinions exist as to the importance of maceral composition on sorption properties. Fusinite has been found to sorb more methane than vitrinite (Ettinger & others, 1966) while the opposite has also been observed (Beamish & others, 1993; Lamberson & Bustin, in press).

Maceral composition has also been found to have little effect (Faiz & others, 1992).

METHODOLOGY

Samples

Hand picked samples of dull and bright coal were selected from drill core. Sorption rate and maceral studies were performed on solid coal blocks weighing 1g which have an approximate diameter of 8mm. Gas sorption capacities were determined on crushed samples (-212µm). Rank ranged from high to low volatile bituminous. Results from three representative pairs of samples are discussed in detail (Table 1).

Gas Sorption Testing

Gas sorption testing was performed using a microgravimetric technique (Beamish & O'Donnell, 1992; Beamish & Gamson, 1993a; Levine & others, 1993).

Sorption rates were determined on samples which had been evacuated, repressured with methane and degassed from 1MPa to atmosphere. The amount of gas sorbed was monitored as a weight change with time.

TABLE 1. SAMPLE PROPERTIES

	1A bright	1B dull	2A bright	2B dull	3A bright	3B dull
MACERAL ANALYSIS						
Telocollinite	99.2	3.3	43.0	8.5	100.0	0.0
Desmocollinite	0.8	6.4	29.9	24.6	0.0	1.9
Sporinite	0.0	0.0	2.7	3.6	0.0	8.5
Cutinite	0.0	0.0	0.3	0.3	0.0	0.0
Resinite	0.0	0.0	0.2	0.0	0.0	0.0
Semifusinite	0.0	79.2	18.8	53.1	0.0	39.0
Fusinite	0.0	4.2	0.8	2.0	0.0	0.0
Inertodetrinite	0.0	2.0	3.6	7.3	0.0	39.4
Micrinite	0.0	0.0	0.5	0.3	0.0	0.0
Macrinite	0.0	0.0	0.0	0.5	0.0	0.0
Detrital Mineral Matter	0.0	4.8	0.3	0.0	0.0	11.2
	1.66		0.81		0.88	
PROXIMATE ANALYSIS						
Ash (%db)	1.9	24.5	2.1	4.2	3.7	13.8
Volatile Matter (%db)	16.5	13.8	33.3	29.2	30.4	20.9
Fixed Carbon (%db)	81.6	61.7	64.6	66.5	65.8	65.3
Langmuir Volume (scc/g, db)	37.9	24.7	32.8	26.9	30.9	24.4

Adsorption isotherms were determined up to a maximum pressure of 7MPa.

Gas Content Calculation

Weight recorded by the microbalance must be corrected for buoyancy effects. A buoyant force is applied to all components within the balance, including the sample, equal to the weight of gas displaced. The weight of displaced gas varies with pressure as well as during sorption, as the sorbing gas changes the sample volume. The weight of displaced gas is estimated from the volume of the balance, including the sample, and the gas density at each pressure, derived from the real gas equation.

Volume of the microbalance components, including weighing arms, sample pans and counterweights, is experimentally determined. Initial sample volume is calculated from its helium density. Knowing the density of sorbed methane on coal, the weight of sorbed methane can be calculated (Crosdale, 1993; Levine & others, 1993) :

$$W_s = (W_{mb} - \rho_g(V_{mb} - V_c))/(1 - \rho_g/\rho_s)$$

where :

W_s	=	weight of sorbed methane
W_{mb}	=	microbalance output weight
V_{mb}	=	microbalance volume
V_c	=	volume of coal
ρ_g	=	gas density
ρ_s	=	sorbate density

Sorbed methane density on coal has been determined as 618.9g/l (van der Sommen & others, 1955).

Helium Density Determination

Coal density is a critical factor in gas content calculation. Helium densities of the coal used in the microbalance were determined by the CSIRO. However, helium density is now also determined in the microbalance. Sample volume is derived from a plot of gas density versus observed weight at a range of pressures up to 10MPa. As sample weight is known, density is readily obtained. Gas density is calculated using the real gas equation.

Maceral Analysis

Following sorption testing, half the sample was mounted in epoxy and polished for maceral analysis. Point counting of 250 to 500 points per sample of both macerals and associated structures was performed. Structures associated with macerals included mineralised and unmineralised fractures and cell lumina.

RESULTS AND DISCUSSION

Results from three representative pairs of samples (Table 1; Figure 1) are discussed in

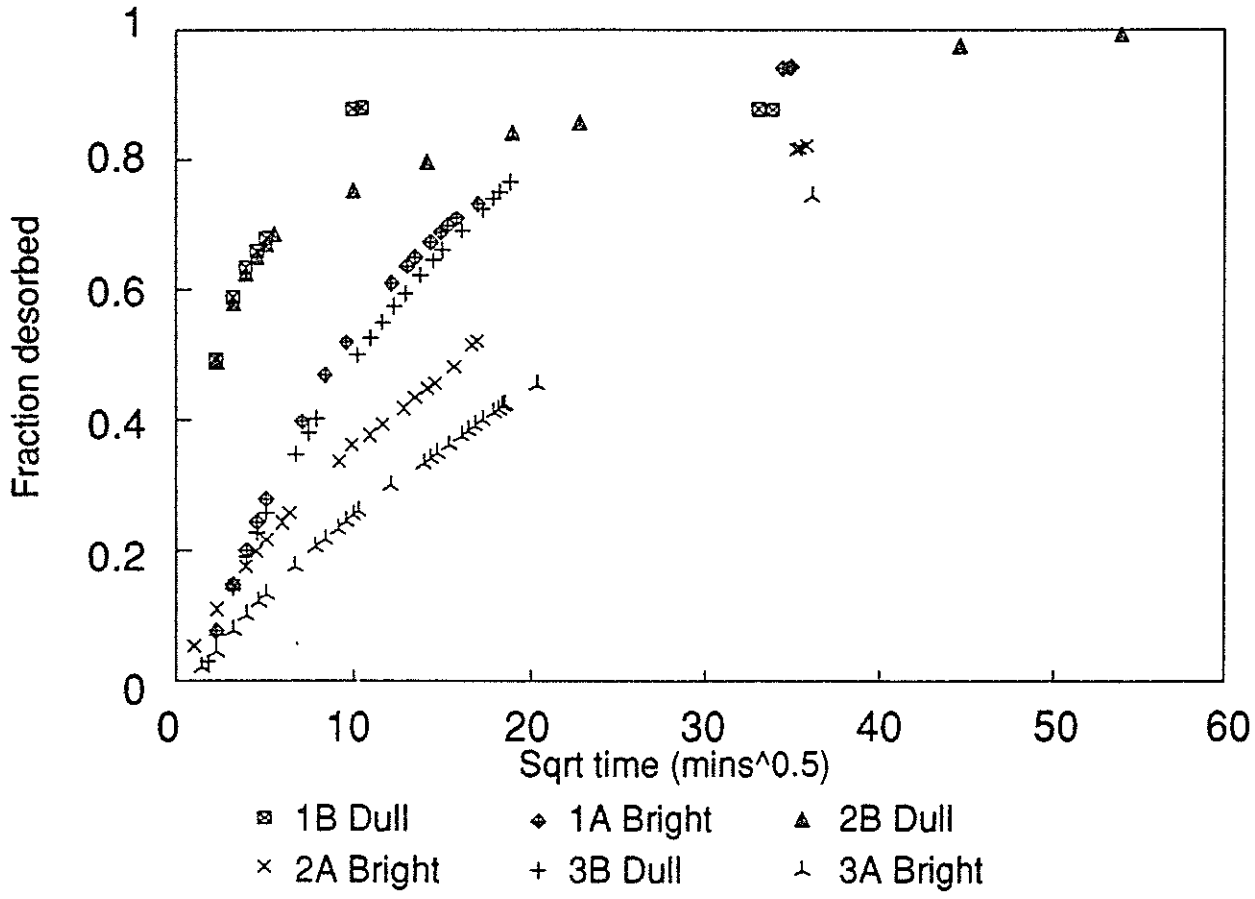

detail but conclusions are drawn from a larger data set (Beamish & Gamson, 1993b).

Maceral Analysis

Bright coal samples 1A and 3A are composed almost exclusively of telocollinite (Table 1). Megascopic description of the polished sample 2A petrographic block indicated it is banded dull and bright rather than bright coal. This is reflected in its maceral content including significant desmocollinite and semifusinite.

Dull coals (1B, 2B and 3B) consist of 40 - 80% semifusinite (Table 1). Sample 3B is characterised by a high percentage of inertodetrinite with much of the semifusinite also fragmentary but too large to be classified as inertodetrinite. Macroscopically, 3B has an appearance similar to a sapropelic coal.

Results on investigation of structures associated with macerals are not presented here. However, semifusinite usually contains around 30% by volume of cell lumina, many of which appear unmineralised. SEM examination (Gamson & others, 1993) confirms generally low degrees of mineralisation which is partly responsible for high gas flow rates associated with inertinite-rich coals.

Sorption Rate Behaviour

Dull coal generally has an initial rapid desorption followed by slow desorption (Figure 1 - 1B, 2B). Desorption rate is little affected by rank for the rapid desorption. Reasons for the change from rapid to slow desorption are clarified by petrographic analysis. In some instances, a more uniform, slower desorption is shown (Figure 1 - 3B).

Bright coals are characterised by slower, more uniform desorption rates (Figure 1 - 1A, 2A, 3A). Rank dependence is shown as the sorption rate increases with increasing rank; samples of rank intermediate between 1A and 3A plot in intermediate positions. Sample 2A has an initial period of more rapid desorption up to 25% desorbed methane before the rate (slope of line) becomes the same as sample 3A, which is of similar rank.

Maceral Effects on Methane Sorption

Dull coals show a variety of sorption characteristics. Those with high semifusinite contents have the lowest sorption capacities but fastest rates. Types dominated by inertodetrinite have intermediate properties. With increase of vitrinite content, characteristics become closer to those of bright coal.

Change from rapid to slow desorption of dull coals occurs at a fraction desorbed of 90% for 1B and 65% for 2B. This corresponds closely to inertinite compositions (mmf) of 88.8% and 63.2% respectively. Similarly, for bright coal 2A an initial period of more rapid desorption up to 25% fraction desorbed corresponds to an inertinite content of 23.7%.

Slowly desorbing dull coal 3B can be petrographically distinguished by its high fragmentary inertinite content. Other dull coal types dominated by vitrinite group macerals may also be expected to show slower desorption characteristics.

Isotherm investigations show bright coal has a higher gas sorption capacity (by up to 30%, expressed as Langmuir volume) as well as lower desorption rates than equivalent rank dull coal (Table 1; Figure 1). Capacity and sorption rate of vitrinite-rich samples also show rank dependence, with lower ranks having lower capacities and slower rates. Dull coals with high semifusinite contents are less influenced by rank.

CONCLUSIONS

Methane sorption rate and capacity vary according to coal type and rank.

Vitrinite-rich coals desorb more slowly but have gas sorption capacity up to 30% greater than inertinite-rich coals of the same rank. Sorption rates of vitrinite-rich coal display a dependency on rank, with higher ranks desorbing more quickly.

Sorption rates of inertinite-rich coals, particularly those with semifusinite and fusinite, are greater than vitrinite-rich coals and are less rank dependent.

ACKNOWLEDGMENTS

The following funding bodies are thanked for their financial support :

- New South Wales Joint Coal Board Health and Safety Trust
- Energy Research and Development Corporation
- James Cook University, Prestige Research Grant

Samples were supplied by MIM Holdings Ltd and MGC Resources Australia.

REFERENCES

BEAMISH, B.B. & GAMSON, P.D., 1993a: Laboratory investigations of Bowen Basin coals for natural gas production. *Australian Coal Geology*, **9**, 16—21.

BEAMISH, B.B. & GAMSON, P.D., 1993b: Volume 2 - Laboratory Studies : Sorption Behaviour and Microstructure of Bowen Basin Coals. *In*: Oldroyd,G.C.(Principal Investigator) *Final Report on EDRC Project 1464 - Prediction of Natural Gas Production from Coal Seams*. Energy Research Development Corporation, Canberra.

BEAMISH, B.B. & O'DONNELL, G., 1992: Microbalance applications to sorption testing of coal. *Symposium on Coalbed Methane Research and Development in Australia, 19-21 November 1992, Townsville* 4, 31—41.

BEAMISH, B.B., CROSDALE, P.J. & GAMSON, P.D., 1993: Characterising the methane sorption behaviour of banded coals in the Bowen Basin, Australia. *Proceedings of the 1993 International Coalbed Methane Symposium, The University of Alabama/Tuscaloosa, May 17-21, 1993*, 145—150.

CROSDALE, P.J., 1993: Determination of Density and Methane Content of Coal Using a High Pressure Microbalance. *Coalseam Gas Research Institute Technical Report CGRI TR93/5*. Department of Geology, James Cook University, Townsville.

ETTINGER, I., EREMIN, I., ZIMAKOV, B. & YANOVSKAYA, M., 1966: Natural factors influencing coal sorption properties I - Petrography and sorption properties of coals. *Fuel*, 45, 267—275.

FAIZ, M.M., AZIZ, N.I., HUTTON, A.C. & JONES, B.G., 1992: Porosity and gas sorption capacity of some eastern Australian coals in relation to coal rank and composition. *Symposium on Coalbed Methane Research and Development in Australia, 19-21 November 1992, Townsville* 4, 9—20.

GAMSON, P.D., BEAMISH, B.B. & JOHNSON, D.P., 1993: Coal microstructure and micropermeability and their effects on natural gas recovery, *Fuel*, 72, 87—99.

LAMBERSON, M.N. & BUSTIN, R.M., (in press): Coalbed methane characteristics of Gates Formation coals, northeastern British Columbia : effect of maceral composition. AAPG.

LEVINE, J.R., JOHNSON, P.W. & BEAMISH, B.B., 1993: High pressure microgravimetry provides a viable alternative to volumetric method in gas sorption studies on coal. *Proceedings of the 1993 International Coalbed Methane Symposium, The University of Alabama/Tuscaloosa, May 17-21, 1993*, 187—195.

OLDROYD, G.C., (Principal Investigator), 1993: *Final Report ERDC Project 1464 - Prediction of Natural Gas from Coal Seams*. Energy Research Development Corporation, Canberra.

VAN DER SOMMEN, J., ZWEITERING, P., EILLEBRECHT, B.J.M. & VAN KREVELEN, D.W., 1955: Chemical structure and properties of coal XII - Sorption capacity for methane, *Fuel*, 34, 444—448.

P.J. Crosdale
*B. B. Beamish**
Coalseam Gas Research Institute
James Cook University of North Queensland
Townsville 4811

**Current address: Department of Geology, University of Auckland*

METHANE SORPTION STUDIES AT SOUTH BULLI (NSW) & CENTRAL (QLD) COLLIERIES USING A HIGH PRESSURE MICROBALANCE

P.J. CROSDALE[1] & B.B. BEAMISH[2]

[1] Dept. of Geology, James Cook University

[2] Dept. of Geology, University of Auckland

ABSTRACT

Bright and dull coal lithotypes from medium volatile bituminous coals of South Bulli and Central (German Creek) Collieries have been characterised for methane sorption properties. In dry, isorank samples, bright (vitrinite-rich) coal has greater sorption capacity but lower sorption rate than dull (inertinite-rich) coal. In equilibrium moist samples, differences in gas properties are less apparent but initial desorption rates of bright coals remain lower than dull coals.

INTRODUCTION

Results of gas sorption studies are presented from two pairs of bright and dull coals from South Bulli ($\bar{R}_{omax}$ 1.27%) and Central (German Creek) Collieries ($\bar{R}_{omax}$ 1.45%). They are representative of a larger suite of results examining gas sorption characteristics in these two collieries in relation to coal type.

A variety of opinions exist as to the importance of coal type on sorption properties. Fusinite has been found to sorb more methane than vitrinite (Ettinger et al., 1966) while the opposite has also been observed (Beamish et al., 1993; Lamberson and Bustin, 1994). Maceral composition has also been found to have little effect (Faiz et al., 1992).

METHODOLOGY

Samples

Samples of dull and bright coal were hand picked from in seam drill cuttings and from underground mine workings following lithotype logging. Particle size greatly influences gas sorption rates and a uniform particle size is required for direct comparison of results. The size selected for analysis was dictated by the drill cuttings. Samples were sieved at -5.60+2.00mm prior to picking, with approximately 1g used. Analyses were performed at both equilibrium moist and dry conditions. Equilibrium moist conditions are thought to simulate the in ground state but analysis is difficult. Dry

coal testing is less complicated and ensures comparability of results. Methane adsorption isotherms were determined on finely crushed (-0.212mm) coal.

Gas Sorption Testing

Gas sorption testing used a microgravimetric technique (Beamish and O'Donnell, 1992; Beamish and Gamson, 1993; Levine et al., 1993). Prior to testing, moist samples were evacuated at -95kPa for one minute, the pressure simulating equilibrium moist conditions and a short time to minimise moisture loss. Oven dried samples were evacuated at greater vacuum and for one hour. Following evacuation, methane was introduced at 5MPa and the -5.60+2.00mm size sample left to resorb gas until the weight change did not exceed 0.01 mg/hr. Pressure was then reduced to the estimated *in situ* gas pressure (3MPa for South Bulli; 2MPa for Central) and the sample left until the weight change did not exceed 0.01mg/hr. Samples were then allowed to degas at atmospheric pressure. Adsorption isotherms were performed on crushed coal (-0.212mm) up to maximum gas pressures of 7 to 10 MPa using 1 MPa steps.

Testing of moist samples was problematic. High relative humidity, necessary to prevent moisture loss during analysis, can be maintained in the sample environment by the use of a K_2SO_4 solution. However, buoyancy correction factors are difficult to calculate with certainty owing to variable and different gas densities in the sample and counterweight chambers of the balance. High humidity environments may also damage the balance.

Moist samples were tested in a dry gas environment. Moisture loss during the course of testing results in the final sample weight being significantly less than its initial weight. A correction factor was applied which assumed a constant rate of moisture loss for the duration of the test. The final weight change for moist samples is therefore zero.

Gas Content Calculation

Weight recorded by the microbalance must be corrected for buoyancy effects. A buoyant force applied to all balance components, including the sample, equals the weight of gas displaced. The weight of displaced gas is estimated from the volume of the balance, including the sample, and the gas density at each pressure, derived from the real gas equation.

Volume of the microbalance components, including weighing arms, sample pans and counterweights, was experimentally evaluated. Initial sample volume was calculated from its helium density as determined in the microbalance prior to methane adsorption. Knowing the density of sorbed methane on coal (= 618.9g/l; van der Sommen et al., 1955), the weight of sorbed methane can be calculated (Crosdale, 1993; Levine et al., 1993) :

$$W_s = (W_{mb} - \rho_g(V_{mb} - V_c))/(1 - \rho_g/\rho_s)$$

where :

W_s = weight of sorbed methane V_c = volume of coal ρ_s = sorbate density
W_{mb} = microbalance output weight V_{mb} = microbalance volume ρ_g = gas density

RESULTS AND DISCUSSION

Adsorption Isotherm

Adsorption isotherms indicate the coal's sorption capacity at different pressures and have been used to estimate the degree of gas saturation (Table 1). The Langmuir Volume (V_L) of the adsorption isotherm represents the maximum gas holding capacity of the coal. Langmuir Pressure (P_L) is the pressure at half the Langmuir Volume.

Results for Central Colliery (Table 1; Fig 1) indicate dry coal holds more gas than moist coal. Coal type influences are shown with dry bright coal having greatest sorption capacity. However, no significant difference in Langmuir volume is observed between bright and dull coals in equilibrium moist samples. Further analyses are required to confirm these trends.

Sorption Rate Behaviour

Gas saturation calculations are derived from the adsorption isotherm and the gas content of the coarse sample. Gas saturations of $>80\%$ are generally achieved (Table 2) prior to desorption to atmosphere. Comparison with known seam gas contents (Tables 2 and 3) indicate the coal in ground is undersaturated with respect to methane except at South Bulli site 1.

Comparison of desorption rates from the *in situ* pressure to atmosphere is made using an estimation of the effective diffusivity (D_e). Calculation is based on the desorption rate during the first ten minutes and assumes a unipore spherical model with uniform pore distribution. As neither assumption is usually true (Smith and Williams, 1984), the calculated diffusivities do not describe the whole desorption curve and separate evaluation of macropore and micropore diffusivities is required (Smith and Williams, 1984; Beamish and Gamson, 1993).

Effective diffusivities for all samples are generally of the same order of magnitude (10^{-6} s^{-1}). Moist samples appear to have greater diffusivities than dry but this result may be influenced by assumptions used for calculating gas contents of moist samples. Bright coals generally have lower diffusivities than their dull coal equivalent in both moist and dry states and release gas more slowly.

Analysis of moist coal desorption is complicated by lack of knowledge of the true moisture state of the sample. Significant moisture loss occurs as sample weight at the end of desorption is less than its initial weight. Calculations have assumed a constant rate of moisture loss for the whole experiment as this gives the most reasonable overall isotherm shape.. This assumption requires the final gas content of the moist coal to be zero, which is unlikely as dry coals show a significant residual gas content.

Moist coal desorption may be similar for both bright and dull coal (Figs 2 and 4) or bright coal may desorb more slowly (Fig 3). In the dry state, dull coal always shows an initial period of more rapid desorption than the bright coal, followed by a

period in which the dull desorption rate is slower (Figs 2 to 5).

CONCLUSIONS

Methane sorption rate and capacity vary according to coal type and rank. The higher rank Central Colliery coal has a greater sorption capacity than the South Bulli coal but is more undersaturated. Moisture state is important in determining gas contents and desorption rates. In comparable moisture states, dull coal always desorbs more quickly than its equivalent bright coal. Bright coals have a greater gas storage capacity than dull coals when dry but the difference is less marked in moist coal.

ACKNOWLEDGMENTS

The following bodies are thanked for their support :
- New South Wales Joint Coal Board Health and Safety Trust
- South Bulli Colliery
- Central Colliery
- The Shell Company of Australia Ltd
- Auckland University Research Committee

REFERENCES

BEAMISH,B.B., GAMSON,P.D. (1993) Volume 2 - Laboratory Studies : Sorption Behaviour and Microstructure of Bowen Basin Coals. *In* Oldroyd, G.C. (Principal Investigator) Final Report on ERDC Project 1464 - Prediction of Natural Gas Production from Coal Seams. *Energy Research Development Corporation*, Canberra, 128pp.

BEAMISH,B.B., O'DONNELL,G. (1992) Microbalance applications to sorption testing of coal. *Symposium on Coalbed Methane Research and Development in Australia*, Vol. 4, pp. 31-41, 19-21 November 1992, Townsville.

BEAMISH,B.B., CROSDALE,P.J., GAMSON,P.D. (1993) Characterising the methane sorption behaviour of banded coals in the Bowen Basin, Australia. *Proceedings of the 1993 International Coalbed Methane Symposium*, pp. 145-150, The University of Alabama/Tuscaloosa, May 17-21, 1993.

CROSDALE,P.J. (1993) Determination of Density and Methane Content of Coal Using a High Pressure Microbalance. Coalseam Gas Research Institute Technical Report CGRI TR93/5. Department of Geology, James Cook University, Townsville. 18 pages.

ETTINGER,I., EREMIN,I., ZIMAKOV,B., YANOVSKAYA,M. (1966) Natural factors influencing coal sorption properties I - Petrography and sorption properties of coals. *Fuel* 45, 267-275.

FAIZ,M.M., AZIZ,N.I., HUTTON,A.C., JONES,B.G. (1992) Porosity and gas sorption capacity of some eastern Australian coals in relation to coal rank and composition. *Symposium on Coalbed Methane Research and Development in Australia*, Vol. 4, pp. 9-20 19-21 November 1992, Townsville.

LAMBERSON,M.N., BUSTIN,R.M. (1993) Coalbed methane characteristics of Gates Formation coals, northeastern British Columbia : effect of maceral composition. *AAPG Bulletin* 77 2062-2076.

LEVINE,J.R., JOHNSON,P.W., BEAMISH,B.B. (1993) High pressure microbalance sorption studies. *Proceedings of the 1993 International Coalbed Methane Symposium*, pp. 187-195, The University of Alabama/Tuscaloosa, May 17-21, 1993.

SMITH,D.M. AND WILLIAMS,F.L. (1984) Diffusion models for gas production from coals - application to methane content determination. *Fuel* 63, 251-255.

VAN DER SOMMEN,J., ZWEITERING,P., EILLEBRECHT,B.J.M., VAN KREVELEN,D.W. (1955) Chemical structure and properties of coal XII - Sorption capacity for methane. *Fuel* 34, 444-448.

P.J. CROSDALE and B.B. BEAMISH

Table 1 Adsorption Isotherm, Central Colliery, Site 1

	Bright Coal		Dull Coal	
Sample Weight (equilibrium moist) (g)	0.44227		0.37833	
Sample Weight (dry) (g)	0.43499		0.36688	
Equilibrium Moisture (%)	1.43		3.03	
Particle Size (mm)	-0.212		-0.212	
Temperature (°C)	23.5		23.5	
Helium Density (dry) (g/cc)	1.34		1.45	
Langmuir Coefficients	moist	dry	moist	dry
Langmuir Pressure (P_L) (MPa)	2.40	1.17	2.08	1.32
Langmuir Volume (V_L) (scc/g)	21.5	28.3	21.1	26.3

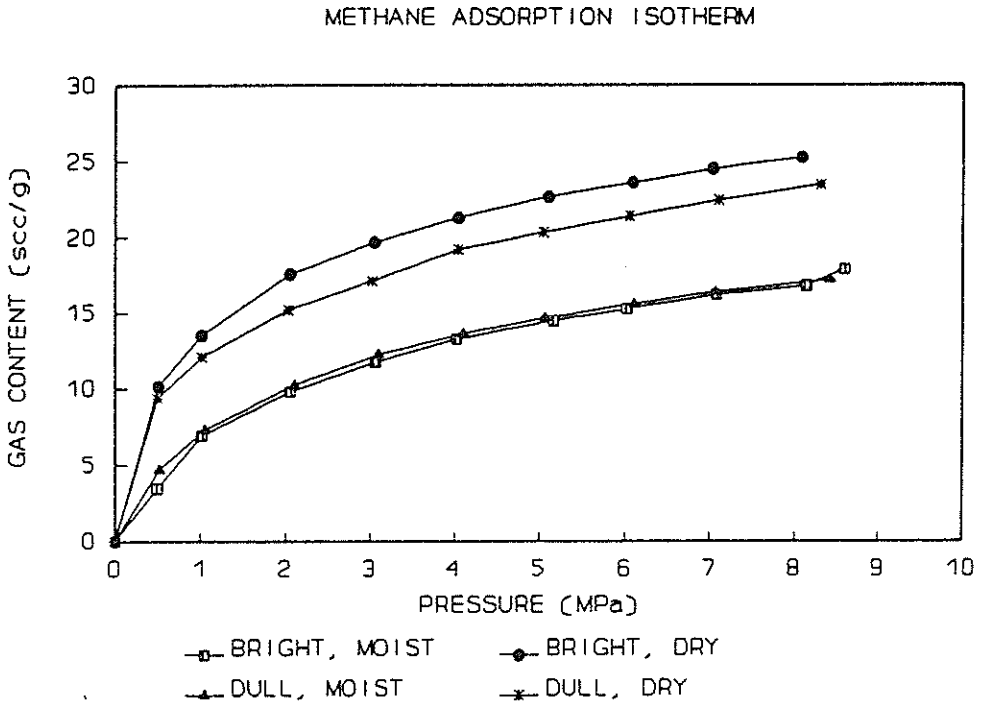

Figure 1 Methane Adsorption Isotherm, Central Colliery, Site 1

METHANE SORPTION AT SOUTH BULLI AND CENTRAL COLLIERIES

Table 2 Central Colliery - coal and gas properties

	SITE 1				SITE 2			
	Bright Moist	Bright Dry	Dull Moist	Dull Dry	Bright Moist	Bright Dry	Dull Moist	Dull Dry
weight (moist) (g)	1.00660		1.00910		1.01404		1.01076	
weight (dry) (g)	0.99170	1.00243	0.99190	0.99190	0.99654	0.99654	0.99219	0.99219
moisture (%)	1.48	0.00	1.70	0.00	1.73	0.00	1.84	0.00
particle size (mm)	-5.60 +2.00	-5.60 +2.00	-5.60 +2.00	-5.60 +2.00	-5.60 +2.00	-5.60 +2.00	-5.60 +2.00	-5.60 +2.00
temp. (°C)	23.5	23.5	23.5	23.5	23.5	23.5	23.5	23.5
He density (g/cc)		1.34		1.45		1.33		1.39
gas cont. at 5MPa (scc/g)	15.6	22.4	12.3	18.4	18.4	22.7	17.1	18.4
% gas saturation at 5MPa	95	98	82	89				
gas cont. at 2MPa (scc/g)	11.6	17.7	8.6	13.7	15.2	18.3	12.9	15.1
% gas saturation at 2MPa	99	98	81	85				
est. final gas cont. (scc/g)	0.0	5.5	0.4	5.9	0.0	6.3	0.0	5.3
effect. diffusivity(D_e)(s^{-1})	3.6E-6	1.5E-6	6.9E-6	5.5E-6	8.9E-7	1.8E-6	2.7E-6	4.0E-6
seam gas content (m^3/t)	5.5				6.0			

Table 3 South Bulli Colliery - coal and gas properties

	Site 1				Site 2			
	Bright Moist	Bright Dry	Dull Moist	Dull Dry	Bright Moist	Bright Dry	Dull Moist	Dull Dry
weight (moist) (g)	1.00372		1.00085		0.90242		0.92664	
weight (dry) (g)	0.98733	0.98733	0.98276	0.98276	0.88908	0.88908	0.91112	0.91112
moisture (%)	1.63	0.00	1.81	0.00	1.48	0.00	1.67	0.00
particle size (mm)	-5.60 +2.00	-5.60 +2.00	-5.60 +2.00	-5.60 +2.00	-5.60 +2.00	-5.60 +2.00	-5.60 +2.00	-5.60 +2.00
temp. (°C)	23.5	23.5	23.5	23.5	23.5	23.5	23.5	23.5
He density (g/cc)		1.29		1.44	1.39	1.28	1.29	1.40
gas cont. at 5MPa (scc/g)	5.7	15.7	8.3	14.5	8.6	14.6	15.6	17.5
% gas saturation at 5MPa								
gas cont. at 3MPa (scc/g)	6.0	14.9	7.8	13.4	8.2	14.1	12.9	15.7
% gas saturation at 3MPa								
est. final gas cont. (scc/g)	0.5	5.6	0.4	4.9	0.1	6.7	0.5	4.9
effect. diffusivity(D_e)(s^{-1})	2.7E-6	8.6E-7	2.3E-6	1.6E-6	1.3E-6	1.1E-6	2.2E-6	2.8E-6
seam gas content (m^3/t)	8.0				5.0			

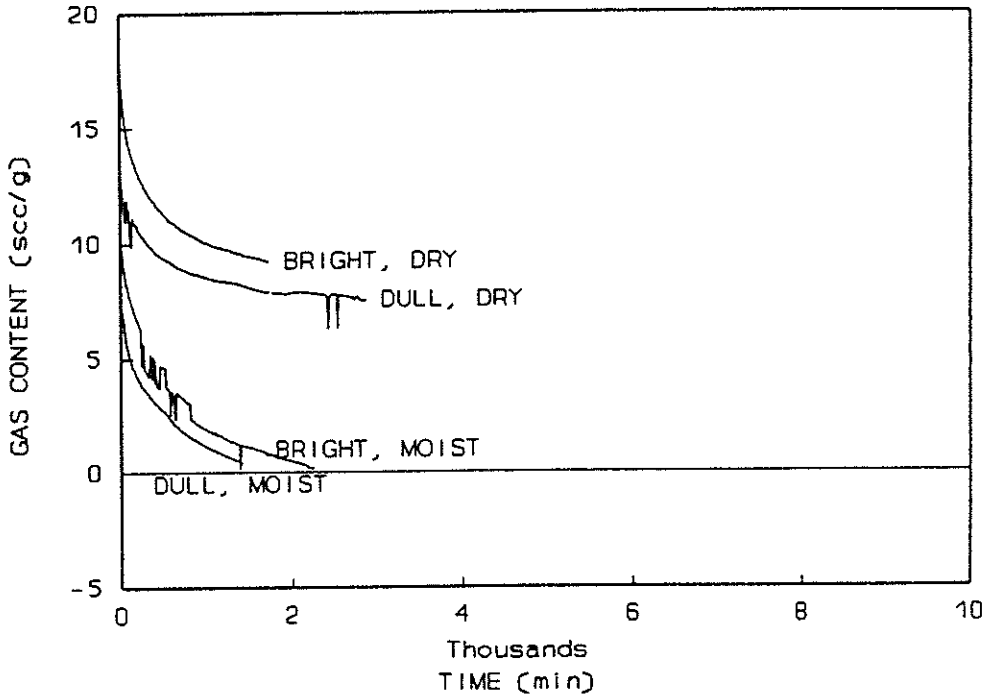

Figure 2 Desorption to atmosphere from 2MPa, Central Colliery, Site 1

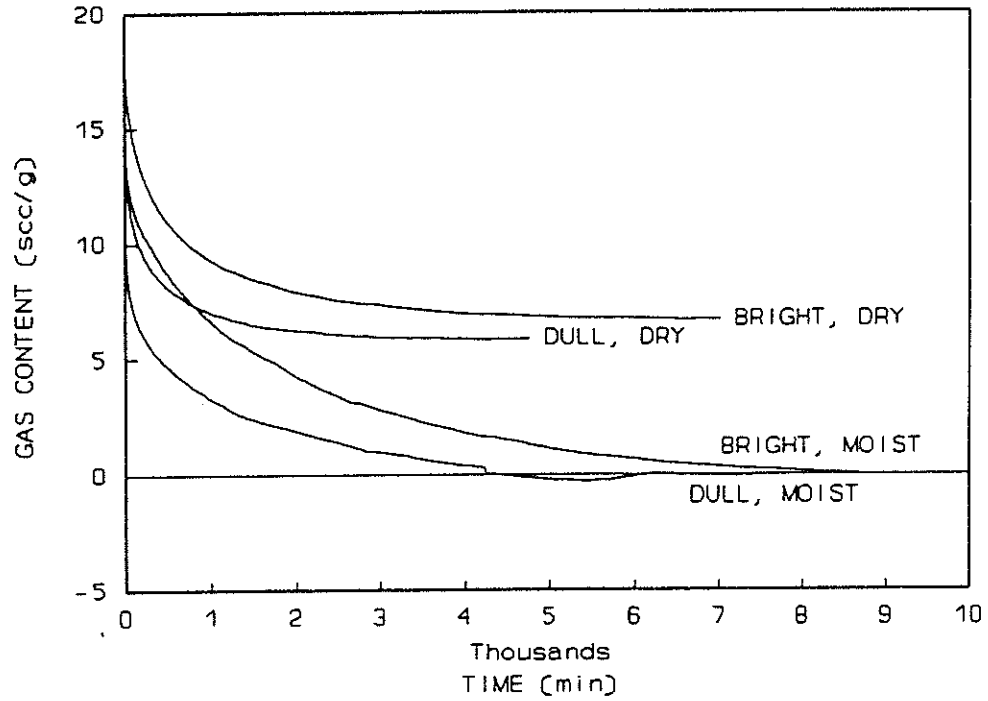

Figure 3 Desorption to atmosphere from 2MPa, Central Colliery, Site 2

METHANE SORPTION AT SOUTH BULLI AND CENTRAL COLLIERIES

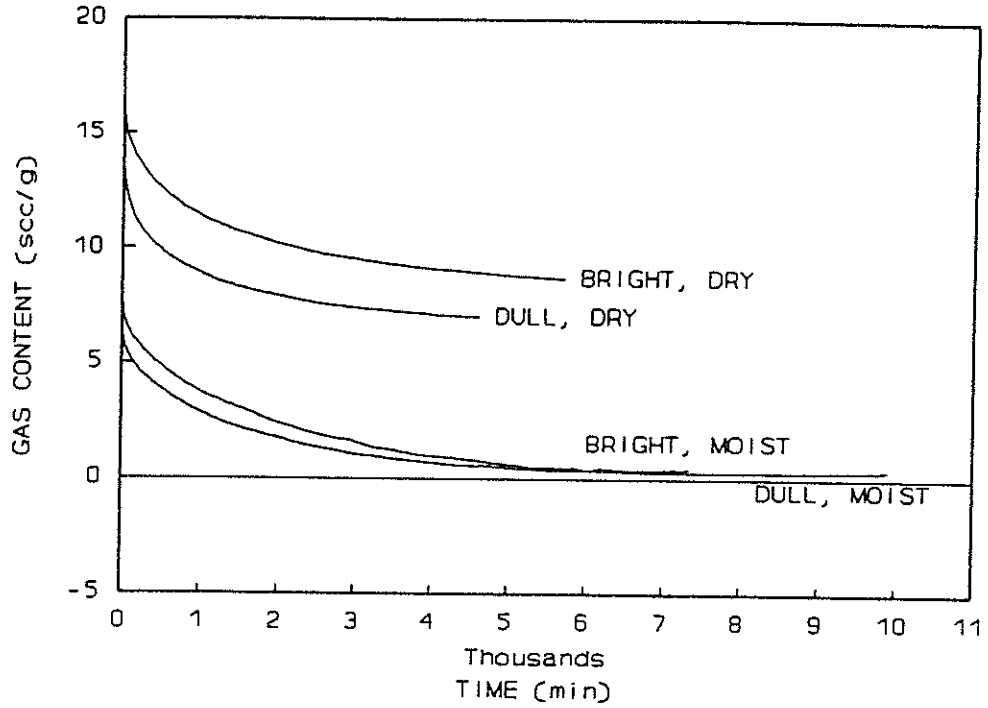

Figure 4 Desorption to atmosphere from 3MPa, South Bulli, Site 1

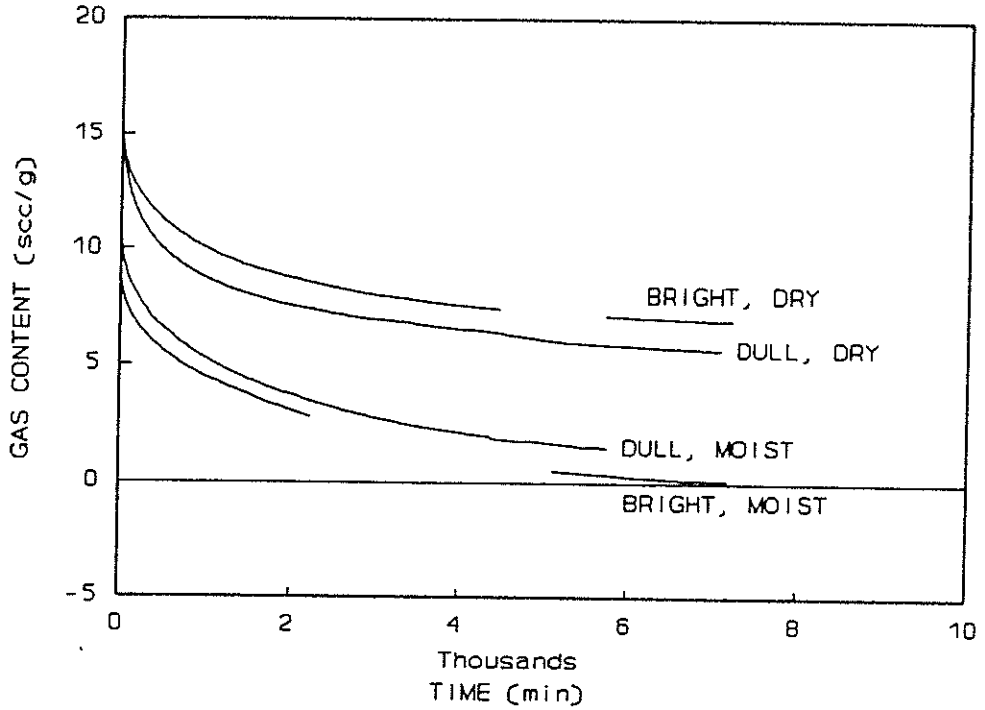

Figure 5 Desorption to atmosphere from 3MPa, South Bulli, Site 2

The influence of maceral content on the sorption of gases by coal and the association with outbursting

B. Basil Beamish
Department of Geology, The University of Auckland, Auckland, New Zealand

Peter J. Crosdale
Coalseam Gas Research Institute, James Cook University, Townsville, Australia

ABSTRACT: This paper considers the application of recent laboratory gas sorption and coal physical properties data to the understanding of gas associated phenomena in underground coal mining. The mechanisms of gas sorption are discussed with relevance to pore structure of the macerals present in coal. Comparison of the laboratory data with mine site information from outburst-prone areas enables a model to be developed for identification of outburst-prone conditions.

1 INTRODUCTION

Fundamental investigations concerning the gases found in coal seams can be related back to the earliest coal mining (von Meyer 1872; Thomas 1876). The primary concern at that time was to assess gas content and composition for ventilation purposes, in order to reduce the hazard of either methane emissions and subsequent explosions or outbursting of coal and gas. This work is still continuing as higher production operations must combat larger quantities of gas into workings (Hargraves 1993), and the complexity of the gas/coal system is recognised (Levine 1992).

The effects of coal type are poorly understood in terms of gas emission and outbursting, and have generally been overshadowed by the inferred relationships with coal rank. Most previous work has focused on bulk sample testing, which confuses the issue of coal rank and coal type effects. Recent investigations of smaller sample sizes (Beamish & O'Donnell 1992; Levine et al. 1993; Crosdale & Beamish 1993) using high pressure microbalances are providing clearer distinctions between the two coal parameters.

The pore nature of coal is well documented for overseas coals (Gan et al. 1972), but little published data exists on Australian coals. To fully understand sorption mechanisms requires a better understanding of pore sizes and distributions in the coals of interest. With this knowledge it is possible to predict the sorption behaviour of the coal, and apply it to field observations. This paper attempts to show the basis for the link between coal sorption behaviour, its pore nature and the resulting experiences of gas emission and outbursting.

2 LABORATORY ASSESSMENT OF THE PORE NATURE OF COAL

The pores in coals vary in size from large cracks of micrometer dimensions to apertures which are even closed to helium at room temperature. It is the large internal surface area within the pores of any porous material that enables significant volumes of gas or liquid to be adsorbed. Porosity in coals influences behaviour during their mining, preparation and utilisation (Mahajan & Walker 1978). The pore volume and pore size distribution of coals determines the extent and ease of diffusion of methane out of the pore structure during mining (Mahajan & Walker 1978).

2.1 *Distribution of total pore volume in coals*

Gan et al. (1972) made a detailed study of the porosities of coals over a wide rank range. They estimated the pore volumes contained in the following different pore diameter ranges:

1. Total open pore volume V_T accessible to He, as estimated from the He and Hg densities.
2. Pore volume V_1 contained in pores greater in

diameter than 300Å, as estimated from penetration of mercury under a pressure of 5800 psi.

3. Pore volume V_2 contained in pores in the diameter range 300 to about 12Å, as estimated from the analysis of the absorption branch of the N_2 isotherms (-196°C).

4. Pore volume V_3 contained in pores smaller in diameter than 12Å as estimated from $V_3 = V_T - (V_1 + V_2)$.

The proportion of V_3 is significant for all coals. Its value is a maximum for anthracite and a minimum for lignite. The results demonstrated that essentially all American coals, irrespective of their rank, show molecular sieve properties. Gan et al. (1972) concluded that (1) porosity in coals with carbon contents less than 75% (sub-bituminous) is primarily due to the presence of macropores, (2) porosity in coals with about 75-84% carbon content (high volatile bituminous) is predominantly due to the presence of micro- and transitional pores, and (3) for coals ranging in carbon content from about 85 to 91%, microporosity predominates.

A large pore volume need not always imply a large pore surface area because the latter is dependent on the pore size distribution. A higher CO_2 surface area is associated with the presence of a larger proportion of micropores. The results of this early work are applicable to vitrinite-rich coals, but no comparison is given for the effects of coal type.

2.2 *Porosity and surface area of Bowen Basin coals*

A series of coals was examined from the Bowen Basin (Tables 1 and 2) to assess the differences in hand selected coal bands. Analysis of total pore volume, porosity and surface area (Tables 3 and 4) were performed by the CSIRO, Division of Coal and Energy Technology. It is quite clear from the data in these tables, that inertinite-rich coals have a greater porosity (6.0-13.7%) than vitrinite-rich coals (0.8-5.3%) of equivalent rank. For surface areas the relationship is reversed. The basic inference of these two results is that inertinite-rich coals are predominantly macroporous, whereas vitrinite-rich coals are predominantly microporous for coals in the rank range of high volatile bituminous to low volatile bituminous. In terms of sorption behaviour these properties of the coal have serious implications for gas emission. The diffusion of gas through vitrinite-rich coals would be micropore dominated, whereas for inertinite-rich coals it would be macropore dominated.

Table 1. Proximate analyses and crucible swelling number (CSN) of Bowen Basin coals investigated.

Sample	Moisture (% adb)	Ash (% db)	VM (% daf)	CSN
1 Bright	3.5	3.7	36.9	3
1 Dull	2.6	3.6	32.9	1
2 Bright	4.0	1.7	34.1	6
2 Dull	2.6	10.6	31.1	½
3 Bright	2.3	4.5	38.0	5½
3 Dull	2.3	7.0	32.1	1
4 Bright	2.8	2.1	37.3	6½
4 Dull	3.1	4.6	31.0	1
5 Bright	3.1	1.8	31.3	5½
5 Dull	2.3	17.2	26.2	½
6 Bright	1.3	3.7	24.3	9
6 Dull	1.6	15.7	24.8	1
7 Bright	1.5	0.7	21.9	9
7 Dull	1.6	9.9	21.3	1½
8 Bright	1.0	0.3	20.1	9
8 Dull	1.6	17.1	17.6	1
9 Bright	1.0	0.5	16.8	8
9 Dull	1.0	18.9	14.9	½

adb = air-dry basis; db = dry basis; daf = dry, ash-free

Table 2. Petrographic analyses of Bowen Basin coals investigated.

	Maceral analysis (%)				Ro max
Sample	Vit	Lipt	Inert	MM	(%)
1 Bright	72.9	3.2	23.7	0.6	0.81
1 Dull	32.8	3.9	63.2	0.8	0.81
2 Bright	96.3	0.0	2.6	0.8	0.81
2 Dull	18.7	3.7	74.3	3.4	0.81
3 Bright	82.7	3.3	12.7	1.2	0.82
3 Dull	23.6	2.3	69.5	4.6	0.82
4 Bright	86.1	1.6	11.7	0.6	0.82
4 Dull	18.9	1.5	78.9	0.7	0.82
5 Bright	99.4	0.0	0.0	0.6	0.88
5 Dull	1.9	8.5	78.4	11.2	0.88
6 Bright	84.3	0.5	14.7	0.5	1.23
6 Dull	26.7	0.0	70.8	2.4	1.23
7 Bright	100.0	0.0	0.0	0.0	1.33
7 Dull	20.1	0.0	73.4	6.4	1.33
8 Bright	92.5	0.0	3.4	4.2	1.65
8 Dull	30.2	2.1	66.7	1.0	1.65
9 Bright	99.4	0.0	0.0	0.6	1.66
9 Dull	9.7	0.0	83.5	6.7	1.66

Table 3. Density and porosity data for Bowen Basin coals.

Sample	Helium density (g/cc, mmcb)		Mercury density (g/cc, mmcb)		Total pore volume[1] (cc/g, mmcb)		Porosity[2] (%, mmcb)	
	Dull	Bright	Dull	Bright	Dull	Bright	Dull	Bright
1	1.39	1.29	1.20	1.27	0.11	0.01	13.7	1.6
2	1.42	1.31	1.26	1.29	0.09	0.01	11.3	1.5
5	1.48	1.29	1.35	1.28	0.07	0.01	8.8	0.8
7	1.39	1.32	1.24	1.25	0.09	0.04	10.8	5.3
8	1.50	1.31	1.41	1.28	0.04	0.02	6.0	2.3
9	1.53	1.30	1.34	1.27	0.09	0.02	12.4	2.3

[1]Total pore volume = $V_T = (1/\rho_{Hg} - 1/\rho_{He})$

[2]% Porosity = $P = 100\rho_{Hg}(1/\rho_{Hg} - 1/\rho_{He})$ mmcb - mineral matter containing basis

Table 4. Surface area measurements for Bowen Basin coals.

Sample	Carbon dioxide surface area (m^2/g, mmcb)	
	Dull	Bright
1	209	237
2	194	247
3	200	228
4	209	245
5	175	277
6	213	269
7	150	196
8	173	213
9	187	261

3 LABORATORY ASSESSMENT OF SORPTION BEHAVIOUR

Two key parameters are obtained from gas sorption measurements on coal. These are the gas sorption isotherm and the gas sorption rate. Both these parameters are fundamental to the understanding of the gas/coal system in outbursting. Detailed studies of maceral effects on sorption capacity (Beamish & O'Donnell 1992; Lamberson & Bustin 1993; Levine et al. 1993; Crosdale & Beamish 1993), have also shown that vitrinite-rich coals store more gas than inertinite-rich coals.

The diffusivity behaviour of coal governs the rate at which gas can be liberated from the coal matrix. Laboratory measurements of this property in coal lithotypes of equivalent rank have shown marked differences (Crosdale & Beamish 1993; Figure 1). The inertinite-rich coal has a much faster desorption rate than the vitrinite-rich coal, which is consistent with the pore nature.

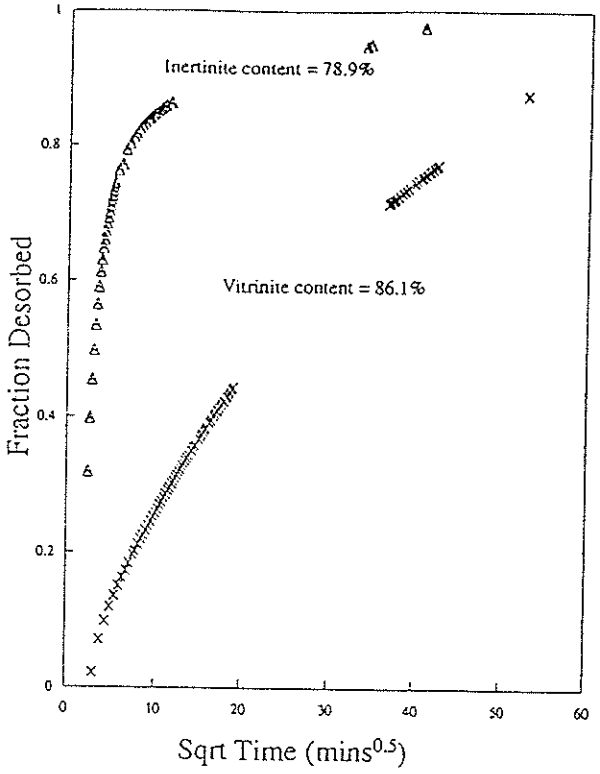

Figure 1. Experimental desorption data for sample 4, Table 1.

4 RELATIONSHIP BETWEEN LABORATORY FINDINGS AND MINE OPERATIONS

From 1954 to 1981, a total of 22 outbursts were recorded for coal mine operations in the Collinsville No.2 Mine of the Bowen Basin, Australia (Figure 2). These ranged in size from 500 tonnes to only 0.5 tonnes, with the seam gas being carbon dioxide. Collinsville Coal Company Pty. Ltd. conducted an extensive research programme into the gas outburst problem (Beamish et al. 1985). The main objectives

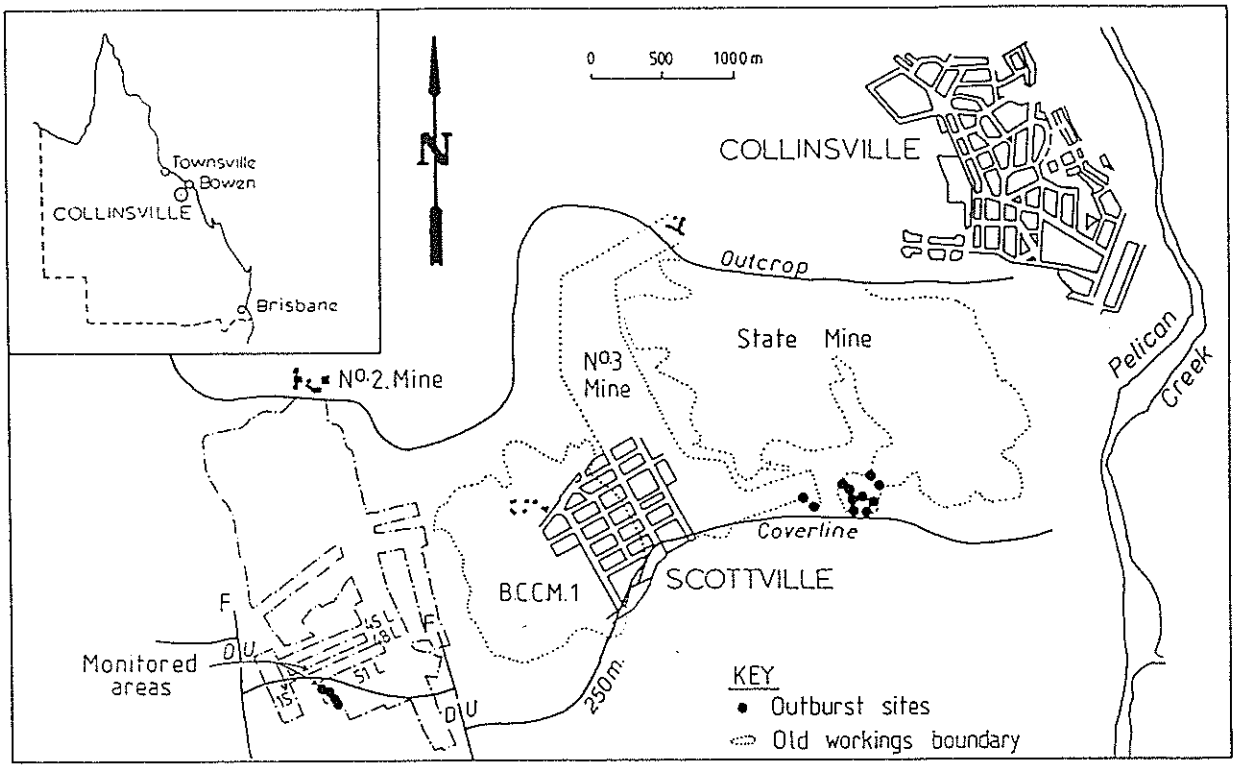

Figure 2 Locality map and workings outline of No.2 Mine, Collinsville, Queensland (modified from Beamish et al. 1985).

of the research were to find reliable methods of:

1. Regional assessment of outburst-proneness (Williams & Giedl 1983; Williams & Rogis 1980).
2. Assessment of outburst-proneness at the mining face (Beamish 1990; Beamish & McKavanagh 1987).
3. Alleviation of the problem (Williams et al. 1986).
4. Determination of operational requirements for mining in outburst-prone areas (Beamish 1984).

4.1 *Regional effect of vitrinite content*

Williams & Rogis (1980) proposed that a distinct relationship existed between the coal rank and outbursting in the No.2 Mine area, such that outbursting only occurred in coal with greater than 1.2% vitrinite reflectance. They also noted that the vitrinite content of the mining section (the top 2.5 m to 2.8 m) increased from 28%, 200 m east of the Western Panels Fault (Figure 3) to a maximum of 48% near the fault. The increase in vitrinite content was confined to the lower half of the mining section, being 63% compared to 26 % in the top section in the vicinity of the fault. When vitrinite reflectance and vitrinite content are plotted (Figure 4) with the Hargraves emission values (EV) readings (Hargraves 1962) along a profile of the Western Panels area (Figure 3), it is clear that the vitrinite content of the coal displays a greater association with the EV readings. Such a correlation would be expected from the laboratory data which suggests the vitrinite-rich coal has a greater sorption capacity.

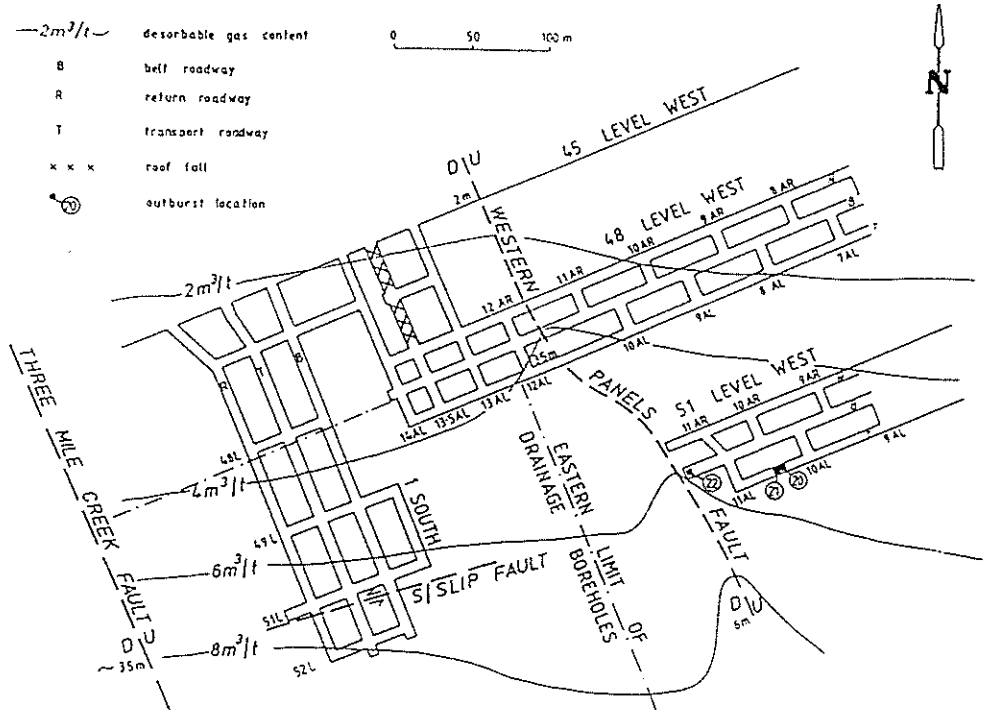

Figure 3. Mining panel layout showing outburst locations (from Beamish 1990).

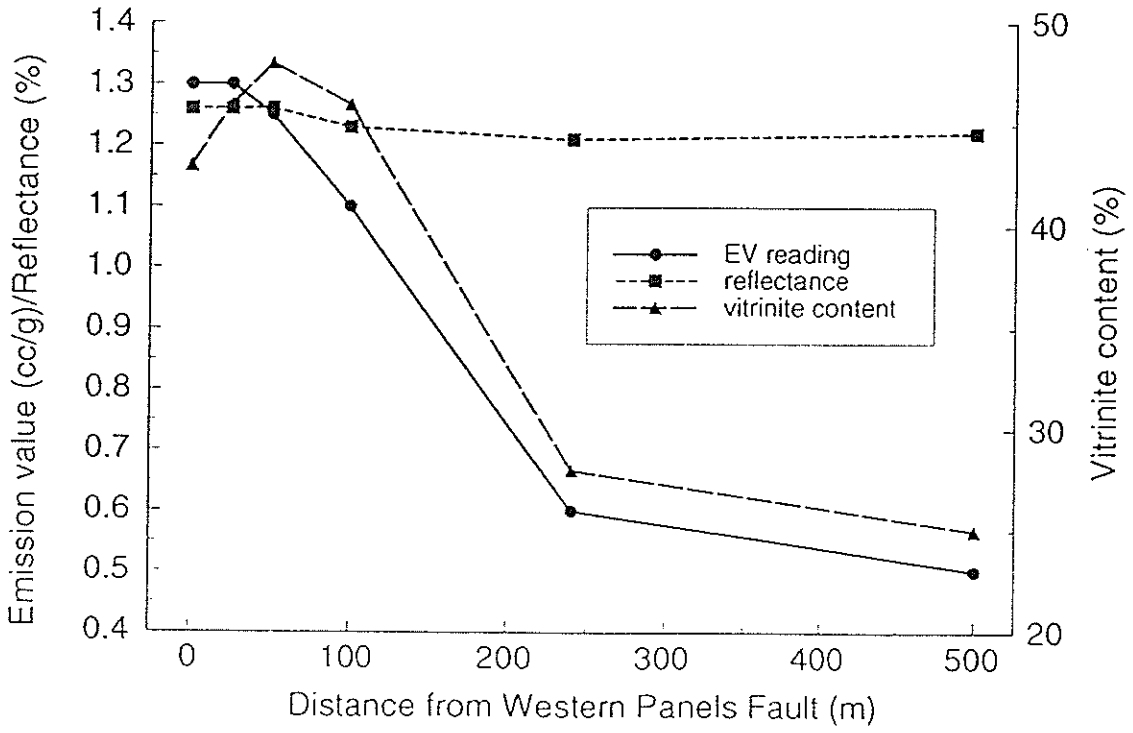

Figure 4. Profiles of vitrinite reflectance, vitrinite content and EV readings approaching the Western Panels Fault.

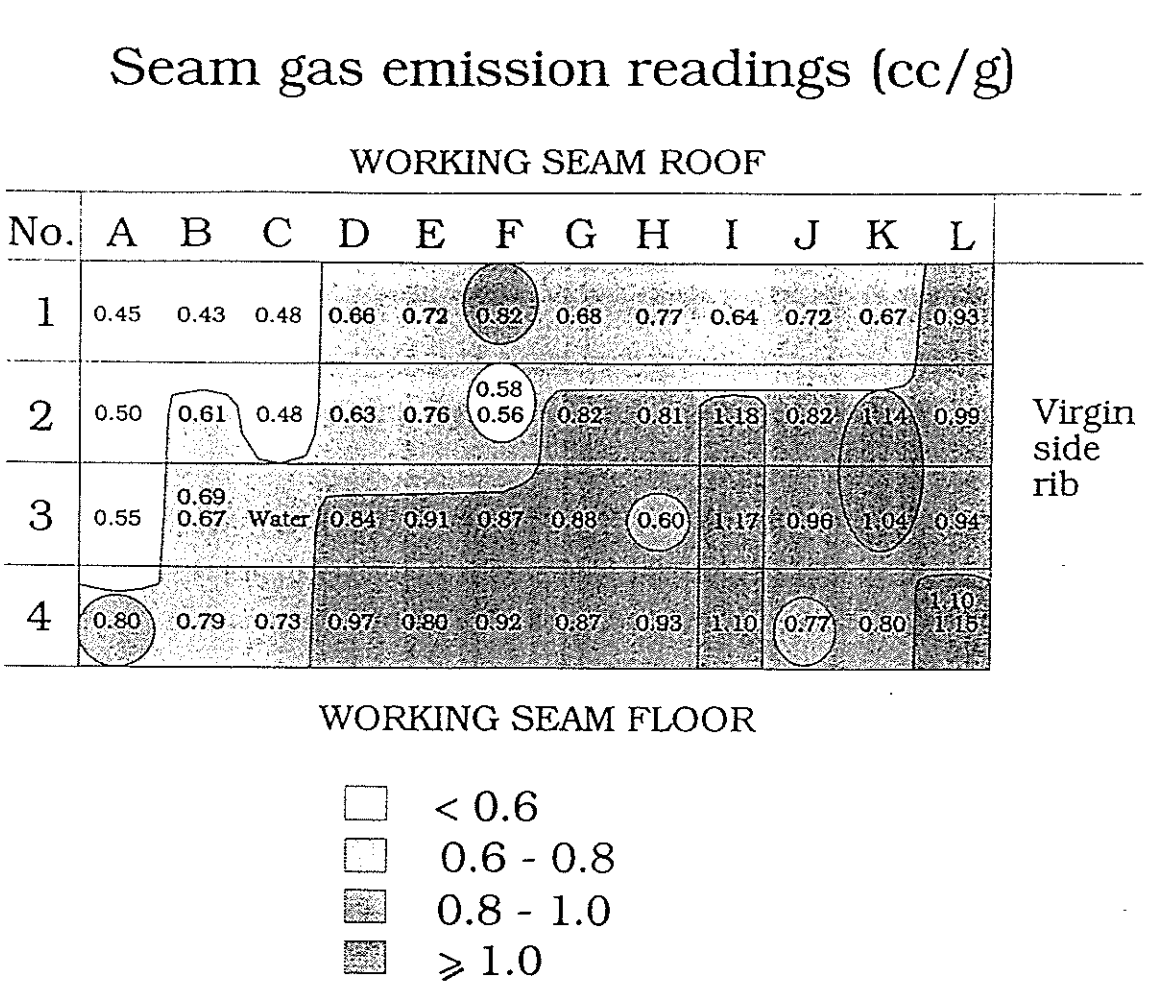

Figure 5. Hargraves EV readings taken across a working face (modified from Biggam et al. 1980).

4.2 *Effect of coal lithotypes in the working face*

Biggam et al. (1980) presented a tabulation of EV readings from a full face exposure in the Western Panels area of No.2 Mine. This data has been redrawn and contoured to emphasise the significance of the results (Figure 5). There is a noticeable increase in values moving from the roof of the seam to the working floor. A visual examination of the seam in this area reveals that the upper half is predominantly dull coal and the lower half is predominantly bright coal, separated by a bedding plane fault. The vitrinite content of the seam, as noted by Williams & Rogis (1980) in the previous section, is consistent with this. Combining the diffusivity and sorption capacity information from laboratory testing it is valid to postulate that the dull coal has rapidly lost its gas in the face area while the bright coal has retained its gas due to the slower desorption rate. This phenomenon is used by Creedy (1986), who suggests that when taking face samples of coal for gas content measurement, bright coal samples should be used.

A second trend is also observable in Figure 5. The EV readings progressively decrease away from the virgin rib side, which is again more noticeable in the upper part of the working section. Bedding plane permeability is high according to Bartosiewicz & Hargraves (1985), which is being reflected in this case by the EV readings.

4.3 *Outburst occurrence*

At 5:27 pm on the 16 April 1981, an outburst at No.2 Mine, Collinsville (No.22, Figure 3) released approximately 35 tonnes of coal and 380 cubic metres of carbon dioxide, in the belt road 29m inbye of 11A cut-through (Beamish 1981). The origin of the outburst appeared to be from the floor line in the centre of the roadway, 4.5 m inbye of the face. A rectangular prism-shaped cavity resulted. Drill hole data placed the intersection of the Western Panels Fault (Figure 3) with the mining section floor, approximately 5 m inbye of the outburst face. Consequently, the disruption to the

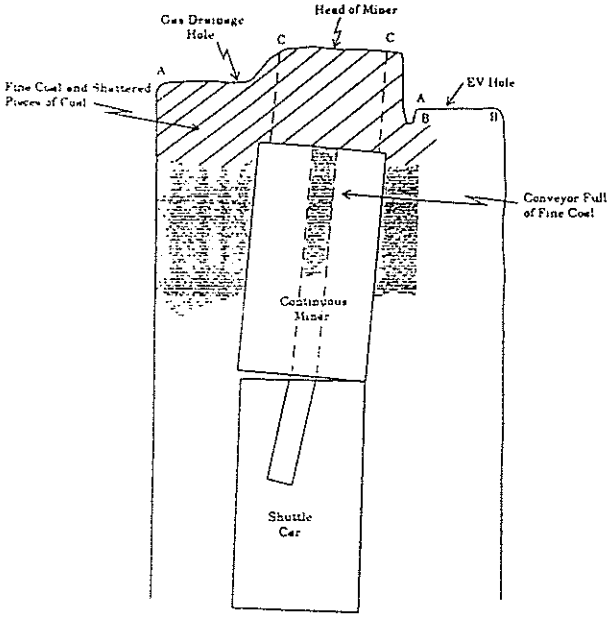

Figure 6. Plan view of continuous miner location at the time of Outburst No.22, No.2 Mine, Collinsville, with face cross-section locations indicated (modified from Beamish 1981).

seam caused by the fault contributed to the outburst.

A plan view of the outburst face is shown in Figure 6 with corresponding cross-sections in Figure 7. As in all previous recorded cases at Collinsville, the outburst material was extremely sheared with a sugary texture.

Table 5. Coal analyses from outburst locality No.22, 51 Level West Panel.

Sample details	IM (%)	Ash (%)	VM (%)	FC (%)	CSN
Outburst coal ejected onto miner head	1.9	16.2	23.0	60.8	8
Coal from outburst cavity	1.1	16.5	22.0	61.5	8
Dull coal from right hand side of the face above slip plane	0.6	16.8	19.4	63.8	2
Sheared coal from right hand side of the face below slip plane	1.6	17.9	19.7	62.4	5

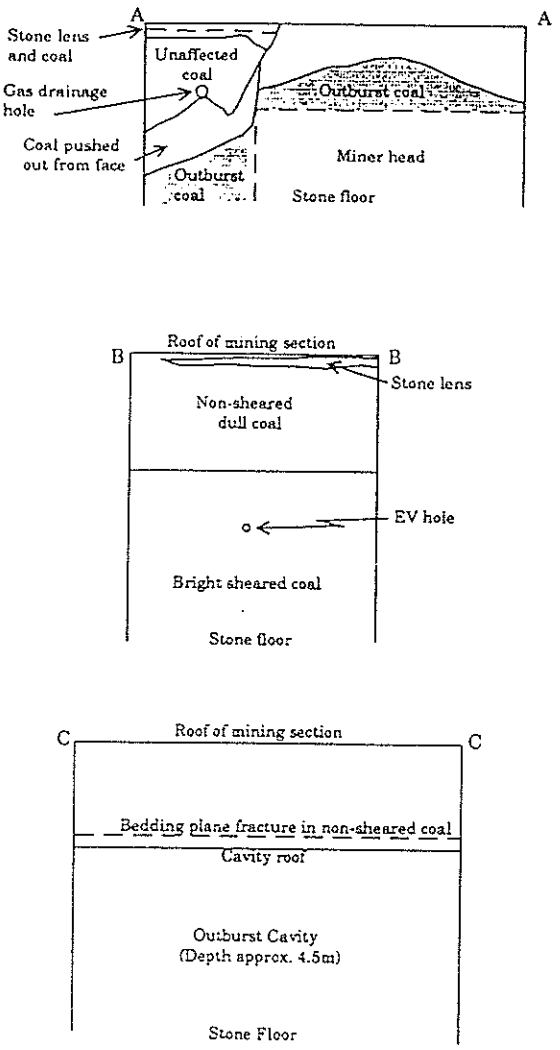

Figure 7. Face cross-sections from Figure 6 (modified from Beamish 1981).

Analyses of coal samples taken from the outburst location (Table 5), reveal that the in-situ sheared coal and outburst coal have:

1. High crucible swelling numbers.
2. Relatively high volatile matter content.

Both these parameters are consistent with vitrinite-rich coal, which matches the seam profile assessment.

The area had been undergoing gas drainage to reduce the gas levels, and a borehole was located in the upper part of the seam (Figure 7). As a result of the different desorption rates of the dull and bright lithotypes, the upper part of the seam would have drained to a safe level, however, the bright lower part of the seam did not.

5 CONCLUSIONS

Coal rank as an outburst-proneness indicator is often misleading, and should only be considered in conjunction with the full sorption behaviour of the coal being assessed. The effect of coal maceral composition on the propensity of outbursting with respect to the gas/coal system is just as important and is twofold:

1. Vitrinite-rich coals appear to have a higher sorption capacity than inertinite-rich coals.
2. Vitrinite-rich coals have a much slower desorption rate than inertinite-rich coals.

The resulting differential throughout a seam can be devastating, particularly, where large thick bands of vitrinite-rich coal is present concurrently with seam disturbances.

ACKNOWLEDGMENTS

The completion of this paper has been financially sponsored by the Auckland University Research Committee and the New South Wales Joint Coal Board Health and Safety Trust.

REFERENCES

Bartosiewicz, H. & A.J.Hargraves 1985. Gas properties of Australian coal. *Proc. Australas. Inst. Min. Metall.* 290(1):71-77.

Beamish, B.B. 1990. Continuous gas monitoring for the assessment of outburst-proneness at a mining face. *Int. J. Min. Geol. Engng.* 8:131-147.

Beamish, B.B. 1984. Control of outbursts at Collinsville. In *The Co-ordinating Committee on Outburst-Related Research, Mini-Seminar Report No. 4*, 14p, (October, 1984).

Beamish, B.B. 1981. CCP No. 2 mine, 51 level west panel, report on continuous face monitoring using a gas analysing system. Collinsville Coal Company Pty Ltd Technical Report R 101, 49p, (June, 1981).

Beamish, B.B. & G.O'Donnell 1992. Microbalance applications to sorption testing of coal. In B.B.Beamish & P.D.Gamson (eds), *Proceedings of Symposium on Coalbed Methane Research and Development in Australia*, Townsville, Queensland, 4, November, 31-41.

Beamish, B.B. & B.M.McKavanagh 1987. Underground rock-noise monitoring at No. 2 Mine, Collinsville. *Geoexploration* 24:347-365.

Beamish, B.B., F.Hungerford, B.McKavanagh & R.J.Williams 1985. Outburst research. (Collinsville Coal Co., Queensland (Australia)). NERDDP-EG-85-495 Canberra, ACT, Australia. National Energy Research, Development and Demonstration Council, 760p, (August, 1985).

Biggam, F.B., B.Robinson & B.Ham 1980. Outbursts at Collinsville - A case study. In *Proceedings of The AusIMM Symposium on The Occurrence, Prediction and Control of Outbursts in Coal Mines*, Brisbane, Qld, September, 41-61.

Creedy, D.P. 1986. Methods for the evaluation of seam gas content from measurements on coal samples. *Mining Science and Technology* 3:141-160.

Crosdale, P.J. & B.B.Beamish 1993. Maceral effects on methane sorption by coal. In J.W.Beeston (ed), *Proceedings of New Developments in Coal Geology Symposium*, Brisbane, November, 95-98.

Gan, H., S.P.Nandi & P.L.Walker 1972. Nature of the porosity in American coals. *Fuel* 51:272-277.

Hargraves, A.J. 1993. Update on instantaneous outburst of coal and gas. *Proc. Australas. Inst. Min. Metall.* 298(2):3-17.

Hargraves, A.J. 1962. Gas in face coal. *Proc. Australas. Inst. Min. Metall.* 203:7-43.

Lamberson, M.N. & R.M.Bustin 1993. Coalbed methane characteristics of Gates Formation coals, Northeastern British Columbia: Effect of maceral composition. *AAPG Bulletin* 77(12):2062-2076.

Levine, J.R. 1992. Oversimplifications can lead to faulty coalbed gas reservoir analysis. *Oil & Gas J.* (November 23):63-69.

Levine, J.R., P.W.Johnson & B.B.Beamish 1993. High pressure microbalance sorption studies. In *Proceedings of the 1993 International Coalbed Methane Symposium*, The University of Alabama/Tuscaloosa. Birmingham, Alabama, May 17-21, 187-196.

Mahajan, O.P. & P.L.Walker 1978. Porosity of coals and coal production. In C.Karr (ed) *Analytical methods for coal and coal production*: 125-160.

Meyer, E. von 1872. Über die in einigen englischen Steinkohlen eingeschlossenen Gase. *Jour. f. praktishce Chemie* 5.407pp.

Thomas, J.W. 1876. On the gases enclosed in cannel coals and jet. *J. Chem. Soc.* 30(2):144.

Williams, R.J. & J.Giedl 1983. Geological parameters affecting seam gas content and composition in the Collinsville Coal Measures, Collinsville, Queensland. In *Proceedings of the 17th Newcastle Symposium on Advances in the Study of the Sydney Basin*, University of Newcastle.

Williams, R.J. & J.Rogis 1980. An analysis of the geologic factors leading to outburst-prone conditions at Collinsville, Queensland. In *Proceedings of The AusIMM Symposium on The Occurrence, Prediction and Control of Outbursts in Coal Mines*, Brisbane, Qld, September, 99-109.

Williams, R.J., J.Allan, D.Truong, B.B.Beamish & F.Hungerford 1986. An evaluation of seam gas drainage by long-hole drilling. *The Coal Journal*, No.10, 13-22.

8. APPENDICIES

8.1 Proximate Analysis by Thermogravimetry

New Zealand Journal of Geology and Geophysics, 1994, Vol. 37: 387–392
0028–8306/94/3704–0387 $2.50/0

Proximate analysis of New Zealand and Australian coals by thermogravimetry

B. BASIL BEAMISH
Department of Geology
The University of Auckland
Private Bag 92019
Auckland, New Zealand

Abstract A technique has been developed at The University of Auckland for proximate analysis of coals by thermogravimetry using sample weights of <20 mg. Samples from three New Zealand coalfields and the Bowen Basin of Queensland, Australia, have been analysed. Coals tested range in rank from subbituminous to semianthracite, and have ash contents from 3.1 to 21.4% on a dry basis. Results obtained using the technique are within acceptable precision limits of the standard procedure. Volatile matter content of the coal shows a logarithmic increase with decreasing sample weight. To minimise this effect on repeatability, and to optimise the equipment capabilities, sample weights of 15.5 ± 0.5 mg should be used. The technique is ideally suited to (1) analysing samples where insufficient material is available for standard proximate analysis, and (2) correlation with microstudies of coal.

Keywords thermogravimetry; proximate analysis; coal; reproducibility; repeatability

INTRODUCTION

Cuttings from petroleum and coal exploration programmes often contain fragmentary material that is useful for rank or quality determination. In some circumstances, only small quantities of coal sample (less than a few grams) are available for analysis, which makes it difficult to obtain a standard proximate result. Proximate analysis of coals follows a standard procedure which measures the moisture, volatile matter, and ash content on three separate 1 g splits drawn from a homogenised sample. The procedure used is prescribed by national standards organisations (e.g., Australian Standard AS 1038.3, 1989; British Standard BS 1016 Pt4; International Standards Organisation ISO 5068/1983 moisture, ISO 562/1981 volatile matter, ISO 1171/1981 ash) and requires the samples to be heated under specified conditions at a selected temperature. Moisture is determined by measuring the weight loss obtained by heating the sample in nitrogen at 105–110°C until constant weight is reached. Volatile matter is determined by heating the sample at 900°C for 7 min in a covered crucible in a nitrogen atmosphere, and the ash content is defined as the residue after heating the sample in air at 815°C until constant weight is reached. The fixed carbon content is obtained by difference from 100%..

Elphick (1960) reported on a technique for analysing small quantities of coal down to 0.1 g, which gave results comparable with normal procedures. The approach relied on using the standard procedure and developing correction factors for sample weight. A more sophisticated approach has been possible with sample weights down to 10 mg using thermogravimetry (TG), which provides a rapid, accurate, low cost method of analysis (Warne 1991). The TG technique also offers the opportunity to complete the determinations for moisture, volatile matter, fixed carbon and ash directly, on a single sample, in a sequential manner.

Proximate analysis of coals by TG has been investigated by Ottaway (1982), Cumming & McLaughlin (1982), Rosenvold et al. (1982), and Elder (1983). Coals tested were from the United Kingdom and the United States. Reasonably good agreement was reported with the standard proximate analysis determinations of all the coals. However, a closer examination of the data from these studies reveals the agreement is not within precision limits set by the standards.

The purchase of a new simultaneous thermal analyser (STA) by the Department of Geology at The University of Auckland has provided the opportunity to assess the applicability of proximate analysis of New Zealand and Australian coals by TG. A series of three coals was supplied by the Coal Research Association of New Zealand, which had already undergone proximate analysis according to the ISO standard (Table 1). Coals selected were Ohai subbituminous (Wairaki No. 6 Mine), Greymouth bituminous (Strongman Mine), and Huntly subbituminous (Huntly East Mine). In addition, three coal samples from the Bowen Basin, Queensland, Australia, were sent to Coal Research for proximate analysis (Table 1), and the remaining homogenised sample returned for comparative studies using the TG technique. This paper describes the major steps used to develop a standard TG test procedure, which produces proximate analysis results within acceptable limits for repeatability and reproducibility.

DEVELOPMENT OF A STANDARD THERMOGRAVIMETRIC PROCEDURE FOR PROXIMATE ANALYSIS OF COAL

A summary of the operating conditions and procedures used in previous studies of thermogravimetric proximate analysis of coals is contained in Table 2. It is evident that a number of variations have been used, without a clear standard procedure being developed, although Larkin (1988) described an attempt to develop a standard method for compositional analysis using TG. This perhaps has contributed to the lack of precision in the results obtained to

G94006
Received 10 June 1994; accepted 15 August 1994

date, which is seen by some as a deficiency of the technique. Another factor that has often been raised is the question of representativeness of the sample used. However, as Charsley & Warrington (1988) point out, if a 1 g sample is seen as representative of 1000 t shipments, then 10 mg may be reasonably extracted from the 1 g.

Variability of test conditions

The equipment used in this work was a Polymer Laboratories Simultaneous Thermal Analyser STA 1500, which is fully computer controlled with data storage/retrieval and software analysis programs. Two parameters were selected to be fixed in all experiments. The first of these was heating rate, which is equipment related. The maximum heating rate of the instrument, 50°C/min, was used, similar to Cumming & McLaughlin (1982). Secondly, samples were prepared by Coal Research as per the standard for proximate analysis at a size fraction of <212 μm.

Initial procedure

Initially three tests were performed on each of the New Zealand coals using sample weights in the upper 75% of the weight range selected (15–20 mg). The operational procedures adopted at this stage were basically those described by Warne (1991), except that the heating rate of the analyser was limited to 50°C/min, and air was used instead of oxygen to burn off the fixed carbon. The sampl was heated in a nitrogen atmosphere to 110°C at a rate o 50°C/min and was maintained at that temperature for 5 mi to ensure a constant weight was achieved. Weight los recorded by the STA is due to moisture (Fig. 1). Th temperature of the STA was then raised to 950°C at 50°C min, and maintained at that temperature for 42 min. A separate timing device was set at 0.92 h at the beginning o the test run, which automatically switched the operatin atmosphere from nitrogen to air (Fig. 1). Weight loss prio to this switch over was due to loss of volatile component from the coal, and weight loss following the introduction o air was due to oxidation of the residual carbon. The timin device setting was found by trial and error by monitorin the volatile release until a reasonably constant weight wa achieved. The residue at the end of the combustion proces is the ash content of the coal.

Results obtained in these initial tests (Table 3) wer encouraging, being comparable with the standard value obtained by Coal Research.

Buoyancy effects

Ottaway (1982) read all values directly from the TG chart However, Cumming & McLaughlin (1982) recognised th need for a buoyancy correction to allow for the smal differences in balance reading at the various temperature

Table 1 Samples used for testing.

			Proximate analysis			
				Volatile matter	Fixed carbon	Ash
Sample	Location	Coal rank	Moisture (%) air-dried basis	(%) dry basis		
New Zealand						
52/085	Huntly	subbituminous	13.4	44.9	50.9	4.2
52/057	Ohai	subbituminous	11.5	41.6	54.8	3.6
52/109	Greymouth	high volatile bituminous	6.3	42.0	54.9	3.1
Bowen Basin						
53/527	Collinsville	medium volatile bituminous	1.9	20.7	57.9	21.4
53/883	Harrybrandt	low volatile bituminous	1.8	13.3	66.0	20.7
53/884	Yarrabee	semianthracite	2.8	8.4	85.9	5.7

Table 2 Summary of TG methods used for proximate analysis.

	Ottaway (1982)	Elder (1983)	Cumming & McLaughlin (1982)	Warne (1991)
Balance	Stanton - Redcroft	Perkin - Elmer	Stanton - Redcroft	Perkin - Elmer
Sample weight (mg)	10	5–10	50 ± 0.5	10
Size fraction (μm)	< 212	< 250	< 210	<212
Moisture				
Temperature (°C)	110	110	105	110
Rate (°C/min)	250	160	50	100
Time (min)	1	4.5	constant weight	constant weight
Gas	nitrogen	nitrogen	nitrogen	nitrogen
Volatile matter				
Temperature (°C)	900	900/950	900	950
Rate (°C/min)	250	160	50	100
Time (min)	1	5	7	constant weight
Gas	nitrogen	nitrogen	nitrogen	nitrogen
Fixed carbon				
Temperature (°C)	900	900/950	815	950
Gas	oxygen	oxygen	air	oxygen
Ash	residual	residual	residual	residual

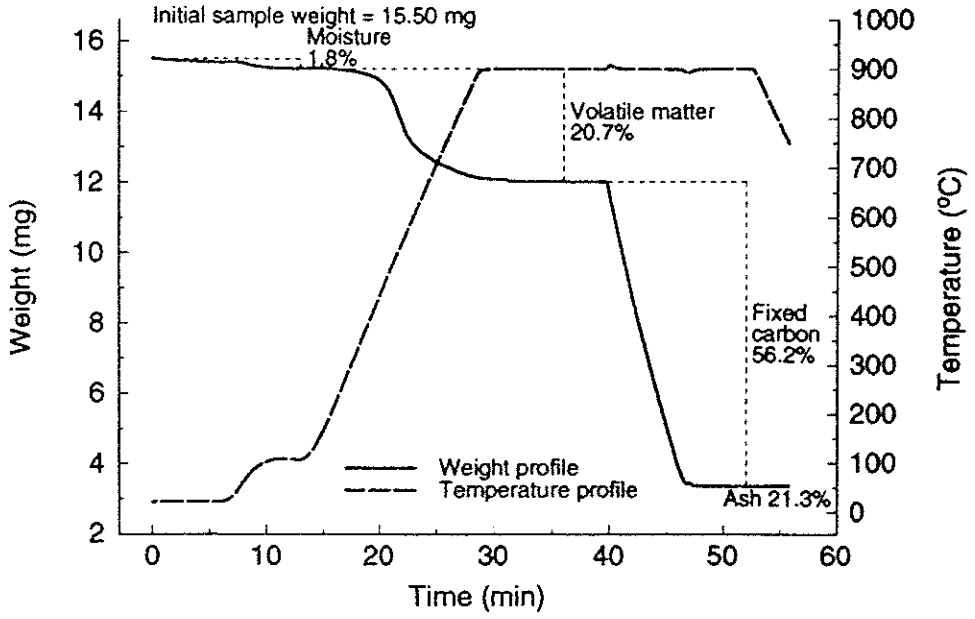

Fig. 1 TG profile for run number 462, sample 53/527.

used in the test. They applied a fixed correction to both the volatile and ash readings, and assumed the correction at the moisture temperature to be negligible.

Applying the Cumming & McLaughlin (1982) corrections to early testing did not prove very successful. Consequently, the buoyancy correction was closely examined, and it was found that the ash value from the TG profile at the end of the test varied significantly from the value obtained by reweighing the residue and crucible (Table 4). The difference between the two values does not appear to be systematic, and is certainly not a constant value as suggested by Cumming & McLaughlin (1982). This is not surprising as the parameters affecting buoyancy are numerous, including the density of coal, which is known to vary according to coal rank and type, and the density of the mineral matter present in the coal (van Krevelin 1993).

As both the volatile matter and fixed carbon content determinations were made at the same temperature, it is reasonable to assume that the volatile matter/fixed carbon ratio can be read directly from the TG data file. Therefore, the true weight losses are apportioned as follows:

Table 3 Initial proximate analysis results for New Zealand coals.

Sample/ Run no.	Sample weight (mg)	Proximate analysis			
		Moisture (%) air-dried basis	Volatile matter (%) dry basis	Fixed carbon (%) dry basis	Ash (%) dry basis
52/057					
228	15.90	10.8	41.9	55.2	2.9
231	14.85	10.8	41.9	54.7	3.4
232	16.66	10.5	41.6	54.5	3.9
Mean	15.80	10.7	41.8	54.8	3.4
σ	0.74	0.1	0.2	0.3	0.4
52/109					
229	16.65	5.9	42.4	54.9	2.7
233	15.39	5.7	42.3	54.7	3.0
234	16.14	5.1	42.3	55.4	2.3
Mean	16.06	5.6	42.3	55.0	2.6
σ	0.52	0.3	0.1	0.3	0.3
52/085					
236	18.37	12.7	45.7	51.3	3.0
237	17.98	12.7	45.9	51.1	3.0
238	18.71	12.9	45.6	51.2	3.2
Mean	18.35	12.8	45.7	51.2	3.1
σ	0.3	0.1	0.1	0.1	0.1

Table 4 Differences in ash values obtained from the TG data at 900°C, and by reweighing at room temperature.

Run no.	TG ash	Reweighed ash
	% air-dried basis	
52/085		
453	4.8	3.3
454	3.8	3.4
457	4.4	3.3
458	4.5	3.2
52/057		
438	3.0	3.1
439	3.9	2.8
440	4.3	3.0
441	3.8	2.8
52/109		
398	3.8	2.8
442	4.5	2.6
455	3.6	3.0
456	4.1	2.9
53/527		
459	22.2	21.4
460	22.4	21.8
461	21.5	21.2
462	21.7	21.3
53/883		
422	22.1	20.5
424	21.6	20.1
426	21.6	20.4
429	21.6	20.1
53/884		
423	6.5	5.5
425	6.4	5.5
427	6.2	5.5
428	6.6	5.6

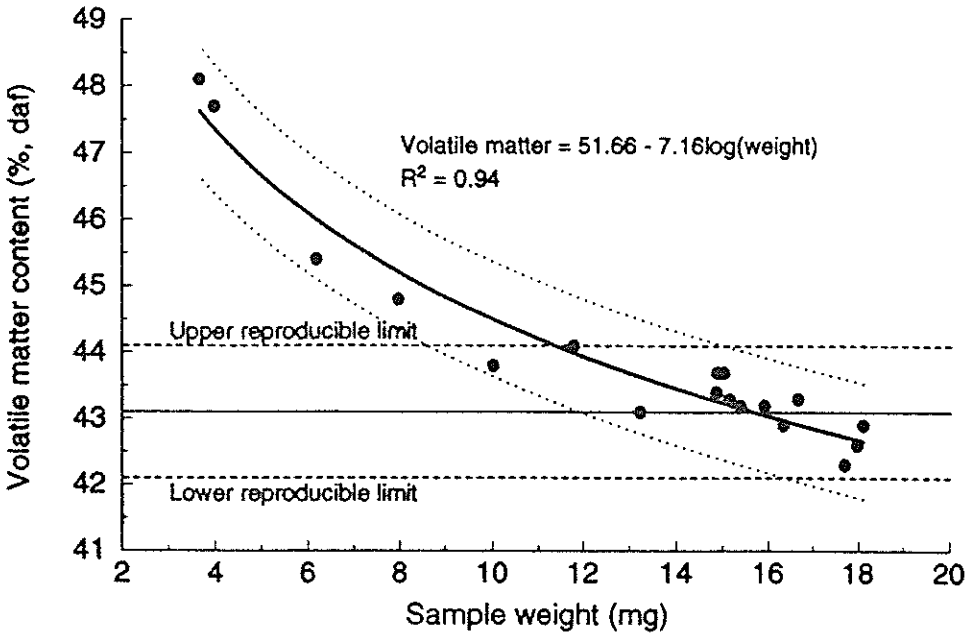

Fig. 2 Dependence of volatile matter on sample weight, as illustrated by sample 52/057.

moisture content (M in mg) = weight loss recorded by TG

ash content (A in mg) = residual weight measured by reweighing at the end of the test

volatile matter (VM in mg) = VM_{TG} * (sample weight – M – A)/(VM_{TG} + FC_{TG})

fixed carbon (FC in mg) = FC_{TG} * (sample weight – M – A)/(VM_{TG} + FC_{TG})

The effect of sample weight

Elphick (1960) reported on the effects of sample weight on the volatile matter yield of New Zealand coals and showed that by decreasing the sample weight from the standard 1 g down to 0.1 g the measured volatile matter yield increased. Therefore, to make the results comparable to the standard, correction factors were necessary. This difference in volatile matter yield with sample weight was not addressed by any of the previous studies on proximate analysis of coals by TG. Ottaway (1982) and Warne (1991) used c. 10 mg of sample, Elder (1983) used 5–10 mg of sample, and Cumming & McLaughlin (1982) used 50 ± 0.5 mg of sample, without justifying the reason for a restricted sample weight range.

Weights of 4–18 mg for sample 52/057 were subsequently used in this study to assess the effect on the proximate analysis determination (Table 5). The ash content values did not vary with sample weight, consistent with the findings of Elphick (1960). The moisture content variations can be attributed to sampling, as it was noted that samples taken from the top layer of the stored coal produced lower moisture values (presumably as a result of surface drying). A plot of volatile matter against sample weight (Fig. 2), yields a similar trend to that observed by Elphick (1960). As the weight of the sample decreases the measured volatile matter increases.

The actual standard value for sample 52/057 and reproducible limits of 1.0% have been superimposed on the volatile matter plot (Fig. 2). As seen from the 95% confidence intervals, sample weights between 8 mg and 22 mg are able to produce volatile matter results within these limits. According to the plot in Fig. 2, the optimum reproducible sample weight for the equipment and technique used at Auckland appears to be 15.5 mg.

For acceptable volatile matter repeatability, however, the weight range of the sample needs to be restricted. Tests performed on sample 52/057 (run numbers 340–342, Table 5), using a weight deviation of ±0.11 mg, did not produce any better repeatability than samples run with weight deviations of ±0.3–0.7 mg. This suggests that a weight deviation of ±0.5 mg is appropriate for acceptable repeatability.

Time and temperature effects on volatile matter determination

Following the success of the initial testing of the New Zealand coals, the first of the high rank Australian coals was tested, using the same procedure. It soon became apparent that the volatile matter measurement was excessively

Table 5 Proximate analysis results for Ohai subbituminous coal (52/057) by TG using different sample weights.

		Proximate analysis		
Run no.	Sample weight (mg)	Moisture (%, adb)	Ash (%, db)	Volatile matter (%, daf)
303	17.68	9.2	3.4	42.3
304	15.37	10.1	3.2	43.2
305	16.32	9.3	3.1	42.9
306	18.09	10.0	3.2	42.8
328	11.78	10.2	3.2	44.1
329	3.98	10.6	3.1	47.7
330	7.96	10.4	3.2	44.8
331	10.01	9.0	3.1	43.8
332	6.18	8.1	2.8	45.4
333	13.21	8.0	3.2	43.1
334	3.66	10.4	3.0	48.1
335	17.95	9.9	3.3	42.6
340	15.01	9.3	3.6	43.7
341	15.13	9.5	3.3	43.3
342	14.87	9.3	3.1	43.7

high. Two possible causes for this were immediately identified as: (1) the time taken for the volatile reading, and (2) the temperature used in the procedure. Consequently, runs were performed on samples 53/527 and 52/085 at 900°C and 950°C, respectively. The resulting data were analysed for volatile matter at varying times to establish an optimum procedure for these parameters (Table 6).

A wide range of times was used for volatile matter determination in previous studies using TG (Table 2). Interestingly, Cumming & McLaughlin (1982) selected the standard procedure time of 7 min from the point at which the sample attained a temperature of 900°C. The results in Table 6 support this procedure, and consequently a new procedure was adopted to compare all the coals in the study with the standard values.

Standard procedure

1. The sample is heated in a nitrogen atmosphere to 110°C at a rate of 50°C/min and is maintained at this temperature for 5 min to ensure a constant weight is achieved. The weight loss recorded by the STA is due to moisture (Fig. 1).
2. The temperature of the STA is then raised to 900°C at 50°C/min, and maintained at this temperature for 24 min. A separate timing device is set at 0.62 h at the beginning of the test run, which automatically switches the operating atmosphere from nitrogen to air (Fig. 1). The volatile matter reading is taken as the weight loss occurring from the end of the moisture loss to 7 min after reaching 900°C. The fixed carbon reading is taken as the weight loss occurring after the volatiles have been driven off till combustion is complete.
3. The residue at the end of the combustion process is the ash content of the coal, and is measured by reweighing.
4. The volatile matter and fixed carbon contents are recalculated for buoyancy effects.

DISCUSSION OF RESULTS

The results of proximate analysis by TG using the standard procedure developed are contained in Table 7. Limits of reproducibility and repeatability are contained in Table 8 for reference. All samples tested in this study are within these precision limits, except for the reproducibility of the ash content of sample 52/085. This may be due to the higher temperature of 900°C used for the ashing as opposed to the

Table 6 Change in volatile matter value with time and temperature.

Sample	53/527		52/085	
Weight (mg)	15.51	15.53	15.45	15.41
Temperature (°C)	950	900	950	900
ISO value	20.7		44.9	
Time after attaining temperature (mins)				
0	20.8	20.5	43.6	43.3
5	21.2	20.8	44.3	44.3
7	**21.3**	**20.9**	**44.5**	**44.4**
10	21.5	21.0	44.8	44.5
15	21.8	21.3	45.2	44.8
20	22.0	21.7	45.6	45.3
25	22.2	21.9	45.9	45.6

Table 7 Proximate analysis results obtained by TG.

	Proximate analysis			
Sample/ Run no.	Moisture (%) air-dried basis	Volatile matter (%) dry basis	Fixed carbon (%) dry basis	Ash (%) dry basis
52/085				
453	11.5	44.1	52.2	3.7
454	11.5	43.5	52.7	3.8
457	11.5	43.7	52.5	3.7
458	11.2	44.0	52.4	3.6
Mean	11.4	43.8	52.4	3.7
σ	0.13	0.23	0.17	0.08
52/057				
438	10.4	40.3	56.3	3.5
439	10.3	40.6	56.3	3.1
440	10.1	39.6	57.1	3.3
441	10.2	39.8	57.1	3.1
Mean	10.3	40.1	56.7	3.3
σ	0.11	0.40	0.41	0.15
52/109				
398	5.6	40.7	56.4	3.0
442	5.6	41.0	56.3	2.8
455	5.4	40.3	56.6	3.2
456	5.3	40.7	56.3	3.1
Mean	5.5	40.7	56.4	3.0
σ	0.13	0.26	0.12	0.15
53/527				
459	1.8	21.1	57.1	21.4
460	1.8	21.1	56.7	22.2
461	1.8	21.1	57.3	21.6
462	1.8	21.1	57.2	21.7
Mean	1.8	21.1	57.1	21.8
σ	0.00	0.00	0.23	0.23
53/883				
422	1.5	13.4	65.8	20.8
424	1.8	13.4	66.1	20.5
426	1.7	13.3	65.9	20.8
429	1.5	13.5	66.1	20.4
Mean	1.6	13.4	66.0	20.6
σ	0.13	0.06	0.13	0.18
53/884				
423	2.4	8.7	85.7	5.6
425	2.7	8.5	85.8	5.7
427	2.6	8.4	85.9	5.6
428	2.5	8.5	85.7	5.7
Mean	2.6	8.5	85.8	5.7
σ	0.11	0.10	0.10	0.04

Table 8 Precision for moisture, ash, and volatile matter as quoted by the ISO standard.

Property	Repeatability, % absolute	Reproducibility, % absolute
Moisture (air-dry):		
< 5%	0.10	See note
≥ 5%	0.15	See note
Ash (dry)		
< 10%	0.20	0.3
≥ 10%	2% of the mean result	3% of the mean result
Volatile matter (dry):		
< 10%	0.3	0.5
≥ 10%	3% of the mean result	0.5%, or 4% of mean, whichever is greater

For the moisture determinations, the results obtained will depend on the humidity conditions in the different laboratories. Since these conditions will vary, it is not practical to quote limiting values for reproducibility.

standard temperature of 815°C. However, this is unlikely as values obtained for all the other samples fall within the acceptable limits. Also, separate TG runs for ash only, at 815°C, produced the same values as those at 900°C.

The increase in volatile matter yield with decreasing sample weight may be due to coal particles being lost with the volatiles, as the STA crucible is open (Matheson pers. comm.). However, as already pointed out, these results are consistent with Elphick (1960), who used a closed crucible. Elphick's explanation was that the effect could be related to the rate of heat conduction through the coal at different loadings. Another contributing factor may be the change in surface area to volume ratio of the coal (Crosdale pers. comm.). At this stage, further testing will be necessary to assess the possible causes of the volatile matter to sample weight relationship.

According to Gray (1983), the New Zealand low rank coals fall within the classification of hard black coals as defined by the Australian Standard. It is therefore not surprising that the one test procedure for proximate analysis by TG is equally applicable to New Zealand and Australian black coals.

CONCLUSIONS

Thermogravimetry has the ability to analyse coal samples where only small amounts have been recovered for testing. It also provides the capability to produce proximate analysis results for small coal samples used in detailed petrographic studies, mineralogic studies, and other microstudies of coal (e.g., high pressure microgravimetry – Levine et al. 1993; Beamish & Crosdale 1993 ; coal microstructure – Gamson et al. 1993).

Proximate analysis results obtained for coals from three New Zealand coalfields and the Bowen Basin are within reproducible limits of the standards. The ash content of the coal is best determined by reweighing at the completion of the test, as the direct result from the STA is in error due to buoyancy effects associated with the elevated temperatures of the ashing. Ash values recorded by reweighing show little deviation and are within the standard limits for repeatability, irrespective of sample weight. The value obtained for the volatile matter content by TG is strongly sample weight dependent, fitting a logarithmic function consistent with earlier work of Elphick (1960). To obtain acceptable repeatability for volatile matter content, it is necessary to minimise these weight effects, and a sample weight of 15.5 ± 0.5 mg is recommended for future testing. The weight deviation value selected here is consistent with that used by Cumming & McLaughlin (1982).

ACKNOWLEDGMENTS

The author would like to thank Ritchie Sims for his diligence and patience in setting up the STA equipment. He also provided valuable assistance in assessing the methodology of the TG technique. Thea DePetris assisted with some of the later TG testing. Financial support for this work was provided by the Auckland University Research Committee. The New Zealand samples used for testing were supplied by Trevor Matheson of the Coal Research Association of New Zealand. The draft manuscript was reviewed by Ian Smith, Department of Geology, The University of Auckland, and Peter Crosdale, Coalseam Gas Research Institute, James Cook University of North Queensland. Peter also supplied two of the Australian coals for testing.

I am grateful to the external referees for their useful and inspiring suggestions to help me fill some of the original gaps in the paper.

REFERENCES

Beamish, B. B.; Crosdale, P. J. 1993: Methane sorption studies using a high pressure microbalance. Fifth New Zealand Coal Conference proceedings vol. 1. Wellington, Coal Research Association of New Zealand (Inc). Pp. 34–38.

Charsley, E. L.; Warrington, S. B. 1988: Industrial applications of compositional analysis by thermogravimetry. *In*: Earnest, C. M. *ed.* Compositional analysis by thermogravimetry. ASTM STP 997. Philadelphia, American Society for Testing and Materials. Pp. 19–27.

Cumming, J. W.; McLaughlin, J. 1982: The thermogravimetric behaviour of coal. *Thermochimica acta 57*: 253–272.

Elder, J. P. 1983: Proximate analysis by automated thermogravimetry. *Fuel 62*: 580–584.

Elphick, J. O. 1960: Analysis of very small samples of New Zealand coals. *Fuel 39*: 183–186.

Gamson, P. D.; Beamish, B. B.; Johnson, D. P. 1993: Coal microstructure and micropermeability and their effects on natural gas recovery. *Fuel 72*: 87–99.

Gray, V. R. 1983: Coal analysis in New Zealand. Coal Research Association of New Zealand (Inc.). *NZERDC report 97*. 75 p.

Larkin, D. E. 1988: Compositional analysis by thermogravimetry. The development of a standard method. *In*: Earnest, C. M. *ed.* Compositional analysis by thermogravimetry. ASTM STP 997. Philadelphia, American Society for Testing and Materials. Pp. 28–37.

Levine, J. R.; Johnson, P. W.; Beamish, B. B. 1993: High pressure microbalance sorption studies. The 1993 International Coalbed Methane Symposium proceedings vol. 1. Birmingham, Alabama, The University of Alabama/ Tuscaloosa. Pp. 187–196.

Ottaway, M. 1982: Use of thermogravimetry for proximate analysis of coals and cokes. *Fuel 61*: 713–716.

Rosenvold, R. J.; Dubow, J. B.; Rajeshwar, K. R. 1982: Thermal analyses of Ohio bituminous coals. *Thermochimica acta 53*: 321–332.

van Krevelen, D. W. 1993: Coal. 3rd ed. Amsterdam, Elsevier.

Warne, S. St J. 1991: Proximate analysis of coal, oil shale, low quality fossil fuels and related materials by thermogravimetry. *Trends in analytical chemistry 10*: 195–199.

8.2 Analysis of Coal Microstructure